Biophysics and Biochemistry of the Pancreatic ß-cell.

Thesis submitted for the degree of

Doctor of Philosophy

at the

University of Oxford.



Trinity Term

1989

Ronan Kelly

St. Cross College

To my parents.

Contents.

Detailed Contents iv

Prologue xiii

Abbreviations xiv

1. Introduction. 1

2. Methods. 7

3. Rb^+ and Na^+ permeability of the ATP-sensitive channel. 28

4. ATP sensitivity: modulation by ADP. 45

5. ATP-sensitive channels in the cell line HIT T15. 53

6. Voltage-activated currents in the rat ß-cell and the cell line HIT T15. 61

7. Electrophysiology of the human ß-cell. 73

8. General discussion 90

Appendix. 112

References. 114

1. Introduction. 1

ß-cell electrical activity 1

Dependence on metabolism 2

Primary and secondary secretagogues 2

Origin of slow waves and spikes 3

Previous patch clamp studies 5

The ATP- and glucose-sensitive channel 5

Regulation by ATP_i 5

Voltage-activated currents 6

2. Methods. 7

Rat ß-cell preparation 7

Islet preparation 7

Islet collection 8

Dispersion of islet cells 9

Solutions for islet preparation 10

Human cells 12

The HIT T15 cell line 13

Biochemical analysis 14

Insulin secretion: static incubations 14

Insulin secretion: superfusion 14

Insulin radio-immunoassay 15

ATP determination 15

Solutions for biochemical analysis 17

Biochemical results

Insulin secretion: islets 18

Insulin secretion: isolated cells 18

ATP content 19

CONT...

Patch clamping

General set-up 20

Pipettes 20

Electrophysiological recording 21

Cell-attached recording 22

Excised patch recording 22

Whole cell recording 23

Junction potentials 24

Data analysis

Single-channel data analysis 25

Whole-cell data analysis 25

Solutions for patch clamping 27

3. Rb^+ and Na^+ permeability of the ATP-sensitive channel. 28

Introduction 28

Methods 30

Junction potentials 30

Solutions 31

Solution exchange 31

Protocols 31

Results

Inside-out patches 33

K^+ and Rb^+ IV's 33

Noise analysis 35

Permeability ratios 36

Outside-out patches 38

Discussion

Rb-experiments 40

Na permeability 43

Relationship to flux studies 44

4. ATP sensitivity: modulation by ADP. 45

Introduction 45

Methods 47

Results

Block by ATP 48

Effect of ADP 48

ATP and ADP concentrations 49

Discussion 50

5. ATP-sensitive channels in the cell line HIT T15. 53

Introduction 53

Methods 54

Results

Whole-cell results

Washout currents 55

Block by Tb and ATP 55

Inside-out patches 56

Channel kinetics 56

Effects of ATP and Tb 57

Discussion 59

6. Voltage-activated currents in the rat ß-cell and the cell line HIT T15. 61

Introduction 61

Methods 62

Results 63

Outward currents 63

Inward currents 63

Inactivation 65

Effect of Glucagon 66

Single-channel currents: T- and L-type channels 67

Discussion 69

Inactivation 70

Modulation by glucagon 71

7. Electrophysiology of the human ß-cell. 73

Introduction 73

Results

Single-Channel Currents 74

Tolbutamide sensitivity. 75

Voltage-Activated Currents

Outward Current 76

Inactivation 77

Activation 77

Inward currents 78

Inactivation of calcium currents 79

Effects of barium as the charge carrier 81

Voltage-dependent inactivation 82

Discussion

ATP-sensitive channels 84

Voltage-activated potassium currents 85

Calcium currents 86

8. General discussion. 90

The ionic basis of electrical activity.

The Initial Depolarisation. 91

Mechanism Of Bursting. 92

Ca^{2+}-activated K^+ channel activation ? 92

ATP-sensitive K^+ channel activation ? 93

Ca^{2+} current inactivation ? 94

IP3-activated K^+ current ? 95

The action potential.

The action potential upstroke. 96

Action potential repolarisation. 96

The regulation of the ATP-sensitive potassium channel. 99

RIN cells vs. ß-cells. 100

The modulatory effect of glucose.

Slow waves. 102

Action potential frrquency. 103

Ca^{2+} current modulation. 103

The biochemical modulation of Ca^{2+} channels. 104

Modulation by hormones and neurotransmitters.

Glucagon. *Microelectrode studies.* 105

Patch clamp studies. 106

Acetylcholine. *Microelectrode studies.* 107

Patch clamp findings. 108

Biochemical mediators. 108

Adrenaline 109

Galanin and somatostatin. 110

Conclusion. 111

Abbreviations.

ADP	adenosine diphosphate
ATP	adenosine triphosphate
BSA	bovine serum albumin
DAG	diacylglycerol
DHP	dihydropyridine
cAMP	cyclic adenosine monophosphate
CTX	α-conotoxin
HK	HEPES- Krebs buffer
I(Ca)	calcium current (amplitude)
I(K)	potassium current (amplitude)
IP3	inositol 1,4,5-tri(s)phosphate
K(ATP)	ATP-sensitive potassium channel or current
K(DR)	delayed rectifier potassium channel or current
K(Ca)	calcium-activated potassium channel or current
NDCB	Nuffield Dept. of Clinical Biochemistry, John Radcliffe Hospital
NIDDM	Non-insulin dependent diabetes mellitus
NMG	N-methyl D-glucamine
P_i	inorganic phosphate (ions)
PKC	protein kinase C
PLC	phospholipase C
PMA	phorbol mystyrate acetate
TPA	tetradecanoyl phorbol acetate
TTX	tetrodotoxin
V_H	holding potential
V_m	membrane potential
V_p	pipette potential
V_r	cell resting potential (in the absence of glucose)

Introduction.

The ß-cells of the pancreatic islets of Langerhans are the endocrine cells which secrete the hypoglycaemic hormone insulin. The primary stimulus for insulin secretion is an increase in the plasma glucose concentration, although secretion can be modulated by a variety of hormones and neurotransmitters. The immediate signal for insulin release is calcium entry through the ß-cell plasma membrane. Primary secretagogues are glucose and those other secretagogues capable of initiating insulin secretion (e.g. glyceraldehyde, leucine, 2-ketoisokaproate); secondary secretagogues are those which potentiate the effect of glucose but which cannot initiate insulin secretion in the absence of glucose (glucagon, ACh, Forskolin, phorbol esters). Both glucose and the various agents which modulate insulin secretion do so by altering the pattern of ß-cell electrical activity, and hence Ca^{2+} influx. This thesis examines the ionic basis of ß-cell electrical activity and the mechanism of its initiation by glucose.

ß-CELL ELECTRICAL ACTIVITY

In the absence of glucose the ß-cell is electrically silent, with a resting potential of ~ -70 mV as shown both by micro-electrode studies (Dean & Matthews, 1970a; Henquin & Meissner, 1982a; Meissner, 1976) and by more recent whole-cell patch-clamp recordings (Ikeuchi et al., 1984; Ashcroft et al., 1984). Micro-electrode recordings have shown that glucose influences ß-cell electrical activity in three ways. First, increasing plasma glucose in the range 0 to 7 mM produces a graded, glucose-dependent depolarisation of the membrane until the threshold for both electrical activity and insulin secretion is reached at glucose concentrations between 5 and 7 mM (Dean & Matthews, 1968; Meissner & Schmelz, 1974). The threshold for electrical activity (~ -50 mV) is 10-15 mV positive to the resting potential (Henquin & Meissner, 1984a) The characteristic electrical activity of the ß-cell consists of oscillations in membrane potential (bursts or slow waves) between a depolarised plateau potential, on which Ca-dependent action potentials are superimposed, and a more hyperpolarised silent phase (Dean & Matthews, 1968; Dean & Matthews, 1970a; Matthews & Sakamoto, 1975; Meissner, 1976) (see figure 1.1)

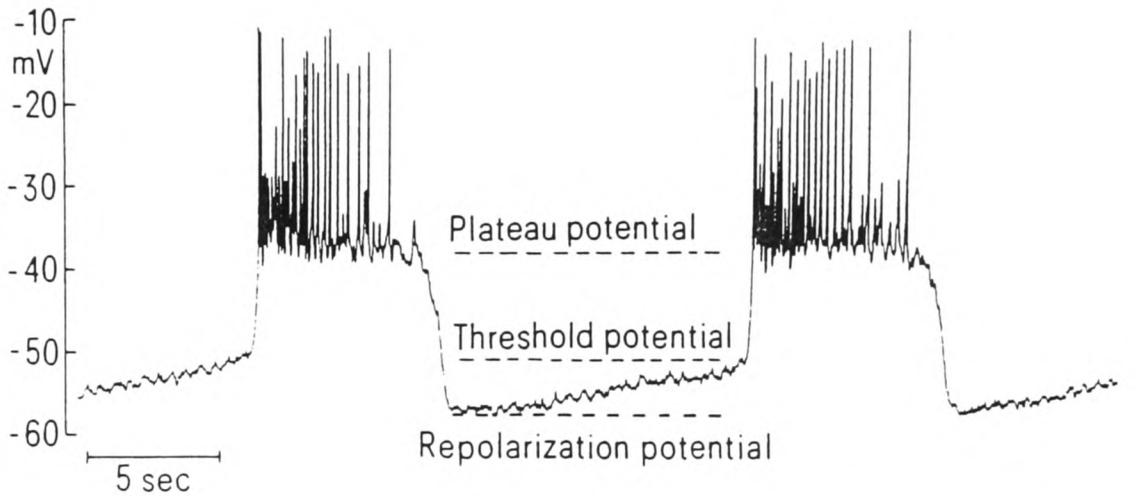


Figure 1.1. Electrical activity of the mouse ß-cell.
Two slow waves, demonstrating the plateau potential, action potentials and the silent phase. (Taken from Henquin & Meissner, 1984a).

The second effect of glucose (> 7 mM) is to increase the duration of the slow waves and decrease the interval between them, until finally (~20 mM glucose), the plateau potential is sustained and action potentials fire continuously (Dean & Matthews, 1970a; Henquin & Meissner, 1984a; Petersen & Findlay, 1987). A third level of control by glucose exists, whereby glucose can increase the rate of generation of action potentials directly, i.e. other than by increasing the amount of time spent at the plateau potential (Meissner & Schmelz, 1974; Bozem & Henquin 1988; supported by recent patch-clamp results: Cook & Ikeuchi, 1988; Ashcroft & Smith, 1989; Smith et al., 1989).

The initiation of electrical activity by glucose is preceeded by a slow depolarisation of the ß-cell membrane to the threshold potential. The origin of this initial depolarisation has been the subject of detailed investigation. K^+ efflux studies (Sehlin & Taljedal, 1975; Henquin, 1978) and microelectrode conductance measurements (Atwater et al., 1978) showed that the depolarisation was caused by a decrease in the resting K^+ permeability of the ß-cell membrane, which they attributed to closure of some channel other than the voltage-sensitive K^+ delayed rectifier, as the silent phase potential was not TEA-sensitive (Atwater et al., 1979a). Atwater et al. (1979b), however, erroneously attributed the initial depolarisation to closure of the calcium-sensitive potassium channel on the grounds that i) the glucose-induced depolarisation could be mimiced by quinine, a known K(Ca) current blocker (Armando-Hardy et al. 1975) and ii) the depolarisation could be prevented by metabolic inhibitors, which had previously been shown to increase intracellular calcium levels (Rojas & Hidalgo, 1968; Blaustein & Hodgkin, 1969)[1].

All these effects of glucose, the initial depolarisation, the increase in electrical activity, the effects upon ion fluxes and the stimulation of insulin secretion, depend upon glucose uptake and its subsequent metabolism by the ß-cell (electrical: Dean et al., 1975, 1978. ionic: Henquin, 1980a, secretory: Ashcroft, 1980, Hedeskov, 1980). The effects of glucose on electrical activity are inhibited by those agents which block glucose uptake (phloridzin: Dean et

[1]It is now known that in the ß-cell, quinine has a much lower K_D for both the K(ATP) channel and the delayed rectifier potassium channel than for the calcium-activated potassium channel (Findlay et al. 1985a, 1985c; Bokvist et al. 1990a,b; Smith et al. 1990), and that the effect of metabolic inhibitors can be attributed directly to the decrease in intracellular ATP levels that they produce (e.g. Rorsman & Trube, 1985).

al., 1975) or metabolism (mannoheptulose, anoxia, iodoacetate: Dean et al., 1975), and structural analogues of glucose which do not induce insulin secretion do not induce electrical activity (e.g. L-glucose, D-galactose, 3-methyl D-glucose, Dean et al., 1975).

All primary secretagogues act via their metabolism. All primary secretagogues investigated have been shown to be capable of triggering the initial depolarisation (L-leucine: Dean & Matthews, 1968; Dean & Matthews, 1970a; Henquin & Meissner, 1981; D-glyceraldehyde, acetoacetate: Dean et al., 1975; 2-ketoisokaproate: Henquin & Meissner, 1981; Hutton et al., 1980). Secondary secretagogues increase the duration of the slow waves or decrease the duration of the interval between them (ACh: Gagerman et al., 1978; Cook et al., 1981a; glucagon: Ikeuchi & Cook, 1984; cAMP: Henquin & Meissner, 1984b, 1984c; Henquin et al., 1983). The mechanism of their action is not yet understood. Catecholamines, which inhibit insulin secretion, have been reported to hyperpolarise the ß-cell membrane and inhibit electrical activity (Dean & Matthews, 1970a) or to have no effect on electrical activity (Cook & Perera, 1982; Santana de Sa et al., 1983).

Origin of slow waves and spikes.

The change of plateau rhythm achieved by depolarisation with high K^+ (Cook et al., 1980; Matthews & Sakamoto, 1975) or injected current (Cook et al., 1980, 1981b) the abolition of slow waves in 0 mM Ca (Meissner & Schmelz, 1974; Matthews & Sakamoto, 1975) and the ability of Ca channel blockers to inhibit the slow waves (Meissner et al., 1980: d600: Matthews & Sakamoto, 1975; nifedipine: Vasseur, et al., 1986) and of dihydropyridine derivatives that prolong Ca channel opening to increase slow wave duration (Henquin et al., 1985) suggest that a voltage-dependent Ca current might be involved in the generation of the slow waves. This idea is supported by the increase in slow wave amplitude found when external Ca is raised (Meissner et al., 1980, Atwater et al., 1983; Meissner & Preissler, 1979; Meissner & Schmeer, 1981; Ribalet & Beigelman, 1980), although the data could also be explained if a Ca^{2+}-activated non-specific cation current contributed to the slow wave (Sturgess et al., 1987). Finally, the ability of DHP agonists to increase insulin release (Henquin et al., 1985) and of DHP antagonists to decrease secretion (Malaisse & Boschero, 1977) is consistent with the

Ca^{2+} influx for insulin release flowing through L-type Ca channels (see Henquin & Meissner, 1984, and Findlay et al., 1989, for reviews).

Repolarisation of the plateau has been attributed to Ca^{2+}-activated K^+ channels (Atwater et al., 1979b, 1979a) or Na-K exchange (Meissner, 1976, Henquin & Meissner, 1982).

Micro-electrode studies had also deminstrated that the upstroke of the action potential is due to the opening of voltage-dependent Ca^{2+} channels (Dean & Matthews, 1970b; Meissner & Schmeer, 1981; Ribalet & Beigelman, 1980). Action potentials can be elicited by injected current (Matthews & Sakamoto, 1975; Dean et al., 1975; Atwater et al., 1978) and are abolished by Ca^{2+} removal (Atwater 1980; Atwater et al., 1980; Dean & Matthews, 1970b; Matthews & Sakamoto, 1975; Meissner & Schmelz, 1974). They increase in amplitude in high Ca^{2+} solutions (Atwater et al., 1980; Dean & Matthews, 1970b; Matthews & Sakamoto, 1975; Ribalet & Beigelman, 1980; Ribalet & Beigelman, 1981) the rate of depolarisation is proportional to the external Ca^{2+} concentration (Ribalet & Beigelman, 1980) and they are blocked by Ca^{2+} channel blockers (Matthews & Sakamoto, 1975; Ribalet & Beigelman, 1980; Ribalet & Beigelman, 1981; Vasseur et al., 1986). There is no significant Na^+-current contribution to the action potential: they are not diminished in amplitude in a low-Na^+ medium (Dean & Matthews, 1970b; Ribalet & Beigelman, 1982) or by TTX (Meissner & Schmelz, 1974; Tarvin & Pace 1981). Neither does TTX block insulin secretion (Milner & Hales, 1969; but see Hiriart & Matteson, 1988 for an effect of TTX). Action potential repolarisation had been demonstrated to involve the activation of potassium currents, which were suggested to be due to activation of voltage-sensitive K^+ channels (Atwater et al., 1979a) (because of the increase in amplitude and duration of the action potentials on addition of TEA, thought to be a selective blocker of voltage-activated K^+ channels (but now recognised as a selective blocker of $K_{(Ca)}$ channels)), or to $K_{(Ca)}$ channels (Ribalet & Beigelman, 1980) (because of the decreased rate of repolarisation in low Ca^{2+} solutions, the unexpectedly rapid repolarisation in the presence of TEA and the increase in the amplitude of the hyperpolarising after-potentials with higher Ca^{2+}).

PATCH CLAMP STUDIES

The advent of patch-clamping in 1981 allowed the individual conductances underlying the electrical activity to be dissected out, and the function and regulation of the individual species of ion channels to be studied in detail.

In 1984 patch-clamp studies identified a glucose-sensitive K^+ channel which was shown to be the dominant permeability in the unstimulated ß-cell, and which, in the absence of glucose, maintains the resting potential of the cell at about -70mV (Ashcroft et al., 1984; Rorsman & Trübe, 1985; Ashcroft et al., 1988a). This channel, in the intact ß-cell, is closed by glucose in a dose-dependent manner in the range 0-20 mM (Ashcroft et al., 1984). Most of the decrease in channel open probability occurs in the range 0-5 mM glucose (Ashcroft et al., 1988a), which is similar to the range of glucose concentrations which produces a graded depolarisation of the ß-cell membrane (Meissner & Schmelz, 1974). The channel was shown to be closed not directly by glucose, but rather by some product(s) of glucose metabolism (Ashcroft et al., 1984) although the intermediate was not immediately identified. In the same year the histirically separate discovery had been reported of a K^+ channel in the ß-cell plasma membrane sensitive to ATP_i with a K_i, in inside-out membrane patches, of 15 μM (Cook & Hales, 1984). The glucose-sensitive and ATP-sensitive K^+ channels were soon shown to be one and the same channel (Rorsman & Trübe, 1985). As glucose was known to increase ATP_i (Ashcroft et al. 1973, Malaisse et al. 1979) it was suggested that supra-threshold concentrations of glucose depolarised the cell and so initiated electrical activity by closing the channel via an increase in ATP_i (Rorsman & Trübe, 1985). This conclusion is further supported by

i) the striking correlation between the glucose dependence of channel inhibition and that of the increase in ATP_i (Ashcroft et al., 1986a).

ii) the initial increase in open probability of the channel (Rorsman, 1986; Arkhammar et al., 1987), accompanied by an increase in K^+ efflux (reviewed in Henquin & Meissner, 1984a) and membrane conductance (Atwater et al., 1978) which coincides with an initial decrease in ATP_i (Malaisse et al., 1979).

iii) the similarity of the effects on channel kinetics of an increase in the concentration of external

glucose or of ATP_i (Rorsman & Trübe, 1985).

Several objections were raised to the hypothesis that glucose closes this channel via an increase in ATP_i, the principal one being that ATP-sensitive channels are visibly active in cell-attached patches on ß-cells in 0 mM glucose, even though ATP_i under these conditions is ~ 5 mM, and the channel had been demonstrated to have a K_i for ATP of 15 µM in excised patches. The selectivity, modulation and role of this channel are the subjects of the first part of this thesis (ch. 3-4); chapter three provides evidence to support a role for the channel in the initial depolarisation, and chapter four investigates the mechanism whereby glucose modulates the channel and explains some of the discrepancy between the K_i for ATP and the reported activity with 5 mM ATP_i. Chapter five characterises the ATP-sensitive channel in the hamster insulinoma HIT T15, a cell line used in biochemical studies of the ß-cell, and a promising source of material for isolation and purification of the ATP-sensitive channel.

Little work had been done on the voltage-activated currents in the ß-cell prior to 1985 (Marty & Neher, 1982). In 1985-6 inward calcium currents and outward potassium currents were reported by several groups (Satin & Cook, 1985, 1986; Findlay & Dunne, 1985, 1986b; Trübe & Rorsman, 1986), and those in the mouse ß-cell were characterised in some detail by Rorsman and Trübe (1986). The second part of this thesis further investigates the properties of these currents in the rat ß-cell and in the HIT T15 cell line.

The final chapter demonstrates the presence of ATP-sensitive channels and voltage-activated K^+ and Ca^{2+} currents in the human ß-cell. It confirms the value of the rodent ß-cell as a model for that of the human, and discusses the possibility that a defect in ion channel regulation is involved in the aetiology of some forms of non-insulin dependent diabetes mellitus (NIDDM).

Methods.

RAT ß-CELL PREPARATION

Single pancreatic ß-cells were prepared by dispersion of isolated islets of Langerhans from normal adult rats using enzymic and mechanical methods, plated onto glass cover-slips and maintained in short-term tissue culture for up to 5 days.

Islet preparation

Two separate methods were used at various times to isolate islets of Langerhans. In the first of these, adapted from that described in Coll-Garcia & Gill (1969), male Wistar rats (200 g) were killed by injection of 1 ml pentobarbitone (Sagital, May & Baker, Dagenham) subcutaneously or intraperitoneally. The rat was soaked in alcohol, the skin cut open and pinned back, then the muscle of the abdominal wall, the pancreas exposed, and then distended by injection of 10 ml of ice-cold bicarbonate Krebs buffer (see below page 10 for details of the solutions used). The pancreas was then rapidly removed, taking care not to cut into the duodenum. It was placed in a petri dish, on ice, was washed in Krebs, carefully trimmed of adherent adipose tissue and placed in a small (15 ml) glass flask. The pancreas was then finely chopped with a pair of scissors and washed three times in ice-cold bicarbonate Krebs by sucking the pieces into a 10ml syringe, allowing the fat to float to the top of the solution, and expelling. The pieces of pancreas were then added to a 10 ml glass conical flask containing 2.3 mg collagenase (Serva, from clostridium histrolyticum, 0.71 U/mg) in 2 ml bicarbonate Krebs solution and the flask was bubbled with 95% O_2, 5% CO_2 for 2 min. The flask was securely stoppered and sealed with Nescofilm. Flasks were shaken vigorously in a water-bath for three periods of five, four and four minutes, alternating with vigourous shaking by hand for one minute after each interval in the water-bath. Sixteen min after the start of the incubation, the pancreatic tissue, now a lump-free digest, was washed three times in buffer by centrifugation (1 min. position 1, MSE bench centrifuge, 100 x *g*) and placed on ice in a disposible petri dish (Gibco, Glasgow, Scotland) for collection of islets.

A second method for islet preparation was developed from that used in the preparation of human islets by Gray, Mcshane, Grant and Morris (1984). In this case the rat was anaesthetised by intra-peritoneal injection of 0.5 ml pentobarbitone, the abdominal wall was opened and pinned back and the pancreas exposed. The pancreatic duct was clamped with a pair of artery forceps and a small incision was made with a pair of microscissors in the wall of the bile duct. A cannula was inserted into this incision, and the wall of the duct tightly ligated round the cannula. The rat was then killed by exsanguination (achieved by section of both carotid arteries) and blood was allowed to drain for ~2 min. 3 ml of HEPES-Krebs solution (without BSA) containing 3 mg/ml Sigma Type Ia collagenase was then injected via the cannula to distend the pancreas. The cannula was removed and the pancreas rapidly excised from the abdomen and placed in 20 ml pre-warmed HEPES-Krebs solution in a water-bath at 38 °C for 17 min. At the end of this period, the solution was poured off and the pancreas (now on the point of falling apart) was triturated using an 18 gauge needle (three to six times, depending on the degree of disintegration of the tissue). The islet suspension was then washed three times by centrifugation in ice-cold HEPES Krebs (1 ml tissue per 9 ml HEPES Krebs) and placed on ice for picking.

This second method was found to give higher and more consistent yields of islets: around 200 per rat, compared with 50-150 per rat when the first method was used. This improvement was attributed to the greater and more equal distension of the pancreas produced by duct cannulation. No qualitative difference was noted between the islets produced by the two methods.

Islet collection

Islets were collected individually, using a small wire loop made from the support for the filament of a standard light-bulb. Picking was performed under a binocular dissecting microscope (magnification x 40) in a flow-hood. The dish containing the islets was kept on ice to prevent islet deterioration. Islets could easily be distinguished from exocrine tissue by their higher opacity when viewed against a black background. The loop was flamed frequently and

the inside of the flow hood and the microscope were thoroughly washed with alcohol before starting to help mantain sterility.

Dispersion of islet cells

50-400 islets were collected in 0.5 ml HEPES-Krebs buffer (HK) in an LP3 tube and washed twice by centrifugation (1 min, ~100 g) in HK/BSA/Ca solution (see page 10 below). They were then incubated for 20 min in 200 µl HK/BSA/Ca/DNase /collagenase solution in a slowly shaking water bath at 37 °C. After 20 min, 1 ml HK/BSA/EGTA was added and the islets spun (1 min, 100 g) in a bench centrifuge. The supernatant was removed and the islets were suspended in 200 µl HK/BSA/EGTA/Dnase at room temperature for 15 min. The islets were then dispersed into single cells by trituration using a Finn pipette. The cells were added to 10 ml RPMI in a universal container and centrifuged for 5 min at 1000 r.p.m. on an MSE Centaur 2 bench centrifuge (~ 300 x g) . The supernatant was sucked off and the cells resuspended in 5 ml RPMI per 100 islets. 5 ml cell suspension was added to a sterile petri dish containing a glass cover-slip (previously washed and sterilised by dipping in alcohol and flaming). Cells adhering to the cover-slip after 24 hrs were used for the patch-clamp experiments. The dishes of cells were maintained at 37 °C in a humidified atmosphere (95% air, 5% CO_2) for 1-5 days, until use. The culture medium was RPMI 1640 (Gibco) supplemented with penicillin (100 U/ml), streptomycin (0.1 mg/ml), and 10% fetal calf serum.

It was later found that the method of cell preparation worked equally well without DNase, and so this was then omitted from the collagenase solution.

Metabolic and secretory responses of cells prepared in this way have been briefly reported (Ashcroft et al., 1988a) and are detailed below on page 18.

SOLUTIONS FOR ISLET PREPARATION

Krebs buffer was made from stock solutions as detailed in table 2.1. Glucose was added (0.6 mg/ml, 3.3 mM) and the buffer was bubbled with a O_2:CO_2 mixture (95:5) for 15 min to bring the pH to ~7.4 before use.

Table 2.1: Krebs buffer.

	stock concentration		volume	mol. wt.	final conc.
	g/l	M	(ml)		(mM)
NaCl	90	1.541	10	58.4	11
KCl	11.5	0.154	4	74.5	4.75
$NaHCO_3$	13	0.155	21	84	25
$CaCl_2$	16.2	0.110	3	147	2.54
$MgSO_4.7H_2O$	38.2	0.155	1	246.5	1.20
KH_2PO_4	20.9	0.154	1	136.1	1.18
H_2O			90		
				Total volume, 130 ml.	

Table 2.2: ($0Ca^{2+}$) HEPES Krebs buffer.

	stock concentration		volume	mol. wt.	final conc.
	g/l	M	(ml)		(mM)
NaCl	90	1.541	10	58.4	11
KCl	11.5	0.154	4	74.5	4.75
$NaHCO_3$	13	0.155	4.2	84	25
($CaCl_2$	16.2	0.110	0	147	0
$MgSO_4.7H_2O$	38.2	0.155	1	246.5	1.20
KH_2PO_4	20.9	0.154	1	136.1	1.18
HEPES			16.8		
H_2O			90		
				Total volume, 130 ml.	

HK/BSA/Ca: for collagenase digestion, 10 µl 100 mM $CaCl_2$ added to 10 ml 0Ca HEPES Krebs buffer containing 10 mg/ml bovine serum albumin.

HK/BSA/Ca/DNase/collagenase: 10 µl 2 mg/ml DNase (646 Kunitz units/mg) in 0Ca HK and 2.3 mg Sigma Type II collagenase (180 U/mg) added to 1.15 ml HK/BSA/Ca.

HK/BSA/EGTA: for cell separation, 100 µl of stock EGTA (3.8 g/100 ml adjusted to pH 7 with NaOH) added to 10 ml HK/BSA/0Ca.

HK/BSA/EGTA/DNase: 10 µl 20 mg/ml DNase (646 Kunitz units/mg) added to 0.72 ml HK/BSA/EGTA.

HUMAN CELLS

Human pancreata were obtained,with appropriate permission from normoglycaemic, heart-beating cadaver organ donors. The results in chapter 7 were obtained from 9 successful preparations (out of a total of 13). The donors were aged between 17 and 64, and died from head injuries, cerebral or subdural haemorrhage. Islets were isolated by collagenase digestion as described by Gray et al. (1984). Briefly, the pancreas was distended by injection of medium (1 ml/g of tissue) containing collagenase (6 mg/ml, Type I, Sigma) into the pancreatic duct. After incubation at 39 °C for 23 min the gland was rapidly cooled and distended by injection of cold medium (1 mg/g) into the pancreatic duct. The pancreas was dispersed by a process of teasing and shaking and the dispersed tissue was collected by centrifugation at 50*g* for 10 s. The pellet was resuspended in medium and further dispersed by gentle aspiration and expulsion through a 14 gauge needle (three times) and a 16 gauge needle (once). The tissue suspension was then passed through a nylon mesh filter (pore size 106 μm). Tissue trapped in the filter was carefully washed and passed through a polyester mesh filter (pore size 500 μm). The trapped tissue was discarded and isolated islets were individually collected from the filtrate, using a wire loop or a pasteur pipette. Tissue which passed through the 106 μm mesh was allowed to settle for 5 min, the supernatent aspirated and the sediment underlaid on a discontinuous Ficoll gradient: islets could usually be recovered from the 1.03/1.00 (specific gravities) interface. About 1000 islets per donor were collected in this way. All stages of the preparation were performed in Hank's balanced salt solution, containing 5 mM glucose. With the exception of that used to inject the collagenase, the medium also contained bovine serum albumin (4 g/l, Fraction V, Sigma).

After overnight culture in RPMI 1640 the islets were dispersed into single cells, plated onto glass coverslips and maintained in short-term tissue culture for up to four days, in exactly the same manner as described for the rat ß-cells. The metabolic and secretory responses of islets prepared in this way have been reported elsewhere (Harrison et al., 1985).

THE HIT T15 CELL LINE

HIT T15 ß-cells (passage numbers 75-90) obtained from Dr. A. E. Boyd III (Baylor College of Medicine, Houston, Texas USA), were cultured in RPMI 1640 tissue culture medium supplemented with penicillin (100 U/ml), streptomycin (0.1 mg/ml), fungizone (0.25 µg/ml) and fetal calf serum (10%) at 37 °C in an atmosphere of humidified air (95%) and CO_2 (5%). Culture medium was replaced every 48 hrs and the cells were passaged weekly after detachment using trypsin-EDTA. The metabolic and secretory properties of the HIT T15 cell line have been fully characterised and reported (Santerre et al., 1981; Hill & Boyd, 1985; Boyd et al., 1985; Swope & Schonbrunn, 1984; Ashcroft et al., 1986; Ashcroft & Stubbs, 1987; Nelson et al., 1987; Hughes & Ashcroft, 1988).

BIOCHEMICAL ANALYSIS

The identity and viability of the islets and cells isolated from the rat pancreas as detailed above were assessed by a variety of tests, principally by their ability to secrete insulin, to respond to glucose and to respond to a selection of hormones and neurotransmitters:

METHODS FOR BIOCHEMICAL ANALYSIS

Insulin secretion: static incubations

Islets: islets were generally used on the day after isolation. 4-6 replicate tubes were used per condition, 5 islets per tube. The islets were collected into 0.3 ml HK + BSA (2 mg/ml) and a similar quantity of glucose solution was added to make final glucose concentrations of 2 or 10 mM. Glucagon, ACh and adrenaline were made up in 20 mM glucose solution before addition to the islets. The tubes were incubated at 37 °C for 1 hr in a humidified incubator, after which 0.1 ml samples were taken and serially diluted 1:10 and 1:50 in PAM.

Cells: after overnight culture, rat ß-cells cells not adherent to the cover-slip were collected and centrifuged for 5 min at 1000 rpm. The supernatant was removed and the cells were resuspended in HEPES-Krebs + BSA (10 mg/ml).

0.3 ml of HK/BSA containing 4 mM or 20 mM glucose was added to 0.3 ml cell suspension (containing ~20 x 10^3 cells), as for islets. 5 replicates were used for each test condition. The tubes were incubated in a humidified incubator at 37 °C for 1 hr, and were then spun for 5 min at 1000 rpm (~2000 g) in an MSE Hi-spin 21 centrifuge. 0.2 ml samples of the supernatant were taken and 1:5 and 1:50 dilutions were made in PAM.

Insulin secretion: superfusion

Biogel powder (BioRad, Watford, Herts) was boiled for 15 min in NaCl (9 g/l, 154 mM). Biogel was placed on glass wool in the lower half of a perifusion syringe. The cells (80 x10^3) were placed on the biogel and the syringe was filled with more biogel. The syringe was stoppered and connected to a flow system in a humidified incubator at 37 °C. The syringe was perfused at 1 ml/min and the perfusate was collected every 2 min and assayed for insulin

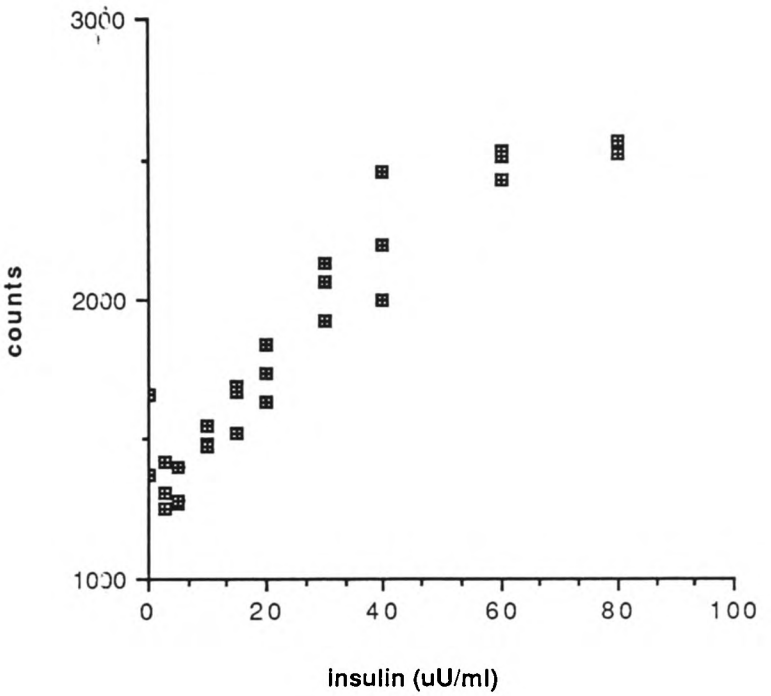


Figure 2.1. Standard curve for insulin radio-immunoassay.
The samples were serially diluted so that the assayed insulin concentration fell on the linear portion of the curve.

without dilution. Solution changes were made by transferring the mouth of the inflow tube between beakers containing the various solutions, care being taken to avoid air locks. The dead space upstream of the cells amounted to ~1 ml, and that downstream was roughly similar.

Insulin radio-immunoassay

100 µl of each diluted sample was taken into an LP3 tube, in duplicate, and 50 µl of a 1:30 dilution of anti-insulin serum was added before incubation for 1-4 hrs at room temperature. At the end of the incubation, 50 µl of radio-labelled insulin (^{125}I-labelled insulin, Amersham Intl., Amersham, Bucks.) was added to each tube, and they were placed in the fridge overnight (~18 hrs). Insulin standards (rat insulin standard from Novo Research Labs. Copenhagen) were made up at 0, 2.5, 5, 10, 15, 20, 30, 40, 60 and 80 µU/ml, 100 µl in triplicate. A suspension of 0.6 mg charcoal per 100 ml PAM for charcoal was made up and stored in the fridge.

The next day, 1 ml of the charcoal suspension was added to each tube and the tube was shaken by touching it briefly to a Whirlimixer (Fisons) to ensure a good mix. The tubes were then spun at 2000 rpm (1500 g) for 20 min in an MSE Mistral 6L centrifuge, the supernatant was sucked off and the residue was counted on a Tracor Analytic 1190. A typical standard curve is shown in figure 2.1.

ATP determination

Rat ß-cells were cultured overnight in a rotating universal container (to prevent clumping or attachment to the walls). The cells were centrifuged for 5 min at 1000 rev (300 g) in an MSE Centaur 2 bench centrifuge, the supernatant was removed, the cells washed in HEPES-Krebs and respun. After the wash the cells were resuspended in 0.9 ml HEPES-Krebs. 0.4 ml cell suspension was added to 0.4 ml HEPES-Krebs (0 mM glucose) in an LP3 tube and a similar volume to 0.4 ml HEPES-Krebs (20 mM glucose).

The ATP content of the cells was assayed 5 min and 60 min after addition of glucose. Triplicate 50 µl samples (each containing 15 x 10^3 cells) were taken from each incubation tube

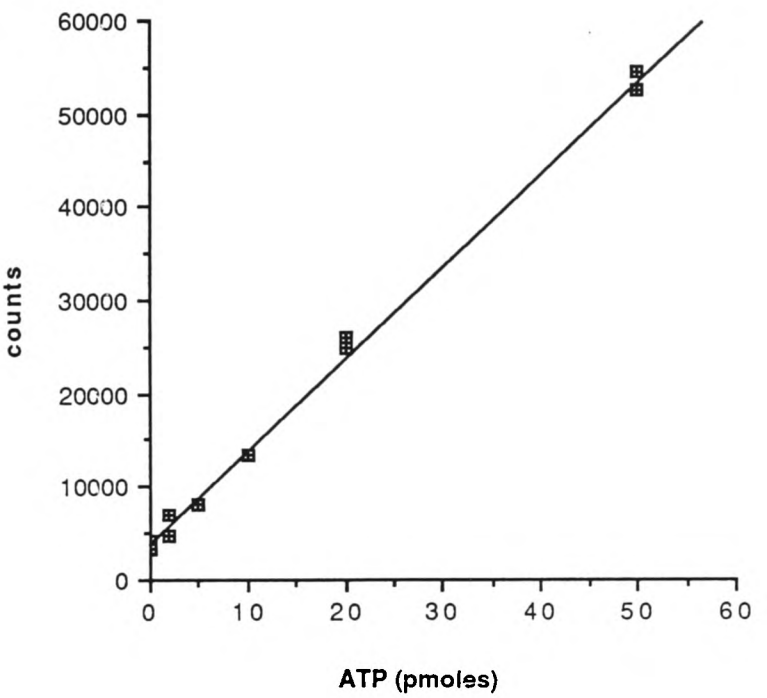


Figure 2.2. Standard curve for ATP determination.

at each time point and each was added to 25 µl 10% PCA in an Eppendorf tube. The samples were then sonicated for 5-10 s to ensure cellular disruption. Duplicate 30 µl samples were taken from the Eppendorfs and added to 3 ml Ars/Phos buffer in scintillation vials.

ATP standards (Bohringer) were made up at 0, 2, 5, 10, 20, 50 pmoles, with PCA added to the same concentration as in the samples. (ATP solution was made up at 1 µM, i.e. 1 pmol per µl, and the required no. of µl was added to 3 ml Ars/Phos buffer in scintillation vials. PCA was added last.)

Luciferin (firefly extract, Sigma) was made up to 5 ml, (i.e. 5 ml water was added to a vial of luciferin). 1 ml was removed and spun to remove the sediment. 25 µl luciferin solution was added to each vial (standard or sample) before counting the sample for 6 s on a Philips 4540 liquid scintillation analyser. To standardise the timing of luciferin addition, the 25 µl were added to one sample as the counter started to print the count for the corresponding vial in the previous row (this allowed about 2 min between luciferin addition and counting of the sample). Care was taken to exclude light from the counting room.

The counts were converted to ATP content using a dedicated linear regression programme on an Apple II microcomputer. The standard curve generated in this experiment is shown in figure 2.2.

BIOCHEMICAL ANALYSIS: SOLUTIONS

All insulin secretion and ATP content experiments were performed in HK/Ca containing 2 or 10 mg/ml BSA. All chemicals were from Sigma unless otherwise indicated.

An arsonate/phosphate buffer was used for ATP determination. This was obtained by mixing arsonate buffer, phosphate buffer and water 1:1:1.

Arsonate buffer.	Na arsonate	15.6 g/ 500 ml
	$MgSO_4$	4.93 g/ 500 ml
Phosphate buffer.	KH_2PO_4	0.68 g/ 500 ml
	$MgSO_4$	0.49 g/ 500 ml

For insulin assay.

PAM buffer.	NaH_2PO_4	1.22 g/l
	Na_2HPO_4	4.57 g/l
	Thiomersal	0.25 g/l
	BSA (RIA grade)	1 g/l

PAM for charcoal. as PAM, substituting BSA (not RIA grade) 4 g/l

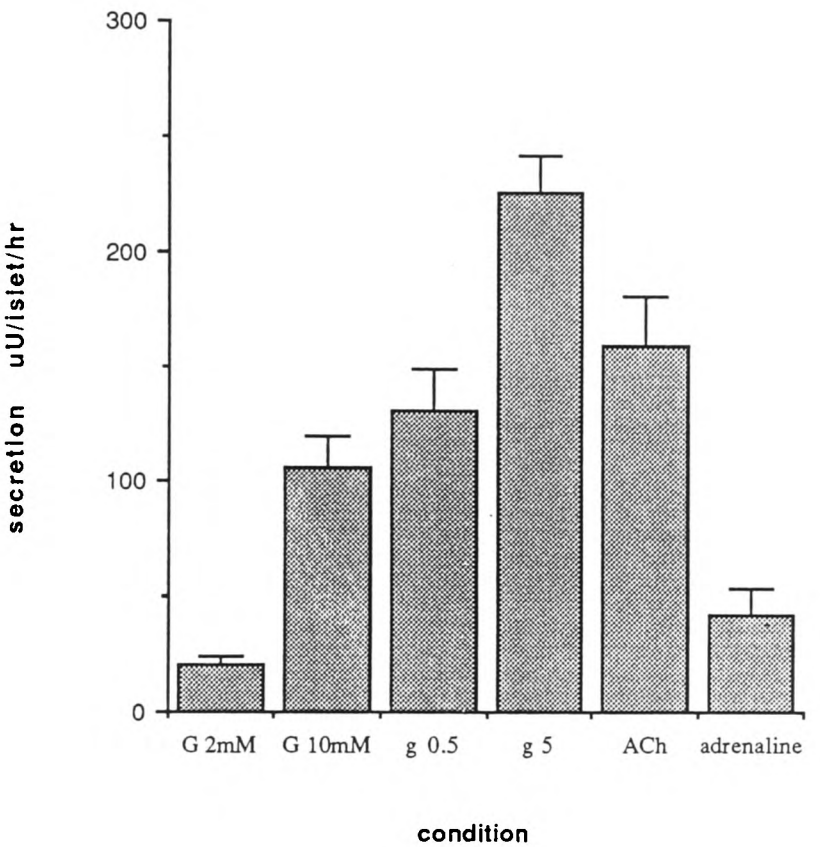


Figure 2.3. Secretory responses of rat pancreatic islets.
Apart from the column labelled "G 2 mM", which represents islet insulin secretion in a 2 mM glucose solution, all the columns represent the secretory response to the indicated hormone or neurotransmitter in the presence of 10 mM glucose. "g 0.5" represents insulin secretion in a solution containing 0.5 μg/ml glucagon, "g5", 5 μg/ml glucagon. The ACh concentration was 5 μM, and that of adrenaline, 2.5 μM.

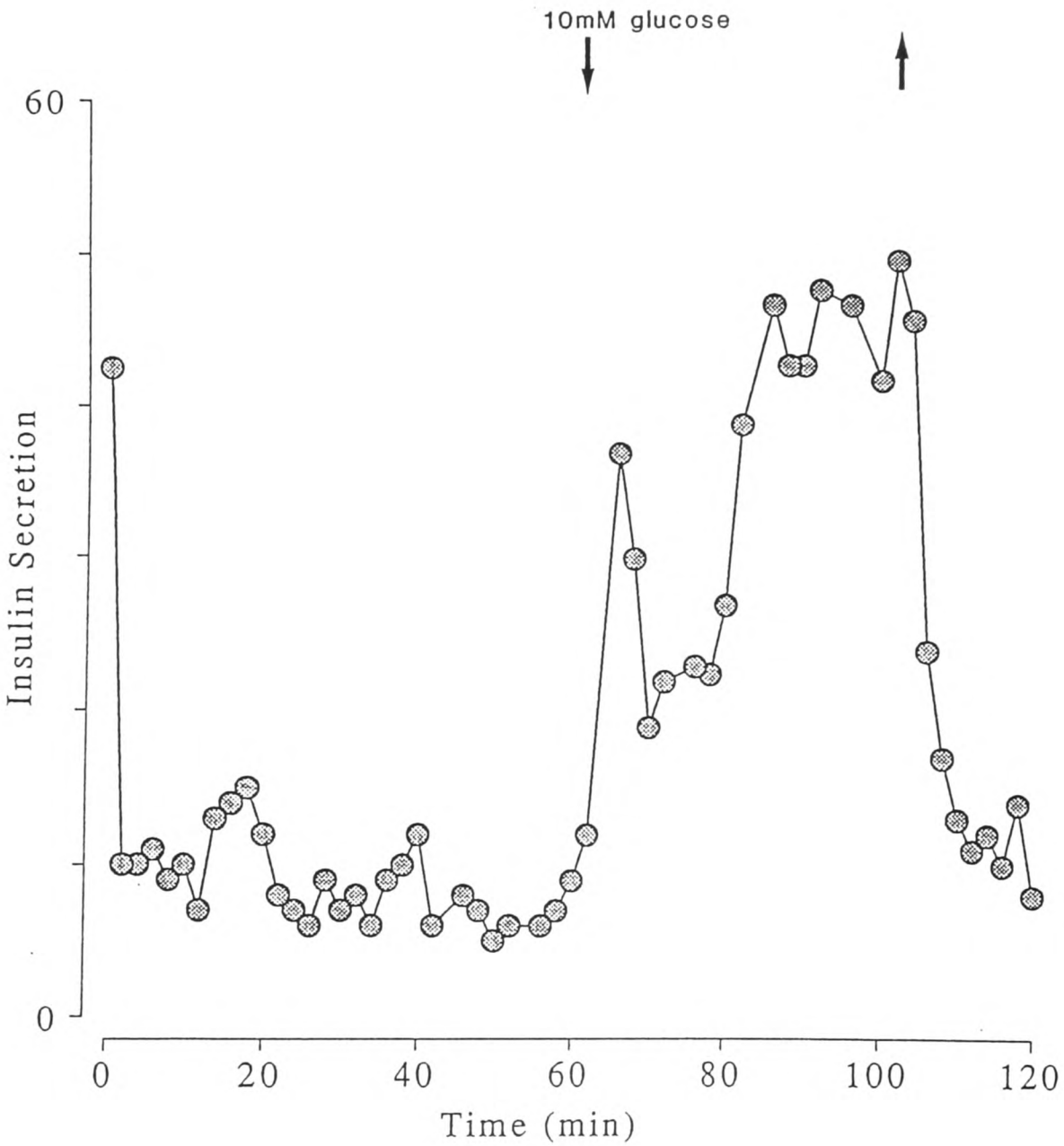


Figure 2.4. The secretory response to glucose of dispersed islet cells.
The baseline represents the rate of secretion in 2 mM glucose. The glucose concentration was raised to 10 mM after 60 min and the cells were returned to control solution at 110 min. The units of secretion are $\mu U/10^6$ cells/hr.

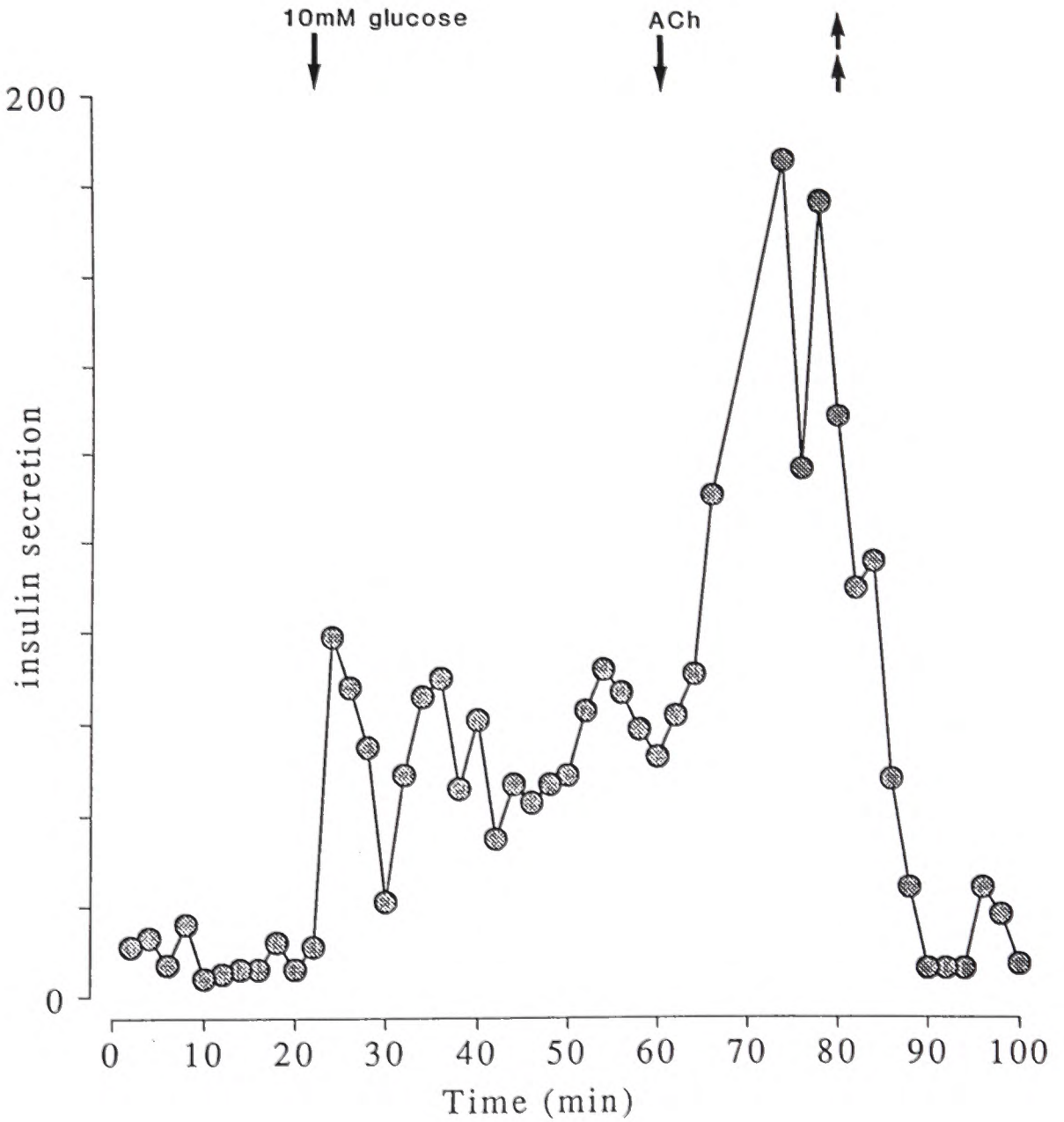


Figure 2.5. Secretory response of dispersed cells to ACh.
The solution was changed to one containing 5 μM ACh at 60 min and was returned to the control at 80 min. Secretion in $\mu U/10^6$ cells/hr.

BIOCHEMICAL ANALYSIS: RESULTS

Insulin secretion: islets

Batches of five islets were tested for the ability to respond to glucose, glucagon, ACh and adrenaline. The results are shown in Table 2.3 and figure 2.3.

Table 2.3.

Glucose (mM)	Addition	Insulin secretion (μU/islet/hr)	n	x
2		20.42 ± 3.4	18	4
10		105.16 ± 13.2	21	5
10	glucagon 0.5 μg/ml	130.32 ± 17.64	4	1
10	glucagon 5 μg/ml	225.8 ± 22.5	26	4
10	ACh 5 μM	159.02 ± 21.94	4	1
10	adrenaline 2.5 μM	42.39 ± 11.24	5	1

The values of n given in the table are the total no. of replicates of each experimental condition. The x values indicate the no. of separate experiments.

Insulin secretion: isolated cells.

Isolated cells were tested for their ability to secrete and to respond to glucose and glucagon in both superfusion and static ("batch") experiments: the results are given in figures 2.4 and 2.5.

The secretion results show that the islets and cells retain the ability to secrete and to respond to glucose, glucagon, ACh and adrenaline: their responses are in accordance with those previously reported by several groups (e.g. Malaisse et al., 1967; Howell & Montague, 1983).

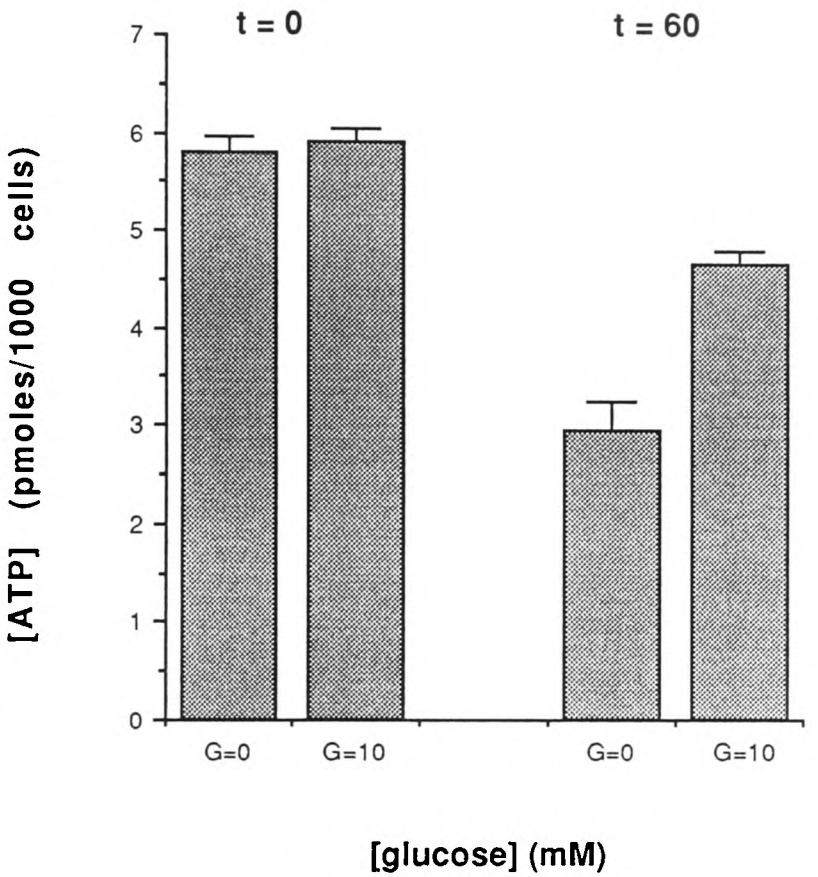


Figure 2.6. ATP content of rat ß-cells.
Cells incubated in 0 or 10 mM glucose for 1 hr.

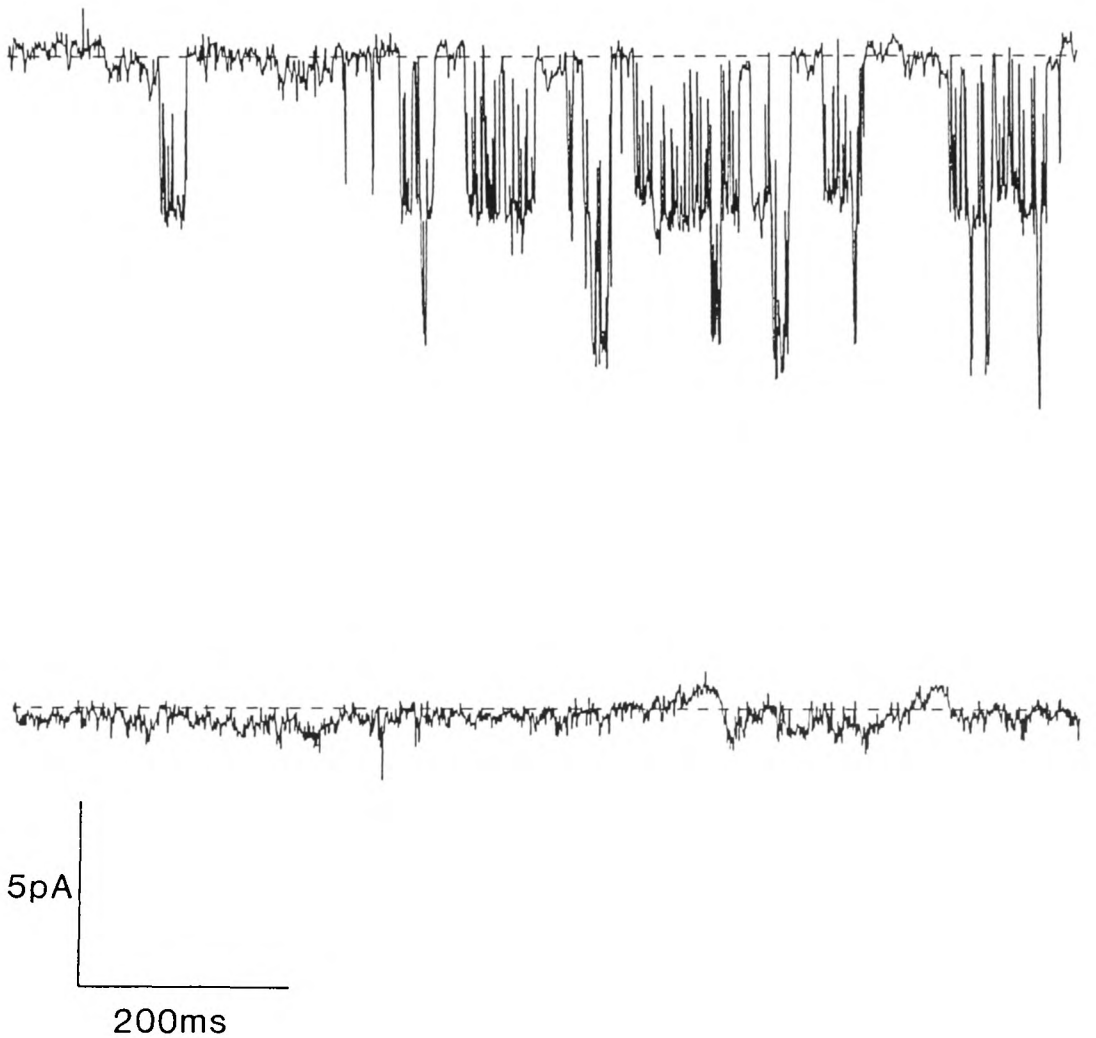


Figure 2.7. The effect of glucose on ß-cell membrane currents.
Cell-attached patch clamp recordings from a rat ß-cell incubated in 0 mM glucose, (upper panel), and about 3 min after the addition of 10 mM glucose. The upper record shows openings of the ATP-sensitive K^+ channel, which are abolished by addition of glucose. The biphasic current variations in the lower record indicate cellular action potentials.

ATP content.

In view of the possible role of ATP as a second messenger for glucose (Cook & Hales, 1984; Rorsman & Trübe, 1985), and as a general indicator of cell viability, the ATP content of isolated cells was measured. A luciferin/luciferase assay was used, and the results are presented in figure 2.6. The ATP content of the isolated cell preparation was glucose-dependent, and the absolute values obtained (4.66 pmol/10^3 cells in 10 mM glucose, 2.95 pmol/10^3 cells in 0 mM glucose) were similar to those previously reported (Hellman et al., 1969; Malaisse et al., 1979; Ashcroft et al., 1973, 1986).

A final demonstration of the identity and viability of the cells was their consistent ability to respond to glucose by inhibition of the ATP-sensitive channel and by production of action potentials in the cell-attached patch clamp configuration. ATP-sensitive channel activity in the absence of glucose and action currents in a 20 mM glucose solution are shown in figure 2.7.

PATCH CLAMPING

General set-up

All the electrophysiological experiments were carried out in a recording chamber on the stage of an inverting microscope (Nikkon Diaphot) mounted on a vibration isolation table (Newport Research Corporation) inside a Faraday cage (built by the mechanical workshop). In general, solution reservoirs were 50 ml syringes attached to the outside of the cage and connected to the bath inlet by narrow polystyrene tubes. Flow was regulated by turning a 3-way valve attached to the syringe nozzle or by means of a crocodile clip pinching a more flexible insert in the tubing.

Various bath designs were used. For the ATP and ADP dose-response experiments in chapter 4, a perspex bath was constructed with a glass floor and five glass inlet tubes: in some of these experiments all five solutions were simultaneously flowing into the bath and the solution in contact with the patch was changed by moving the patch from the mouth of one tube to the mouth of another. For the whole-cell experiments and the single-channel experiments in chapter 5, a simple perspex bath was used, ~3 mm deep and with a glass floor (formed from a cover-slip, cut to size and glued in place with epoxy resin). These two baths had volumes of ~1 ml and the solution could be exchanged in less than 1 min. 4 ml of solution was perfused before recording currents in each new solution. Except for some experiments in chapter 4, the perfusion was stopped during recording.

For most patch-clamp experiments, small pieces of cover-slip, about 5 mm x 5 mm, were preincubated in glucose-free 5 mM K^+ external solution at room temperature or at 4 °C, until use. These small sections of coverslip could conveniently be transferred to the recording chamber.

Pipettes

Patch pipettes were pulled on a modified (solenoid disabled) Kopf (David Kopf Instruments, Tujunga, CA, USA) puller, using a three-stage pull, from 1.5 mm borosilicate

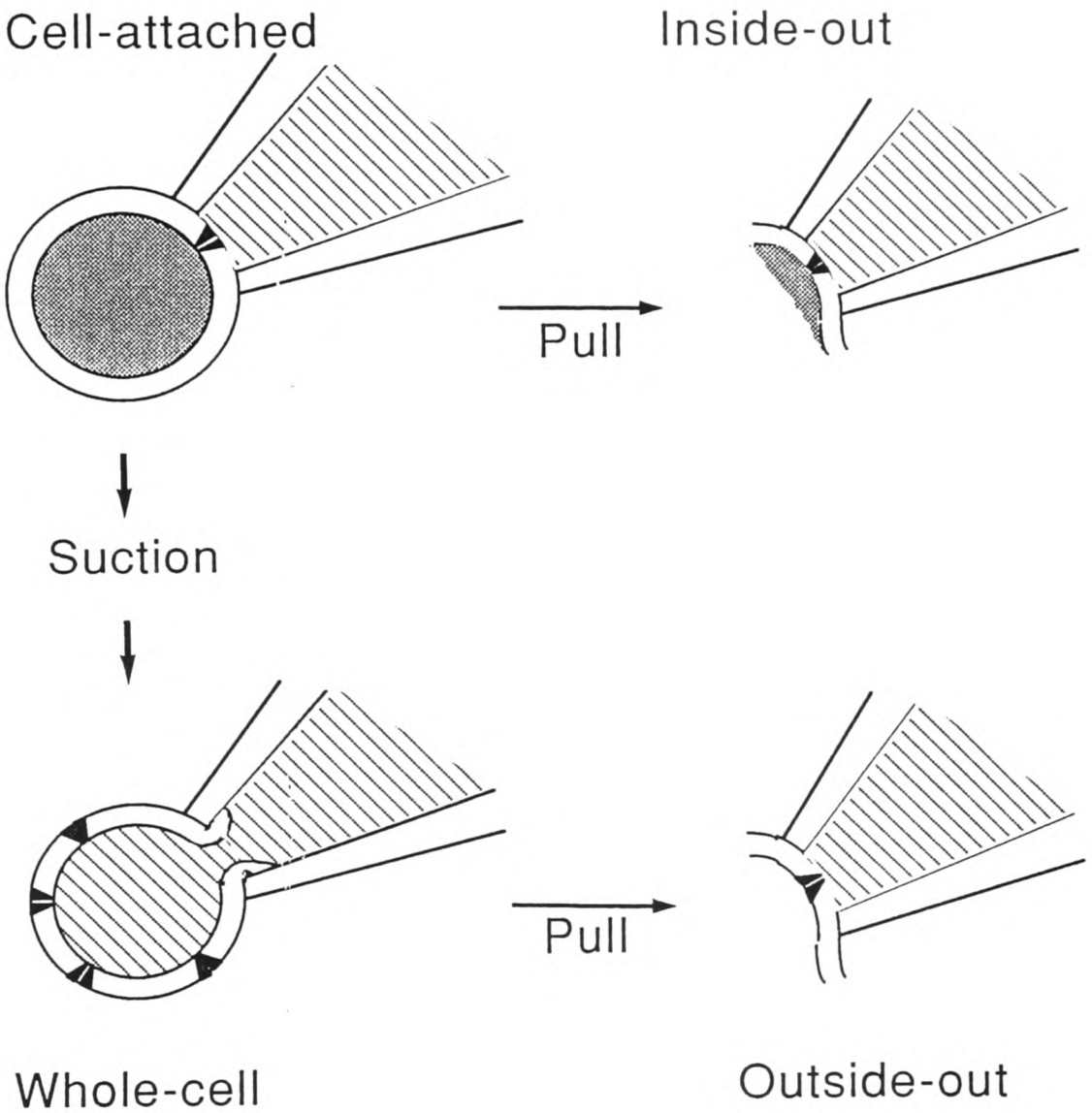


Figure 2.8. Patch-clamp configurations.
The cell-attached configuration (upper left) is the first step in any patch-clamp experiment. Inside-out patches can then be formed directly by withdrawing the pipette from the cell. The whole-cell configuration is achieved by applying a pulse of negative pressure. Outside-out patches are obtained by pulling the electrode away from the whole-cell configuration.

glass haematocrit capillaries (Boralex, Rochester Scientific, Rochester, NY), coated witl Sylgard close to their tips (within 100 μm) to reduce their electrical capacitance and fire polished immediately before use. The sylgarding jig and the fire-polisher were home-made The pipettes had resistances between 3 and 10 Mohm when filled with 140 mM KCl.

Electrophysiological recording

Currents were recorded using a List EPC-5 (chapters 3 and 5) or a List EPC-7 patch clam amplifier (List Electronic, Darmstadt, FRG). The current signals were stored on FM-tap (Store 4DS at a tape speed of 15ips, -1db down at 8kHz; Racal recorders, Hythe, UK) fo later analysis or digitised using a modified digital audio processor (Sony PCM 7O1ES) an stored on videotape; the frequency response of the recording system was 10 kHz for bot whole-cell and single-channel experiments.

The patch-clamp techniques used to study whole-cell and single-channel currents wer similar to those described by Hamill et al., (1981). The cell-attached, whole-cell, inside-ou and outside-out configurations of this technique were all used.

The cell-attached patch clamp configuration (figure 2.8) is formed by gently placing the ti of the recording pipette on the cell membrane and applying gentle suction. A tight seal i formed between the glass and the cell membrane (Corey & Stevens, 1983). The seal has high shunt resistance (usually > 10 Mohm), allowing low-noise recording of single-channe currents. The seal is also mechanically strong, allowing the membrane patch to be ripped fror the rest of the cell, so forming an inside-out patch. If a strong suction pulse is applied to th pipette in the cell-attached mode, the membrane patch ruptures, forming a communicatio between the cell cytoplasm and the interior of the pipette. This is the whole-cell recordin configuration. Outside-out patches are formed by withdrawing the pipette from the cell onc the whole-cell mode has been achieved.

Cell-attached recording

Cell-attached recording has the advantage of an intact cell with a functional metabolism and undisturbed cytosolic contents. This allows study of the effects of those channel modulators (e.g. glucose) which require metabolism, and avoids the phenomenon of rundown, i.e. the decrease of channel activity with time, which is frequently seen in whole-cell or excised patch recordings. This rundown is probably related to diffusion of some intracellular constituent (e.g. nucleotide or enzyme) away from the channel. On the other hand, the cell-attached configuration does not allow change of the solution on either side of the patch under study, and it is not a true voltage-clamp, as the potential across the membrane (V_m) depends on both the pipette holding potential (V_p) and the resting membrane potential of the cell (V_r): $V_m = V_p - V_r$. If the membrane potential of the cell changes for any reason, the patch potential will change independently of any change in the pipette potential. This effect is most obvious in studies on the glucose-sensitive channel, with pipettes containing 140 mM K^+, with a 10 mM glucose solution, where few channels are open and the cell has a very high input resistance; opening of a single channel in the patch can allow sufficient K^+ into the cell to depolarise it (change V_m) and cause a reduction in the single-channel amplitude (Ashcroft et al., 1984). Similarly, addition of glucose to a ß-cell sometimes causes the cell to depolarise sufficiently (by decreasing the hyperpolarising outward current) to reduce the channel amplitude (and elicit action potentials). To achieve a more stable voltage-clamp, the studies on the single Ca^{2+} channels in chapter 6 were carried out in a 140 mM K^+ external solution, which holds the membrane potential steady close to 0 mV (as demonstrated by the reversal of single K^+-channel currents close to 0 mV with 140 mM K^+ in bath and pipette or by superposition of current-voltage curves before and after patch excision).

Excised patch recording

Excised patches, inside-out or outside-out, allow good voltage control and the possibility of changing the solution on the side of the patch facing the bath . This is particularly useful in inside-out patches for testing the effects of second messangers which modulate channel activity

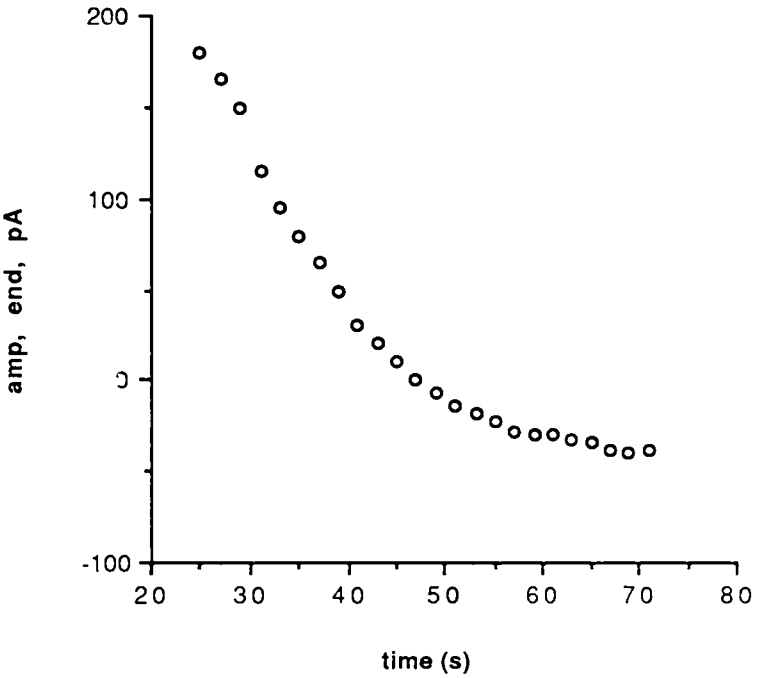


Figure 2.9. Time-course of cellular dialysis.
The current amplitude at the end of a 200 ms depolarising voltage step is plotted against time (in seconds after going whole-cell. The first 20 s were spent compensating the cell membrane capacitance). The pipette contained 145 mM N-methyl D-glucamine to block outward K^+ currents.

(e.g. ATP and ADP in chapter 5). The problems with excised patches are channel rundown and a tendency for the patches to form vesicles on excision. Vesicles could usually be detected by the high resistance of the "patch", the aberrent channel properties (e.g. decreased or variable channel amplitudes, or a declining channel amplitude during an opening being evidence for a "patch" with a high input resistance) or the unresponsiveness of the channel to ATP (chapters 3-6). These vesicles could usually be ruptured by briefly taking the tip of the electrode through the solution-air interface. For inside-out patches, the standard protocol was to form a gigaseal (usually > 10 Gohm) on a cell exposed to 5mM-K^+ external solution and then to exchange this for the control internal solution (130mM-K^+) before excising the patch; outside-out patches were formed with internal solution in the pipette.

Single channel currents were recorded at different potentials (in the cell-attached, inside-out and outside-out configurations) by changing the holding potential applied to the pipette.

Whole-cell recording

In the whole-cell configuration, currents through the ensemble of open channels in the cell membrane are recorded rather than currents through single channels. When used on small cells such as the ß-cell, voltage-clamp experiments can be performed with current measurement and voltage control achieved with a single electrode. Rundown can be a problem (see figures 5.1 and 6.7), particularly for Ca^{2+} currents, since the cell interior is dialysed with the pipette solution.

On going whole-cell with 145 mM NMG^+ in the pipette, depolarising voltage steps initially elicited both inward and delayed outward currents. Within two or three minutes, the outward current was abolished and only an inward current remained: this was taken as an indication of the exchange of K^+ and NMG^+. An example of the time course of this exchange is shown in figure 2.9. No experiments were performed on inward currents until internal dialysis was complete.

One common problem with the whole-cell voltage clamp is that of series resistance. No series resistance compensation was used for the experiments in this thesis. The cell membrane

potential will differ from the nominal patch-clamp potential by an amount $V_{sr} = I.R_m$, where I is the current flowing and R_m is the cell membrane resistance. For inward currents in the ß-cell, I_{max} is < 100 pA and R_m in the order of 20 Mohm, giving an maximum estimated error of 2 mV. The error will be somewhat larger (maybe 10 mV) for the largest outward currents (~500 pA).

The holding potential in all whole-cell experiments was -70 mV, unless otherwise stated.

Junction potentials

The reference potential for all measurements was the zero current potential of the pipette before establishment of the seal, and no corrections have been made for liquid junction potentials (< 5 mV), except in chapter 3, where corrections have been made for junction potentials as detailed in the methods section of that chapter.

All electrophysiological experiments were done at room temperature (18-23 °C).

DATA ANALYSIS

Single-channel Data Analysis

In chapters 3 and 7, single channel current amplitudes were measured directly from a digital oscilloscope. For analysis of single channel recordings in chapter 5, for most of the single-channel records shown in this thesis and for construction of mean current- voltage relations, the recorded currents were amplified (x 10 or 25) and low pass filtered at less than half the sample frequency using an 8-pole Bessel filter (Frequency Devices, Haverhill, Mass). They were subsequently digitised using a 12-bit ADC (INDEC, California, USA) controlled by a PDP 11/73 computer (Digital Equipment Corporation). Filter cut-off frequencies given in the text refer to -3 dB values.

The construction of mean current-voltage relations (chapter 3), dose-response curves (chapter 4), amplitude histograms (chapter 5) and open- and closed-time histograms (chapters 5 and 6) is described in the relevant chapters.

Whole-cell data analysis:

In most cases, the current amplitudes were measured directly from a digital oscilloscope. For most illustrations in this thesis, the recorded currents were amplified (x 5 or 10), low-pass filtered (-3dB down at 1 kHz) and digitised at 2 kHz, in the same manner as the single-channel data. For some figures the records were replayed onto a Gould 2200 (Gould, Cleveland, USA) chart recorder which has a frequency response of 150 Hz. Leak correction for the current-voltage relations was by linear extrapolation of currents elicited by 30 mV hyperpolarising steps from the holding potential. No voltage-dependent currents were active in this potential range. For the activation and inactivation curves of voltage-dependent currents, the current amplitudes were fitted by a non-linear least squares regression method to an equation derived from the Boltzman relation:

$$I/I_{max} = 1/\{1+\exp[(V_{0.5} - V)/k]\}$$

where $V_{0.5}$ is the potential at 50% inactivation and k is the slope factor. Determination of the

current amplitudes is described in detail in chapters 6 and 7.

Data are expressed as the mean ± S.E.M. for n observations.

In this thesis, all currents and potentials are displayed using the usual sign convention, that is, potentials are expressed relative to the external membrane surface and currents flowing inwards across the membrane (from the outside to the inside of the cell) are displayed as downward deflections of the current trace and denoted negative currents.

SOLUTIONS USED IN PATCH CLAMPING:

The composition of the most frequently used bath and pipette solutions is given in Table 2.4 below. Details of other solutions used are given in the relevant chapters. Nucleotides were obtained from Bohringer, all other chemicals from Sigma, unless otherwise stated.

Table 2.4

Patch-clamp solutions.

Solution	KCl	NaCl	$CaCl_2$	HEPES	EGTA	$MgSO_4$	NMG	HCl
External								
5 mM-K^+	5	135	5	5	-	2	-	-
140 mM-K^+	140	-	5	5	-	2	-	-
Internal								
130 mM-K^+	107	-	1	11	11	2	-	-
145 mM-NMG^+		-	2	10	5	4*	145	120

* $MgCl_2$

The external solutions were titrated to pH 7.4 with NaOH, and the internal to pH 7.2 with KOH. Magnesium and sodium ions were omitted from most of the intracellular solutions used in chapter 3, as these ions have been reported to produce a voltage-dependent block of outward currents through ATP-sensitive K-channels (Cook & Hales, 1984; Horie et al., 1987; Findlay, 1987). 3 mM Na_2ATP was added to the internal solutions when measuring voltage-activated currents, as it blocks the ATP-sensitive current (Cook & Hales, 1984; chapter 5) and helps prevent rundown of the inward calcium current (Cavalie et al., 1986; Belles et al., 1988).

The 11 mM EGTA and 1 mM $CaCl_2$ used in the standard internal solution resulted in ~0.06 μM free Ca^{2+}. Tolbutamide (chapters 5 & 7) was dissolved in di-methyl-sulphoxide (DMSO) and solutions containing tolbutamide were made fresh each day. DMSO at the concentrations used here were without effect on ATP-sensitive K^+-channels.

All the solutions used in the patch-clamp experiments were passed through a 0.22 μm filter before use.

Rb^+ and Na^+ permeability of the ATP-sensitive channel.

INTRODUCTION

It was proposed in chapter one that the initial glucose-induced depolarisation of the ß-cell membrane could be attributed to closure of ATP-sensitive K^+ channels. Evidence that this initial depolarisation is due to a decrease in the K^+ permeability of the ß-cell membrane originally came from ion efflux studies. Sehlin and Taljedal (1975) found that islets incubated in the presence of 20mM glucose retained more $^{86}Rb^+$ (used as a substitute for K^+) than islets in incubation media containing 3mM glucose. Subsequently, the idea has been confirmed by measurements of $^{42}K^+$ efflux from perifused rat islets which showed that 9mM glucose markedly decreased the rate of K^+ efflux (Henquin, 1978). The short half-life of $^{42}K^+$ (12.4hrs) requires correction for decay of the isotope during the experiment and therefore, in general, the more stable $^{86}Rb^+$ (half-life, 19.5 days) has been used as a tracer (Malaisse et al., 1978; Boshero & Malaisse, 1979; Dawson et al., 1983). A ratio of the efflux rate constants k_{Rb}/k_K of 0.62 in the absence of glucose was reported from separate experiments in rat islets (Boschero et al. 1977; Malaisse et al., 1978; Boshero & Malaisse, 1979). However, as the values of efflux rate constants vary considerably between batches of islets made at different times (Dawson et al., 1986) it is important to compare efflux rate constants for ^{42}K and ^{86}Rb in simultaneous flux experiments. Two studies have compared Rb^+ and K^+ fluxes in double-labelled experiments (Henquin, 1980; Dawson et al., 1986); these found permeability ratios (from the ratios of the efflux rate constants, k_{Rb}/k_K), of 0.87 and 0.8 respectively. These authors concluded that $^{86}Rb^+$ is an acceptable tracer for qualitative changes in K^+ efflux from ß-cells although the magnitude of the resting K^+ permeability is underestimated, by a factor equal to the ratio of the efflux rate constants. Dawson et al. (1986) also pointed out that the permeability ratio could represent contributions from several channel types, and suggested that this was indeed the case, because the ratio of efflux rate constants varied as the external ion

concentration was varied.

The results of the $^{86}Rb^+$ efflux experiments would imply that, if the reduction in the membrane K^+ permeability is due to a decrease in the open probability of the glucose- and ATP-sensitive K^+ channel identified in patch clamp experiments, this channel must be permeable also to Rb^+. K^+ and Rb^+ are of similar size and have similar physical and chemical properties but whereas some K^+ channels do not disciminate between these two ions (Gay & Stanfield, 1978; Gallacher et al., 1984), other K^+ channels have a considerably lower conductance in Rb^+ (Standen & Stanfield, 1980; Gallacher et al., 1984). The Rb^+ permeability of the glucose-sensitive K^+ channel was examined therefore, to confirm that its closure could account for the reported decrease in $^{86}Rb^+$ efflux by glucose stimulation and so to provide evidence further supporting its role in ß-cell stimulus-secretion coupling.

Study of the channel's permeability to rubidium also allows investigation of the intrinsic properties of the channel, in particular the mechanism of ionic permeation through the channel.

METHODS

Junction potentials

If the solution in the pipette or the agar bridge of the reference electrode differ in ionic composition from the bath solution, junction potentials may develop at the solution interfaces as a results of the differences in ionic mobilities. This can lead to errors in the measurement of the membrane potential: first, any junction potential present between the bath and pipette solution no longer exists after seal formation; secondly, changes in the bath solution can produce changes in the junction potential at the reference electrode. Junction potentials were measured by comparing the zero current pipette potential recorded in each of our experimental solutions against a reference of 140mM-K external solution (Table 3.1). In these measurements the pipette was filled with 140mM-K external solution and the test solution was connected to the reference electrode by a 3M-KCl agar bridge. Measured values were close to those calculated from Henderson's eqn. (Henderson, 1908, quoted in Schultz, 1980). The potentials in the text of this chapter were corrected for the presence of junction potentials at pipette and reference electrodes using the measured values given in Table 3.1.

Table 3.1: liquid junction potentials.

Solution	Junction potential (mV)
External	
140 mM-K^+	0
5mM-K^+	-2.6 $\pm$ 0.4 (6)
70 mM-Rb^+	0.46 $\pm$ 0.29 (3)
140 mM-Rb^+	0.27 $\pm$ 0.2 (3)
Internal	
130 mM-K^+	1.4 $\pm$ 0.06 (7)
70 mM-Rb^+	0.47 $\pm$ 0.29 (3)
107 mM-Rb^+	1.46 $\pm$ 0.18 (3)
140 mM-Rb^+	1.4 $\pm$ 0.75 (3)
70 mM Na^+	0.18 $\pm$ 0.3 (3)

All junction potentials were measured with respect to external 140 mM-K^+ solution, at room temperature. Values in parentheses indicate the number of samples.

Solutions

Table 3.2 details the solutions used in the experiments described in this chapter and not used elsewhere. For solutions also used in other experiments, see chapter 2, "Methods".

Patch-clamp solutions.

Solution	KCl	RbCl	NaCl	$CaCl_2$	HEPES	EGTA	$MgSO_4$
External							
70 mM-Rb^+	70	70	-	2	5	-	-
Internal							
140 mM-Rb^+		107	-	1	11 (Rb)	11 (Rb)	-
107 mM-Rb^+		107	-	1	11 (K)	11 (K)	-
70 mM-Rb^+	37	70	-	1	11 (K)	11 (K)	-
70 mM-Na^+	37	-	70	1	11 (K)	11 (K)	-

Solution exchange

In some of the experiments in this chapter, a rapid perfusion system was used, the excised patch being inserted through a small (300 μm) hole into a short (1 cm) stretch of glass haematocrit capillary which served as a bath of small volume. Details of this system are published in Kakei & Ashcroft, (1987).

Protocols

The variance-voltage relation (figure 3) was measured by slowly ramping the membrane potential by hand, recording on FM tape and subsequently digitising the voltage and the AC-coupled current record simultaneously after amplification and filtering at 2 kHz (Butterworth filter; Kemo, Beckenham). Current data were sampled at 5 kHz and the variance calculated for blocks of 512 data points (bandwidth 10 Hz-5 kHz). The mean variance for several blocks of data was calculated in steps of 1 mV. In solutions containing internal Rb^+, the variance of the background noise in the presence of 5 mM ATP was subtracted from that recorded in the absence of ATP to obtain the variance of the ATP-sensitive current.

The mean current-voltage relation in figure 4 was constructed from multi-channel patches by slowly ramping the voltage (by hand) from -40 mV to +60 mV. Voltage and current data

were subsequently digitised simultaneously at 2.5 kHz (filter 1 kHz). The leak conductance was measured either from sweeps in which the baseline current was visible or estimated from the current-voltage relation in the presence of 5 mM ATP, and was then subtracted from the data.

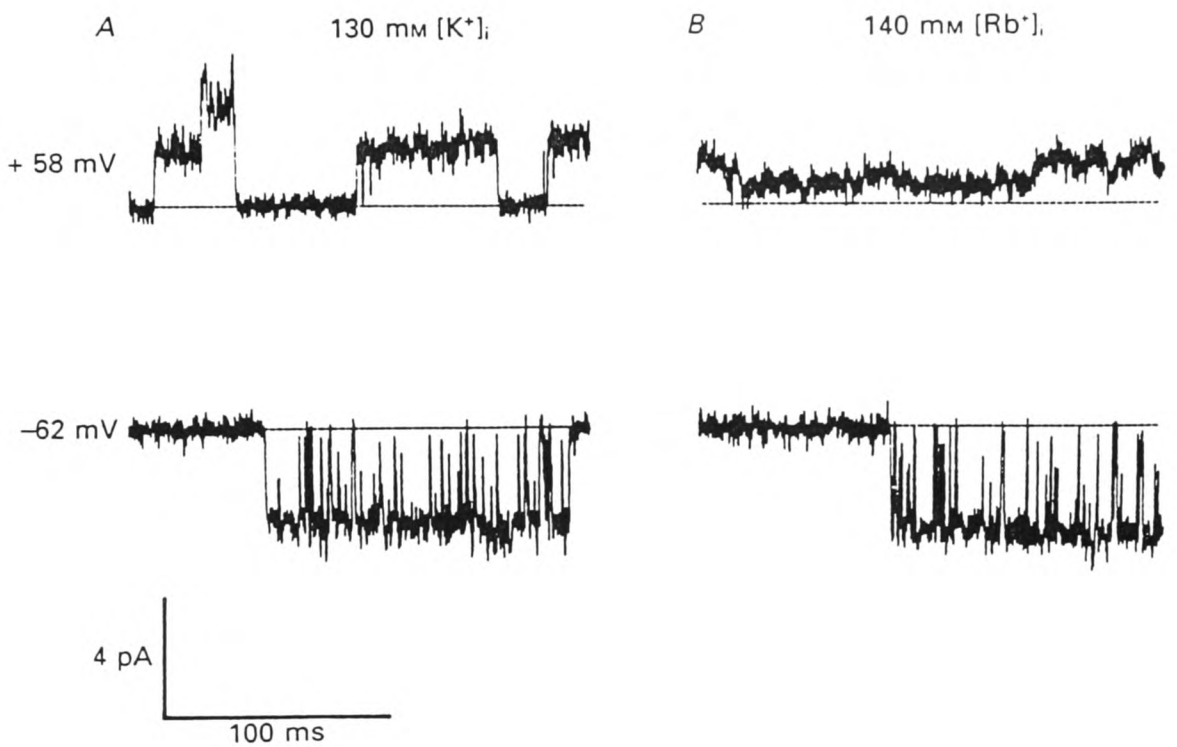


Fig.3.1. Single channel currents recorded from an inside-out patch at +58 mV (upper traces) and at -62 mV (lower traces) with an intracellular (bath) solution of 140 mM-K (left) or 140 mM-Rb (right). External (pipette) solution, 140 mM-K. Records come from the same patch. Sample rate 5kHz; filter, 2kHz. Room temperature.

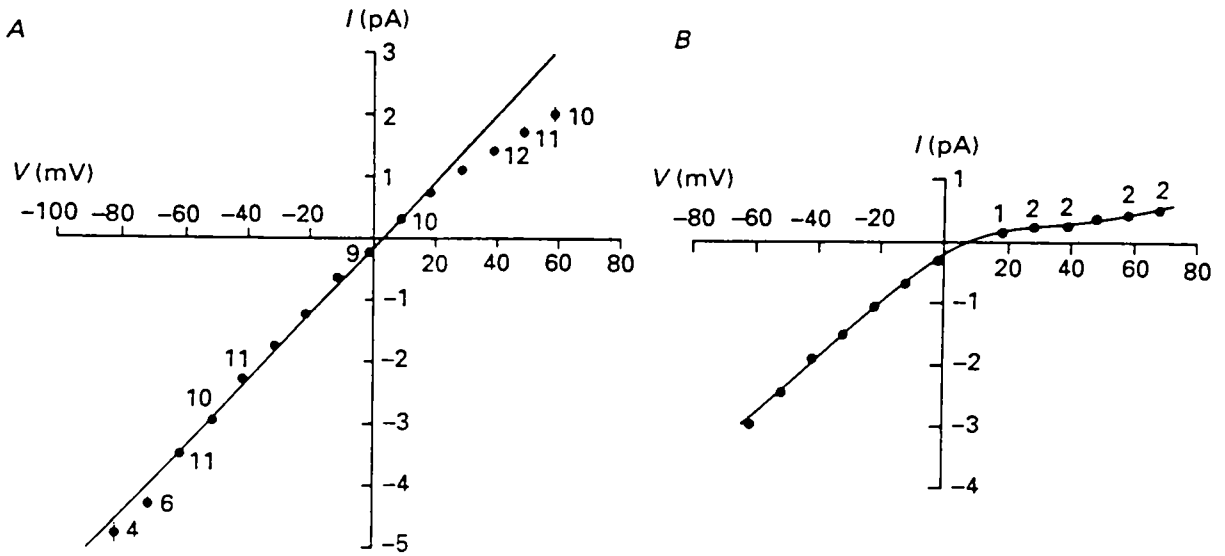


Figure 3.2A. Mean relation between the amplitude of the single channel current (I) and membrane potential (V) for 4-13 inside-out patches exposed to an internal (bath) solution containing 130 mM-K and to a 140 mM-K external (pipette) solution. In this and all subsequent figures in this chapter, the number of samples is indicated adjacent to the data point and the vertical bars indicate ± 1 S.E.M. where this is larger than the symbols. The line is drawn to eqn. 3.1 taking $P_K = 1.05 \times 10^{-13}$ cm^3/sec, $[K]_o = 140$ mM and $[K]_i$ as 130 mM. B. Mean current-voltage relation for 1-3 inside-out patches with 140 mM-K external solution and 140 mM-Rb intracellular solution. The line is drawn through the points by eye.

RESULTS

The first part of this section describes results obtained using inside-out membrane patches: the results of experiments using outside-out patches are considered subsequently.

Inside-out patches

First, the ability of Rb^+ to carry outward currents through the ATP-sensitive K^+ channel was investigated. In this series of experiments the inside-out patch recording configuration was used and in general the pipette was filled with a 140 mM-K^+ external solution. In some experiments the pipette contained a 5 mM-K^+ solution.

Figure 3.1A shows single channel currents and figure 3.2A the corresponding mean current-voltage relations recorded from inside-out patches exposed to 140 mM-K^+ externally and 130 mM-K^+ internally. Under these conditions, single K^+ channel currents reversed at a membrane potential of +2 mV, as expected for a K^+-selective channel. The continuous line in figure 3.2A is drawn to the general form of the Goldman-Hodgkin-Katz equation (Hodgkin & Katz, 1949):

$$I_X = P_X \frac{VF^2}{RT} \frac{[X]_i \exp(VF/RT) - [X]_o}{\exp(VF/RT) - 1} \qquad \text{eqn. 3.1}$$

where X is potassium and R, T and F have their usual meanings, $[K^+]_o$ is 140 mM, $[K^+]_i$ is taken as 130 mM, and P_K, the K^+ permeability coefficient is 1.05×10^{-13} cm^3/s. This value is very similar to that found for the ATP-sensitive K^+ channel in cell-attached patches on ß -cells (0.98×10^{-13} cm^3/s; Ashcroft et al., 1988a) and to that reported for ventricular myocytes (1.4×10^{-13} cm^3/sec at 150 mM-K^+: Kakei et al., 1985). It is evident from figure 3.2A that the outward K^+ currents are smaller than predicted by eqn. 3.1, indicating that the channel shows some inward rectification. This rectification cannot be attributed to a voltage-dependent block by intracellular ions (such as Na^+ or Mg^{2+}) as the only free cation in the internal solution was potassium. The single-channel slope conductance, obtained from a least-squares fit of a

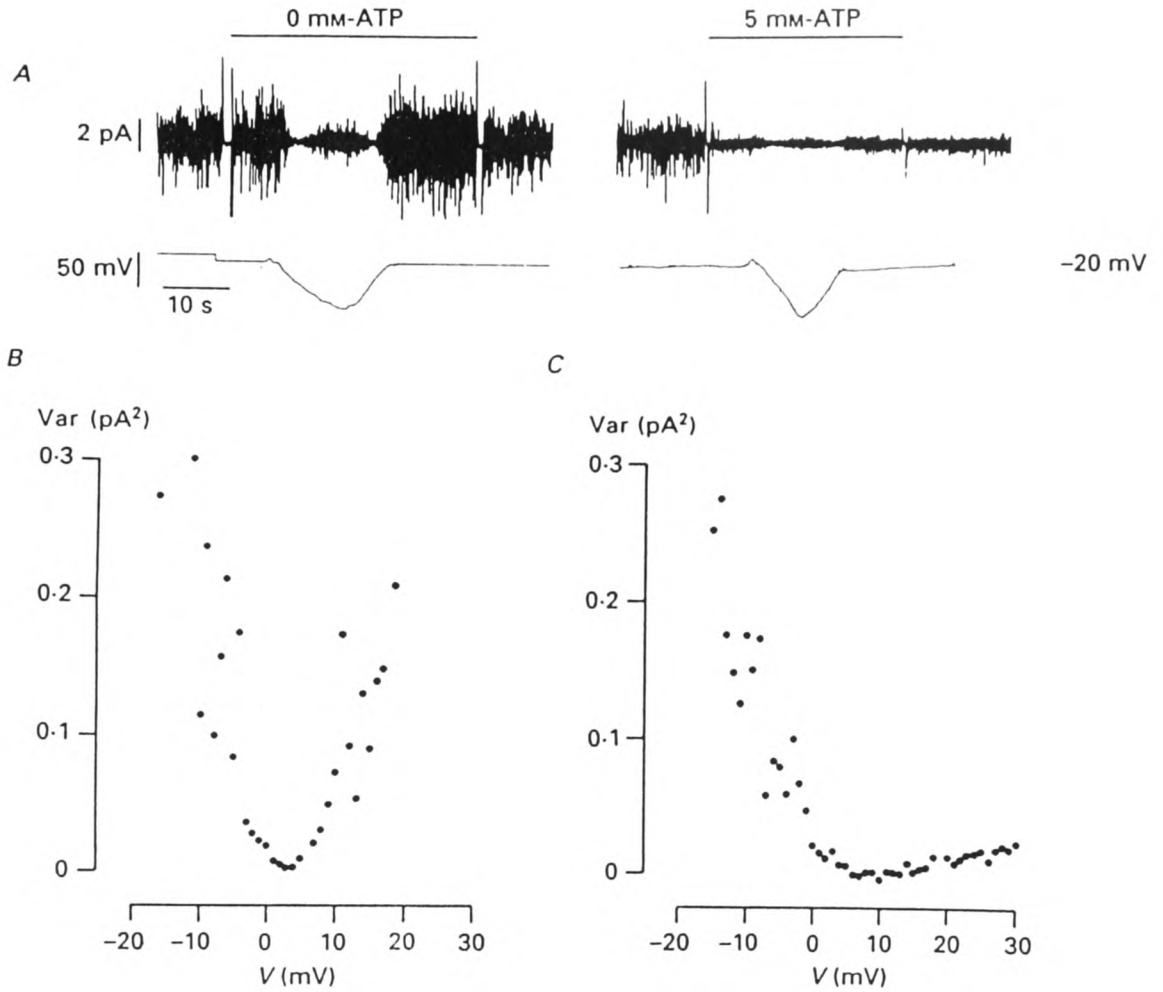


Fig.3.3. ATP-inhibition of outward and inward Rb-currents.
A, AC- coupled current records (above) and membrane potential (below) recorded in the absence (right) and the presence (left) of 5 mM ATP. The bar indicates the time of exposure to the test solution and the glitches on the current record are associated with the solution change (Kakei & Ashcroft, 1987). The bath contained control solution (0.1 mM ATP, 0.1 mM ADP, 2 mM Mg) during the rest of the recording. External solution, 140 mM-K. Bath solution, 140 mM-Rb plus additions as indicated.
B. Variance-voltage relation of the ATP-sensitive current measured with 140 mM-K external solution and an internal solution of 130 mM-K (left) or 140 mM-Rb (right).

straight line to the data points, was 49.1 pS for the inward currents (-10 to -60 mV) and 31.3 pS for the outward currents (20 to 60 mV). These values are in good agreement with those reported previously for ATP-sensitive K^+ channels (Ashcroft, 1988).

When Rb^+ replaced internal K^+, there was no significant change in the amplitude of the inward currents but outward currents were substantially smaller (Fig. 3.1B). At +60 mV, outward currents decreased from about 2 pA in K^+ solution to approximately 0.5 pA in Rb^+ solution. The single-channel slope conductance for the inward currents, carried by K^+, was 45.2 pS (-10 to -60 mV), close to that found when K^+ was the internal ion. The slope conductance for outward Rb^+ currents, however, was considerably smaller than that in K^+ (6.8 pS, 20 to 60 mV). The reversal potential of the mean single-channel current-voltage relation shifted by +6 mV to +8 mV when Rb^+ replaced K^+ (figure 3.2B). The relative Rb^+ permeability can be obtained from the reversal potential (E_{rev}) using the general expression:

$$E_{rev} = \frac{RT}{F} \ln \frac{[K^+]_o + P_X/P_K\,[X]_o}{[K^+]_i + P_X/P_K\,[X]_i} \qquad \text{eqn. 3.2}$$

where P_X/P_K is the permeability of X with respect to K^+. In this case X is Rb^+, $[Rb^+]_i$ and $[K^+]_o$ = 140 mM and $[Rb^+]_o$ and $[K^+]_i$ = 0 mM. This gives a P_{Rb}/P_K ratio of 0.73 (Table 3.2).

One problem encountered in attributing these outward Rb^+ currents to outward current flow through ATP-sensitive K^+ channels is that a few of the patches contained an additional type of K^+ permeable channel of low conductance (approximately 9 pS for outward currents). This channel was seen infrequently, but in K^+ solutions also had a unit amplitude of about 0.5 pA at +60 mV, similar to that of the currents recorded in Rb^+ solutions. In determining the outward Rb^+ conductance of the ATP-sensitive K^+ channel, therefore, data were selected from patches in which these small channels were absent (or only rarely seen) in control solutions. To confirm that outward Rb^+ currents indeed flowed through ATP-sensitive K^+ channels, the ability of ATP to produce inhibition of outward currents was tested. As shown in figure 3.3A both inward and outward currents in Rb^+ solutions were substantially blocked by 5 mM ATP.

The very small outward currents recorded with internal solutions containing 140 mM-Rb^+ mean that it is difficult to obtain an accurate estimate of the reversal potential from the single channel current-voltage relation. An alternative way to measure the reversal potential, which may be more suitable when single channel currents are small, is to look for the potential at which the current trace shows the least noise. For these experiments it is preferable to use patches containing large numbers of channels and maintain a stable level of activity in the patch. Therefore the test solution was alternated with a control solution containing 0.1 mM ATP, 0.1 mM ADP and 2 mM Mg^{2+}, as Ohno-Shosaku et al. (1987) have shown that a similar protocol is effective in minimising channel run-down.

Figure 3.3A shows AC-coupled current records recorded with 140 mM-Rb^+ internally both before and after the addition of 5 mM NaATP when the patch potential was slowly ramped from -20 mV to +40 mV. It is clear that in ATP-free solution, the current noise is greatest at negative membrane potentials, passes through a minimum around 0 mV, and increases again at more positive membrane potentials. Membrane potential has little effect on current noise in the presence of 5 mM NaATP, indicating that most of the voltage-dependent noise originates from the opening and closing of ATP-sensitive K^+ channels.

In 130 mM-K^+ internal solution the variance was least at $+3 \pm 0.5$ mV (n=4; figure 3B) close to the reversal potential of the single channel current-voltage relation (compare figure 2A). The variance-voltage relation of the ATP-sensitive current measured with 140 mM-Rb^+ internal solution is shown in figure 3C. Compared with controls in K^+ solution, in the same patch, the potential at which the variance was least was shifted by $+6.3 \pm 1$ mV (n=4). In the presence of ATP there was little difference in the variance-voltage relation in Rb^+ and K^+ solutions. The predicted P_{Rb}/P_K ratio of 0.72 is in good agreement with that estimated from the reversal potential of the single-channel currents.

The reversal potential of the ATP- sensitive K^+ channel was also measured in patches containing large numbers of channels, by constructing the macroscopic ATP-sensitive current-voltage relation. A difficulty with this method was that of leak correction: the base-line was not usually visible in patches containing a large number of channels. The leak was measured either

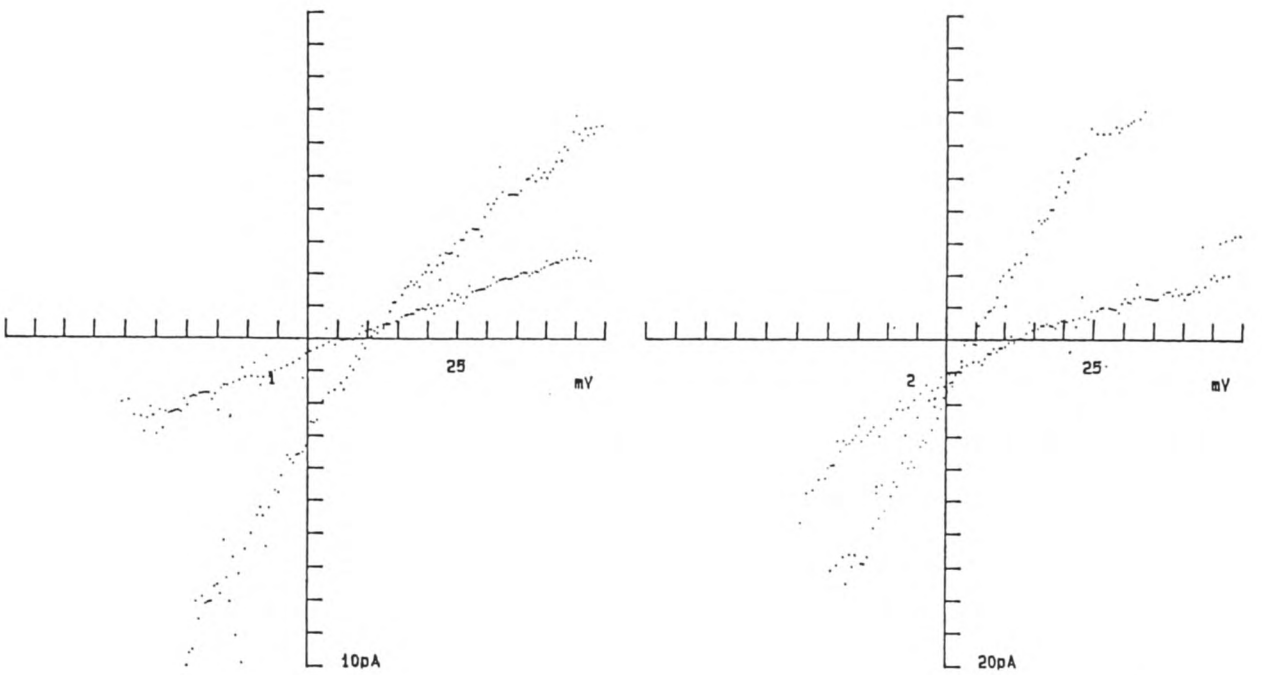


Figure 3.4. Macroscopic current-voltage relations.
Determined for a multi-channel patch as described in Methods.
A. External solution, 140 mM-K, internal solution, 140 mM-Rb, 0 mM (IV with greater slope) or 5 mM (IV with lower conductance) ATP.
B. The current-voltage relation in the presence of 5 mM ATP was subtracted from the IV relation recorded in the absence of ATP to produce the ATP-sensitive IV with either 140 mM-K or 140 mM-Rb in the internal solution. The IV with 140 mM-Rb (the IV with the lower conductance) was formed by subtraction of the two IV's in 4A.

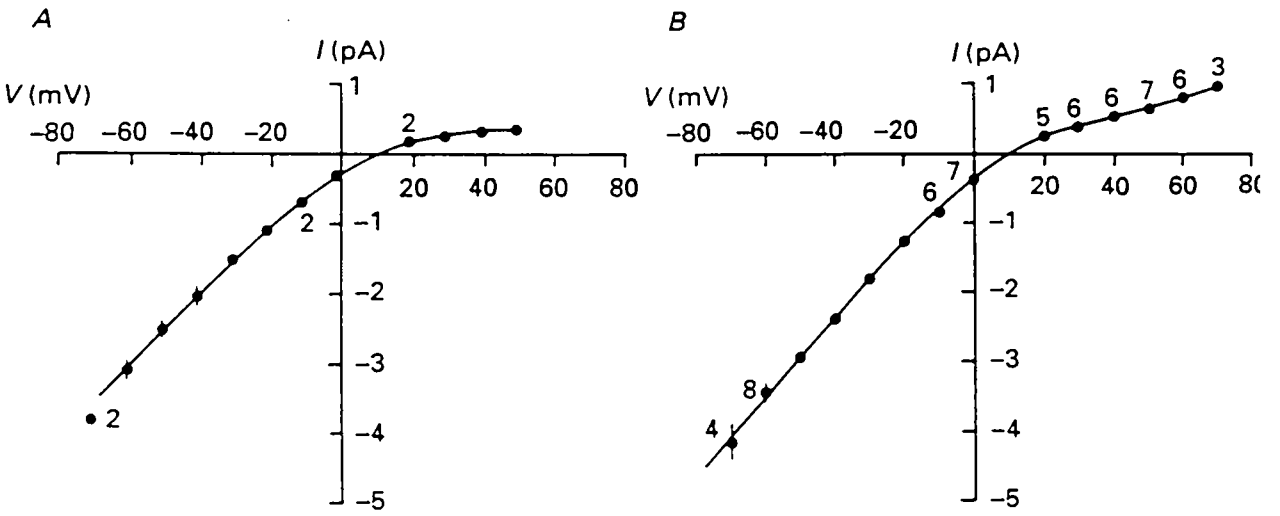


Fig.5 A,B. Mean single channel current-voltage relations for inside-out patches exposed to an internal solution containing 107 mM-Rb (A; n = 2-3) or 70 mM-Rb (B; n = 3-9). External solution, 140 mM-K. The lines are drawn through the points by eye.

Table 3.3 Permeability ratios.

External solution	Internal solution	configuration	E_{rev} (mV)	P_X/P_{Rb}
140 mM-K^+	130 mM-K^+	i-o	+2.1	
140 mM-K^+	130 mM-K^+	o-o	+1.9	
140 mM-K^+	140 mM-Rb^+	i-o	+8	0.73
140 mM-K^+	107 mM-Rb^+	i-o	+9.6	0.51
140 mM-K^+	70 mM-Rb^+	i-o	+10	0.49
70 mM-Rb^+	130 mM-K^+	o-o	-4	0.59
140 mM-K^+	70 mM-Na^+	i-o	+12	0.39
5 mM-K^+	130 mM-K^+	i-o	-78	0.007

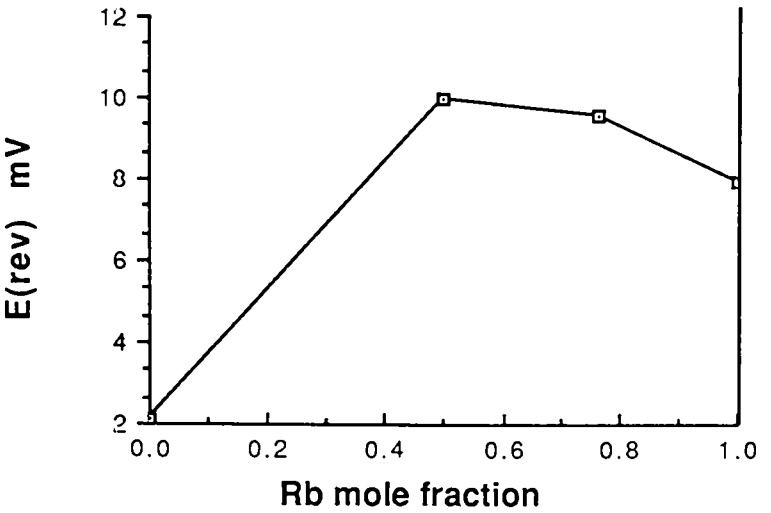
Configuration = patch clamp configuration; i-o = inside-out; o-o = outside-out. Reversal potentials have been corrected for the presence of a liquid junction potential at both the pipette andthe reference electrode using the measured values given in Table 3.1. P_X/P_{Rb} ratios were calculated using equation 3.2.

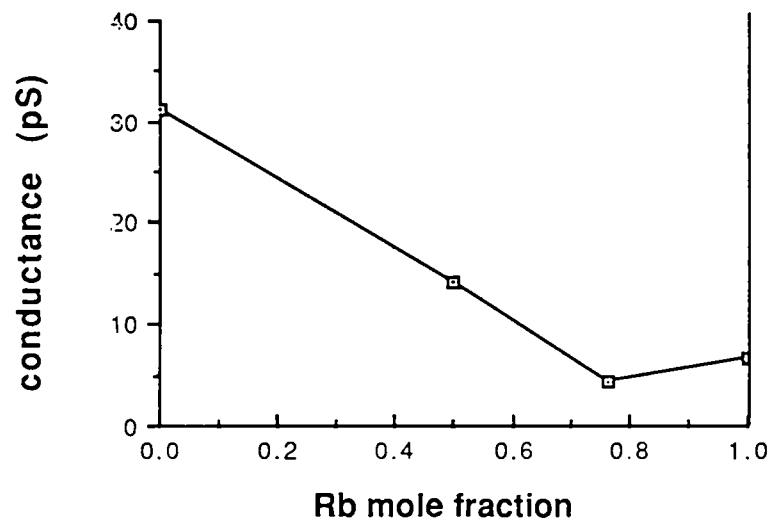
Figure 3.6. Anomalous mole-fraction effects in K^+-Rb^+ mixtures.

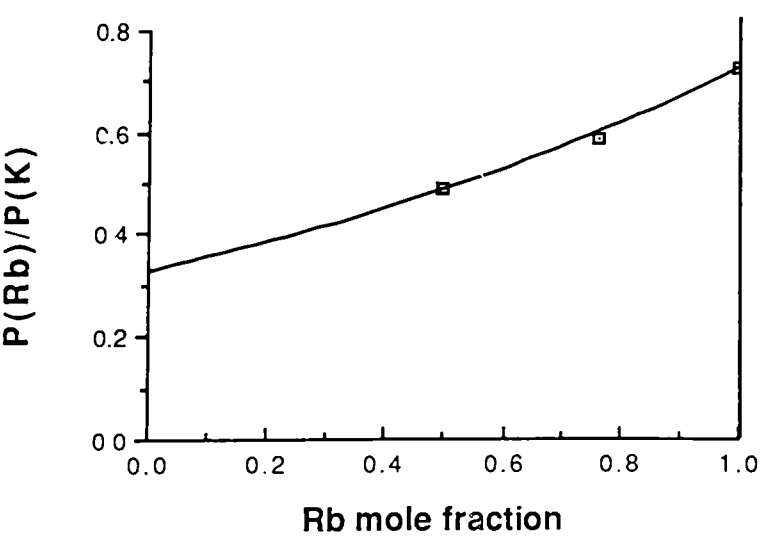
A (top panel). Reversal potentials of single-channel IV relations in K^+-Rb^+ mixtures. The data values are given in Table 3.3.

B (middle). Single channel outward chord conductance (from the data plotted in figures 3.2 and 3.5)

C (lowest panel). P_{Rb}/P_K as a function of Rb mole fraction. The data were fitted to a single exponential by a least squares routine.


E(rev) mV
12
10
8
6
4
2
0.0
0.2
0.4
0.6
0.8
1.0
Rb mole fraction


conductance (pS)
40
30
20
10
0
0.0
0.2
0.4
0.6
0.8
1.0
Rb mole fraction


P(Rb)/P(K)
0.8
0.6
0.4
0.2
0.0
0.0
0.2
0.4
0.6
0.8
1.0
Rb mole fraction

in those sweeps in which it was visible or from the current-voltage relation in the presence of 5 mM ATP, and was then subtracted from the macroscopic IV curve. Figure 3.4A shows the macroscopic current-volage relation in 140 mM Rb^+ internal solution in 0 mM ATP and in 5 mM ATP, for a single cell, and figure 3.4B shows the corresponding leak-subtracted (ATP-sensitive) macroscopic IV curves in 140 mM K^+ and in 140 mM Rb^+ in the same cell. In four cells, shifts of between 6 and 9 mV were found when K^+ replaced Rb^+ as the internal cation.

In intracellular solutions containing a mixture of K^+ and Rb^+ (figure 3.5), outward currents are larger than in 140 mM Rb^+ solution and the reversal potential may be estimated from the I-V relation with more confidence. Estimated permeability ratios found in these solutions were around 0.5 (Table 3.3). Outward currents were also reduced in these Rb^+ solutions, even being smaller than those expected from the GHK equation if K^+ were the only ion carrying current. This raises the possibility that internal Rb^+ may interfere with the outward movement of K^+. In order to determine this, it is neccesary to measure outward K^+ currents separately (in the absence of Rb^+) because the rectification of outward K^+ currents in control solutions (figure 3.2A) means that they cannot be predicted from constant field theory. Unfortunately, a suitable K^+ substitute which did not either permeate or block the channel (or both) was not found and this idea could not be tested experimentally.

Although it is difficult to determine the reversal potential accurately when the internal solution contains Rb^+, the data in Table 3.3 indicate that the reversal potential in internal K^+/Rb^+ mixtures is in fact more positive than in either K^+ or Rb^+ alone. The reversal potential is plotted against the mole fraction of Rb^+ in figure 6A. The single-channel outward slope conductances, (from the data used in figures 2 and 5), in K^+/Rb^+ mixtures are plotted in figure 3.6B. These too show an anomalous mole fraction effect, suggesting that the channel is a multi-ion pore (Hille & Schwarz, 1978). Figure 3.6C shows that the biphasic variations in E_{rev} are underlain by a simple, monotonic decrease in P_{Rb}/P_K as the mole fraction of Rb^+ decreases. Similar effects have been observed in other types of K^+ channels (Hille & Schwarz, 1978; Hille, 1984).

No current-voltage relations could be constructed when both the pipette and the bath

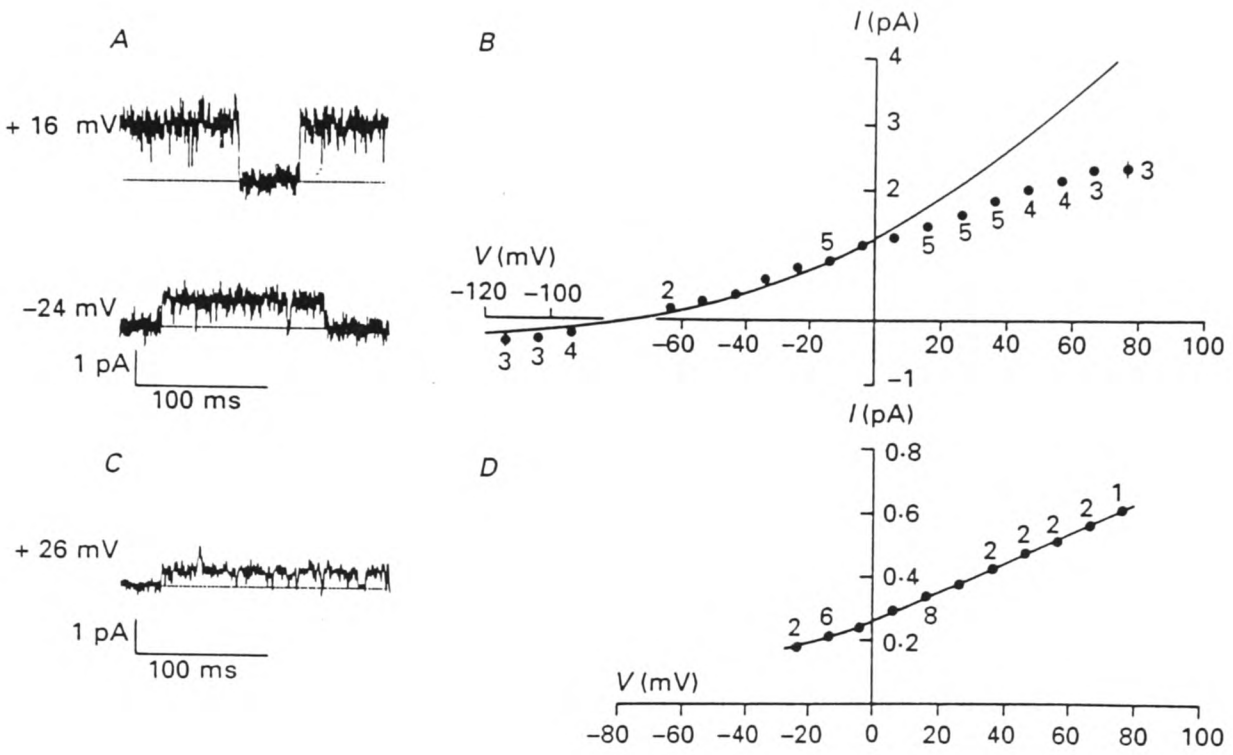


Fig.3.7A. Single channel currents recorded at different membrane potentials from an inside-out patch with a pipette solution of 5 mM-K. Internal solution, 130 mM-K. Sample rate, 5 kHz; filter, 0.5 kHz.

B. Mean I-V relation for between 2 and 6 inside-out patches exposed to an intracellular solution of 130 mM-K. External solution 5 mM-K. The line is drawn to $I_m = I_K + I_{Na}$ (eqn.3) where I_K and I_{Na} are given by eqn.3.1 and P_K is taken to be 1.05×10^{-13} cm^3/s (as in control 140 mM-K) and P_{Na} is given by $P_K \times 0.007$ (P_{Na}/P_K). $[K]_o = 5$ mM, $[K]_i = 130$ mM, $[Na]_o = 140$ mM and R,T and F have their usual values.

C. Single channel current recorded at +30 mV. External solution 5 mM-K, internal solution 107 mM-Rb. Sample rate 5 kHz; filter 0.5 kHz.

D. Mean I-V relation for 2 to 8 inside-out patches exposed to an intracellular solution containing 107 mM-Rb. External solution, 5 mM-K. The line is drawn through the points by eye.

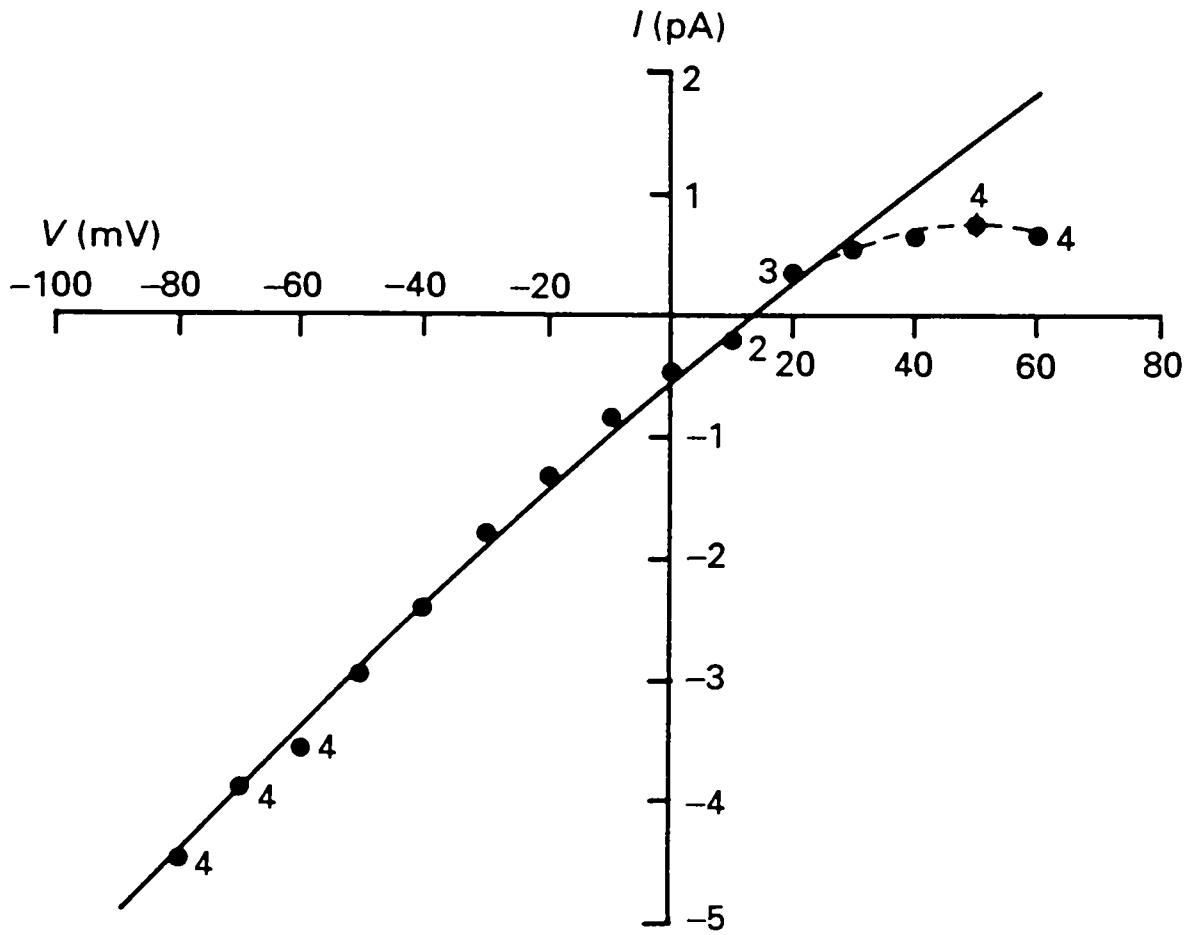


Fig.3.8. Mean single channel current-voltage relation for 4-5 inside-out patches. External solution, 140 mM-K. Internal solution, 70 mM-Na. The line is drawn to eqn.3.2 where $X=Na^+$ and with $P_K = 1.05 \times 10^{-13}$ cm^3/sec, $P_{Na} = 0.41 \times 10^{-13}$ cm^3/sec, $[K]_o$ = 140 mM, $[K]_i$ = 60 mM, $[Na]_o$ = 5 mM, $[Na]_i$ = 70 mM.

contained 140 mM-Rb^+ as the currents were then very small.

The relative Rb^+ permeability under more physiological cation gradients was next examined, using a pipette solution containing 5 mM-K^+ and an intracellular solution of 130 mM-K^+ or 107 mM-Rb^+ (figure 3.7A). Single channel currents reversed at a membrane potential of -78 mV when the pipette contained an external solution of 5 mM-K^+ + 140 mM-Na^+ (130 mM-K^+ internally) giving a P_{Na}/P_K ratio of 0.007 (figure 3.7B). This is close to the selectivity of the ATP-sensitive K^+ channel in skeletal muscle measured under similar conditions (0.012; Spruce et al., 1987). A reasonable fit to the currents (I_t) at potentials negative to about +20 mV was provided by the following equation:

$$I_t = I_K + I_{Na}, \qquad \text{eqn. 3.3}$$

where I_K and I_{Na} are defined as in eqn. (3.1), using a Na^+ permeability of 7.35×10^{-16} cm^3/s (P_{Na}/P_K = 0.007), and the same K^+ permeability as in figure 3.2A. However, at more positive potentials the outward currents again showed significant rectification. The single-channel slope conductance, measured between 0 and +70 mV, was 18.7 pS, comparable to that found for the ATP-sensitive K^+ channel in the ß-cell previously (19 pS; Trübe, Rorsman and Ohno-Shosaku, 1986).

Outward currents were considerably reduced at all potentials when Rb^+ was the internal cation and it was not possible to measure the reversal potential under these conditions (figure 7C,D). The single-channel slope conductance was reduced to 4.5 pS (0 to 70 mV).

Internal Na^+ ions can also permeate the channel. In an intracellular solution containing 70 mM-Na^+ + 60 mM-K^+ single-channel currents reversed at a potential of +12 mV (figure 3.8) indicating that K^+ is more permeant than Na^+. The continuous line is that predicted by equation (3.3), assuming a P_{Na}/P_K ratio of 0.39 and $P_K = 1.0 \times 10^{-13}$ cm^3/sec. These results suggest that it is about fifty-five times easier for Na^+ to enter the channel from the internal than from the external side of the membrane. Outward currents showed greater rectification in the presence of internal Na^+, confirming that internal Na^+ ions can also block outward K^+ currents (Cook & Hales, 1984).

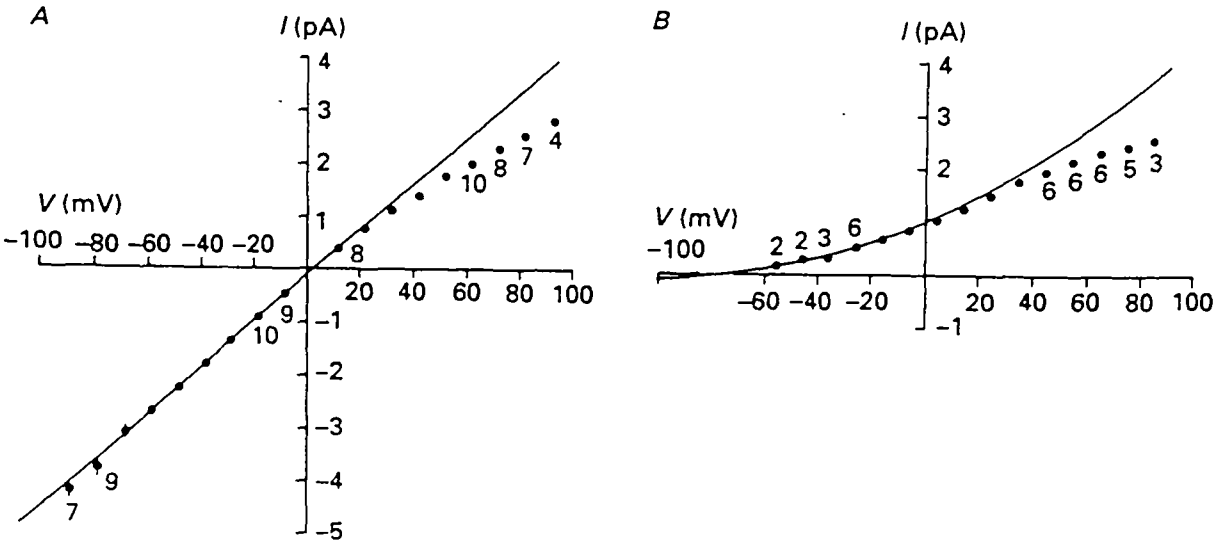


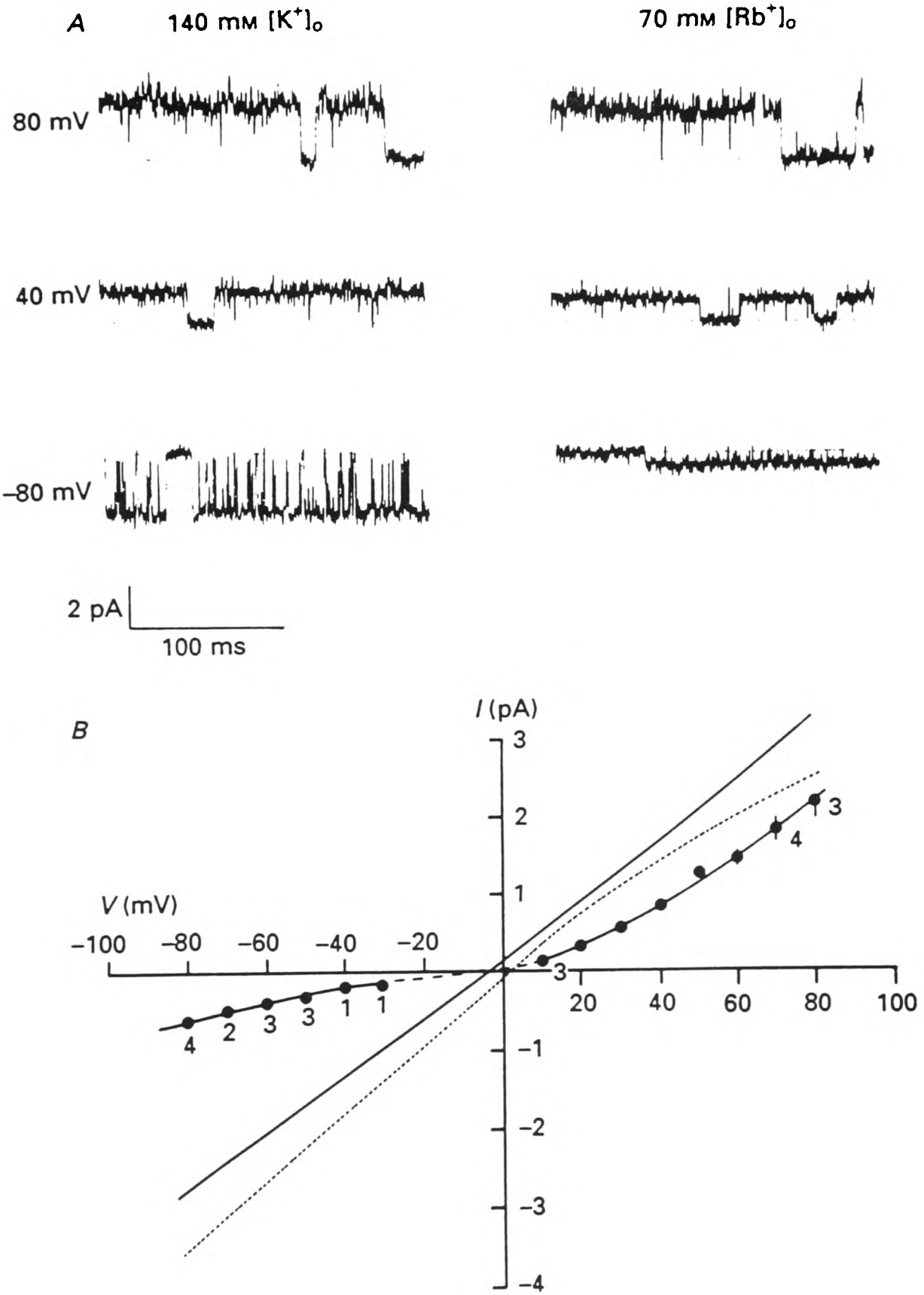
Fig. 3.9A. Mean single channel I-V relation for 4-11 outside-out patches exposed to 140 mM-K extracellularly. Internal (pipette) solution, 130mM-K. The line is drawn to eqn.3.1 with $P_K = 0.86 \times 10^{-13} cm^3/s$.

B. Mean current-voltage relations for 2-7 outside-out patches exposed to an external (bath) solution of 5mM-K (Na 140 mM). Internal (pipette) solution, 130mM-K. All symbols are larger than 1 S.E.M. The line is drawn to eqn. 3.2 with $X=Na^+$ and using $P_K = 0.86 \times 10^{-13}$ cm^3/s, $P_{Na} = 0.007 \times P_K$, $[K]_o = 5$ mM, $[K]_i = 130$, $[Na]_o = 140$ mM.

Figure 3.10.

A. Single channel currents recorded from the same outside-out patch with an external solution of 140 mM-K (left) and subsequently of 70 mM-Rb (right). Internal solution, 130 mM-K. Sample rate, 5 kHz; filter, 2kHz. The potential is indicated next to each trace.

B. Mean single-channel current-voltage relation for 1-5 outside-out patches exposed to 70 mM-Rb solution externally. Internal solution, 130 mM-K. The solid line through the points is drawn by eye. The dashed line is the mean IV relation in control solution (figure 3.9A), and the continuous line is drawn to the equation $I = I_K + I_{Rb}$, where I_K and I_{Rb} are calculated as in equation 3.1, with $P_{Rb}/P_K = 0.59$, $P_K = 0.86 \times 10^{-13}$ cm^3/sec, $[Rb]_o = 70$ mM, $[K]_o = 60$ mM and $[K]_i$, 130 mM.


A
140 mM [K+]o
70 mM [Rb+]o
80 mV
40 mV
–80 mV
2 pA
100 ms
B
I (pA)
V (mV)
–100
–80
–60
–40
–20
20
40
60
80
100
3
2
1
–1
–2
–3
–4
4
2
3
3
1
1
3
4
3

Outside-out patches

The permeability of the channel to extracellular Rb^+ and Na^+ ions was investigated using outside-out patches and pipettes filled with 130 mM-K^+ internal solution.

Figure 3.9A shows the mean single channel I-V relation recorded from outside-out membrane patches with 140 mM-K^+ external and 130 mM-K^+ internal solutions. The line is fitted to eqn 3.1 assuming a K^+ permeability of 0.85 x 10^{-13} cm^3/s, somewhat smaller than that found for the inside-out configuration. The effect of replacing external K^+ with Na^+ in outside-out patches is illustrated in figure 3.9B. When $[K^+]_o$ was 5 mM, the current-voltage relation was reasonably well fitted by eqn. 3.3, asssuming a P_{Na}/P_K ratio of 0.007, the same as that measured for the inside-out patch, and a P_K of 0.86 x 10^{-13} cm^3/s (as for outside-out controls). Thus, the patch configuration does not affect the P_{Na}/P_K ratio.

Single channel currents (A) and current-voltage relations (B) obtained in an external solution of 70 mM-Rb^+ + 70 mM-K^+ are illustrated in figure 3.10. Partial replacement of K^+ with Rb^+ reduced both the inward and the outward currents. The line drawn by eye through the points in Rb^+ solution has a reversal potential of - 4 mV, giving a P_{Rb}/P_K of 0.59, although the difficulty of measuring the reversal potential makes this a very tentative estimate. However, the current noise was less at 0 mV than at +10 or -10 mV consistent with the idea that single channel currents do in fact reverse between these two potentials. Spruce et al. (1987) found a P_{Rb}/P_K ratio of 0.76 for the ATP-sensitive K^+ channel of skeletal muscle measured with 60 mM-$[Rb^+]_o$ and 0 mM-$[K^+]_o$.

The single-channel conductance for inward currents was substantially reduced in 70 mM-Rb^+ + 70 mM-K^+ external solution. With 140 mM $[K^+]_o$, the slope conductance was 47.1 pS (-30 to -80 mV) and decreased to 9.7 pS (-30 to -80 mV) in the Rb^+ - K^+ mixture. The reduction in the outward currents, as shown by the difference between the data points and the dotted line which indicates the control current-voltage relation, (Fig 3.10B) suggests that external Rb^+ also interferes with the outward movement of K^+. This effect is voltage-dependent, and decreases with depolarisation (figure 3.10A, B).

Figure 3.11 shows single-channel currents (A) and mean current-voltage relations (B)

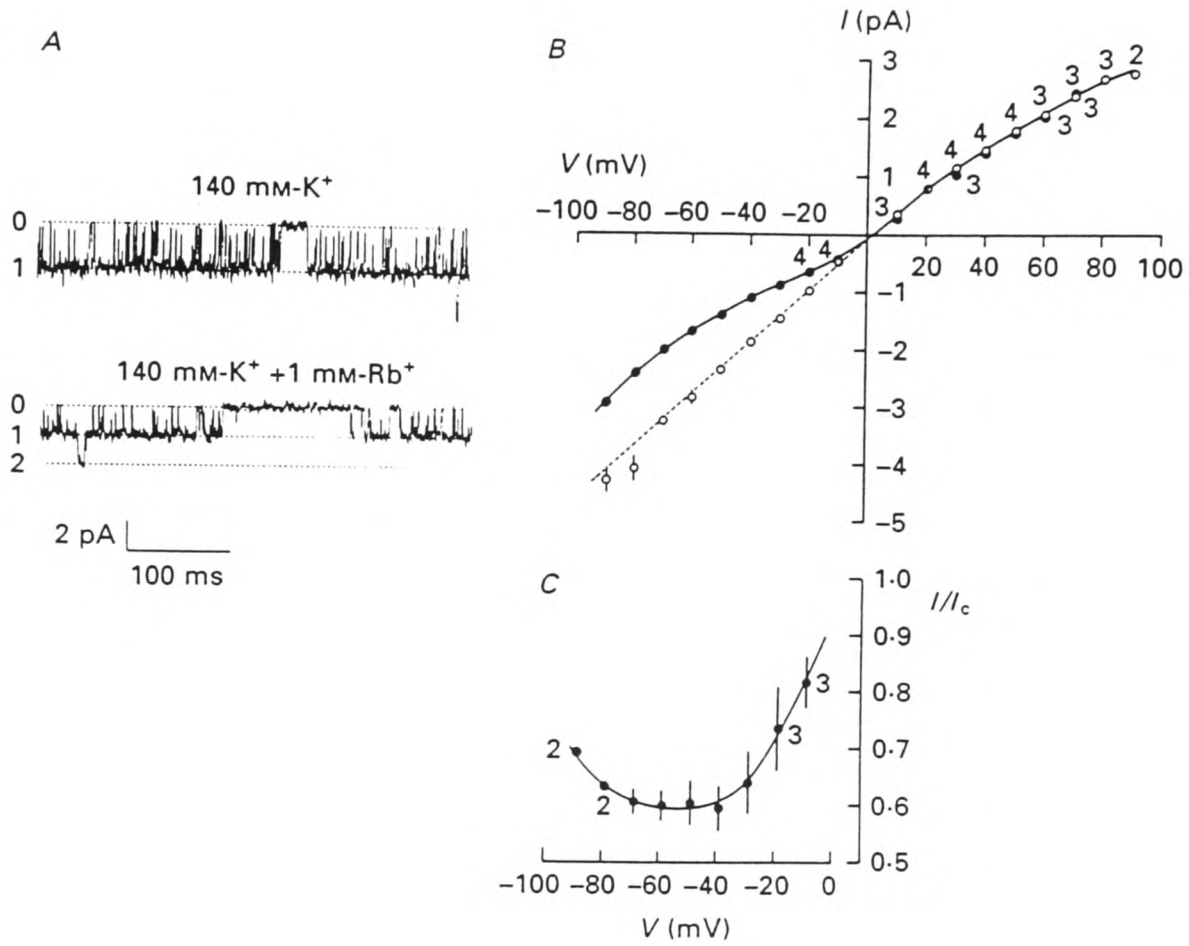


Fig. 13.11A. Single channel currents recorded from an outside-out patch at -58mV in an external solution of 140mM-K (above) and after addition of 1mM Rb (below). Internal solution, 130mM-K. Sample rate, 5kHz; filter 2 kHz.

B Mean single channel current-voltage relations for 5 outside-out patches exposed to an external solution of 140mM-K (o) and for 4 of these patches subsequently exposed to 140mM-K + 1mM-Rb (o). Internal solution, 130mM-K. The lines are drawn through the points by eye.

C. Voltage-dependence of the Rb-block. Mean conductance in the presence of 1mM Rb^+ is plotted as a fraction of that in the absence of Rb^+. The line is drawn through the data points by eye.

obtained in 140 mM-K^+ solution (o) and in the same solution after addition of 1 mM Rb^+ (o). In the presence of 1 mM Rb^+, inward currents are reduced at all potentials, but the extent of the block is voltage-dependent, initially increasing and then decreasing with membrane hyperpolarisation. It was not possible to follow the Rb^+ block to potentials negative to -90 mV because the patch membrane was usually destroyed by strong hyperpolarisation. Outward currents were not affected by 1 mM Rb^+. The voltage-dependence of the Rb^+ block is examined in figure 3.11C. Here the single channel conductance in the presence of Rb^+, expressed as a fraction of that in control solution, is plotted against membrane potential. The maximum block occurs somewhere between -40 mV and -60 mV. These results resemble those found by Standen and Stanfield (1980) for the effect of Rb^+ on macroscopic currents through the inwardly rectifying K^+ channel of skeletal muscle.

A simple interpretation of the effect of Rb^+ on inward K^+ currents is that external Rb^+ can enter the channel and bind to a site lying within the membrane voltage field, thereby blocking the conduction pathway for K^+. If the rate of blocking and unblocking of the channel is rapid with respect to the time constant of the recording equipment (~3kHz), then the measured single channel conductance will be a time averaged value of the blocked and unblocked states. This value will be voltage-dependent because the binding site lies within the membrane voltage field, (this point is considered at greater length in the discussion). Consistent with this idea, open times appeared increased by Rb^+ around the potential at which the blocking effect is greatest (-60 mV). This is expected if Rb^+ acts as an open channel blocker (Neher & Steinbach, 1978). A similar prolongation of K^+ channel openings by Rb^+, in skeletal muscle, has been reported by Spruce et al. (1984) . The increase in the measured conductance at more extreme hyperpolarisation can be interpreted as Rb^+ being forced on through the channel by a further increase in the voltage field.

DISCUSSION

Rb-experiments

The results of the experiments described in this paper lead to the conclusion that Rb^+ acts as a permeant blocker of the ATP-sensitive K-channel.

The results do not allow a very precise estimate of the relative Rb^+ permeability because of the difficulty in measuring the reversal potential when the channel conductance is very low. However, from the results of the noise analysis experiments, and the current-voltage relations, it seems likely that the P_{Rb}/P_K ratio lies around 0.73 and is thus in reasonable agreement with the value of 0.76 found for the ATP-sensitive K^+ channel in skeletal muscle (Spruce et al., 1987). It is also close to the permeability ratio deduced for the resting K^+ permeability of the ß-cell from measurements of the resting potential (0.72; Rosario & Rojas, 1986) and from flux studies of the glucose-sensitive Rb^+ and K^+ efflux (0.87; Henquin, 1978; 0.80; Boschero & Malaisse, 1979). This would be expected if the ATP-sensitive K^+ channel contributes most of the resting K^+ permeability of the ß-cell. The Rb^+ permeability of the ATP-sensitive K^+ channel (relative to that of potassium) also resembles that found for the Ca^{2+}-activated K^+ conductance of pancreatic acinar cells (Gallacher et al., 1984).

Compared with K^+, Rb^+ had a similar permeability but a considerably lower conductance, regardless of whether the ion was moving inward or outward through the pore. The low conductance implies that the absolute permeability of the channel to Rb^+ (in 140 mM Rb_i) is low, although P_{Rb}/P_K is close to unity.

The paradox can be explained by modifying an argument from Hille (1984, chapter 11). It comes about from measuring the absolute P_K and P_{Rb} (i.e. channel conductances) in different solutions, i.e. in 140 mM K_i and 140 mM Rb_i respectively. If the absolute permeabilities had been measured by fluxes, using double-labelled experiments in a mixed K^+/Rb^+ solution, a ratio of 0.74 would have been obtained, but the absolute permeabilities would both have been higher if the major ion present were K^+ rather than Rb^+. Double-labelled efflux experiments have indeed shown permeability ratios close to 0.8 (Dawson et al., 1986).

In terms of a barrier model, (Lauger, 1973; Woodhull 1973; Hille & Schwarz, 1978; Spruce et al., 1987), the highest energy barrier for Rb^+ is only slightly higher than for K^+, ($0.74 = \exp[(G_K - G_{Rb})/RT]$, where G_K and G_{Rb} are the peak barrier energies for K^+ and Rb^+ respectively), but the greatest energy step (from well to peak) is considerably greater for Rb^+ than for K^+ (ratio of conductances = $\exp[(G'_K - G'_{Rb})/RT]$ where G'_K and G'_{Rb} are the greatest energy steps for K^+ and Rb^+). This is equivalent to saying that the dwell time for Rb^+ is considerably greater than for K^+, or that the channel contains an ion binding site within the pore which has a much greater affinity for Rb^+ than for K^+.

It has previously been shown that ion fluxes through the ATP-sensitive channel do not obey the independence principle. This has been shown by 1) demonstration of saturation (Ashcroft et al., 1988) 2) block of outward currents by magnesium and sodium (Horie et al., 1987; Ciani & Ribalet, 1988) and 3) block of inward currents by external rubidium (Stanfield et al., 1987). The present study confirms the effect of internal sodium and external rubidium, and suggests that to these deviations from independence can now be added an anomalous mole-fraction effect (figure 6), as has previously been observed in several other types of potassium channel (Hille & Schwarz, 1978). Spruce et al. (1987) accounted for rectification and non-independence using a two-binding site three-barrier model based on Eyring rate theory, but used a simplifying assumption that only one ion could occupy the pore (channel) at any one time. The anomalous mole-fraction effect shown in figure 6 cannot be accounted for in a one-ion model: it provides evidence of a multi-ion pore (Hille & Schwarz, 1978). Extrema in both the conductance and reversal potential curves (figure 6A, 6B) require that the ion with the lower bi-ionic permeability (Rb^+ here) binds more tightly, and a conductance minimum implies repulsion between ions in the channel (Hille & Schwarz, 1978). It should be borne in mind, however that the anomalous mole-fraction effect suggested here depends upon a rather subjective estimate of reversal potentials in the various ion mixtures; the accuracy of the determination is probably of the same order as the proposed increase in E_{rev} in 107 mM Rb^+ (2-3 mV). In any case, it should not be assumed (Dawson et al., 1986) that any particular type of potassium channel has a fixed selectivity ratio for two different ions.

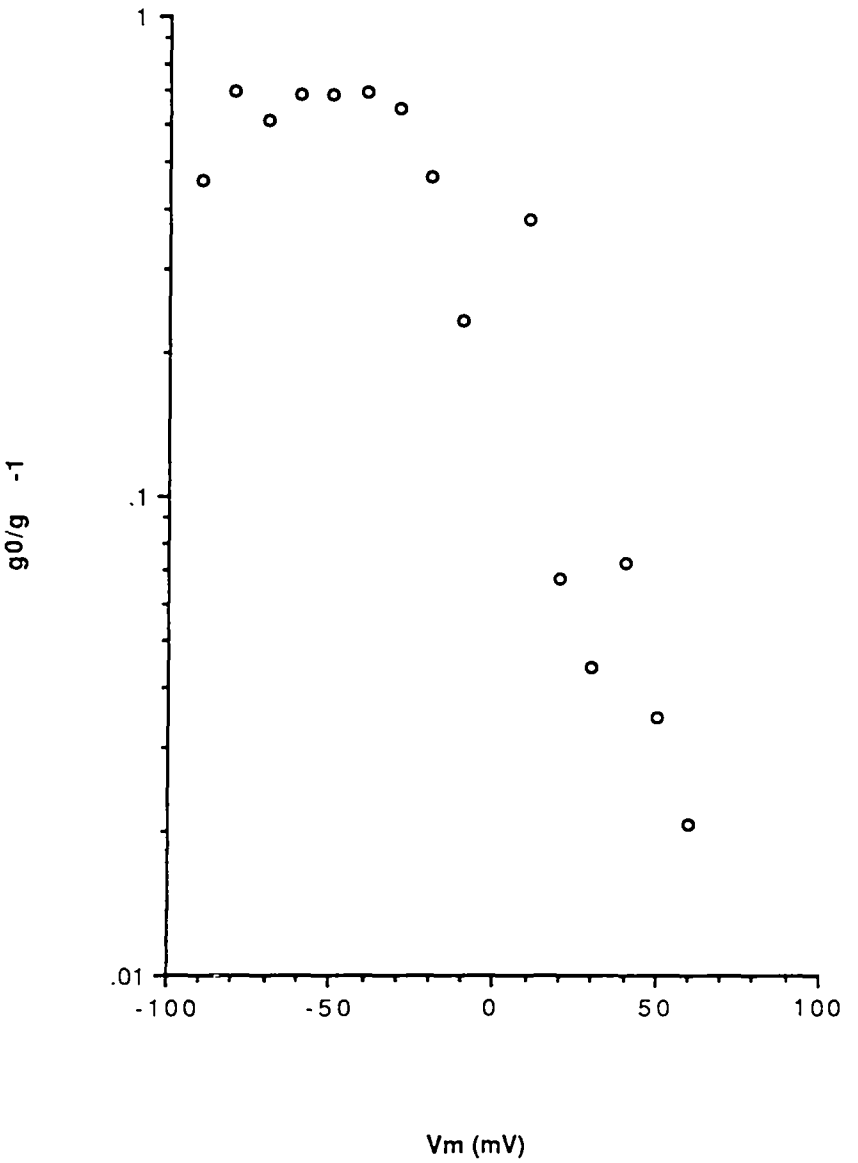


Fig. 3.12. Voltage-dependence of block by 1 mM Rb^+.
Details are given in the text and in appendix 1.

Three pieces of evidence suggest that Rb^+ ions can block K^+ fluxes through the pore. First, the addition of a low concentration of Rb^+ to the external solution produced a voltage-dependent block of inward currents characteristic of a permeant blocking ion (figure 3.11; Standen & Stanfield, 1980; Ashcroft & Stanfield, 1983). Secondly, in 70 mM-Rb^+ external solution, outward K^+ currents were reduced in a voltage-dependent mannner (figure 3.10). A possible explanation of this second effect is that Rb^+ ions sit within the outer entrance of the channel and so block the outward movement of K^+. The decrease in Rb^+ block with increasing depolarisation is consistent with this view as larger depolarisations would be expected to reduce the possibility of external Rb^+ entering the channel. Thirdly, the anomalous mole fraction effect suggests that internal Rb^+ is able to block the outward movement of K^+ ions, due to greater binding of Rb^+ within the pore.

In principle, if a simple blocking scheme is assumed, the effective valence of the blocking ion ($z\partial$) and the dissociation constant at 0 mV (K(0)) can be obtained from the voltage-dependence of block (Coronado, 1980):

$$\gamma/\gamma_0 = [\ 1 + [B] / \{Kb_{(0)} \exp(-z\partial FV/RT)\}]^{-1}$$

which can conveniently be linearised:

$$\ln\{\gamma_0/\gamma - 1\} = \ln\{[B] / Kb_{(0)}\} + z\partial FV/RT \qquad \text{eqn. 3.4}$$

where γ/γ_0 is the ratio of the apparent channel conductance in the presence of the blocking ion to the control conductance, $z\partial$ is the effective valence of the blocking ion, [B] is the blocker concentration (here $[Rb^+]$ = 1 mM), $Kb_{(0)}$ is the equilibrium constant for blocking at 0 mV and R, F and T have their usual meanings (Coronado 1980). (See appendix one for derivation of the equations).

ln (γ_0/γ) is plotted as a function of membrane potential in figure 3.12. In accordance with eqn. 3.4, $z\partial$ = 0.9 and K(0) = 5 mM can be obtained from the slope and intercept of the best-fit straight line through the data points from -20 to +60 mV. There is reason to distrust these parameters, so obtained, in that while the conductance data for V_m < -20 mV are distorted by "punch through", the data for V_m > 0 mV are to be treated warily because they depend on the ratio between two very similar values (see figure 3.11), and a small error would greatly change the value of ln (γ_0/γ - 1): e.g. a 0.1 pA error in estimation of the "blocked" channel amplitude at +40 mV would change ln (γ_0/γ -1) from -2.6 to -3.48 (overestimation of γ) or -2.35 (underestimation of γ). In spite of these caveats, the channel does seem to be somewhat less than 50% reduced in amplitude at -10 mV in 1 mM Rb_o.

Na permeability

Unlike the case for Rb^+, the relative permeability of the channel to sodium was strongly dependent on whether the ion was moving inward or outward across the membrane. Sodium was able to enter the inner mouth of the channel far more readily than the external mouth. The permeability ratio, P_{Na}/P_K, was 0.007 for external Na^+, close to that found for the ATP-sensitive K^+ channel of skeletal muscle (0.015; Spruce et al., 1987). It is, however, slightly lower than the value of 0.047 reported for the resting potential of the unstimulated ß-cell (Rosario & Rojas, 1986). The difference is consistent with the activity of an additional channel type with a significant Na^+ permeability in the resting ß-cell. (Dunne et al., 1989b)

The strong rectification of the I-V relation seen in internal solutions containing both Na^+ and K^+ confirms previous reports that internal Na ions can block the outward flux of K^+ ions (Cook & Hales, 1984; Horie et al., 1987; Ciani & Ribalet, 1988). This block probably results from the voltage-dependent binding of Na^+ to a site within the pore. The results do not indicate whether this is the same site as that to which Rb^+ ions bind.

The relative permeability to external ions was $K^+ > Rb^+ >> Na^+$ and for internal ions was $K^+ > Rb^+ > Na^+$.

There were some differences between inside-out and outside- out patches in these experiments. First, the channels appeared to run down less rapidly in the outside-out configuration. Secondly, the K^+ permeability of the channel appeared to be rather lower in the outside-out configuration (0.86×10^{-13} cm^3/s as compared with 1.05×10^{-13} cm^3/s for inside-out patches). At present I have no explanation for these differences.

Relationship to flux studies

The results presented here suggest that the reversal potential of the ATP-sensitive channel will change only slightly if internal K^+ is partially replaced with Rb^+, as will occur in $^{86}Rb^+$-loaded islets. The magnitude of the Rb^+ efflux from $^{86}Rb^+$-labelled islets will be a good estimate of the K^+ efflux from that islet (when corrected for the P_K/P_{Rb} ratio.) $^{86}Rb^+$ efflux will considerably underestimate K^+ efflux from islets not loaded with Rb^+, as Rb^+ decreases the conductance of the ATP-sensitive K^+ channel. The decrease in conductance depends on the intracellular concentration of $^{86}Rb^+$, which (from the data given in Henquin (1978)) can be estimated at about 15 mM. Therefore, although Rb^+ serves as an acceptable tracer substitute for K^+ when changes in K^+ permeability are of interest, it is not suitable for determining the absolute magnitude of K^+ fluxes.

The results imply that the membrane will depolarise in the presence of internal Rb^+ as the resting potential is determined by both the membrane K^+ permeability and a background Na^+ permeability (Atwater et al., 1978; Dunne et al., 1989b). The extent of this depolarisation will depend on the relative contribution of the Na^+ and K^+ permeabilities to the resting potential and on the extent to which the K^+ channel is blocked, and hence on the internal Rb^+ concentration. If internal Rb^+ were high enough to significantly depolarise the ß-cell, lower glucose concentrations would be required to stimulate insulin secretion than in the absence of $[Rb]_i$. Since the shape of the relationship between insulin release and ion efflux is similar for both Rb^+ and K^+ efflux (Henquin, 1980), Rb^+ must not accumulate in preloaded islets in sufficient concentration to produce a significant depolarisation of the ß-cell.

ATP sensitivity: modulation by ADP.

INTRODUCTION

The origin of the initial depolarisation of the ß-cell membrane, in response to glucose, is a decrease in the possassium permeability (e.g. Henquin, 1978), resulting from closure of the ATP- and glucose-sensitive potassium channel, as discussed previously. Cell-attached patch clamp recording first showed that this channel was closed by some product of glucose metabolism (Ashcroft et al., 1984). Several lines of evidence now support a role for ATP as the link between ß-cell metabolism and channel inhibition. First, in inside-out patches the glucose-sensitive channel is blocked by ATP (Cook & Hales, 1984, Findlay et al., 1985a, Rorsman & Trübe, 1985, Ashcroft et al., 1985). Secondly, changes in $[ATP]_i$ produced by glucose and by metabolic inhibitors are accompanied by reciprocal changes in the channel open probability (Ashcroft et al. 1985, 1988). Thirdly, the time course of channel activity parallels that of the glucose-induced changes in intracellular ATP (Rorsman, 1986; Rorsman & Trübe, 1989). Fourthly, glucose and ATP have similar effects on channel kinetics (Rorsman & Trübe, 1985).

In spite of the evidence suggesting a role for ATP as physiological modulator of channel function, there remained an apparent discrepancy between the ATP sensitivity of the channel in the intact cell and that found for the excised patch. In intact cells, the ATP-sensitive channel is open in glucose-free solutions in which the intracellular ATP concentration is around 4-5 mM (Hellman et al., 1969; Ashcroft et al., 1973; Malaisse et al., 1979; Ashcroft et al. 1988a; chapter two), whereas a K_i of ~15 μM has been reported from excised membrane patches (Cook & Hales, 1984; Misler et al, 1986; Ohno-Shosaku et al., 1987). Several explanations for this discrepancy seemed possible:

i) that only a very small fraction of ATP-sensitive channels is open at rest.

ii) that intracellular ATP is compartmentalised and the sub-membrane [ATP] is much lower than 4 mM.

iii) that the open probability of the channel is affected by intracellular enzymes or products of glucose metabolism other than ATP.

The first of these explanations is certainly true (e.g. Findlay et al., 1985a) while they second is also probably true, due, among other things, to the mitochondrial production of ATP and the high rate of its consumption by plasma membrane ATPases. Nevertheless, these seem not to account for all of the apparent discrepancy, and the studies in this chapter were undertaken to examine the last of these possibilities and show that the ATP sensitivity of the channel is modulated by ADP.

METHODS

Channel activity (NP) was calculated by integrating the recorded, amplified and digitised current (stretches of at least 30s: see chapter 2), subtracting the baseline current (determined by eye) and dividing this total channel current (NPi) by the single-channel amplitude (i, determined by eye) to obtain the index of channel activity NP.

The dose-response curves were determined by calculating NP in each ATP concentration and normalising it against the relevant control activity (as described in the text).

Other methods for this chapter were as described in chapter 2.

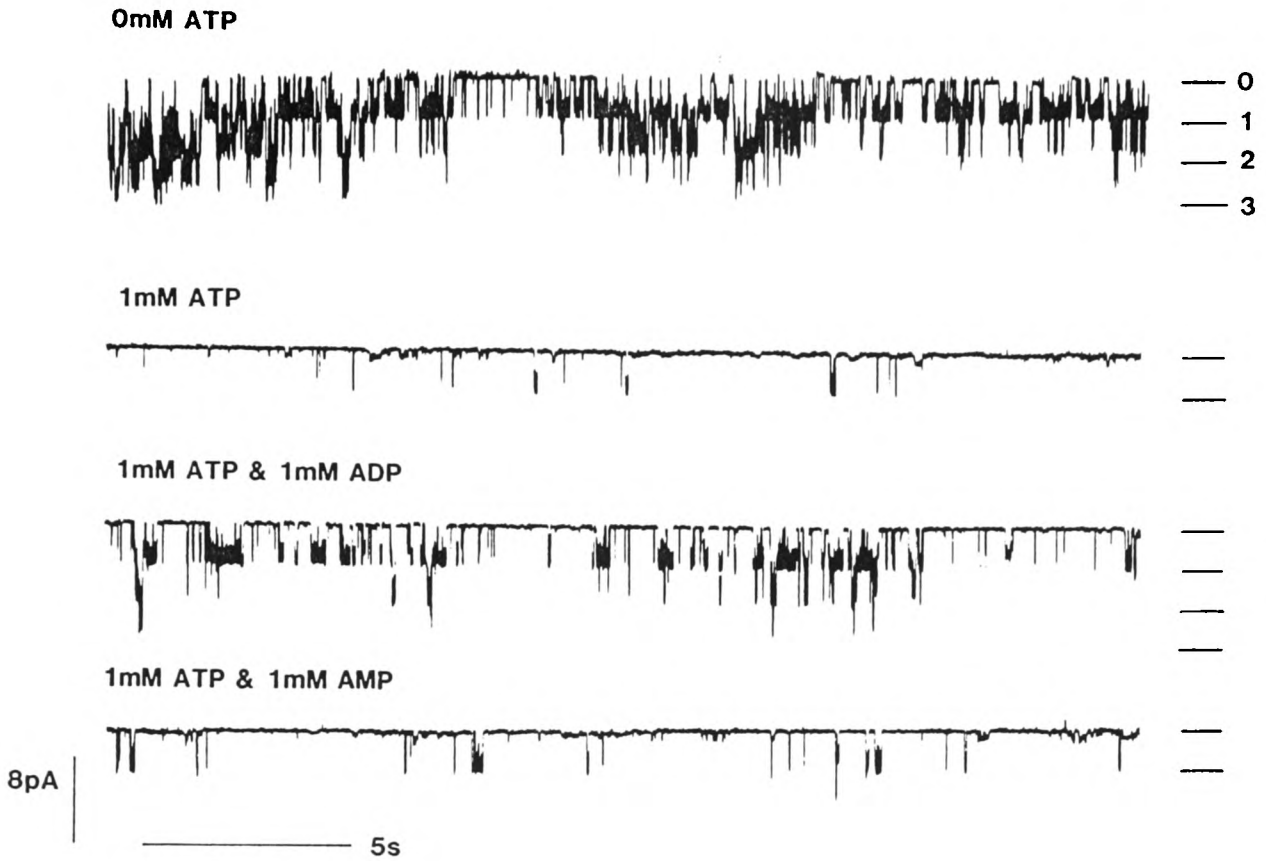
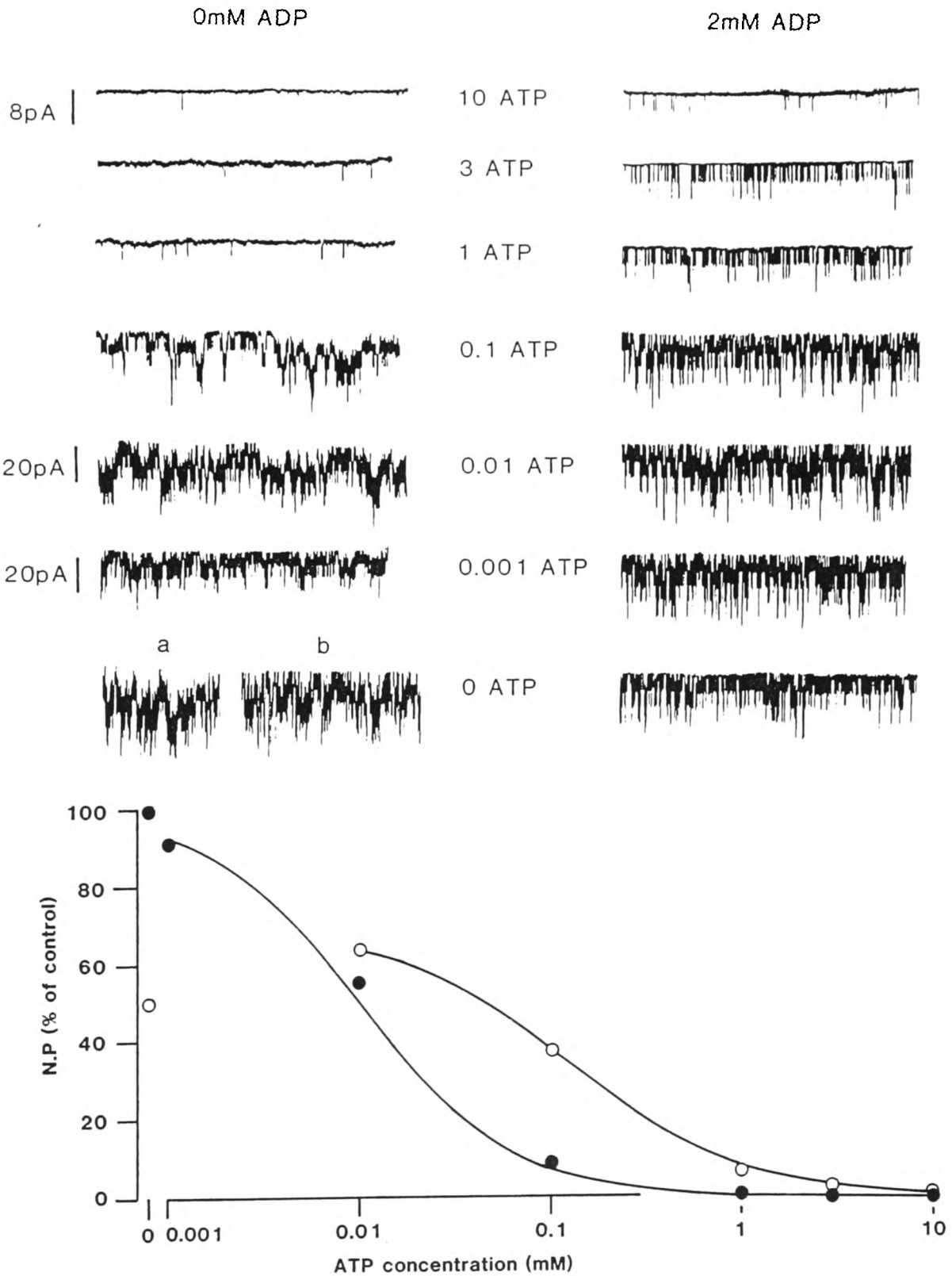


Figure 4.1. Effect of adenine nucleotides on single K^+ channel currents recorded at a membrane potential of -60 mV from an inside-out patch exposed to a 0 mM ATP control solution (a) and about 2 s after exposure to an intracellular solution containing 1 mM ATP (b), 1 mM ATP + 1 mM ADP (c) or 1 mM ATP + 1 mM AMP (d). The records are filtered by the chart recorder at about 300 Hz.

Figure 4.2. Effect of 2 mM ADP on the dose-response curve for the inhibitory action of ATP on the average current measured for a single patch. The upper part of the figure shows selected sections of the current recordings from which NP was calculated, and the lower panel shows the corresponding ATP dose-response curves. Filled circles, 0 mM ADP, open circles, 2 mM ADP. Channel activity is plotted as a percentage of that in the control solution (0 mM ATP, 0 mM ADP). Solutions containing ATP and/or ADP concentrations greater than 1 mM were adjusted to maintain a constant $[K]_i$.


0mM ADP
2mM ADP
8pA
10 ATP
3 ATP
1 ATP
0.1 ATP
20pA
0.01 ATP
20pA
0.001 ATP
a
b
0 ATP
100
80
60
40
20
0
N.P (% of control)
0
0.001
0.01
0.1
1
10
ATP concentration (mM)

RESULTS

ATP added to the intracellular face of inside-out membrane patches from rat ß-cells reduces channel activity in a dose-dependent manner. As shown in figure 4.1a,b, 1 mM ATP reduces the degree of channel activity by about 95%. Channel activity (NP) may be calculated from I = NPi where I is the mean value of the current during the recording period, i is the amplitude of the single channel current, N is the number of channels in the patch and P is the channel open probability. In this patch, NP was reduced from 0.77 to 0.048 by 1 mM ATP. Channel activity was partially restored however by addition of 1mM ADP to this solution (figure 4.1c, NP = 0.29). This result was oberved in each of seven patches. AMP did not reverse channel inhibition at either 1 mM (figure 4.1d, NP = 0.049, and 2 other patches) or 5 mM (2 patches). Adenosine (5 mM, n = 2) and phosphate (5 mM, n = 2) were also ineffective.

The dose-response curves for inhibition by ATP in the absence and presence of 2 mM ADP are shown in figure 4.2. The upper part of the figure shows selected stretches of the current recordings from which NP was calculated, and the lower panel shows the corresponding dose-response curves. In this patch, the half-maximal inhibitory concentration of ATP was 12 µM (2 mM Mg^{2+}); figure 4.2 also shows that ADP, in the absence of ATP, can inhibit channel activity, but is considerably less effective than ATP (50% inhibition by 2 mM ADP, compared with 12 µM ATP). In the presence of 2 mM ADP, the ATP dose-response curve is shifted to higher concentrations, with a half-maximal inhibition at 145 µM ATP. The curves through the data points are drawn to the equation:

$$y = y_{max} - y_{max}/(1 + [ATP]/K_i)^H.$$

where K_i is the ATP concentration giving half-maximal inhibition and H is the Hill coefficient. In the absence of ADP, y_{max} = 100, K_i = 12 µM and H = 1.1 (correlation coefficient of 0.996 when fitted using linear regression analysis to the logarithm of the data). In the presence of 2 mM ADP, y_{max} = 64, K_i = 145 µM and H = 1 (correlation coefficient, 0.993). In many patches it was not possible to construct an ATP dose-response curve either because of the simultaneous presence of a 20 pS K^+-channel or because of a decrease in the

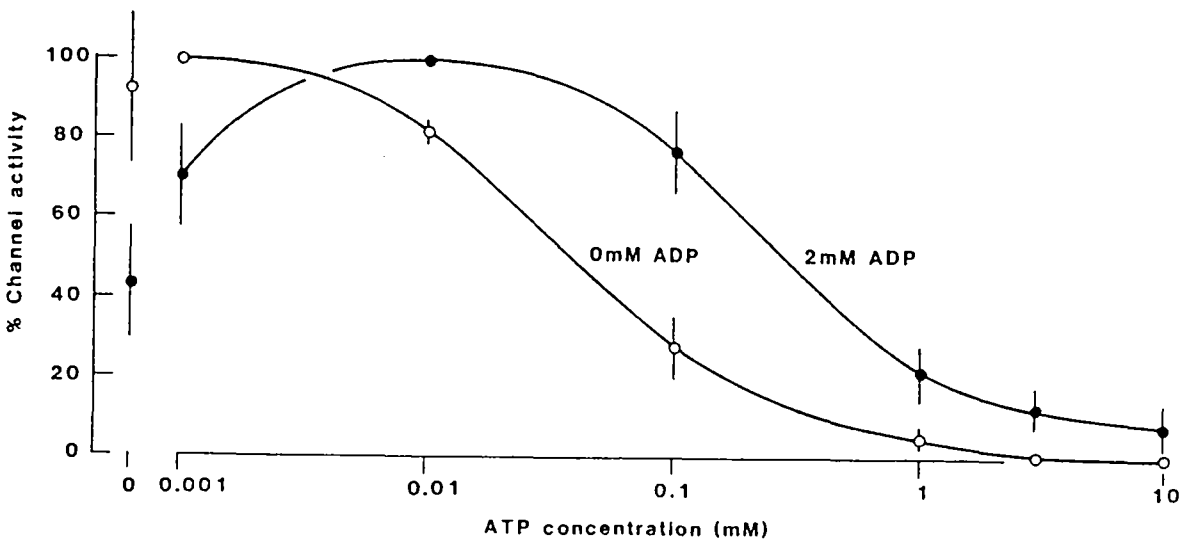


Figure 4.3. The mean ATP dose-response curves from three cells, normalized to the maximum NP in 0 mM or 2 mM ADP (at 0.001 mM ATP and 0.01 mM ATP) respectively.

	[ATP] (mM)	[ADP] (mM)	[ATP/ADP]
0 mM glucose	3.8 ± 0.2	1.5 ± 0.1	2.85 ± 0.12
20 mM glucose	5.3 ± 0.2*	1.0 ± 0.1*	5.52 ± 0.4*
% change	+39	-39	+94

* $p < 0.001$

Table 4.1

Effect of glucose on the concentration of adenine nucleotides in the rat ß-cell.

ATP and ADP were measured by a luciferase method, similar to that described in chapter 2. Results are expressed as the mean ± SE for 7 observations. Data provided by Dr. S.J.H. Ashcroft.

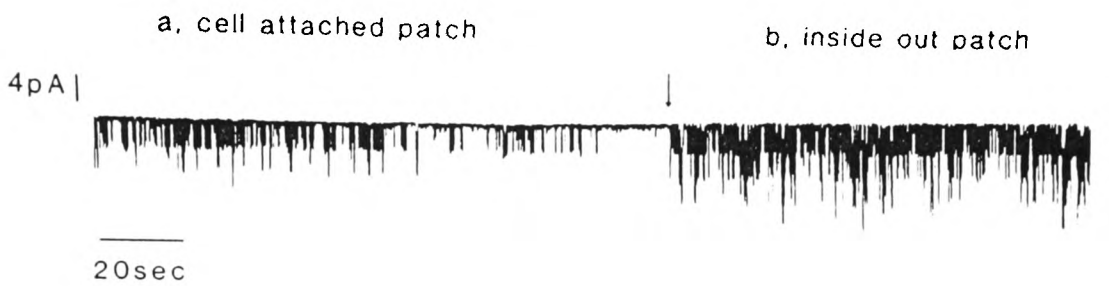


Figure 4.4. Single-channel currents recorded at a membrane potential of -60 mV before and after patch excision. The bath contained the standard intracellular solution plus 4 mM ATP and 1.5 mM ADP.

activity of the ATP-sensitive channel with time (rundown). The results shown in figure 4.2 are representative of three similar experiments for patches in which the 20 pS channel was absent and in which the activity of the ATP-sensitive channel did not decline with time. The mean ATP dose-response curves in the absence and presence of 2 mM ATP for these three patches are shown in figure 4.3. In this figure the curves are normalised so that the maximal activity in the presence or absence of ADP is taken as 100%. The figure clearly shows the rightward shift of the ATP dose-response curve produced by ADP, and also indicates that maximal channel activity occurs at an ATP concentration greater than zero, as if low concentrations of ATP activated the channel (Misler et al., 1986; Ohno-Shosaku et al., 1987; Findlay, 1987).

In a collaborative study, Dr. S.J.H. Ashcroft of the Nuffield Department of Clinical Biochemistry, John Radcliffe Hospital, Headington, measured the intracellular concentrations of ATP and ADP in the ß-cell, in the absence and presence of 20 mM glucose, at room temperature. The results are presented in Table 4.1. As glucose causes opposite changes in the concentrations of ATP and ADP, it produces a considerably larger change in the ATP/ADP ratio than in the concentration of either nucleotide, consistent with a role for the ATP/ADP ratio in determining the degree of channel activity in the intact cell.

To confirm that ADP_i might be sufficient to account for ATP-sensitive channel activity in the intact cell, a patch was excised from a ß-cell incubated for one hour in the absence of glucose into a solution containing ATP and ADP at concentrations chosen to approximate their measured total intracellular concentrations under the same experimental conditions (4 mM ATP and 1.5 mM ADP, Table 4.1). Channel activity did not decrease on excision (figure 4.4), suggesting that the measured ADP_i is able to relieve the inhibitory effect of 4 mM ATP_i.

DISCUSSION

Although it was already known, when the work in this chapter was performed, that glucose and ATP inhibited the same channel type in the ß-cell membrane it was not clear that ATP was the physiological second messenger for glucose-induced closure of the ATP-sensitive K^+-channel. The main objection to the idea was the apparent discrepancy between the activity of the channel in intact cells (with high ATP_i) and the extreme sensitivity of the channel to ATP in excised patches. The results presented in this chapter (and see also Dunne & Petersen, 1986a, Misler et al., 1986, Dunne et al., 1988b) indicated first that the ATP-sensitivity of the channel is reduced by ADP, and secondly that the channel is regulated by changes in the ATP/ADP ratio rather than simply by the absolute level of ATP. The first of these conclusions is supported by the luciferin/luciferase assay of the ADP concentration as 1.5 mM, a concentration sufficiently high to exert a significant relief of ATP inhibition (figure 4.4). In many cell types free ADP is thought to be much lower than total cellular ADP (< 100 µM), due to binding of ADP to cytosolic proteins (Hebisch et al.,1984; Gamkema et al., 1983). In the ß-cell, however, the ADP concentration measured by ^{31}P-NMR (~2 mM) is very similar to that measured by the luciferin/luciferase technique (Dunne et al., 1988b), implying that the ADP is not immobilised by binding. The second conclusion is supported by the reciprocal changes in ATP and ADP concentrations caused by glucose metabolism (Table 4.1, Malaisse & Sener, 1987), and by the findings of Dunne et al. (1988) that, in inside-out membrane patches from RIN cells, ATP-sensitive channel activity increased whenever the ATP/ADP ratio was decreased, and channel activity decreased whenever the ATP/ADP ratio was increased (Dunne et al., 1988b). These authors also found that relatively modest changes in ATP and ADP concentrations can produce clear changes in ATP-sensitive channel activity, supporting a role for the ATP/ADP ratio as the primary physological regulator of ATP-sensitive channel activity.

It has now been shown that it is free ATP^{4-} rather than MgATP which is the efficient regulator of ATP-sensitive channel activity (Kakei & Ashcroft, 1987, 1989; Dunne et al., 1987), and it has been shown that ADP^{3-} is capable of stimulation of ATP-sensitive channel activity in the presence of ATP, i.e. neither ATP inhibition nor ADP stimulation of ATP-

sensitive channel activity (in the presence of ATP) depend on protein phosphorylation (Ohno-Shosaku et al., 1987; Findlay, 1987; Dunne et al., 1988b). This is confirmed by those studies which have shown that non-hydrolysable analogues of ATP and ADP are effective in inhibiting or stimulating ATP-sensitive channel activity (Cook & Hales, 1984; Dunne & Petersen, 1986a; Misler et al., 1986; Ohno-Shosaku et al., 1987; Findlay, 1987; Ashcroft & Kakei, 1987, 1989; Dunne et al., 1988b). These effects are therefore distinct from the "refreshing" effect of ATP, which requires Mg^{2+} ions and which non-hydrolysable analogues of ATP are incapable of producing (Findlay & Dunne, 1986a; Misler et al., 1986; Ohno-Shosaku et al., 1987; Findlay, 1987; Ashcroft & Kakei, 1987, 1989).

Two other points concerning the ATP-sensitivity of ATP-sensitive channels are the discrepancy between the single-channel and whole-cell sensitivities and the open probability of the channel in the intact cell. In whole-cell wash-out experiments (human ß-cells: Ashcroft et al., 1989b) and in the "open cell" configuration (cardiac ventricular cell: Kakei et al., 1985; Noma & Shibasaki, 1985) concentrations of ATP < 0.3 mM have little inhibitory effect, while inside-out patches from the same preparations were highly sensitive to ATP. Similarly, ATP-depleted HIT cells demonstrate a tolbutamide-sensitive Rb efflux sensitive to ATP_i with a K_i of ~1.5 mM (Niki & Ashcroft, 1989). This discrepancy may well relect the conversion of ATP to ADP by cell metabolism (e.g. Jones, 1986).

From the data in this chapter, the expected p(open) of the ATP-sensitive channel can be calculated as 0.17% if 4 mM ATP were the only determinant of channel activity, and as 2.24% if the effect of 4 mM ATP were relieved by that of 2 mM ADP. In two HIT cell experiments in which 500 µM tolbutamide was applied to block the whole-cell washout current (chapter 5), NP immediately after going whole-cell was calculated to be 3% of that at the peak of the washout current. Hence, it would appear that most of the discrepancy between the observed and calculated p(open) can be accounted for by the modulatory effect of ADP.

Other nucleotides are also known to affect ATP-sensitive channel activity: various effects of GDP, GTP, NAD, NADH, NADP and NADPH have been reported, depending on the concentration used (Dunne & Petersen, 1986b; Dunne et al., 1988a). The intracellular

concentrations of these nucleotides will also contribute to the level of ATP-sensitive channel activity.

Finally, the possible role of diacylglycerol-mediated phosphorylation in stimulus-secretion coupling must be considered. It has been shown in the RINm5F cell line that glyceraldehyde stimulation increases the intracellular concentration of 1,2-diacylglycerol and that a phorbol ester (PMA) and a cell-permeable diacylglycerol analogue (DC_{10}) mimic the effect of glyceraldehyde in closing ATP-sensitive channels (Dunne & Petersen, 1987; Wollheim et al., 1988). The strength of the argument in favour of a major role of this pathway was increased by the demonstration that glyceraldehyde induces closure of ATP-sensitive channels in RIN cells before there is a significant increase in their ATP content (Wollheim et al., 1988). In the normal ß-cell, however, ATP does increase with sufficient speed to account for the inhibition of ATP-sensitive channels (Malaisse et al., 1979; Malaisse & Herchuelz, 1982), and , furthermore, a separate study on the RIN cell line found that the protein kinase C activator TPA *increased* ATP-sensitive channel activity (Ribalet et al., 1988). It is therefore still unclear what role DAG-stimulated phosphorylation might play in stimulus-secretion coupling in the normal ß-cell.

ATP-sensitive channels in the cell line HIT T15.

INTRODUCTION

In addition to playing a central role in glucose-stimulated insulin release (Ashcroft, 1988), the ATP-sensitive K^+ channel is the site of action of the sulfonamide drugs used in the treatment of NIDDM (rodent: Sturgess et al., 1985; Trübe et al., 1986; human: Ashcroft et al., 1987b; Sturgess et al., 1987; Ashcroft et al., 1989b) suggesting that a defect in the channel or its regulation may be implicated in the aetiology of diabetes (see chapter 7). Isolation and cloning of the channel would allow a more detailed understanding of the physiological and pharmacological regulation of the channel and a knowledge of its structure would facilitate the design of anti-diabetic drugs. The isolation of the channel requires a considerable quantity of ß-cell membrane, more than can conveniently be prepared from rodent islets. A suitable source of membrane appeared to be the SV40-transformed hamster ß-cell line HIT T15, which can be cultured to provide any desired quantity of material, which responds to glucose and which has frequently been used as a model in biochemical studies of stimulus-secretion coupling in the ß-cell (Santerre et al., 1981; Hill & Boyd, 1985; Boyd et al., 1985; Swope & Schonbrunn, 1984; Ashcroft et al., 1986; Ashcroft & Stubbs, 1987; Nelson et al., 1987; Hughes & Ashcroft, 1988). This chapter identifies and characterises the ATP-sensitive K^+ channel in the HIT T15 cell line.

METHODS

The whole-cell washout currents in figure 5.1 were obtained by holding the cell at a potential of -70 mV and giving alternate +10 mV and -10 mV 200 ms voltage pulses every 200 ms. The current elicited by this pulse protocol increased with time (in figure 1A) as ATP was washed out of the cell and ATP-sensitive channels were activated.

Amplitude histograms were constructed by digitizing the recorded current at a 5 kHz sample rate and sorting the digitized current amplitudes into 0.1 pA bins. The frequency per bin is plotted against amplitude in figures 5.3 and 5.4.

Open and closed time durations were determined from the current records after digitization at 5 kHz. The threshold for opening or closing was 50% of the single-channel amplitude determined from the amplitude histograms. Only stretches of recording with a single active channel were used for the determination of channel kinetics, and at least 30 s of channel activity was analysed for each histogram.

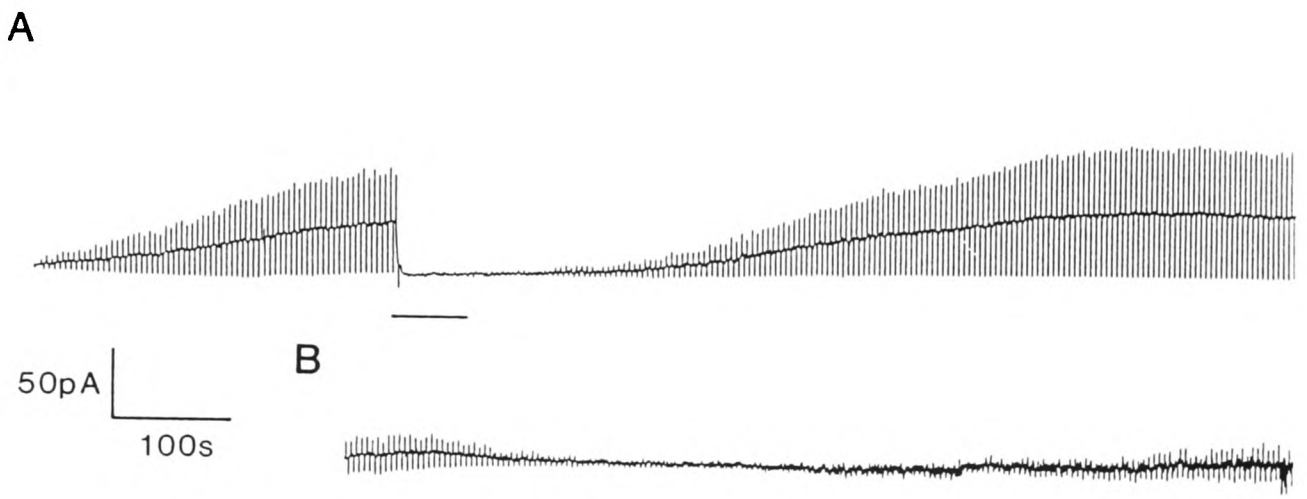


Figure 5.1. Effect of tolbutamide on whole-cell K-currents.
A . Whole-cell washout currents with a 0 mM ATP intracellular solution. The holding potential was -70 mV and current responses to ± 10 mV amplitude pulses appear as vertical lines due to the compressed time scale. 500 μM tolbutamide was added to the bath for the period indicated by the horizontal line.
B . Whole-cell currents recorded with 5 mM ATP, 0 mM ADP in the pipette solution. The initial input conductance decreases after rupture of the membrane as the intracellular ATP/ADP ratio increases due to dialysis of cellular contents with the pipette solution.

RESULTS

Whole-cell currents

The protocol developed by Trübe et al. (1986) was used to study ATP-sensitive K^+ currents in the whole-cell configuration. Cells were held at -70 mV and ±10 mV pulses were applied alternately at a frequency of 0.5 Hz. Most of the resulting current flows through ATP-sensitive K^+-channels since voltage-dependent currents are not activated by these low pulse amplitudes (Rorsman & Trübe, 1986) and activation of Ca-dependent K^+-channels (Findlay et al., 1985a) was prevented by buffering the free Ca^{2+} in the intracellular solution to <0.1 μM.

As observed for rodent ß-cells (Trübe et al., 1986), following establishment of the whole-cell configuration there was a progressive increase in the cell input conductance, as indicated by the increase in the current elicited in response to a 10 mV voltage step (Fig.1A). The input conductance increased from an initial value of 0.47 ± 0.11 nS to 6.44 ± 1.02 nS (n=9). This corresponds to a maximal washout conductance of 0.69 ± 0.1 nS/pF (9 cells; measured as maximum minus initial value). This increase in conductance can be interpreted as the opening of ATP-sensitive K^+-channels due to washout of ATP from the cell interior, because it was prevented by including 3 mM ATP in the pipette solution (6 cells, figure 1B).

The average cell capacitance was 8.5 ± 0.4 pF (n=19).

Sulphonylureas appear to act as selective inhibitors of ATP-sensitive K^+-channels in ß-cells (Trübe et al., 1986). We tested the effect of the sulphonylurea tolbutamide once the wash-out current was maximal. Figure 1A shows that 500 μM tolbutamide reversibly decreased the current response to a 10 mV pulse and the holding current required to maintain the cell at -70 mV. The input conductance was reduced by more than 95%, consistent with the dose-response relationship previously reported for ß-cells (Trübe et al., 1986; Sturgess et al., 1988; Zunckler et al., 1988a, 1988b; Ashcroft et al., 1989b).The change in holding current results from inhibition of the outward current flowing through ATP-sensitive K^+-channels and in an unclamped cell would produce membrane depolarization.

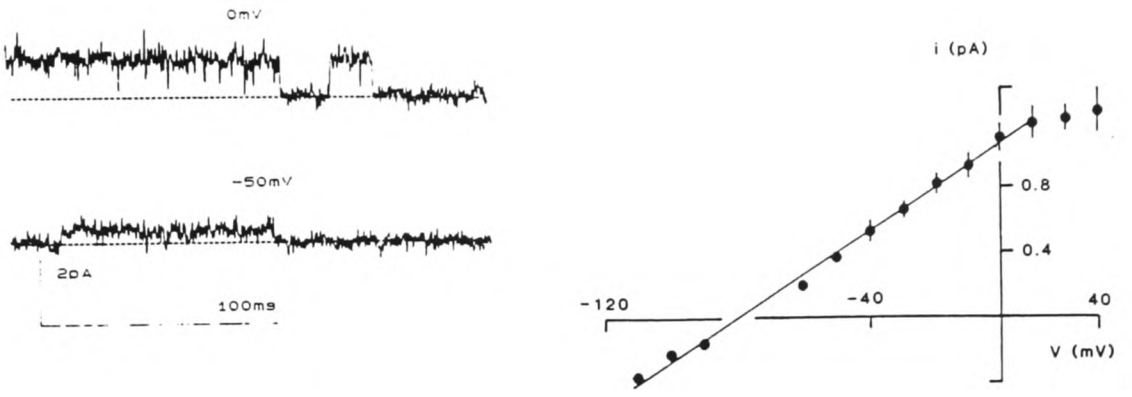
If the tolbutamide-sensitive current is taken as the maximal ATP-sensitive washout

Figure 5.2A. Single channel currents recorded at the indicated membrane potentials (left) and the corresponding mean IV for three cells from an inside-out patch with a pipette solution of 5 mM K^+. Intracellular solution, 130 mM K^+. The dashed line indicates the current level when the channel is closed. Sample rate 5 kHz, filter 2 kHz. The line through the data points at negative potentials has a slope of 13.5 pS.

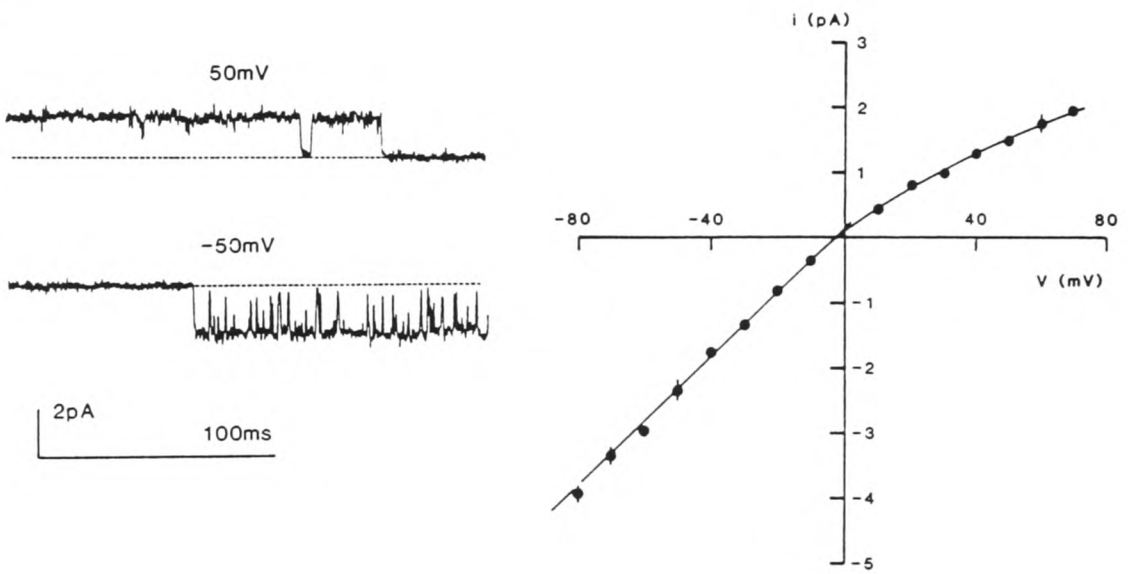
B. Single-channel currents and mean IV for 7 cells exposed to a 140 mM-K+ extracellular solution. Intracellular solution, 130 mM K^+. Filter 1 kHz.

C. Open and closed time histograms from a patch demonstrating activity of only a single channel; most of the open and closed intervals could be fitted with a single exponential.

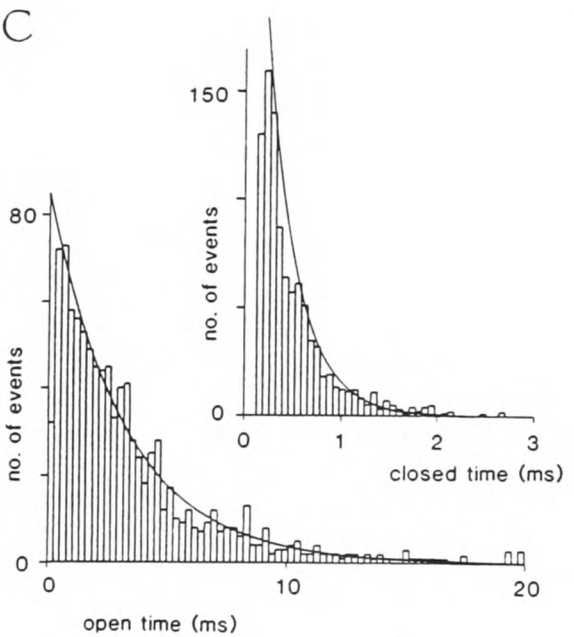
A


0mV
-50mV
2pA
100ms
i (pA)
0.8
0.4
-120
-40
40
V (mV)

B


50mV
-50mV
2pA
100ms
i (pA)
3
2
1
-80
-40
40
80
V (mV)
-1
-2
-3
-4
-5

C


150
80
no. of events
0
0
1
2
3
closed time (ms)
no. of events
0
0
10
20
open time (ms)

conductance, the mean p(open) of the ATP-sensitive channel immediately on going whole-cell (in two cells to which 500 μM tolbutamide was applied) was 3% of that at the peak of the washout current. This must be a high estimate of the channel open probability, as some increase in channel activity is likely to have occcured before the pulse protocol was started, as p(open) < 1 at the peak of the washout current, and as 500 μM tolbutamide may not have blocked 100% of the channels. This calculation is consistent with the great increase in channel activity seen on patch excision into ATP-free solutions (Findlay et al., 1985a) or when glycolytic or mitocondrial inhibitors are added to the ß-cell (Ashcroft et al., 1985; Misler et al., 1986; Ribalet & Ciani, 1987).

Inside-out patches

Following excision of the inside-out patch, the activity of ATP-sensitive K^+-channels initially increases, indicating that they are subject to resting inhibition in HIT T15 cells, as has been described previously for rodent ß-cells (Ohno-Shosaku et al., 1987; Misler et al., 1986) and ß-cell lines (Findlay & Dunne, 1986a) and as demonstrated by the whole-cell wash-out current (; figure 5.1). Subsequently, channel activity declines with time. This run-down of activity can be prevented by intermittent exposure of the patch to phosphorylating solutions containing MgATP (Ohno-Shosaku et al., 1987; Misler et al., 1986; Findlay & Dunne, 1986a). In the presence of MgATP channel activity is low but, as has been shown in chapter 4, it can be substantially increased by the addition of ADP. This nucleotide reduces the ATP-sensitivity of the channel in rat ß-cells (chapter 4; Kakei et al., 1986; Misler et al., 1986) and ß-cell lines (Dunne & Petersen, 1986a; Ribalet & Ciani, 1988). To prevent rundown of channel activity, the single channel properties were therefore measured in intracellular solutions containing 0.1 mM ATP, 0.1 mM ADP and 2 mM Mg^{2+}.

Figure 5.2A shows single channel currents (on the left) and the corresponding mean current voltage-relation (on the right) recorded from inside-out patches exposed to 140 mM K^+ internally and 5 mM K^+ externally. Figure 5.2B shows the single-channel currents and the current-voltage relation recorded in symmetrical 140 mM K^+ solutions. With 140 mM $[K^+]_o$,

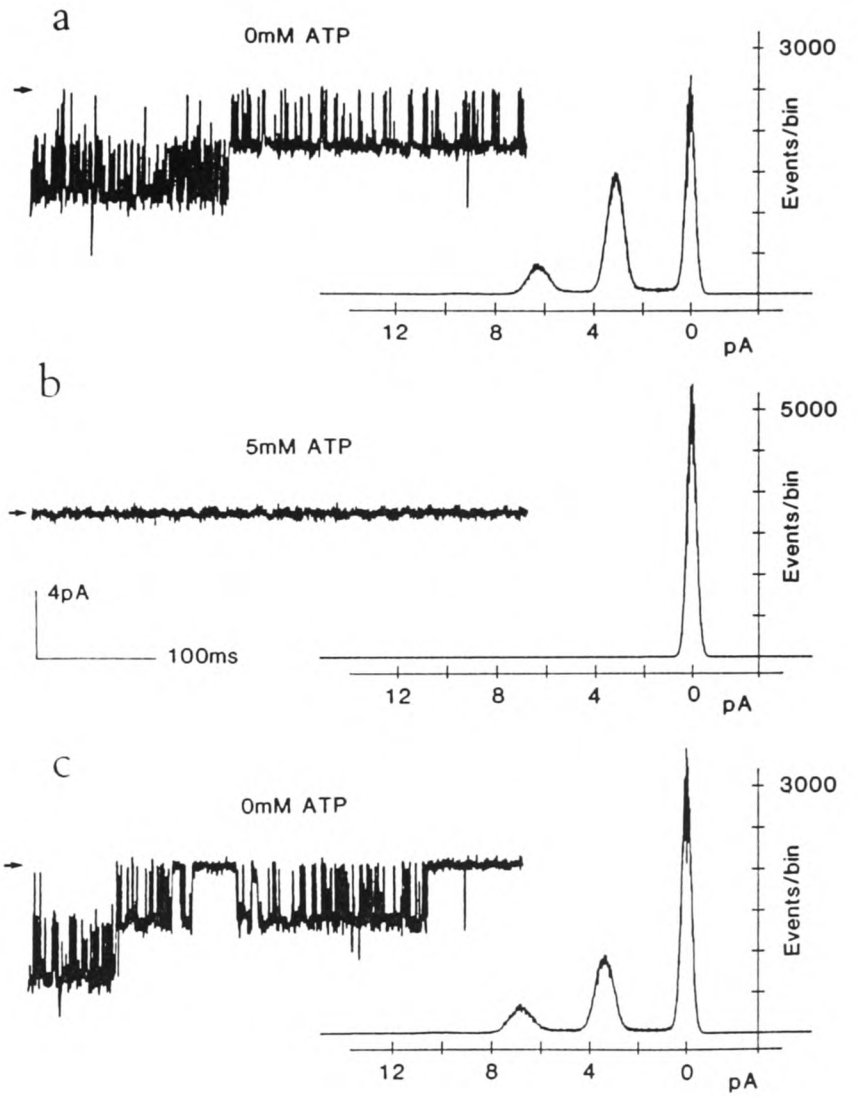


Figure 5.3. Single channel currents (inset) and associated amplitude histograms recorded at -60 mV from an inside-out patch before (**A**) during (**B**) and after exposure (**C**) to intracellular solution containing 5 mM ATP. The arrow indicates the closed channel current level. The numbers above the histogram peaks indicate the number of channels open. External solution: 140 mM K^+; intracellular solution: 130 mM K^+ internal. Sample rate 5 kHz, filter 2 kHz. Amplitude histograms were constructed from 30 s of data record in each case.

single channel currents reversed close to 0 mV, as expected for a K^+-selective channel. The mean slope conductance, measured between -80 mV and -10 mV, was 51.5 pS and the single channel permeability over the same voltage range was 0.83 x 10^{-13} cm^3 /s. These values are in good agreement with those reported previously for ATP-sensitive K^+-channels in ß-cells (chapter 3; Ashcroft, 1988). The rectification seen at positive potentials results partly from the presence of 1.3 mM free Mg^{2+} in the intracellular solution, as Mg^{2+} has been reported to produce a voltage-dependent block of outward currents through this channel (Findlay, 1987; Horie et al., 1987; Ciani & Ribalet, 1988).

Channel openings are grouped into bursts as previously described for ATP-sensitive K^+-channels in ß-cells (Ashcroft, 1988). Mean open and closed times (in 0.1 mM ATP + 0.1 mM ADP) within the burst were 3.8 ± 0.3 ms (n=5) and 0.68 ± 0.02 ms (n=5) respectively (-60 mV). These values are similar to those previously reported for inside-out patches from normal ß-cells; open times between 1.8 ms (Rorsman & Trübe, 1986) and 5.4 ms (Isenberg et al., 1988) and closed times of 0.3 ms (Rorsman & Trübe, 1986; Isenberg et al., 1988).

When $[K^+]_o$ was reduced to 5 mM, the reversal potential shifted to -78 mV (figure 2A), indicating that the channel is highly K^+-selective. The relative permeability to Na^+ (P_{Na}/P_K) was 0.01. This is close to that found for rat ß-cells (0.007, chapter 3; Ashcroft et al., 1989c; Trübe et al., 1986).

As shown in fig. 5.3, single channel currents were completely and reversibly blocked when the control intracellular solution (containing 0.1 mM ATP, 0.1 mM ADP and 2 mM Mg^{2+}) was replaced by 5 mM ATP. The same result was found in 9 other patches. Channel activity was greatly increased by intracellular solutions which lacked all adenine nucleotides, but the effect was transient as channel activity subsequently declined due to run-down. The ATP-sensitivity of the channel is similar to that found for other ß-cells with a reported K_D of 60 µM (Eddlestone et al., 1989).

It is well established that the sulphonylurea tolbutamide is a specific inhibitor of the ATP-sensitive K^+-channel in ß-cells (Trübe et al., 1986; Sturgess et al., 1988; Zunckler et al., 1988a; Ashcroft et al., 1989b). ATP has no effect on tolbutamide action, but ADP appears to

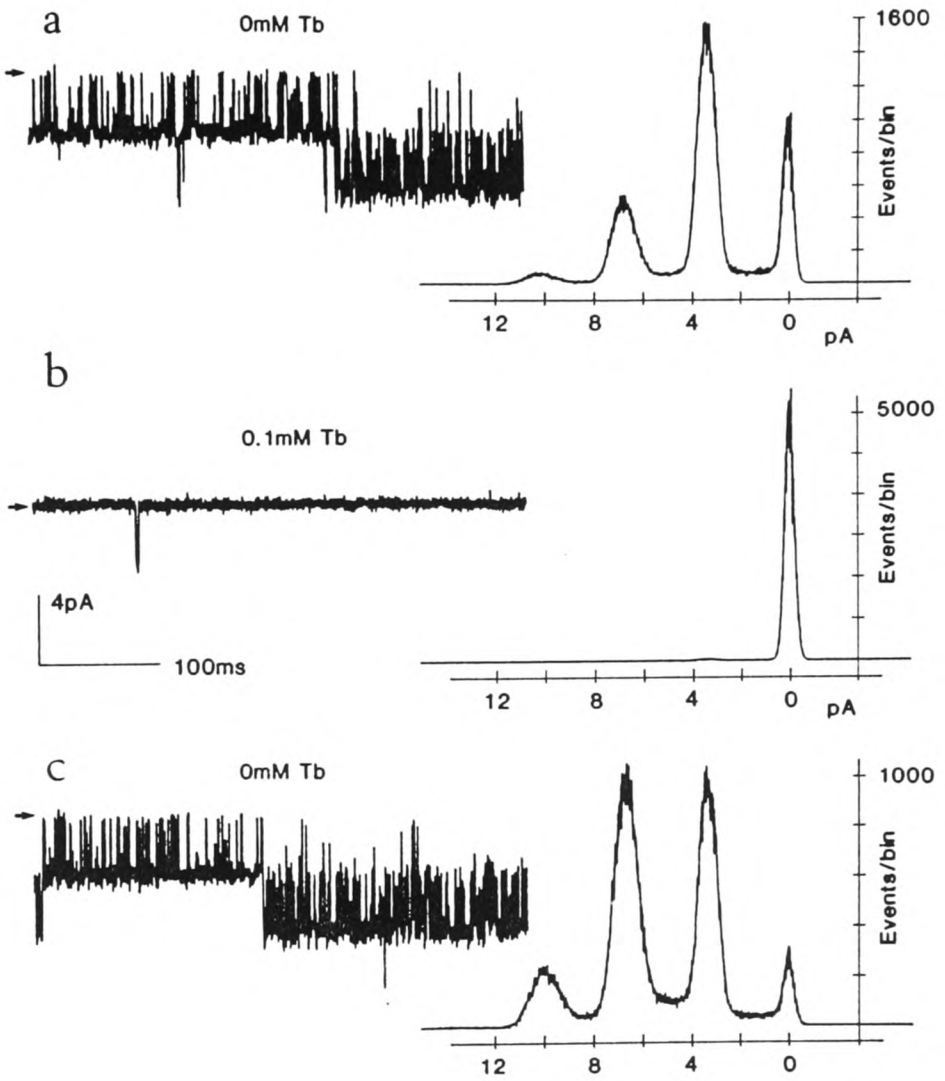


Figure 5.4. Single channel currents (inset) and associated amplitude histograms recorded at -60 mV from an inside-out patch before (**A**), during (**B**) and after (**C**) exposure to 100 μM tolbutamide. The arrow indicates the closed channel current level. The numbers above the histogram peaks indicate the number of channels open. External solution: 140 mM K^+; intracellular solution: 130 mM K^+ plus 0.1 mM ATP and 0.1 mM ADP (to prevent rundown). Sample rate 5 kHz, filter 2 kHz. Amplitude histograms were constructed from 30 s of data recording in each case.

facilitate inhibition by the drug (Zunckler et al., 1988b). Tolbutamide was applied in intracellular solution containing 0.1 mM ATP and 0.1 mM ADP (+ 2 mM Mg^{2+}). Figure 5.4 illustrates that 100 μM tolbutamide reversibly blocks single channel currents in HIT cell membranes. The same result was found in 6 other patches.

DISCUSSION

The aim of the present study was to characterize the ATP-sensitive K^+-channel of the HIT cell.

The electrophysiological properties of the ATP-sensitive K^+-channel described here closely resemble those reported for normal ß-cells and other ß-cell lines. Thus the channel is highly K^+-selective (P_K / P_{Na} ~ 0.01), has a conductance of ~50 pS in symmetrical 140 mM K^+ solutions and exhibits kinetics similar to those reported for rodent ß-cells. It is inhibited by intracellular ATP and by tolbutamide (applied from either side of the membrane).

A rough estimate of the number of ATP-sensitive channels per HIT cell can be made by combining the results of the whole-cell and single channel experiments using the equation

$$I = NPi$$

(where I is the whole-cell current, i the single channel current, P the open probability and N the number of channels). The maximum wash-out conductance in whole-cell recordings was around 7 nS and the single channel conductance under the same ionic conditions was 14 pS. Taking the maximum open probability as 0.8 (Ashcroft et al., 1988a), this suggests around 630 ATP-sensitive K-channels per HIT cell. This must be considered a minimum estimate, however: the actual number of channels will undoubtedly be higher since it is unlikely that the maximum open probability was achieved in the whole-cell recordings, both because chloride was the intracellular anion (Trübe et al., 1989) and because it was not possible to prevent rundown of channel activity completely in these experiments. If an open probability of 0.1 is taken (Rorsman & Trübe, 1989), the estimate rises to ~5000 channels per cell.

In a collaborative study, Drs Niki and Ashcroft of NDCB identified a high-affinity binding site (K_D = 1.2 nM) for glibenclamide in the HIT cell membrane, and obtained an estimate of about 5000 binding sites per cell. This binding site is likely to be the ATP-sensitive channel, and the low K_D indicates that the sulphonylureas will provide a suitable high-affinity ligand for channel isolation and purification.

Sulphonylurea binding is high in the brain, and Bernadi et al. (1988) have isolated a

sulphonylurea-binding protein which they postulate may be the ATP-sensitive K^+ channel. It is not certain, however, that this sulphonylurea-binding protein is the ATP-sensitive channel. Only one report of ATP-sensitive channels in the brain has appeared (Ashford et al., 1988), and those channels were not the normal ATP-sensitive channel, being dissimilar in selectivity, conductance, kinetics and ATP-sensitivity (Ashford et al., 1988). Sulphonylurea binding is particularly heavy in the substantia nigra (Moure et al., 1989), but neurones from this area show no ATP-sensitive washout current (Kapoor & Ashcroft, 1988, personal communication).

The results presented in this chapter suggest that the HIT T15 cell line is suitable as a source of material for isolation and purification of the ATP-sensitive K^+ channel, as it possesses a large number of normal ATP-sensitive channels, as it can be grown in large quantities and as specific binding of glibenclamide to HIT cell membranes has been demonstrated, with a number of binding sites similar to the estimated number of ATP-sensitive channels. Photoaffinity labelling by ^{3}H-glibenclamide of a 140-150 kDa protein has now been demonstrated, both in the HIT cell (Ashcroft & Ashcroft, 1989) and in membranes from RIN cells and from pig brain (Kramer et al., 1988; Bernadi et al., 1988). It is still possible that the sulphonylurea receptor is not the ATP-sensitive channel, but a regulatory protein closely associated with it. This question will have to be settled by reconstitution experiments.

Voltage-activated currents in rat ß-cells and the cell line HIT T15.

INTRODUCTION

The electrical activity of the pancreatic ß-cell, consisting of slow waves and action potentials (chapter one, figure 1.1), is underlain by potential-dependent currents. The rising phase of the Ca^{2+}-dependent ß-cell action potential has been attributed to the voltage-activated calcium current demonstrated in the neonatal rat ß-cell (Satin and Cook, 1985; 1986), in the rat insulinoma RINm5F (Findlay & Dunne, 1986b) and in the mouse ß-cell (Trübe & Rorsman, 1986; Rorsman & Trübe, 1986). In the mouse ß-cell (Rorsman & Trübe, 1986), this current can be activated at -40 mV and has a peak amplitude of ~40 pA (at -15 mV, in 2.56 mM Ca^{2+}). It inactivates slowly, is dihydropyridine sensitive and exhibits fast deactivation kinetics, properties similar to those of L-type calcium currents in other cells (e.g. Fox et al., 1987a). It seems likely that the slow waves too are supported by a voltage-activated Ca^{2+} current, as the slow waves are sensitive to $[Ca^{2+}]_o$ and to calcium agonists and antagonists (see chapter one for references), and as it has been shown that the rhythm of the slow waves in an intact islet can be reset by current injection via a suction electrode (Cook, Crill & Porte, 1980). This chapter investigates the nature and properties of the voltage-dependent currents, particularly the inward currents, in the rat ß-cell and in the hamster cell line HIT T15. Particular attention is paid to the mechanism(s) of calcium current inactivation and to the question of whether a second (low-threshold) type of Ca^{2+} current exists in the ß-cell.

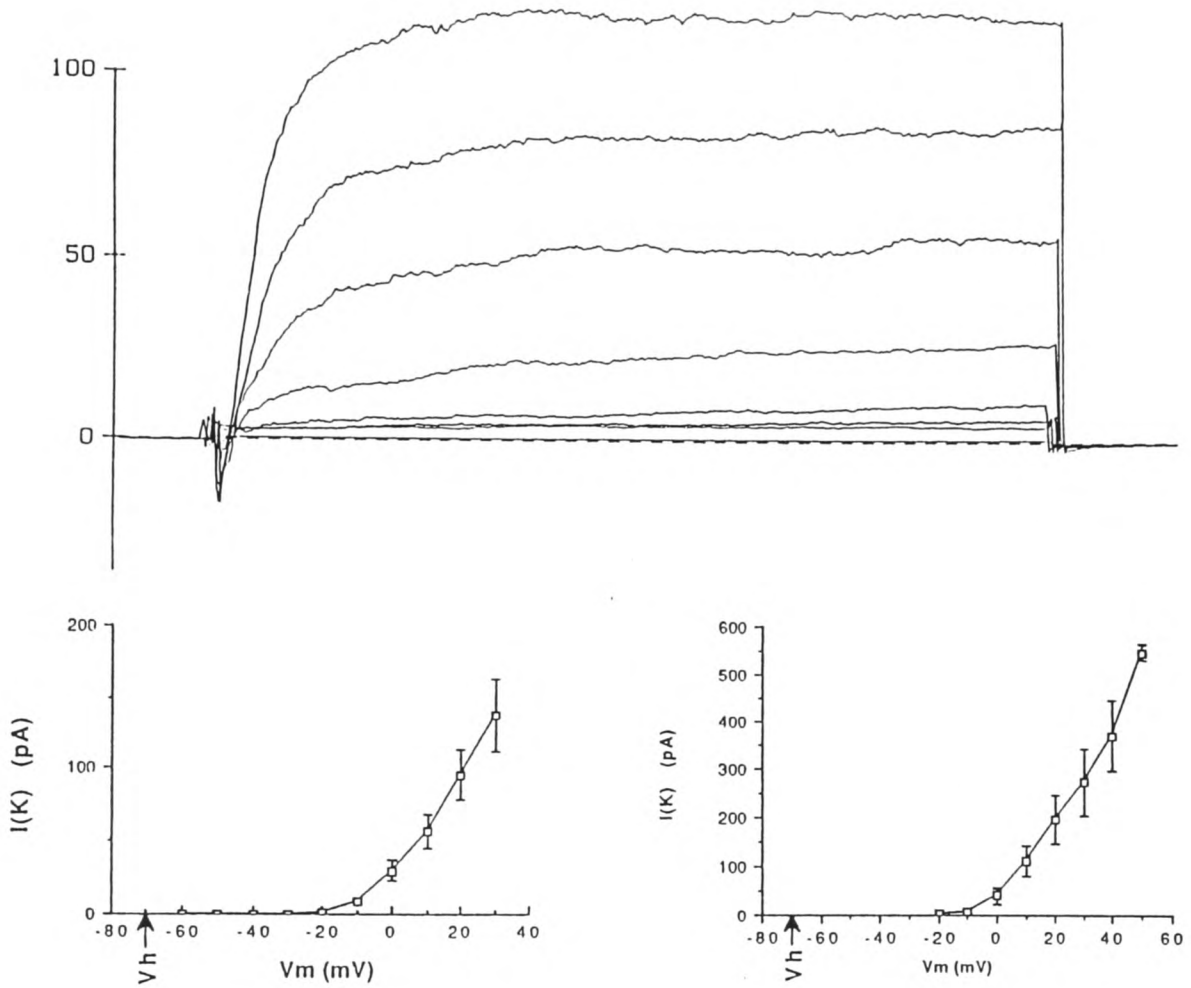


Figure 6.1. Voltage-activated outward currents.

A. Outward currents elicited in a HIT cell by 200 ms depolarising voltage steps from a holding potential of -70 mV. The pipette contained standard internal solution and 3 mM ATP. Digitised at 8 kHz, filtered at 1 kHz. The currents represent increments of 10 mV in the voltage pulses; the uppermost current was elicited at a membrane potential of +30 mV. The vertical scale is in pA.

B. Mean current-voltage relationships for the outward current in 7 HIT cells (left) and in 4 rat ß-cells (right).

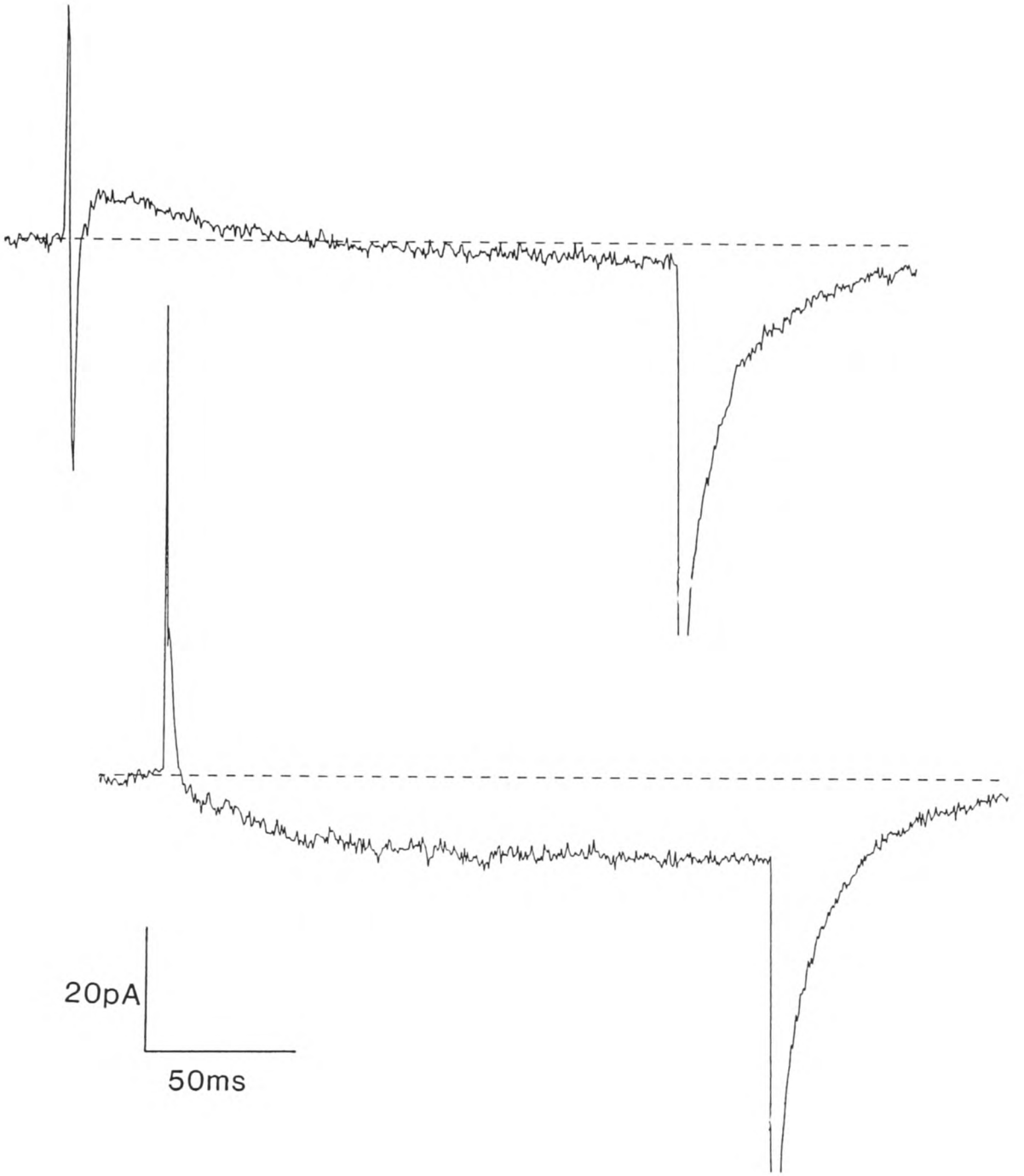
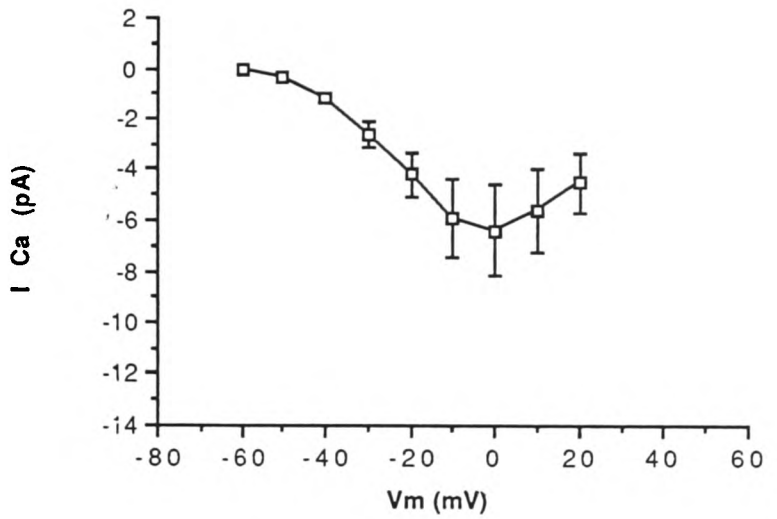
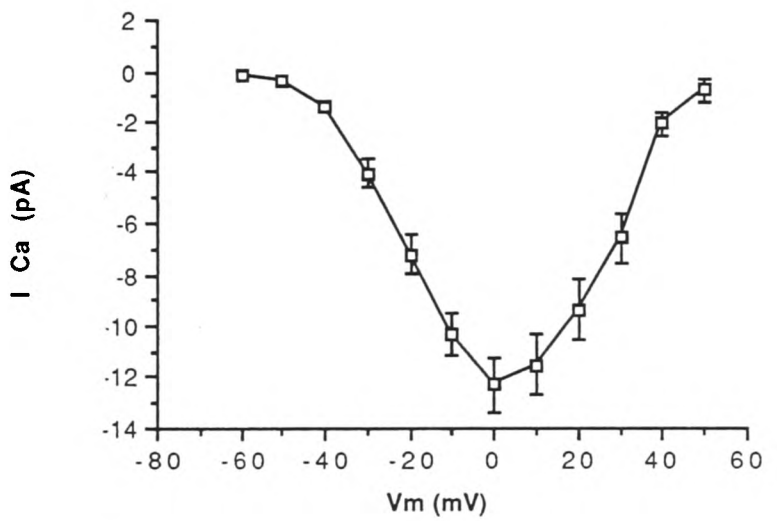
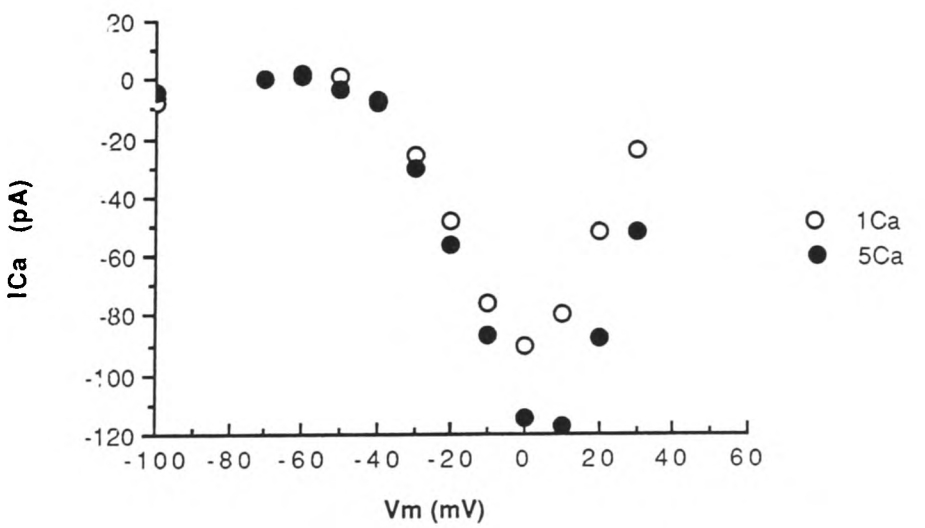


Figure 6.2. The effect of TTX.
Whole-cell currents elicited at 0 mV membrane potential, from a holding potential of -70 mV, recorded with a pipette solution containing 145 mM NMG (as are all the remaining whole-cell records in this chapter). 5 mM Ca external solution, before (**A**, upper record) and after (**B**, lower record) addition of 10 μM TTX. The upper record was made shortly after rupture of the membrane: the smaller amplitude of the inward current can be attributed to a potassium leak

Figure 6.3. The effect of external Ca^{2+} on inward current amplitude. Mean IV curves from HIT cells in 1 mM Ca^{2+} (**A**, top IV) or 5 mM Ca^{2+} (**B**, middle IV) The bottom record (**C**) shows IV's from one cell in which the current-voltage relation was recorded first in 1 mM Ca^{2+} and subsequently in 5 mM Ca^{2+}.


I Ca (pA)
2
0
-2
-4
-6
-8
-10
-12
-14
-80
-60
-40
-20
0
20
40
60
Vm (mV)


I Ca (pA)
2
0
-2
-4
-6
-8
-10
-12
-14
-80
-60
-40
-20
0
20
40
60
Vm (mV)


ICa (pA)
20
0
-20
-40
-60
-80
-100
-120
-100
-80
-60
-40
-20
0
20
40
60
Vm (mV)
1Ca
5Ca

RESULTS

Depolarising voltage steps in the whole-cell mode of patch-clamping in rat or HIT cells elicit both inward and outward currents (figure 6.1). With standard internal solution in the pipette, the delayed outward currents are much larger than the inward currents (at least, at potentials more positive than about -20 mV), as can be seen from the current records in figure 6.1A. Similar currents were observed in both rat ß-cells and HIT cells. This delayed outward current was not investigated in detail in these cells: it was taken to be a potassium current because of its similarity to the potassium currents of human (Ashcroft et al., 1989a; chapter 7) and mouse (Rorsman & Trübe, 1986; Plant, 1987) ß-cells, and because it was abolished when internal K^+ was replaced by the impermeant cation N-methyl glucamine (NMG), (figure 6.2). The current-voltage relation for this outward current is plotted in figure 6.1B.

The nature of the inward currents was investigated in both rat ß-cells and in HIT cells, but more extensively in HIT cells. Outward currents were abolished by replacing internal potassium with NMG. The inward current elicited by depolarising voltage steps from a holding potential of -70 mV was similar in both rat ß-cells and HIT cells, except that HIT cells often exhibited an initial spike-like component of inward current (figure 6.2A) which was absent from rat cells. This initial component was rapidly, completely and reversibly blocked by 10 µM TTX (figure 6.2B; reversal not shown), suggesting that it was carried by Na^+ ions. The nature and properties of this current were not further investigated, and all remaining experiments on HIT cell currents were carried out in the presence of 10 µM TTX.

The slow time-course of the TTX-insensitive currents suggested that they were carried by Ca^{2+} channels, which are known to inactivate only slowly (Rorsman & Trübe, 1986; Plant, 1987). This was confirmed by changing the external calcium ion concentration. Figure 6.3 shows the IV relations for the inward current in the HIT cell in 1 mM Ca^{2+} (A) and 5 mM Ca^{2+} (B). The current in 1 mM Ca^{2+} is smaller than that in 5 mM Ca^{2+} (the maximum current amplitudes being 7.0 $\pm$ 1.5 pA in 1 mM Ca^{2+} (n = 7) compared with 12.3 $\pm$ 1.1 pA in 5 mM Ca^{2+} (n = 12)), and the current-voltage relation is shifted to more negative potentials. This latter effect is probably due to increased screening of negative surface charges by higher

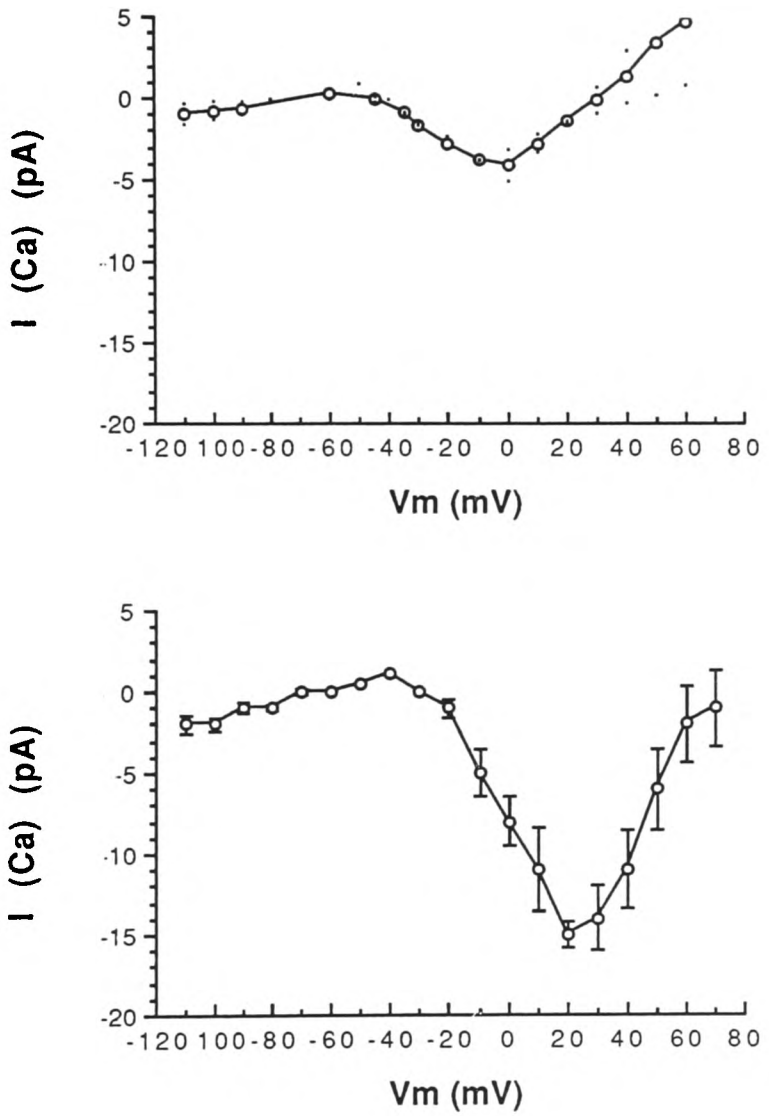
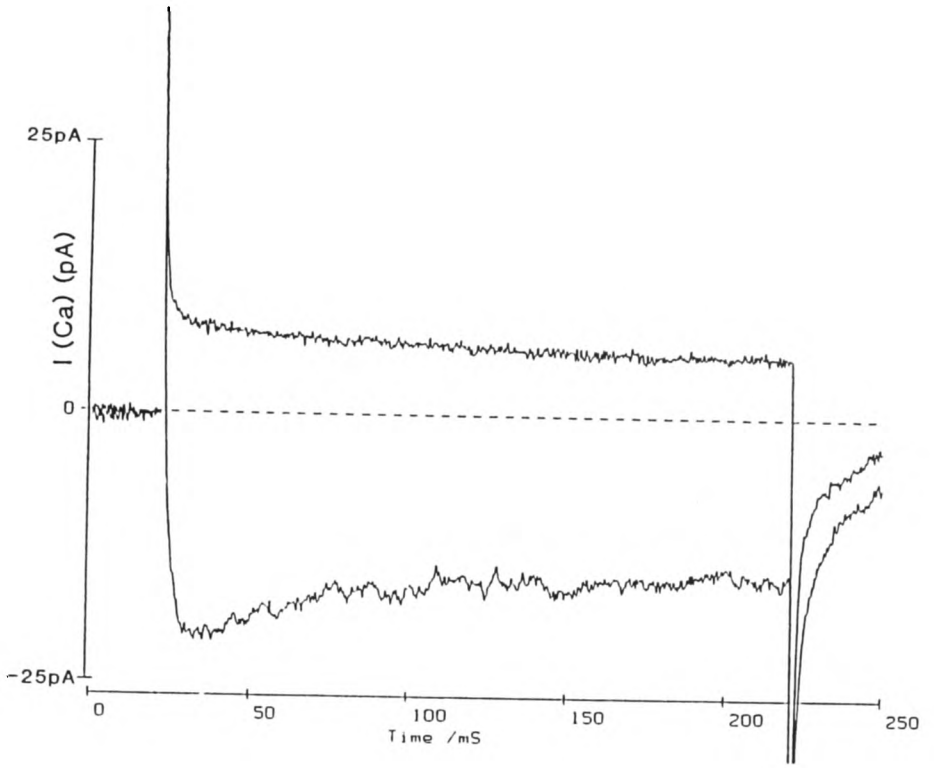
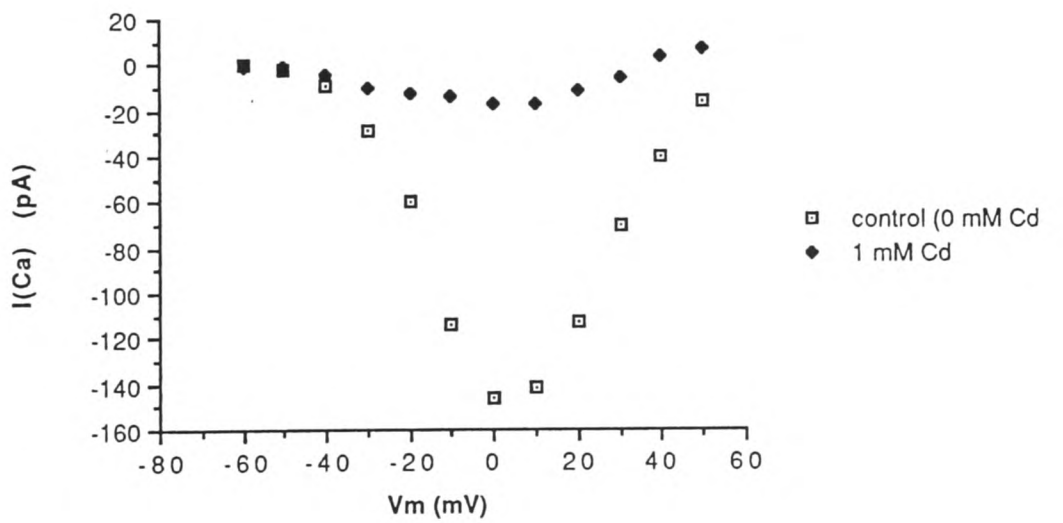
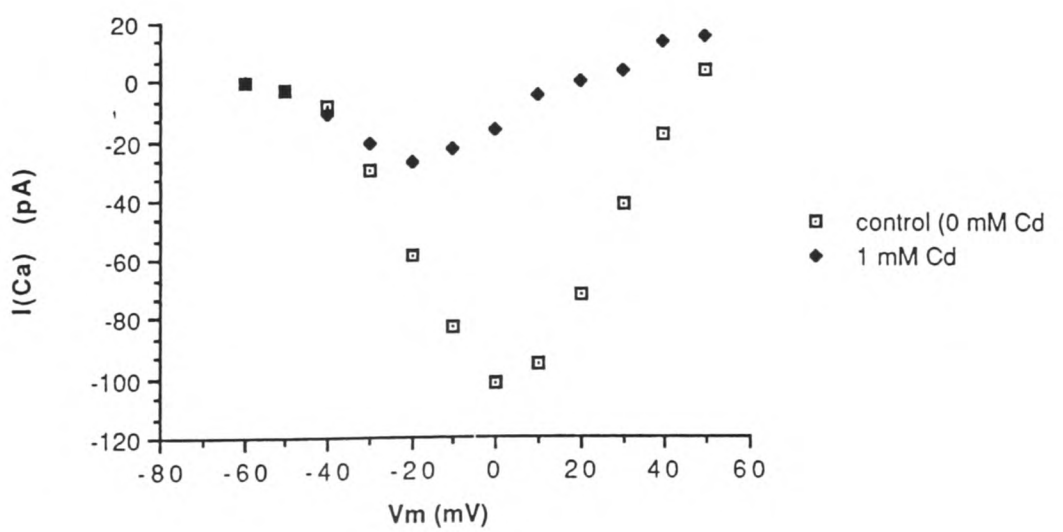


Figure 6.4. The effect of external Ca^{2+} on inward current amplitude in the rat ß-cell. Mean IV curves from rat ß-cells in 5 mM Ca^{2+} (**A**, top IV) or 20 mM Ca^{2+} (**B**, lower IV, n = 3). The upper IV is a mean from only two cells: the individual current amplitudes are indicated by the smaller dots.

Figure 6.5. The effect of Cd^{2+} on Ca^{2+} currents in the HIT cell.
A. Block of a current elicited at a membrane potential of 0 mV. Cd^{2+} block was probably not complete: a component of tail current remains.
B, C. Current-voltage relations for two HIT cells before and during block of I(Ca) by Cd^{2+}. The concentration of Cd^{2+} at the cell is likely to have been considerably lower than 1 mM.


25pA
I (Ca) (pA)
0
-25pA
0
50
100
150
200
250
Time /mS


20
0
-20
-40
-60
-80
-100
-120
-140
-160
I(Ca) (pA)
-80
-60
-40
-20
0
20
40
60
Vm (mV)
control (0 mM Cd
1 mM Cd


20
0
-20
-40
-60
-80
-100
-120
I(Ca) (pA)
-80
-60
-40
-20
0
20
40
60
Vm (mV)
control (0 mM Cd
1 mM Cd

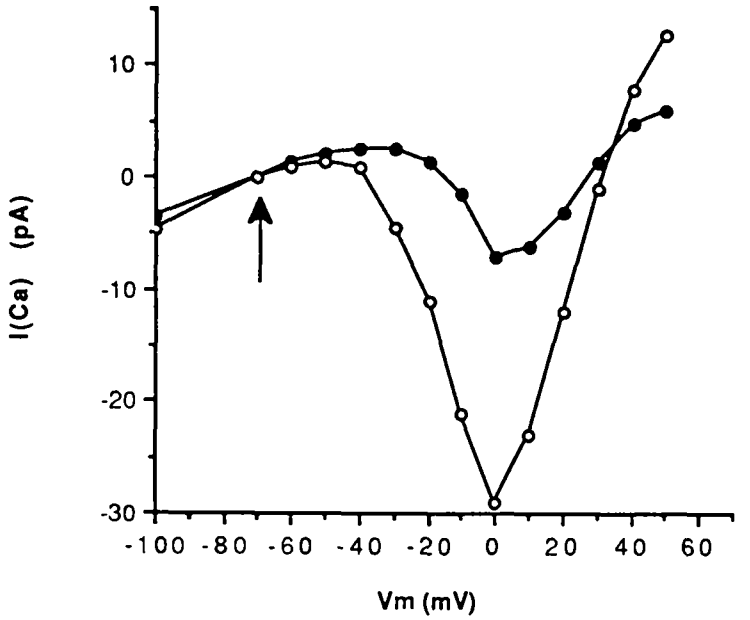


Figure 6.6. The effect of nifedipine on I(Ca).
Current-voltage relations from a HIT cell during incubation in 50 μM nifedipine (filled circles) and during recovery from nifedipine (open circles). The arrow indicates the holding potential (-70 mV). The solution in the bath contained 5 mM Ca. Pulse frequency, 0.5 Hz. The experiment was done in a darkened room and the nifedipine solution reservoir and tubing were shielded from light.

calcium concentrations (Weidmann, 1955; Frankenhauser & Hodgkin, 1957; Frankenhauser, 1957), and is most easily seen in the superimposed current-voltage relations from those cells where the IV relation was obtained in both 1 mM and 5 mM Ca^{2+}, as shown in figure 6.3C.

A similar phenomenon is seen in the inward currents in rat cells: figure 6.4 shows the current-voltage relation for rat ß-cells in 5 mM and in 20 mM Ca^{2+}. Again the current is larger (I_{max} = 4.1 ± 1.3 pA/pF (2 cells) in 5 mM Ca^{2+}, I_{max} = 15.2 ± 0.8 pA/pF, (n = 4) in 20 mM Ca^{2+}, not corrected for leak) and is shifted to more positive potentials in the higher Ca (I_{max} at ~0 mV in 5 mM Ca^{2+}, at ~15 mV in 20 mM Ca^{2+}).

The slow inactivation time-course of the calcium current in the ß-cell is similar to that reported for L-type calcium currents in other cell types (figure 6.5A; Nowycky et al., 1985; Cavalie et al., 1986; Droogmans & Callewaert, 1986). (Calcium current inactivation is considered at much greater length in chapter seven). The effects of cadmium and of nifedipine, both of which are known to be effective blockers of L-type currents are shown in figures 6.5 and 6.6. Figure 6.5A shows currents elicited in a rat ß-cell by depolarising steps to 0mV before and after application of 1mM Cd^{2+} from a puffer pipette placed close (~ 20 µm) to the cell. A similar block by cadmium was seen in rat ß-cells (n = 6). Figure 6.5B shows IV curves from two HIT cells before and during application of cadmium, while figure 6.6 shows similar IV curves demonstrating block by 50 µM nifedipine. In those cells where only a partial block of Ca^{2+} current by Cd^{2+} was observed, (as in the lower cell in figure 5B), the block appeared to be more effective at positive potentials. (The difference between the two cells in the degree of block is probably due to a difference in the concentration of Cd^{2+} at the cell.) The same result was found by Satin & Cook (1988), who attributed it to the presence of two populations of Ca channels in the ß-cell - suggesting that most of the Ca^{2+} current at more negative potentials is carried through T-type Ca^{2+} channels, which are known to be less sensitive to block by Cd^{2+} (Bean, 1989).

Like L-type Ca^{2+} currents in other cells (Cavalie et al., 1986; Belles et al., 1988), the ß-cell Ca^{2+} current runs down with time: this phenomenon is illustrated in figure 6.7, where the amplitude of the current elicited by a depolarisation to 0 mV is plotted against time after

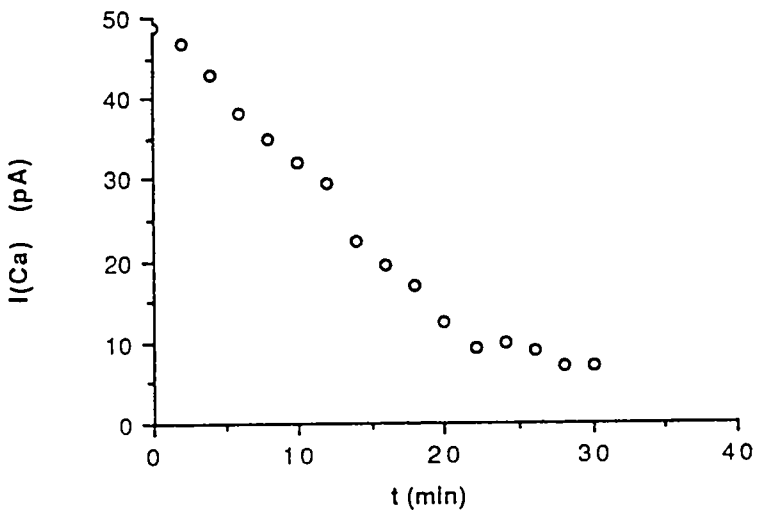


Figure 6.7. Rundown of I(Ca).
Time-course of the decline in inward current amplitude; currents elicited by 200 ms depolarisations to 0 mV from a holding potential of -70 mV in a rat ß-cell. The bath solution contained 20 mM Ca^{2+} and the pipette 5 mM EGTA and 3 mM ATP. Room temperature.

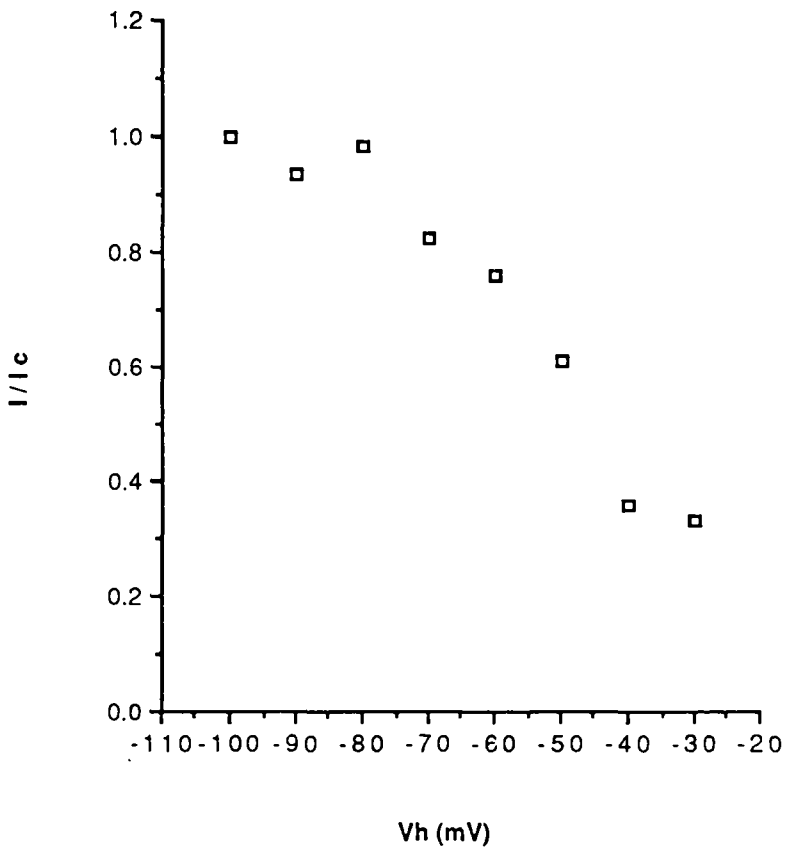


Figure 6.8. Inactivation of I(Ca) at depolarised holding potentials.
The peak amplitude of the inward current elicited by depolarising voltage steps to 0 mV is plotted against the holding potential. 5 mM Ca^{2+} in the external solution.

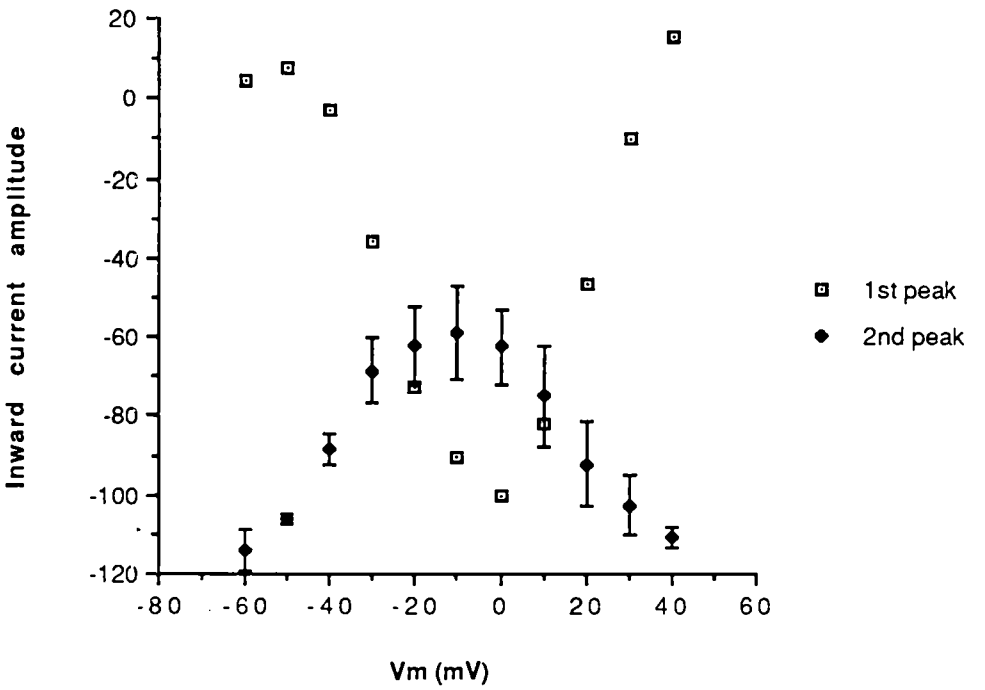


Figure 6.9. Inactivation of I(Ca) in double-pulse experiments.
HIT cells in 5 mM Ca^{2+}_o. The protocol is described in the text, and currents obtained in a similar experiment on human ß-cells are shown in figure 7.9. 5 mM EGTA in the pipette solution. The SEM is not shown for the prepulse IV, to avoid cluttering the figure.

finishing compensating the capacitance of the cell. The current in the rat ß-cell was reduced to 50% of the initial amplitude in about 15 min.

Inactivation

The inactivation properties of the calcium current were investigated using two separate protocols. In the first of these, the IV curve was determined in a HIT cell from a series of holding potentials between -100 mV and -30 mV; in each case the IV protocol was started immediately after changing the holding potential, and the pulse to 0 mV occurred about 15 s after the change. In figure 6.8 the maximum amplitude of the inward current elicited by depolarising voltage steps to 0mV is plotted as a function of holding potential. The maximum amplitude of the inward current is constant for holding potentials below -80 mV, but decreases as the holding potential is made more positive: it is half-inactivated at roughly -45 mV.

A second protocol investigated the presence of calcium-dependent inactivation in the ß-cell. In this protocol (Eckert & Tillotson, 1981; Eckert & Chad, 1986) a 150 ms prepulse of variable amplitude was followed by a 200 ms test pulse to 0 mV after a 10 ms gap. The mean peak amplitudes of both the prepulse current and the test current from three HIT cells are plotted on the same axes in figure 6.9. The abscissa represents the potential during the prepulse and the ordinate the current amplitude. As the amplitude of the current during the prepulse increases, the amplitude of the test current decreases, and for voltage steps to positive potentials the amplitude of the current during the prepulse decreases, (as the potential approaches E_{Ca}) while the amplitude of the current during the test pulse recovers. This recovery is most probably due to the decrease in calcium entry during the prepulse, and is an indication of calcium current inactivation by a mechanism dependent on calcium entry.

The fact that the peak currents during the second (test) pulse are larger than those during the first pulse suggests that the 10 ms gap used was not sufficiently long to allow the activation parameter of the inward current to return to its resting state: this was rather surprising as the inward current was seen to deactivate completely within a couple of ms in these experiments and deactivation time constants in the order of 200 µs have been reported for the Ca^{2+} current

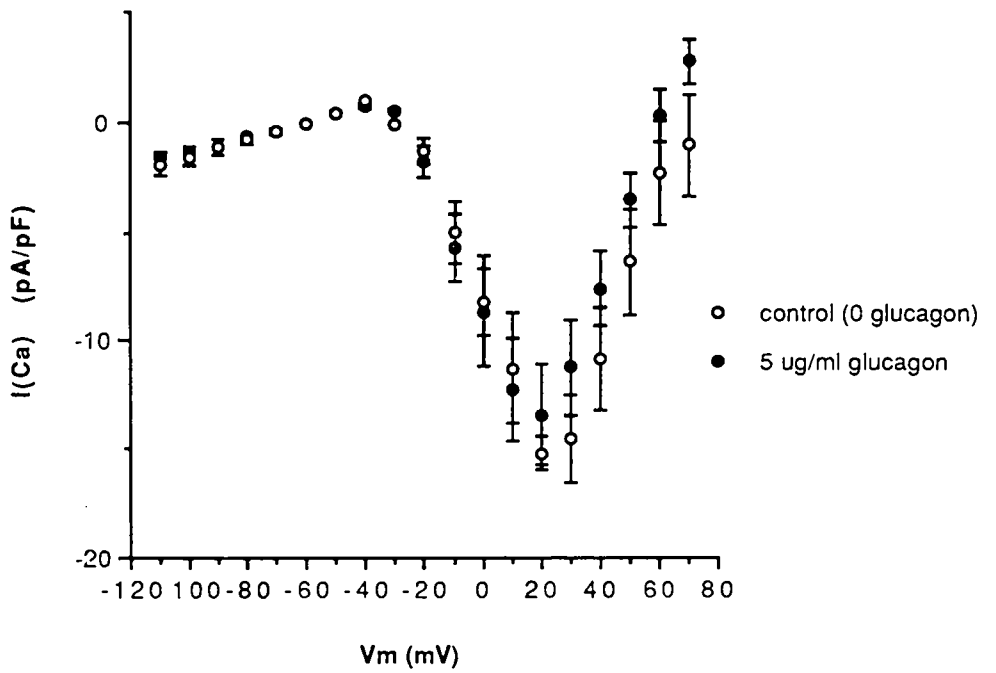


Figure 6.10. The effect of glucagon on I(Ca).
Mean current-voltage relations for 3 control cells and 4 cells in 5 μg/ml glucagon (20 mM Ca^{2+}). Room temperature. NMG internal solution with 3 mM ATP, 0 mM GTP. The control data are also used for figure 6.4.

in mouse and rat ß-cells (Rorsman & Trübe, 1986; Hiriart & Matteson, 1988); this persistent activation could indicate more than one step between the open and "fully closed" states for the ß-cell Ca^{2+} current (Brown et al., 1982; Fenwick et al., 1982; Cavalie et al., 1986).

(Fenwick et al. (1982) argued against the idea that similar evidence in the chromaffin cell indicated an excess of "less closed" states, but their results differ in several respects from those presented here. The results in this chapter could be explained by either a residual increase in the number of partially activated channels or a small shift of the voltage dependence of channel activation as suggested in Fenwick et al. (1982).)

Effect of glucagon

Glucagon potentiates insulin secretion from the rat ß-cell (chapter 2, also e.g. Pipeleers et al., 1985 for a potentiating effect of glucagon on insulin secretion from a population of pure dispersed ß-cells) and the HIT T15 cell line (Ashcroft et al., 1986). Glucagon increases electrical activity (Ikeuchi &Cook, 1984) and is known to increase the intracellular concentration of cyclic AMP (Schuit & Pipeleers, 1985; Gorus et al., 1988). As cAMP increases L-type calcium currents in other cells via phosphorylation of the calcium channel (e.g. cardiac myocytes: Kameyama et al., 1985), it was investigated whether glucagon increased the calcium current in the rat ß-cell. In initial experiments, inward currents were elicited by stepping the membrane to 0 mV for 200 ms once every 2 s, first in a standard external solution (control) and then as the bath solution was exchanged for a solution containing 5 µg/ml glucagon. It was impossible to see if glucagon had any effect, however, because the amplitude of the current was prone to run-down, and run-down was accentuated by solution exchange, independently of any effect of glucagon. Therefore, the protocol was changed, and the calcium currents in cells in an external solution containing glucagon were compared with those in cells in a control solution. The IV curves for 4 cells in glucagon and 3 control cells are shown in figure 10. No difference was observed between the two sets of cells: activation threshold (-40 to -30 mV) and peak amplitude (15.19 $\pm$ 0.76 pA/pF for the controls, 13.39 $\pm$ 2.31 pA/pF in glucagon) were unchanged, the time-courses of the currents were very similar and the holding current (at -60mV) was unchanged (3.2 $\pm$ 1.1 pA/pF for the controls, 3.75 $\pm$ 0.9 pA/pF in glucagon).

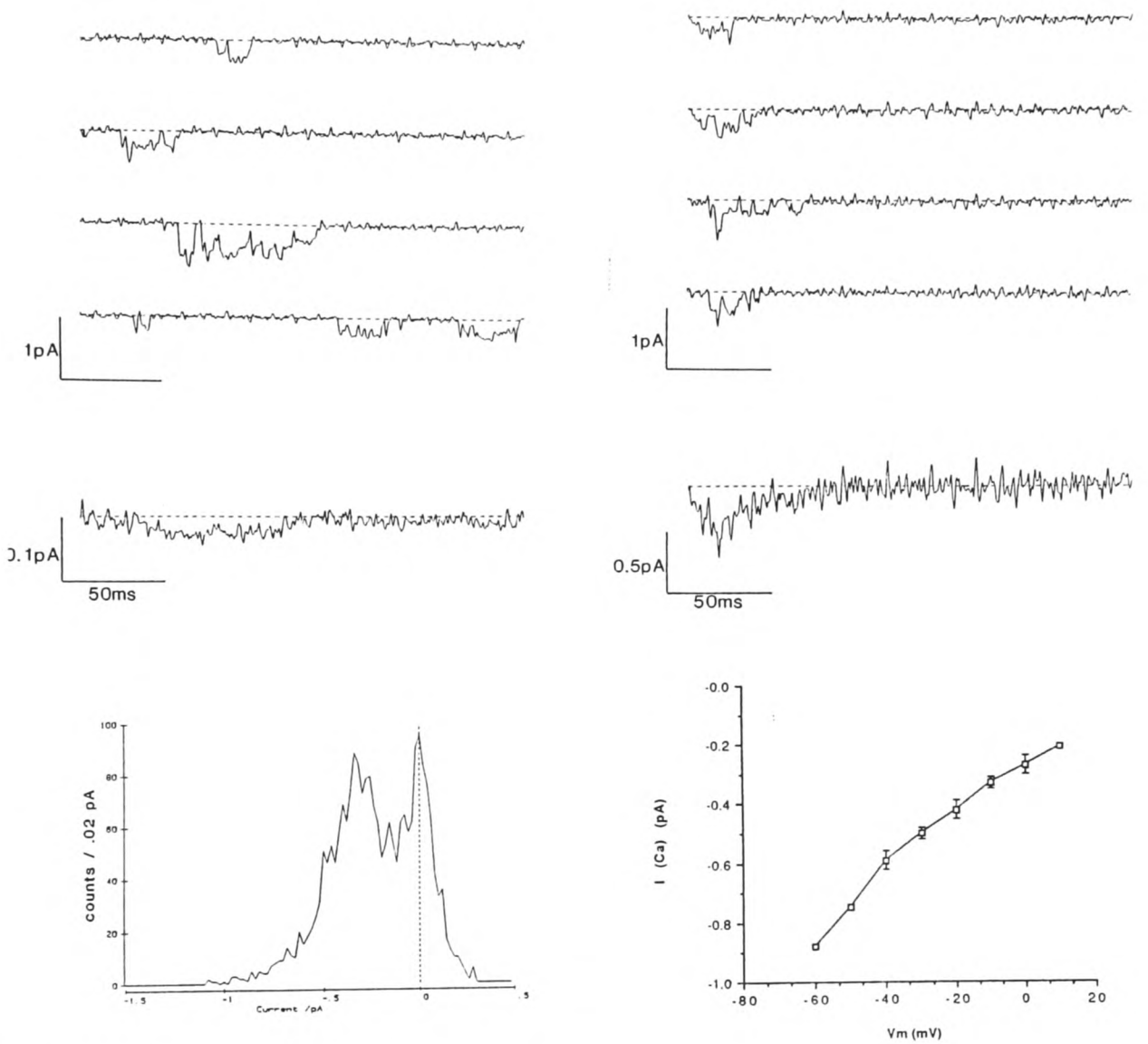


Figure 6.11. T-type Ca^{2+} channels in the rat ß-cell.

A. (top left). Single-channel records elicited 30 mV positive to the cell resting potential, from a cell-attached holding potential of 40 mV negative to the resting potential (i.e. elicited at about -40 mV, V_m). 5 mM K^+ in the bath, 100 mM Ba^{2+} in the pipette solution.

B. (middle left). Average current from 53 sweeps like those in A.

C. (top right). Single-channel currents elicited 70 mV positive to the resting potential, from the same cell and resting potential as in A.

D. (middle right). Mean current from nine depolarisations to V_r + 70 mV. The current is completely inactivated within 100 ms.

E. (bottom left). Amplitude histogram (0.02 pA bin size) from the sweeps included in D.

F. (bottom right). Current-voltage relation for T-type channels, measured in 3 cells in 140 mM K^+_o.

Single channel currents

The next stage in characterisation of the function and modulation of the calcium currents is to examine them at the single-channel level. A preliminary characterisation of the single-channel currents was carried out in rat ß-cells, in cell-attached patches using a pipette solution containing 110 mM $BaCl_2$. Barium was used as it is more permeant than Ca^{2+} in L-type Ca-channels; a high concentration was used to increase the single-channel current amplitude (e.g. Fox et al., 1987b). Two types of single Ca^{2+} channels were found in these rat ß-cells: their characteristics are described in figures 6.11 and 6.12. The channels shown in figure 11 were observed in 11 of 14 patches. Openings of this channel type were concentrated near the beginning of a depolarising voltage step, particularly at more positive potentials. Figure 11A shows four representative sweeps elicited at a potential of (V_r + 30) mV from a holding potential (V_h) of (V_r - 40) mV (where V_r is the resting potential of the cell in 5 mM K^+_o, i.e. elicited at about -40mV from a holding potential of about -110 mV). The ensemble current from 53 similar sweeps is shown in figure 11B. Figure 11C shows four representative current records, from the same cell, elicited at an estimated membrane potential of 0 mV (i.e. a pipette potential of +70 mV), and the ensemble current from 9 similar depolarisations is shown in figure 11D. The ensemble current inactivates rapidly, with a time constant of about 30 ms at 0 mV (determined from currents elicited in a 140 mM K^+ external solution, to control the membrane potential). The single-channel amplitude at 0 mV was 0.27 $\pm$ 0.02 pA (n = 5; figure 11E), and the single-channel slope conductance was 8.9 $\pm$ 1.2 pS over the voltage range 0 mV to -40 mV (n = 3; figure 11F). The mean single-channel open lifetime at 0 mV for the cell shown in figure 11A was 2.99 ms. This type of channel was sometimes elicited by voltage steps to -60 mV from a holding potential of -70 mV and in some cells could also be elicited by voltage steps to -70 mV from a holding potential of -100 mV; at these negative potentials the channel openings were not clustered at the beginning of the trace but occurred throughout the course of a 200 ms depolarisation. In several patches greater channel activity was observed from more negative holding potentials, and channel activity was very largely inactivated at a

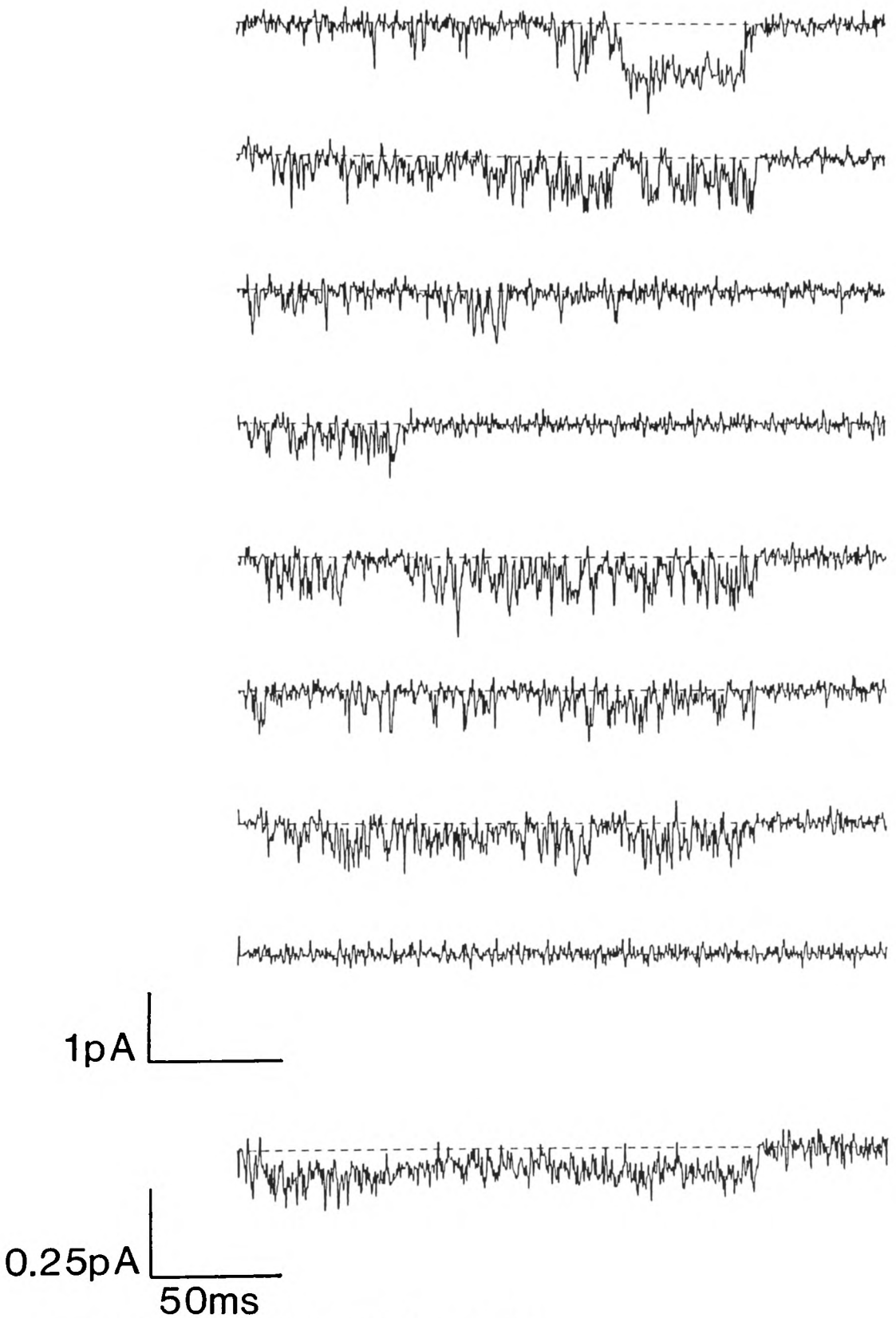


Figure 6.12. L-type Ca^{2+} channels in rat ß-cells.
Single-channel currents and the associated ensemble current elicited in a cell-attached patch on a rat ß-cell in a 140 mM K solution. Depolarisations to 0 mV (Vm) at 0.5 Hz. 110 Ba solution in the pipette.

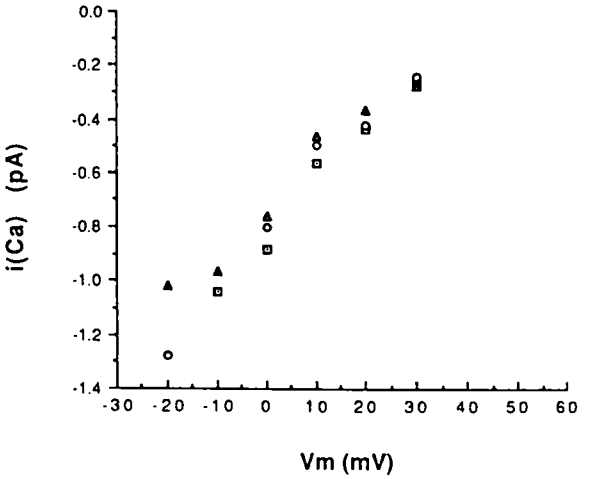
holding potential of -60 mV. The properties exhibited by this channel are typical of those of low-threshold (T-type) Ca-channels reported from other cell types (see Bean, 1989 for a review).

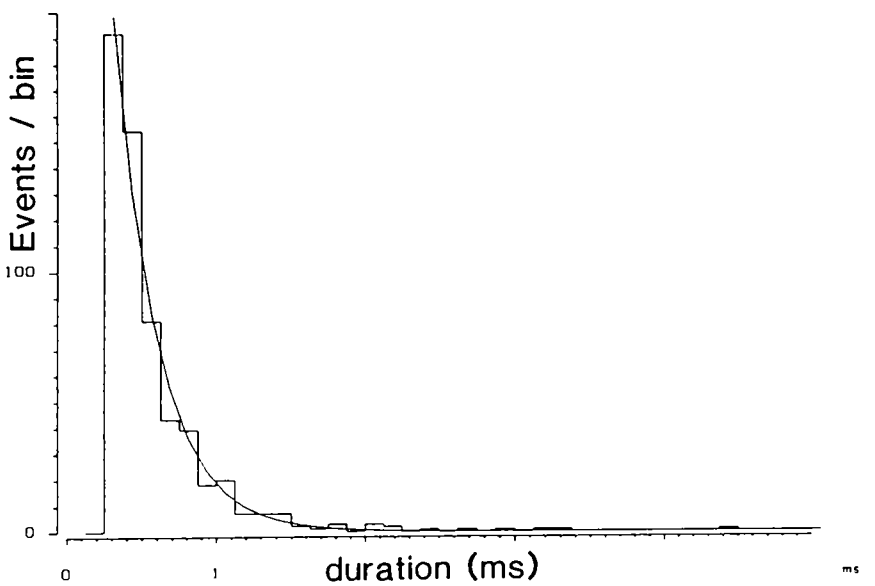
The second type of Ca^{2+} channel observed in the rat ß-cells is illustrated in figure 6.12. This type of channel generally appeared as brief spike-like openings of a variable amplitude (up to about 0.8 pA at 0 mV), similar to L-type Ca^{2+} channel openings previously reported in ß-cells (Velasco & Petersen, 1987; Velasco et al., 1988; Rorsman et al., 1988). The apparent variation in amplitude is probably due to the inability of the recording system to resolve the very brief openings, and is a common phenomenon, e.g. Fox et al. (1987b), Rosenberg et al. (1988). The openings did not show a tendency to cluster at the beginning of the sweep. Occasionally, much longer openings were observed, similar in amplitude to the larger spikes. These openings were attributed to the same channel type as the spikes ("mode 2" openings, see Hess et al., 1984) and were used where possible to construct a current-voltage relation for this channel (figure 13A). The IV gave a mean single-channel slope conductance of 19.6 $\pm$ 1.0 pS for this channel (n = 3). The ensemble current in patches containing only this channel (3 patches in 14) showed little inactivation during the course of a 200 ms depolarisation: an example is shown in figure 12B. The open and closed times of this L-type channel were measured in three patches: the open times were well fitted by a single exponential with a time constant of 0.30 $\pm$ 0.01 ms, and the closed times could be fitted by two exponentials with time constants of 0.61 $\pm$ 0.02 ms and 13.9 $\pm$ 5.3 ms (3 cells; the variability of the slow component of the closed times reflects the variability of channel activity from patch to patch). The open and closed time histograms for the L-type channels at 0 mV in one cell are shown in figure 13B, C. In addition, long runs of identical depolarisations often contained several consecutive sweeps without any openings, suggesting a long-lasting closed state for these channels. The open and closed time characteristics are both qualitatively and quantitatively similar to those in mouse ß-cells (Smith, personal communication) and guinea-pig ventricular cells (Cavalie et al., 1986).

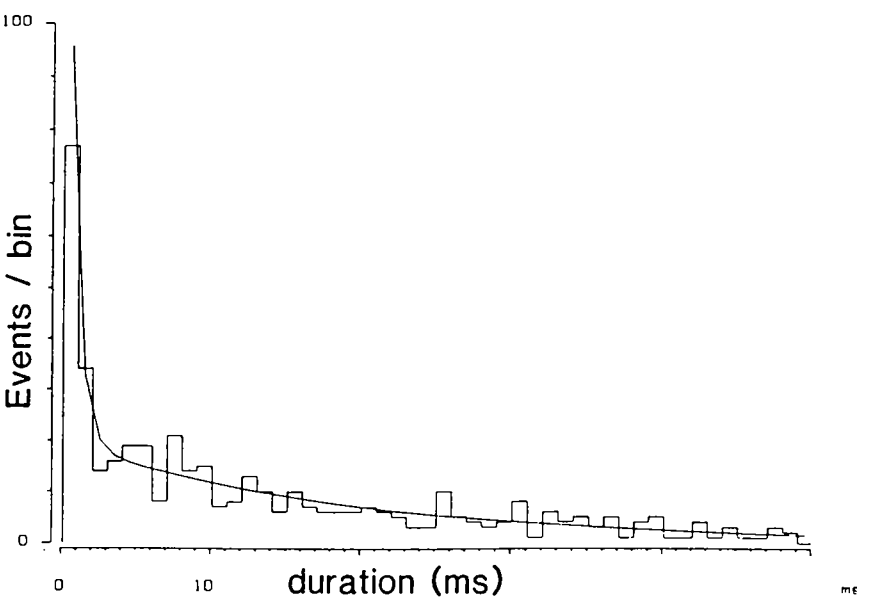
Figure 6.13.

A. Current-voltage relations for L-type Ca^{2+} channels in 3 rat ß-cells. The symbols refer to different cells. The IV's were measured from the (occasional) long ("mode 2") openings of this channel, and with 140 mM K^+ external solution in the bath.

B,C. Examples of open (A) and closed (B) time histograms for the L-type Ca^{2+} channel at 0 mV. The open times were well fitted by a single exponential, while the closed times required at least two exponential components. Detection of an opening or closing event was set by a crossing of a threshold set at 0.4 pA for at least two consecutive digitised points. (Digitisation at 8 kHz; filter 1 kHz).


i(Ca) (pA)
0.0
-0.2
-0.4
-0.6
-0.8
-1.0
-1.2
-1.4
-30 -20 -10 0 10 20 30 40 50 60
Vm (mV)


Events / bin
100
0
0
1
duration (ms)
ms


100
Events / bin
0
0
10
duration (ms)
ms

DISCUSSION

Both rat ß-cells and HIT cells possess voltage-activated potassium and calcium currents. The properties of these currents are similar in the two types of cells, and the whole-cell currents are similar to those in the mouse (Satin & Cook, 1985; Rorsman & Trübe, 1986; Plant, 1988) and human (Ashcroft et al., 1989a; Ashcroft & Kelly, 1990; chapter seven). The inward whole-cell current is carried by calcium and has properties generally similar to those of L-type currents reported in other cell types. T-type channels have been directly recorded in a ß-cell line, RINm5F (Velasco, 1988; Rorsman, personal communication) and have been proposed to exist in rat ß-cells on the basis of evidence from tail-current analysis (Hiriart & Matteson, 1988): recordings of T-type channel activity have not previously been reported in normal ß-cells. As indications of a T-type component of whole-cell Ca^{2+} current,it may be of significance that the Ca^{2+} currents activate at relatively negative potentials, that they were only partially blocked by 50 µM nifedipine and that Cd^{2+} was more effective as a blocker at more negative potentials. (It is common, however, for nifedipine not completely to block L-type channel activity, as it has a partial agonist effect, and its action is often dependent on the holding potential (Bean, 1989; Sanguinetti & Kass, 1984; Rane et al., 1987)). Cd^{2+} has been shown to permeate L-type Ca^{2+} channels at hyperpolarised potentials (Lansman, Hess & Tsien, 1986) but it seems unlikely that this effect could account for the very small degree of block at negative potentials. The view that the small degree of block is due to current through T-type channels implies that there must be only a very small activity of L-type channels at potentials below -30 mV. This is consistent with the potential-dependence of single-channel activation seen in the rat ß-cell (above) and elsewhere (mouse ß-cell: Rorsman et al., 1988; chick DRG cells: Fox et al., 1987b). The whole-cell IV's show no sign of two humps to indicate two populations of channels, as are seen for example in the pancreatic alpha-2 cell. This was noted previously by Hiriart & Matteson (1988), who nevertheless demonstrated two types of Ca channel in the rat ß-cell on the basis of tail current experiments. Clearer whole-cell evidence for the presence of a T-type current in the ß-cell can be obtained from recordings of Ba^{2+} currents, as in chapter 7, where a transient component of inward current can be activated

at more negative holding potentials, but not at more depolarised holding potentials (figure 7.12D). The identity of three of the cells demonstrating T-type channel activity was confirmed by perfusing the bath with a 5mM K+ solution containing 10 mM glucose: all three cells responded by spiking, confirming their identity as ß-cells (Pancreatic alpha-cells are known to possess both L- and T-type Ca^{2+} channels (Rorsman, 1988), but they do not respond to glucose by producing action potentials.)

The properties of the L-type channels in the rat ß-cell appear similar to those of L-type channels reported elsewhere (Brown et al., 1982; Fox et al.,1987b; Kalman et al., 1988). More thorough single Ca-channel studies have been performed in the mouse ß-cell (Rorsman et al.,1988) and in the ß-cell line RINm5F (Velasco et al., 1988); both of these groups have confirmed the presence of L-type Ca-channels in the ß-cell. The conductance of the L-type channel in the rat, reported in this chapter (19.6 + 1.0 pS), is slightly smaller than that reported for the L-type channel in the mouse ß-cell (24 +1.5 pS; Rorsman et al., 1988), but was measured over a more positive voltage range (-20 to +30 mV in the rat compared with -90 to -10 mV in the mouse). If measured over the same voltage range (-90 to -10 mV) the channel conductance in the rat would increase, because of the high degree of inward rectification of Ca^{2+} channels.

Inactivation

The results point to whole-cell Ca^{2+} currents in the ß-cell being subject to both Ca^{2+}- and potential-dependent inactivation. The interpretation of the results of the experiments on inactivation should be treated with some caution: the biphasic change in test current amplitude in figure 7 could be explained by a combination of potential-dependent inactivation and activation, while the apparently potential-dependent inactivation in figure 8 could be due to an increased intracellular Ca^{2+} concentration caused by a small increase in Ca^{2+} influx at more positive potentials. Also, the demonstration of the presence of two types of Ca^{2+} current in the ß-cell implies that the results from the inactivation experiments may be contaminated by a T-type component. It remains possible that there was contamination of the Ca^{2+} currents by K+

currents , especially K(Ca) current, in spite of cellular dialysis with NMG. The interpretation of there being both Ca^{2+}- and potential-dependent mechanisms of inactivation of L-type currents is supported, however, by the studies on Ba^{2+} current inactivation in the human ß-cell described in chapter 7. The results in this chapter suggest that inactivation during the course of an action potential would be primarily dependent on Ca^{2+} entry, while potential-dependent inactivation might contribute to inactivation during the course of the slow wave plateau; this inactivation is likely to be the reason that action potentials are less frequent (Meissner & Schmelz, 1974) and of smaller amplitude (Dean & Matthews, 1970) toward the end of the plateau (figure 1.1). An L-type Ca^{2+} "window current" contributes to maintainence of the plateau: this possibility is supported by the overlap of the activation and inactivation curves for the Ca^{2+} current (compare the IV curves in figures 3 and 4 with the inactivation curve in figure 8). The possibility that the plateau of the slow wave is supported by an L-type window current is in agreement with the DHP-sensitivity of the slow waves (Henquin et al., 1985; Vasseur et al., 1986), but a non-specific Ca-activated cation current underlying the plateau could also appear DHP-sensitive.

The properties and role of T-type channels in the ß-cell remain to be investigated in greater detail, but by analogy with other cell types (Jahnsen & Llinas, 1984; Hagiwara et al., 1988; see Bean, 1989 for a review), they may contribute to the depolarisation during the silent phase or to the rise of the plateau.

Modulation by glucagon

The lack of effect of glucagon does not imply that glucagon does not act by increasing the Ca^{2+} current *in vivo*. It is possible that glucagon had no effect in the experiments shown here because some intracellular constituent, essential for its action was removed from the cell by the whole-cell dialysis: the pipette solution did not contain GTP, for example. A second possibility is that glucagon effect would be visible only at temperatures close to physiological as is the case for the increase in I_K or the generation of the sodium current evoked by isoproterenol in cadiac myocytes (Walsh et al., 1989; Egan et al., 1988). The question of

modulation of calcium currents in the ß-cell is probably best tackled using cell-attached studies of single calcium channels, under conditions where the metabolism of the cell is undisturbed. Such studies proved very effective in investigating the modulation of potassium channels by glucose and α-ketoisokaproate (Ashcroft et al., 1984; Ashcroft et al., 1987a, 1988a), and have already shown that the activation curve of L-type Ca^{2+} channels in RINm5F cells is shifted to the left by glyceraldehyde (Velasco et al., 1988), as is that of L-type Ca^{2+} channels in the mouse ß-cell by glucose (Ashcroft & Smith, 1989; Smith et al., 1989).

Electrophysiology of the human ß-cell.

INTRODUCTION

The previous chapters have investigated and discussed the properties of the ATP-sensitive channel and of the voltage-activated currents in the rat ß-cell and in the hamster insulinoma HIT T15. In this chapter, the properties of the ionic currents in the human ß-cell are described and discussed and they are compared with those of the rodent ß-cell. Finally, the possible malfunction of the ATP-sensitive K^+ channel in diabetes is examined.

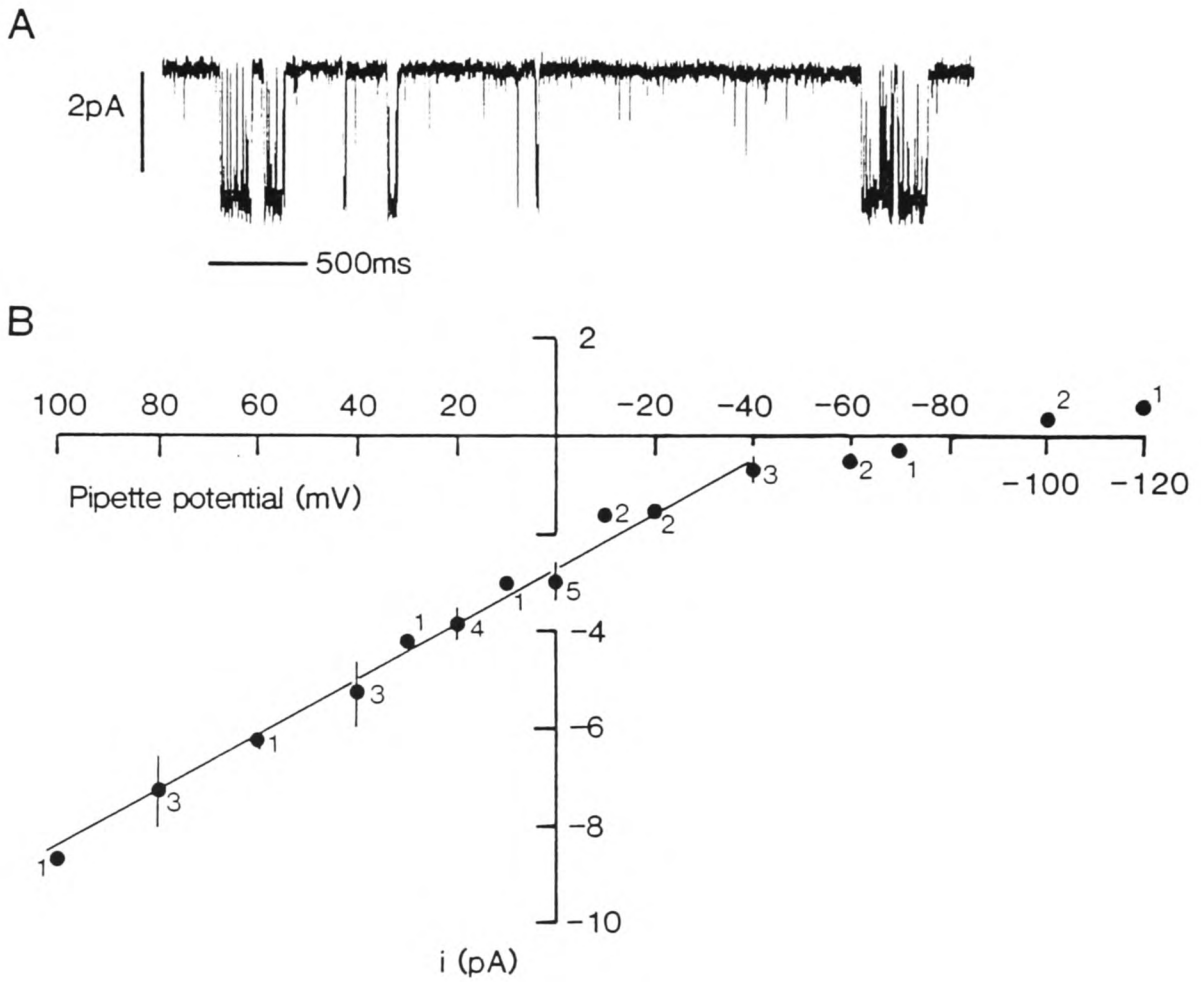


Figure 7.1 A. Single-channel currents recorded at the resting potential from a cell-attached patch on a human ß-cell in 0 mM glucose 5 mM K^+ external solution. 140 mM K^+ in the pipette solution.

B. Cell-attached single-channel current-voltage relation for the channel shown in A). The number of patches is indicated next to each data point.

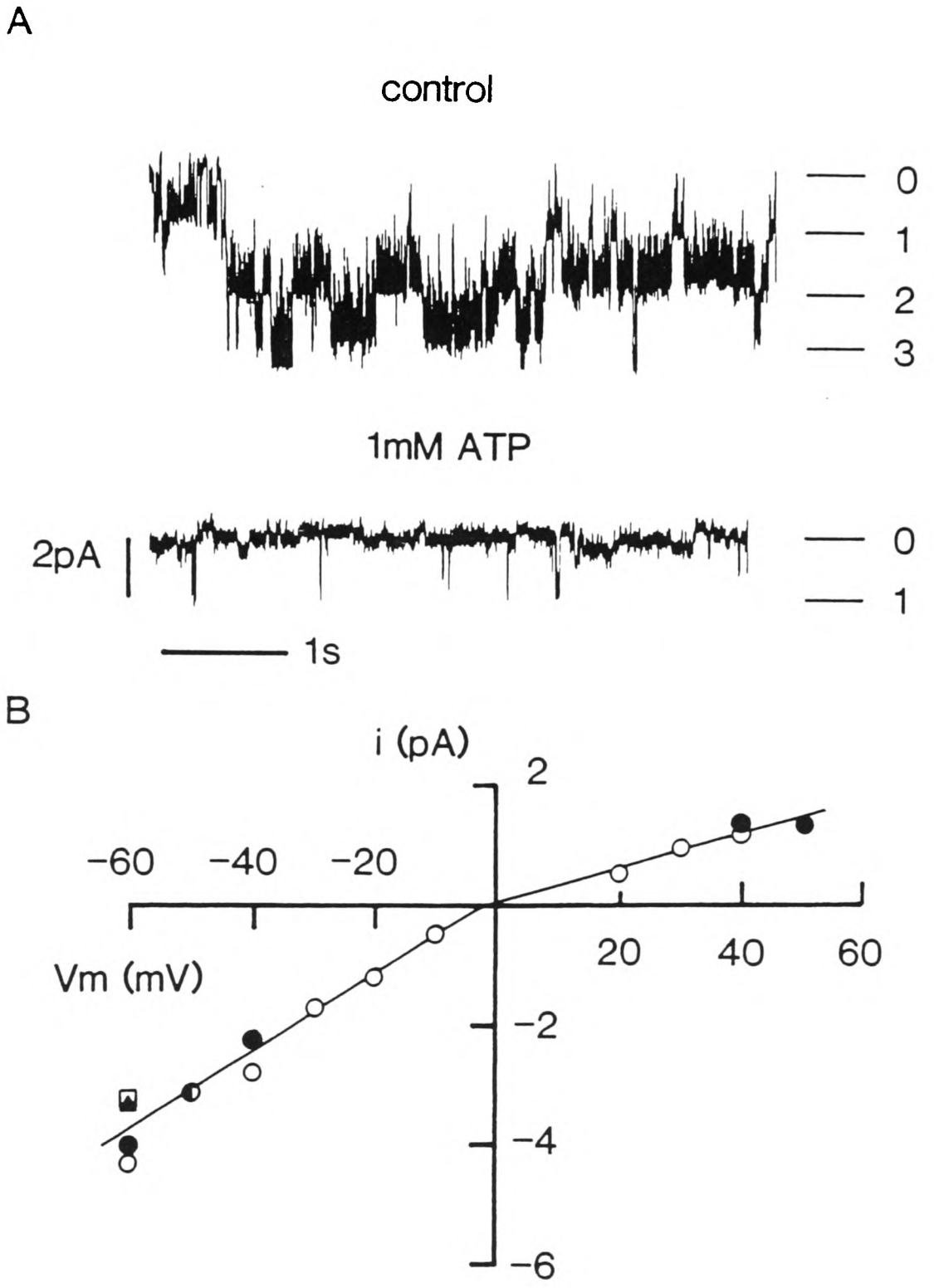


Figure 7.2. **A.** ATP inhibition of single K^+ channel currents.
Single-channel currents recorded at a membrane potential of -60 mV from an inside-out patch of a human ß-cell exposed to intracellular solution before (above) and after (below) the addition of 1 mM ATP. The number of channels is indicated to the right of each trace.
B. Mean current voltage relation of the ATP-sensitive K^+ channel, inside-out patch in symmetrical 140 mM K^+ solutions. The symbols refer to different cells (n = 4).

RESULTS

SINGLE-CHANNEL CURRENTS

The predominant channel type visible in cell-attached patches on human ß-cells exposed to glucose-free solution is shown in figure 7.1. Channel openings occurred in bursts, with an amplitude of about 3 pA at 0 mV pipette potential, i.e. at the resting potential of the cell (140 mM K^+ in the pipette). The single-channel current-voltage relation is shown in figure 7.1B. The channel had a mean inward slope conductance of 56 pS, measured over the linear portion of the current-voltage relation, (between pipette potentials of 80 and -20 mV). Reversal of the single-channel currents occurred at pipette potentials between -45 and -80 mV (mean -61 $\pm$ 9 mV, n = 4; 4 preparations; E_{rev} was extrapolated in 2 patches). This value is somewhat less than that found for rodent ß-cells (about -70 mV; Ashcroft et al., 1984; Rorsman & Trübe, 1985), suggesting that either $[K^+]_i$ is higher in human ß-cells or that the resting potential is on average around 10 mV more positive (i.e. about -60 mV). The amount of channel activity was very variable from patch to patch. In some cell-attached patches a large-conductance (~ 200 pS) K^+ channel was observed at positive membrane potentials, similar to that reported in rodent ß-cells (Cook et al., 1984; Ashcroft et al., 1984; Findlay et al., 1985; Trübe et al., 1986; Ashcroft et al., 1988).

Figure 7.2 shows inward single-channel currents recorded at -60 mV (membrane potential) in an inside-out patch exposed to symmetrical 140 mM K^+ solutions. The channels are substantially inhibited by addition of 1 mM ATP to the intracellular (bath) solution. Inhibition was reversed when ATP was removed. This result was observed in each of 4 patches (2 preparations).

The current-voltage relation for the ATP-sensitive channel is given in figure 7.2B. Single-channel currents reverse at approx. 0 mV, as expected for a K^+-selective channel in symmetrical K^+ solutions. Under these conditions, the single-channel conductance for inward currents was 64 pS, close to that found for ATP-sensitive channels in other cells (Ashcroft et al., 1984; Rorsman &Trübe, 1985; Noma, 1983; Spruce et al., 1985), and close to that found in cell-attached patches in these cells.

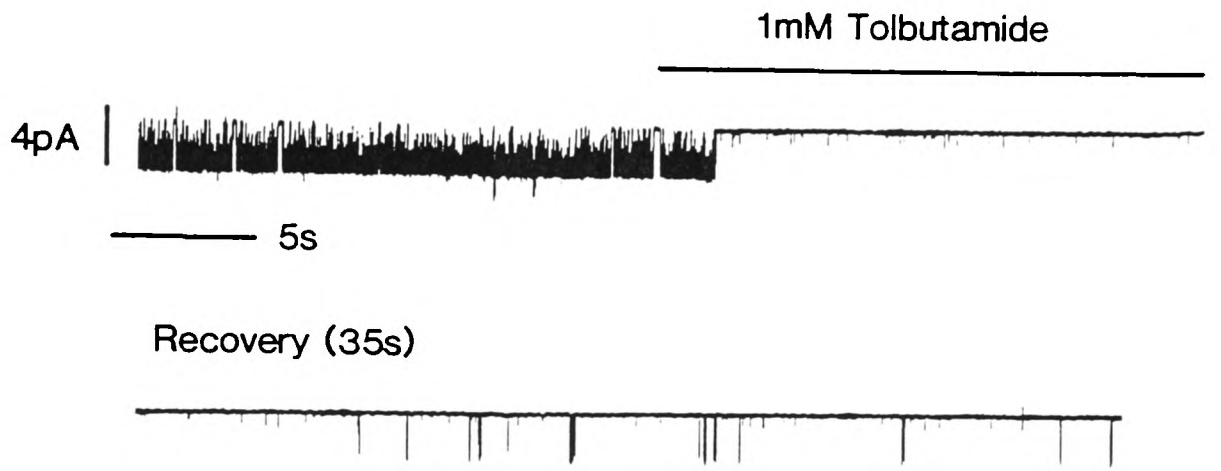


Figure 7.3. Effect of tolbutamide on the ATP-sensitive K channel.
Channels recorded at -60 mV in an inside-out patch. 1 mM tolbutamide applied in the absence of nucleotides.

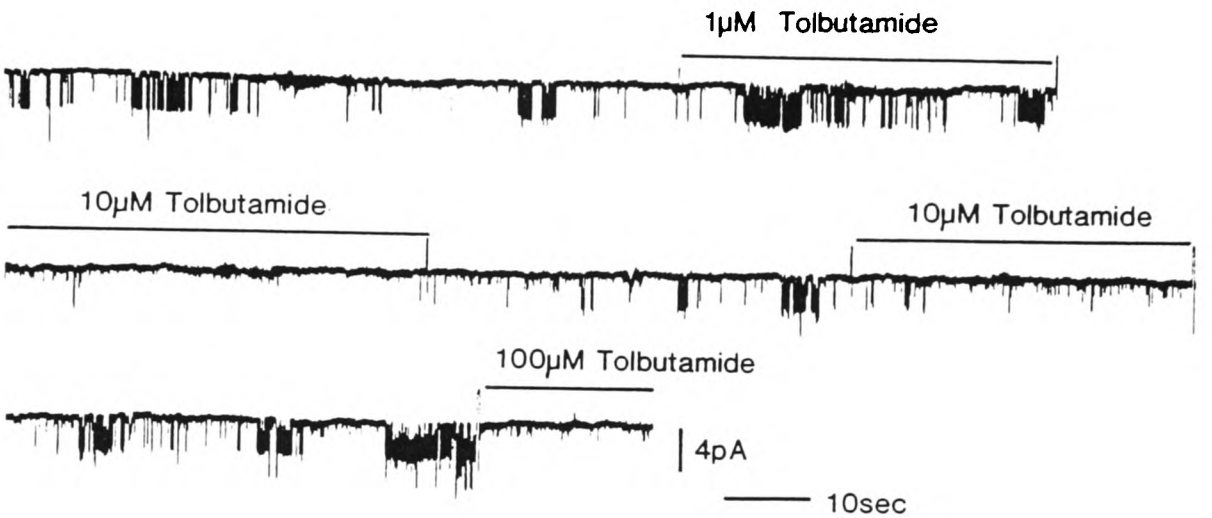


Figure 7.4. Effect of different tolbutamide concentrations on ATP-sensitive channel activity in the presence of 0.1 mM Na_2ATP, 0.1 mM KADP and 2 mM Mg. Channel activity recorded at -60 mVfrom an inside-out patch. The traces are a continuous recording from one patch.

The kinetics of the ATP-sensitive K^+ channel resemble those reported for rodent ß-cells (Ashcroft et al., 1984; Rorsman & Trübe, 1985) and the HIT cell line (chapter four) in consisting of bursts of channel openings separated by long interburst intervals (figures 7.2 - 7.4). At least two closed states are therefore indicated. Figure 7.2 further suggests that ATP reduces channel activity by decreasing the number of openings per burst. As in the rat ß-cell (e.g. Cook & Hales, 1984), no effect of ATP on the amplitude of the single channel currents was observed.

Tolbutamide sensitivity.

The sulphonylureas constitute a class of selective blockers of the ATP-sensitive K^+ channel (Sturgess et al., 1985; Trübe et al., 1986) and are used clinically in the treatment of NIDDM (Balant, 1981). It was therefore of great interest to test the ability of these drugs to block ATP-sensitive K^+ currents in human ß-cells (2 patches from different preparations). Tolbutamide (1 mM) applied to the intracellular membrane surface rapidly produced a complete block of single-channel currents (figure 7.3). Channel activity only partially recovered on removal of the drug. This may be attributable to rundown (rather than a partially reversible effect of tolbutamide), as even in the absence of the drug channel activity ran down with time in isolated patches from human ß-cells, as it does in excised patches from other cells (Findlay & Dunne, 1986; Ohno-Shosaku et al., 1987). To avoid the problem of rundown, tolbutamide was tested in the presence of 0.1 mM ATP + 0.1 mM ADP + 2 mM Mg^{2+} (Trübe et al., 1986). In the presence of these concentrations of ATP and ADP, channel activity was stable; 1 µM Tolbutamide was ineffective, 10 µM greatly decreased the frequency of channel opening, and channel activity was totally inhibited by 100 µM tolbutamide (figure 7.4). Block by tolbutamide was completely reversible and could be repeated several times on the same patch. These preliminary observations on tolbutamide block suggest that the sulphonylurea-sensitivity of the ATP-sensitive channel in the human ß-cell is similar to that reported for mouse ß-cells, where half-maximal inhibition is produced by 7 µM tolbutamide (Trübe et al., 1986).

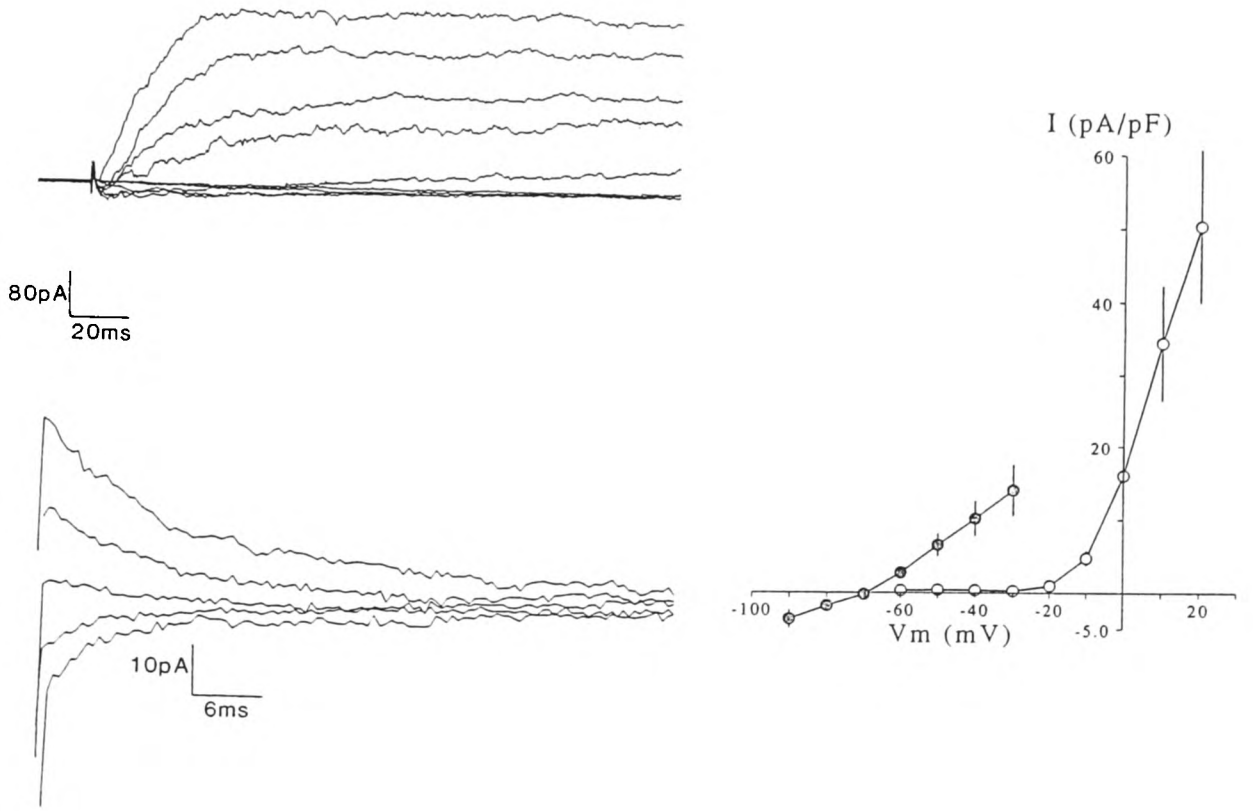


Figure 7.5 Whole-cell membrane currents of a single isolated human ß-cell.
A, (upper left) currents elicited by depolarising voltage steps from a holding potential of -70mV. Stimulation frequency 0.5Hz. Bath solution 5K ext. Pipette solution 140K int. The currents were elicited with 10 mV increments in the amplitude of the step; the current of largest amplitude was elicited at a potential of +30 mV.
B, (right) Open circles: the mean current-voltage relation of the peak outward current for six cells. Filled circles: the mean instantaneous IV curve for 6 cells. (See text for details). The current amplitudes in each cell were divided by the cell capacitance to allow for the differences in cell size.
C, (lower left) tail currents recorded on repolarisation from 0mV to the potentials between -50 mV (uppermost trace) and -90 mV (lowest trace).

VOLTAGE-ACTIVATED CURRENTS

Outward Current

Currents elicited by depolarising voltage steps from a holding potential of -70 mV in human pancreatic ß-cells are shown in figure 7.5. At -40 mV a small inward current is elicited; at more positive potentials increasingly large delayed outward currents are seen. The current-voltage relation for the peak outward current during a 200 ms depolarisation is plotted in figure 5B (open circles). The outward current is activated at about -20 mV, and the current amplitude increases approximately linearly with depolarisations to more positive potentials. The reversal potential was determined from the instantaneous current-voltage relation for the current. This was obtained from the initial amplitudes of tail currents flowing on repolarisation to potentials between -30 and -90 mV after a 400 ms activating depolarisation to 0 mV. Representative tail currents are shown in figure 5C, and the instantaneous IV curve, given by the initial amplitudes of the tail currents, is plotted in figure 5B (filled circles). (The initial tail current amplitudes were calculated by fitting a single exponential (tau = 13 ms) to the tail currents at time points greater than 2 ms, (to avoid uncompensated capacitive transients), and extrapolating back to zero time.) The tail currents in figure 5C reverse between -80 and -70 mV and the instantaneous IV crosses the zero current axis close to -70 mV. This is close to the calculated reversal potential for potassium (about -84 mV), suggesting that the outward current is primarily K^+-selective. This was confirmed by the abolition of outward current when internal K^+ was replaced by the impermeant cation N-methyl-D-glucamine (as in figures 7-10). The deviation of the reversal potential from E_K could be due to an effect of junction potentials (about 3-5 mV, Fenwick et al., 1982) or to an incomplete selectivity for potassium (estimated $P_{Na}/P_K = 0.01$, assuming no junction potential). The relation between the time constant of tail current deactivation and the repolarisation potential is plotted in figure 7.5D. The time constant decreases at more negative potentials, as has been reported in many cell types (e.g. Hodgkin & Huxley, 1952).

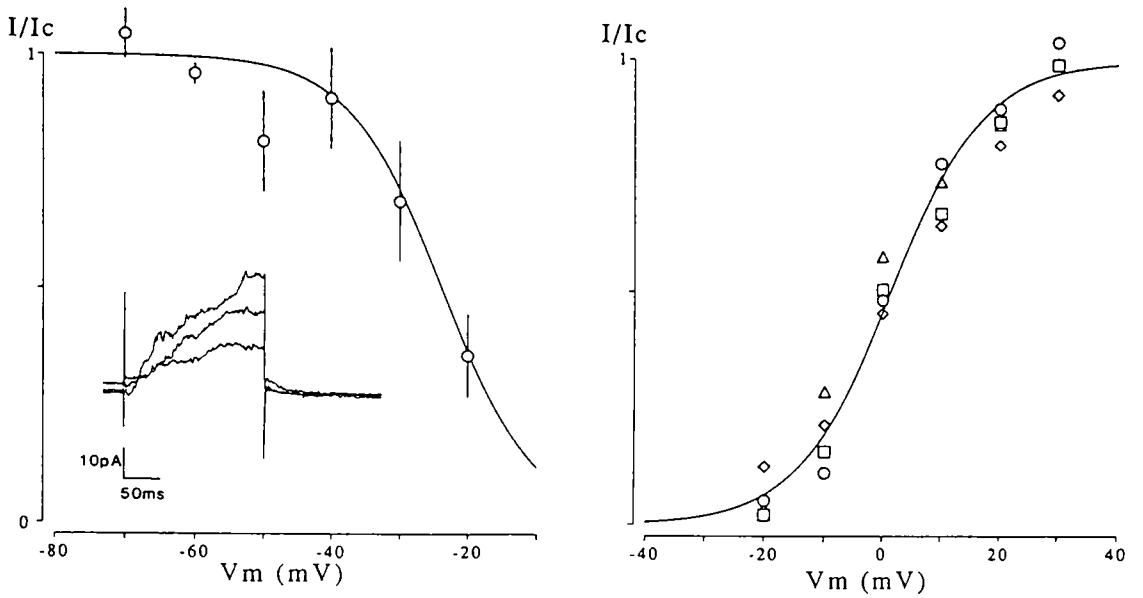


Figure 7.6. Potassium current inactivation and activation.

A, (left) normalised inactivation curve. Inactivation calculated from tails following a 200 ms test depolarisation to 0mV after a 15s inactivating prepulse. Pulse frequency 0.033Hz The means and SEM from 3 cells are shown. The data points are fitted with a smooth curve based on the Boltzman relation, $I/Imax=1/\{1+\exp[(V_{0.5}-V)/k]\}$. $V_{0.5}$ = -24.7 mV, k = 7.3 mV, as described in the text. The inset shows currents elicited at 0 mV from holding potentials of -70, -40 and -20 mV.

B, (right) potassium current activation. Activation determined from tail currents as described in the text. The normalised values of four cells are shown. The curve is similar to that described in A).

Inactivation

Although inactivation of the potassium current was not generally observed during a 400 ms depolarisation, long depolarisations did inactivate the current. The voltage-dependence of inactivation was determined by holding the membrane at the inactivating potential for 15 s prior to a test depolarisation to 0 mV. The potential was then stepped to -50 mV and the degree of inactivation determined from the initial value of exponentials fitted to the tail currents. The inactivation curve is shown in figure 7.6A, and the data are fitted with a smooth curve derived from the Boltzman relation. The function

$$I/Imax = 1/\{1+\exp[(V_{0.5} - V)/k]\} \qquad \text{(eqn. 7.1)}$$

was fitted by a least squares routine to the results of three individual experiments, where $V_{0.5}$ is the potential at 50% inactivation and k is the slope factor. The curve in figure 6A is drawn to eqn. 7.1, using the mean values $V_{0.5} = -24.7 \pm 3.1$ mV and $k = 7.3 \pm 2.6$ mV. The inset to figure 7.6A shows outward currents elicited at 0 mV with prepulses to -70, -40 and -20 mV: a pre-depolarisation to -40 mV decreases the current amplitude, while a prepulse to -20 mV largely inactivates the current.

Activation

The activation curve for the delayed potassium current is shown in figure 7.6B. A 400 ms activating pulse allowed the potassium current to reach a steady state, and activation was determined from the initial amplitudes of exponentials fitted to tail currents which flow on stepping back to -50 mV. Eqn. 7.1 was fitted to the amplitudes of the tail currents for each of the cells in figure 7.6B. The mean and standard errors obtained for the activation parameters were $V_{0.5} = 1.3 \pm 1.0$ mV and $k = -8.5 \pm 0.9$ mV. The curve in figure 7.6B is drawn using these mean values.

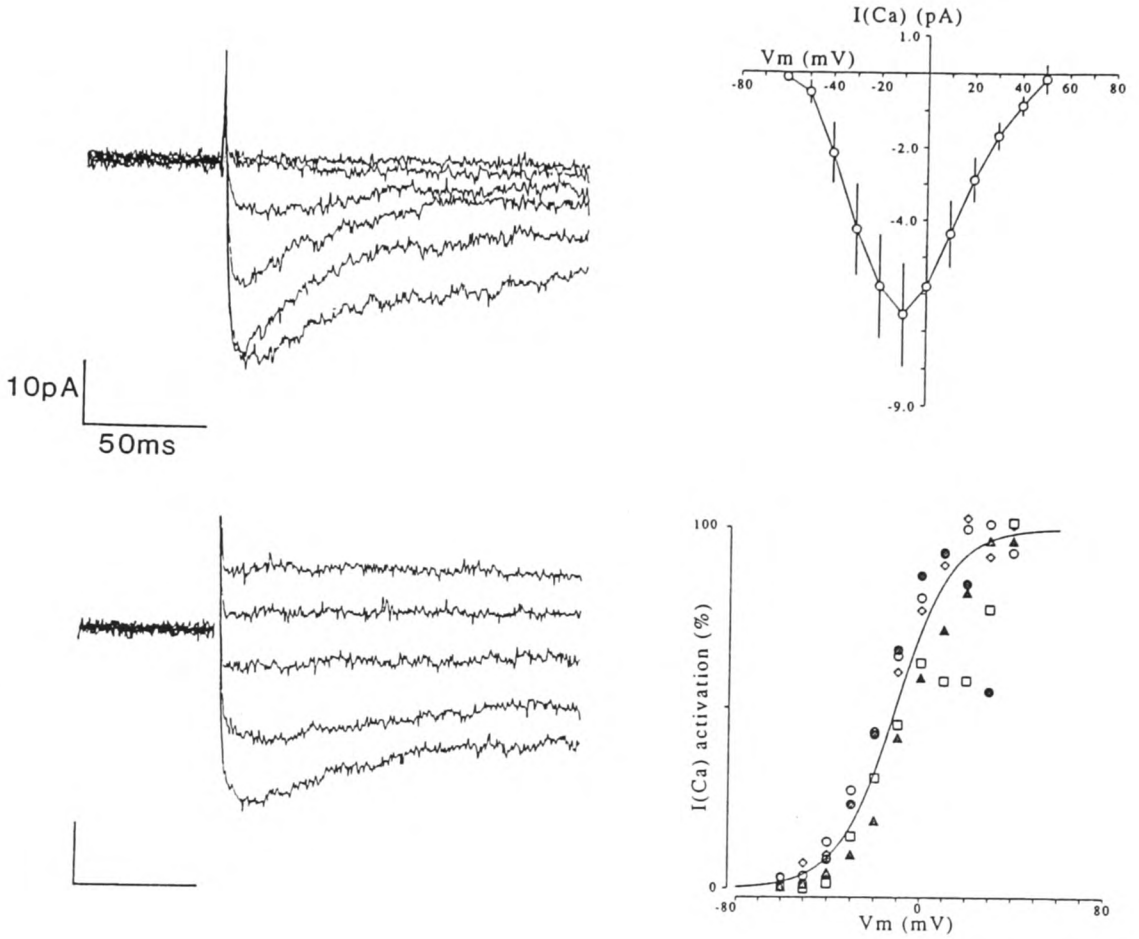


Figure 7.7 Ca^{2+} inward currents.

A and **B**. (left) Currents recorded when intracellular K^+ was substituted by N-methyl glucamine. The extracellular solution contained 10μM TTX and 5mM Ca^{2+}. Holding potential -70mV, test potentials -60 mV to -10 mV (upper panel) and 0 mV to + 40 mV (lower panel). Pulse rate 0.5Hz. The traces are not corrected for leak.

C. (upper right) Average leak-corrected current-voltage relation for five cells; the current amplitudes from different cells were divided by the cell capacitance to compensate for differences in cell size.

D, (lower right), activation curve for Ca^{2+} currents in the human ß-cell. The protocol and curve are as described in the text.

Inward currents

Inward currents (figure 7) were isolated by replacing internal K^+ with 145 mM N-methyl glucamine (NMG). NMG has been shown to be effective in abolishing outward current in rodent beta-cells and in GH3 cells (Rorsman & Trübe, 1986; Fernandez, et al., 1984). With outward currents blocked, depolarising voltage steps from a holding potential of -70 mV to potentials less negative than -50 mV, in 5 mM Ca^{2+}_o elicit slow inward currents (figure 7A). The inward currents increase in amplitude with depolarisation, reaching a maximum amplitude at -10 mV, and then decrease in size as the potential is made more positive (figure 7A,B). The leak-corrected current-voltage relation (figure 7C) did not cross the voltage axis below +60 mV.

The inward current activated during a voltage-clamp step peaks within 5 ms at -10 mV, and then relaxes during a sustained depolarisation. The activation curve of this current was determined by dividing the peak amplitude of the inward current by a function derived from the Goldman-Hodgkin-Katz current equation for calcium:

$$I = \frac{(VF^2)(Ca_i - Ca_0)\exp(-zVF/RT)}{(RT)\quad(1-\exp(-zFV/RT))},$$

to correct for the reduced driving force at more positive potentials. The resulting sigmoid activation curve (figure 7D) was fitted with the equation $I/Imax = 1/\{1 + \exp[(V_{0.5} - V)/k]\}$, derived from the Boltzman relation. The curve in the figure is drawn to the mean values from four cells, $V_{0.5}$ = -10.8 mV and k = 10 mV. The amplitude, activation properties and time course of this current are similar to those of calcium currents measured in rodent beta-cells (Rorsman & Trübe, 1986; Rorsman & Hellman, 1988; Plant, 1988; Hiriart & Matteson, 1988). The maximal current amplitude and the degree of inactivation during a 200 ms depolarisation were quite variable from cell to cell, as has also been reported for calcium currents in beta-cells from other species (Plant, 1988; Rorsman & Trübe, 1986; Satin & Cook, 1988).

Figure 7.8 shows that the inward current is blocked by cadmium. 1 mM Cd^{2+} in the standard external solution was puffed onto the cell from a distance of about 20 μm for 1 s. The

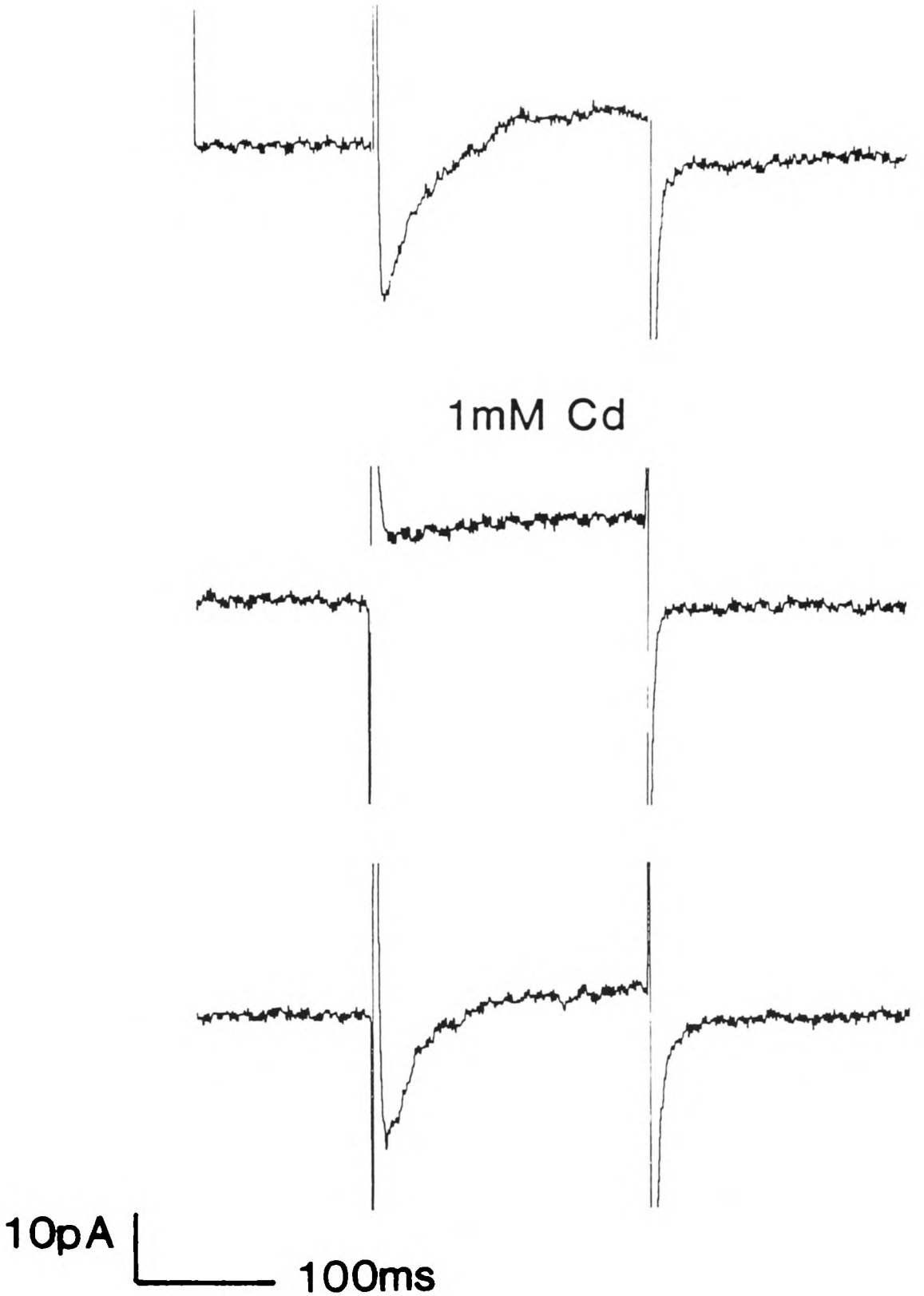


Figure 7.8. Inhibition of Ca^{2+} current by Cd^{2+}.
Currents elicited by voltage steps to 0mV from a holding potential of -70mV before (A), during (B), and after (C) application of 1 mM Cd^{2+} from a puffer pipette. Ca^{2+}_o = 5 mM.

inward current was rapidly and reversibly blocked: the lowest trace in figure 8 shows the recovery of the inward current about 8 s after ceasing cadmium application. The concentration of Cd^{2+} at the cell cannot be estimated accurately, but it must be considerably lower than 1 mM.

From the results above, the inward currents in the human beta-cells can be identified as calcium currents by i) the very positive reversal potential ii) the similarities of the activation properties, amplitude and time course to those of calcium currents in rodent ß-cells iii) their insensitivity to 10 µM TTX, and iv) their sensitivity to Cd^{2+}.

Inactivation of calcium currents.

Although the extent of inactivation during a 200 ms pulse varied considerably from one cell to another the amplitude of the inward current was always seen to decline whenever Ca^{2+} was the current carrier. The relaxation of inward current during the pulse is identified as inactivation (rather than development of an outward current) because i) it occurs even when internal potassium is replaced with N- methyl glucamine, and ii) for currents of similar amplitude, inactivation is less at more positive potentials (where K^+ currents would be expected to be greater). Calcium-activated K^+ currents might be expected to show a similar voltage-dependence to the Ca^{2+} current inactivation shown here, but these currents should be blocked by NMG. Calcium-dependent activation of chloride channels cannot contribute to the inactivation, for inactivation is maximal near 0 mV, which is the chloride reversal potential. (Opening of these channels may however contribute to the non-linear leak sometimes seen at positive potentials.) Inactivation was most pronounced at potentials close to -10 mV and was less for weaker or for stronger depolarisations. This resembles the voltage-dependence of the Ca^{2+}-current, which peaks at -10 mV and is smaller at potentials approaching E_{Ca}. The correspondence between calcium entry and the degree of inactivation suggests that Ca^{2+}-current inactivation in human beta-cells, like that in rodent beta-cells (Plant, 1987), may be dependent on Ca^{2+} entry.

The contributions of potential and calcium entry to inactivation of the calcium current were

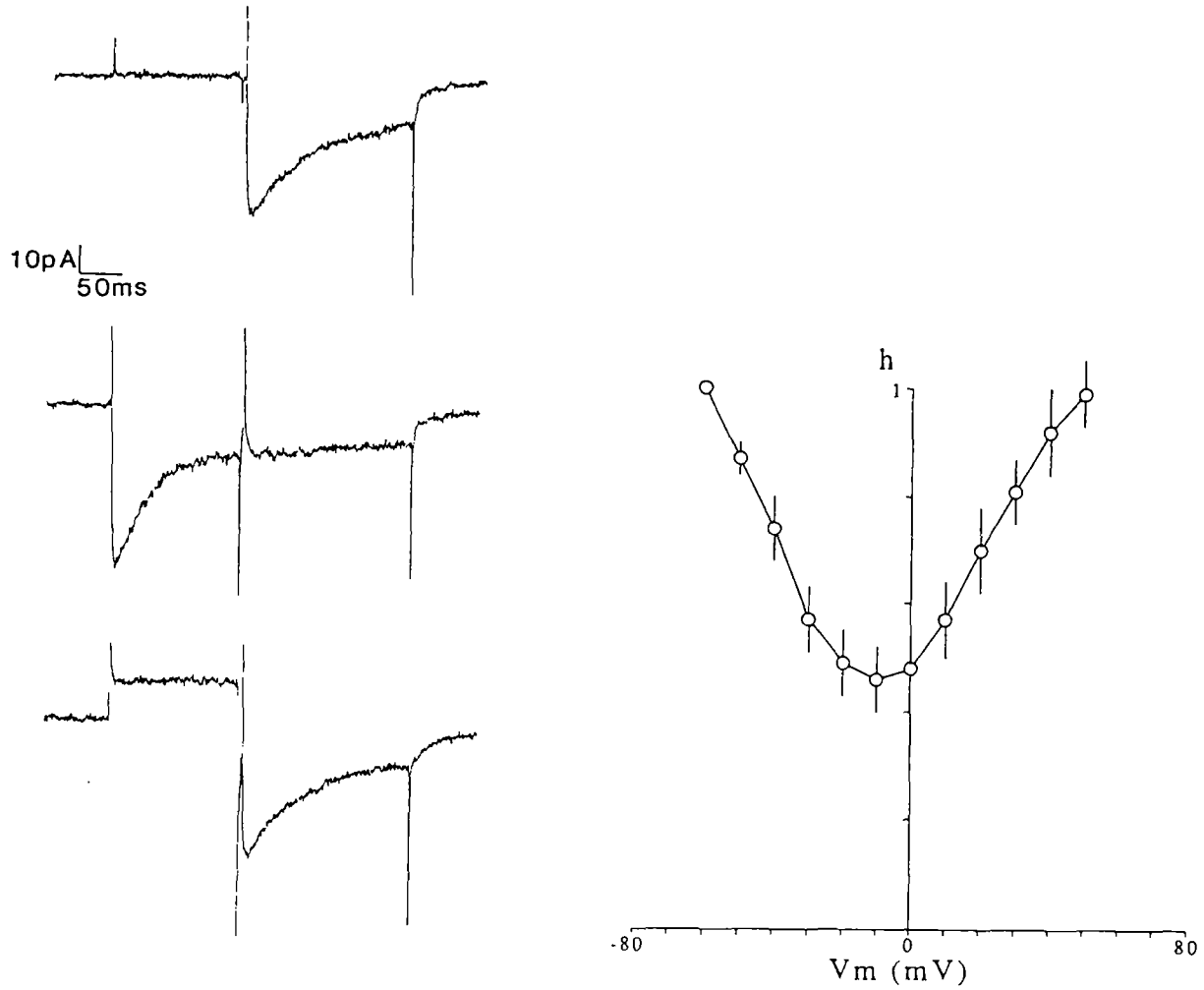


Figure 7.9. Inactivation of calcium currents.

A, (left) current traces during a 200 ms test pulse to 0 mV with 150 ms prepulses to -60 mV, 0 mV and +40 mV. A 10 ms gap separates the two pulses.

B. (right) mean inactivation curve for three cells. The current amplitude (I) during the test pulse is divided by that obtained with a prepulse to -60 mV (I_c) to obtain an index of inactivation. 5 mM Ca^{2+} external solution in the bath.

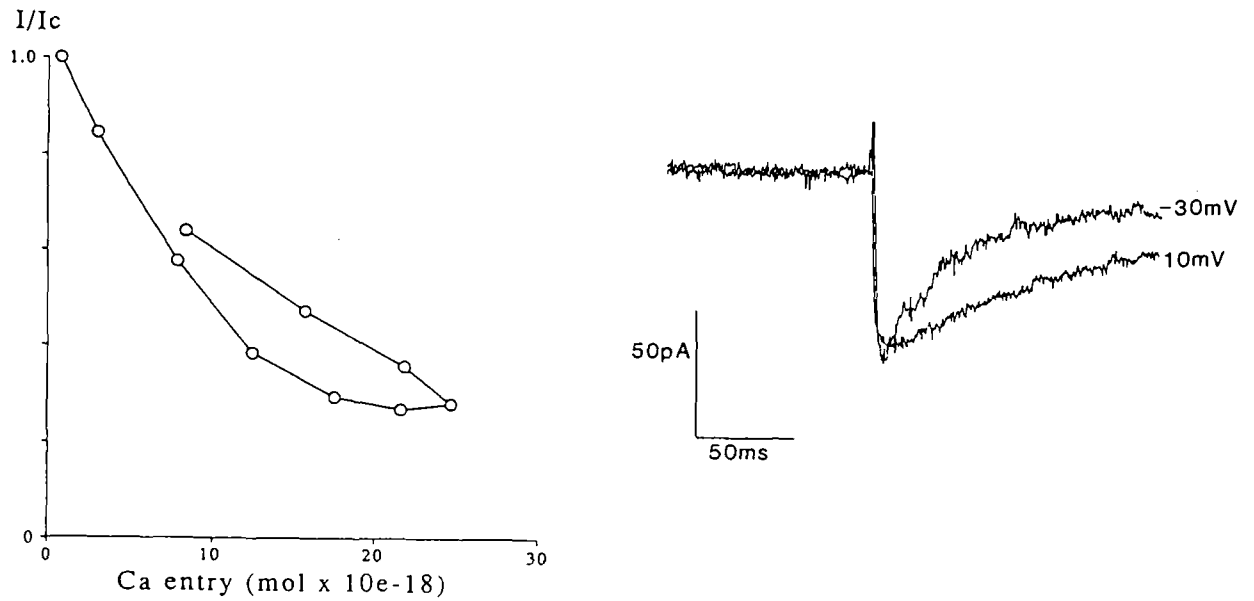


Figure 7.10 The effect of potential on Ca^{2+}-dependent inactivation.

A, (left) Ca^{2+} current inactivation as a function of charge entry. The degree of inactivation (as in figure 7.9) is plotted against total Ca^{2+} entry during the prepulse, calculated by integrating the leak-corrected currents during the prepulse, and dividing the charge by zF, where z is the charge on the ion (= +2), and F the Faraday constant.

B, (right) differing time courses of inactivation of calcium current elicited by potential steps to -30 mV and +10 mV. The traces are from the same cell, and are not leak-corrected. After leak-correction the two currents are of almost identical amplitude.

investigated using a two-pulse voltage protocol (figure 7.9; Eckert & Tillotson, 1981). A constant test pulse to 0 mV from a holding potential of -70 mV was preceeded by a 200 ms test pulse to potentials between -60 mV and +40 mV. A gap of 10 ms between the inactivating and test pulses allowed activation to return to the steady state.(Gillespie & Meves, 1980; Plant, 1988) Figure 7.9A shows how the current during the test pulse is affected by prepulses to -60, upper, -10, middle and +40 mV, lower traces. With a prepulse to -60 mV virtually no inward current is activated, and the current during the test pulse is large. When the current during the prepulse is large (as during the prepulse to -10 mV) the amplitude of the test current is greatly reduced. However, the amplitude of the test pulse current then increases with prepulses to more positive potentials, as the inward current during the prepulse decreases. The relationship between amplitude of the test current and prepulse potential was investigated in four cells; the degree of inactivation is plotted as a function of potential in figure 9B. Inactivation is greatest at -10 mV, where the amplitude of the current during the test pulse is largest, but the amplitude of the test current returns towards its control amplitude when the potential of the prepulse approaches E_{Ca}. This restoration of current amplitude shows that a 200 ms depolarisation is not effective per se in inactivating the calcium current in these cells; rather the inactivation of calcium current during a depolarising voltage step appears to be primarily due to depolarisation-induced calcium entry. This conclusion is supported by the results shown in figure 10: the right-hand panel shows currents elicited by pulses to -30 mV and to +10 mV. Although the amplitudes of the two currents are almost identical, the current at -30 mV inactivates much more rapidly than that at +10mV: the relaxing portions of the current traces can be well fitted with single exponentials of time constants 32 ms (-30 mV) and 113 ms (+10 mV). This result also provides further evidence that development of an outward current does not produce an apparent inactivation. If the difference in inactivation were due to development of an outward current, the current at the more positive potential would be expected to show greater and more rapid inactivation.

The relationship between inactivation of the test current in a two-pulse protocol and the magnitude of Ca^{2+} entry during the prepulse is shown in figure 7.10A. Surprisingly, inactivation of the test current depends not only on calcium entry, but also on the potential at

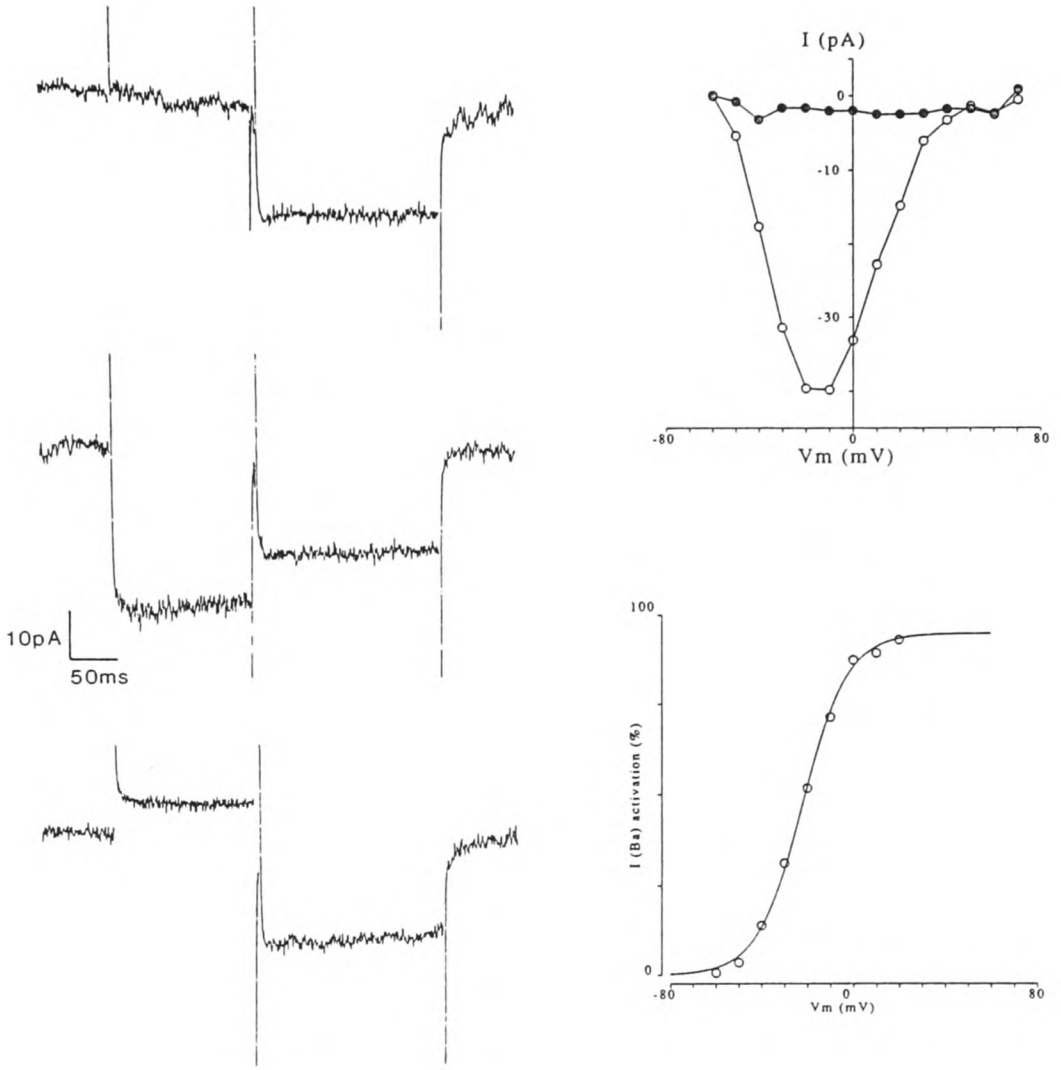


Figure 7.11. Two-pulse protocol in 5 mM Ba^{2+}.

A, (left) Ba^{2+} currents elicited at 0 mV with 150 ms prepulses to -60mV, 0mV and +40mV, as in figure 7.9. The bath solution contained 5mM Ba^{2+}.

B,.(upper right) the amplitude of the Ba^{2+} current during the prepulse (open circles) and the absolute reduction in amplitude of the current during the test pulse (filled circles). (To determine the reduction, the current was compared with the amplitude of the test current elicited with a prepulse to -60 mV)

C, (lower right) Ba^{2+} current activation curve for one cell, determined as in figure 7.7.

which that calcium entry occurred. Specifically, calcium entry during a more depolarised prepulse is less effective at producing inactivation than (a similar amount of) entry at more negative potentials. The effects of potential shown in figures 10A and 10B (i.e. depolarisation appearing to decrease inactivation of the Ca current) are inconsistent with a Hodgkin-Huxley mechanism of voltage-dependent inactivation: they provide support for a mechanism of inactivation dependent upon Ca^{2+} entry, and are considered at greater length in the discussion.

Effects of barium as the charge carrier.

It is known that other divalent cations are unable to substitute for calcium in many of its roles. In particular, the specific effects of Ca^{2+} in mediating inactivation can be investigated by using barium to carry current, as Ba^{2+} has been shown to be permeant through many types of calcium channel but not to produce inactivation of calcium channels in other cells (Fox et al., 1987a, 1987b; Kalman et al., 1988).

Figure 7.11A shows results of the two-pulse protocol repeated in a 5 mM Ba^{2+} solution. Identical results were obtained in two other cells. The barium currents show very little inactivation during the course of a 200 ms depolarisation and, in the two-pulse experiment, the amplitude of the current during the prepulse has little effect on the amplitude of the test current. The current- voltage relation for the current during the prepulse is indicated by the open circles in figure 11 B and the filled circles represent the extent of inactivation of the current during the test pulse.

In Ba solutions, the current- voltage relation is shifted 5-10 mV in the negative direction , relative to that in calcium; barium currents can be elicited even at -60 mV and the maximum current is elicited by a step to -20 mV. The shift in the IV curve is probably due to an effect on surface potential (Frankenhaeuser & Hodgkin, 1957), with Ba^{2+} being less effective than Ca^{2+} at screening negative surface charges, and reflects a similar shift in the activation curve (figure 11C), which has a midpoint of -22 mV in 5 mM Ba^{2+}, compared with one of -10.8 mV in 5 mM Ca^{2+}. The values of the midpoints of activation are similar to those reported from rodent ß-cells (+4 mV in 10 mM Ca^{2+}, (Rorsman & Trübe, 1986), -24 mV in 110 mM Ba^{2+} (Rorsman, Ashcroft & Trübe, 1988)).

Unlike calcium currents, barium currents show little inactivation, confirming that the inactivation seen in figure 9 is dependent on calcium entry. The lack of inactivation of barium

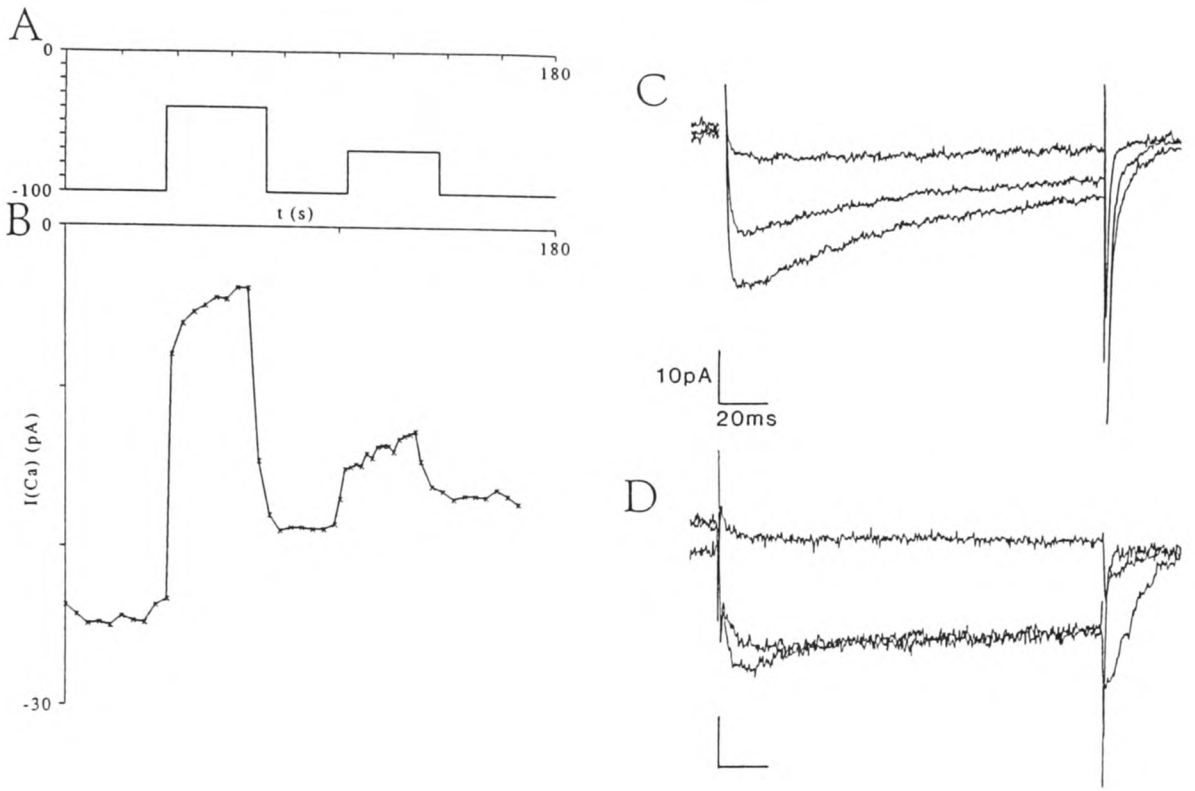


Figure 7.12. Voltage-dependent inactivation of calcium and barium currents.
A, holding potential protocol: the holding potential was stepped from -100 mV to -70 mV and to -40 mV.
B, effect of changes in holding potential on the maximum amplitude of the Ca current elicited by steps to 0mV.
C, Ca current records demonstrating the effect of holding potential on current amplitude. The currents elicited by depolarising pulses to 0 mV, from holding potentials of -100 mV (largest current), -70 mV and -40 mV (smallest current).
D, Ba currents elicited at 0 mV from holding potentials of -100 mV (largest), -70 mV and -40 mV (smallest).

currents indicates not only that barium does not produce inactivation, but that there is no potential-dependent inactivation on a millisecond time-scale in these cells.

Voltage-dependent inactivation

Although no inactivating effect of potential was seen on the calcium currents during 200 ms depolarisations, a slow inactivating effect of depolarisation could be demonstrated by changing the holding potential, (figure 12). Figure 7.12A shows the changes in holding potential while 7.12B shows the effect of holding potential on calcium current amplitude during depolarising pulses to 0 mV. Representative calcium current traces are shown in 7.12C. The currents elicited by steps to 0 mV are largest with a holding potential of -100 mV, are partially inactivated at - 70 mV and greatly (>80%) inactivated at a holding potential of -40 mV. The effects of an increase or decrease in holding potential develop on a time scale of seconds, and would probably be of little importance during short depolarisations such as those used to demonstrate calcium-dependent inactivation.

The decrease in calcium current amplitude at more depolarised holding potentials could be due either to increased (steady-state) calcium-dependent inactivation (caused by entry of calcium into the cell through calcium channels open at more depolarised potentials) or to a genuine inactivating effect of voltage. To distinguish between these possibilities, the experiment was repeated in 5 mM Ba^{2+}, where the effects of potential can be seen in isolation.

Barium current records are shown in figure 7.12D. The currents were elicited by voltage steps to 0 mV from holding potentials of -100 mV, -70 mV and -40 mV. The current elicited from a holding potential of -100 mV shows a transient component which is not observed with more depolarised holding potentials. This component may be a T-type Ca^{2+} current, corresponding to the T-type Ca^{2+} channel activity seen in rat ß-cells. This transient component of whole-cell Ba^{2+} currents was observed at a holding potential of -100 mV (but not at -70 mV) in each of the three human ß-cells where this voltage protocol was tested.

The sustained component of the barium current is similar to L-type currents described elsewhere (Rorsman et al., 1988). Its amplitude is unaltered by changing the holding potential

from -100 mV to -70 mV, but the current is almost totally inactivated at a holding potential of -40 mV. (The barium current baseline shows an inward shift at -40 mV, due to an inward current through Ca^{2+} channels which has not inactivated after 30 s at -40 mV. The current in response to a depolarising voltage step from -40 mV appears as a net outward current because of this shift and the decreased driving force at more positive potentials.) This pattern of inactivation suggests that the inactivation of calcium current at -70 mV may be due to an increase in calcium-dependent inactivation, while that at -40 mV is probably due to both calcium- and potential-dependent inactivation.

Figure 7.12B also indicates that calcium currents in the beta-cell are subject to rundown, as is common for L-type calcium currents in other cell types (Fenwick, Marty & Neher, 1982; Belles, Malecot, Hescheler & Trautwein, 1988). Rundown is present even though the intracellular solution contains ATP and EGTA, and it is accentuated by depolarisation, although this is most likely to be due to increased intracellular calcium levels (Belles, Malecot, Hescheler & Trautwein, 1988).

DISCUSSION

ATP-sensitive channels

ATP-sensitive channels have been identified in the membrane of the human ß-cell on the basis of their inhibition by micromolar ATP, (for the dose-response curve see Ashcroft et al., 1989b), their conductance, permeability to K^+, characteristic burst kinetics and block by tolbutamide. The dominant activity of the ATP-sensitive K^+ channel in intact cells exposed to glucose-free solutions suggests that, as in rodents (Ashcroft et al., 1984; Trübe et al., 1986), this channel may make the major contribution to the resting membrane K^+ permeability. The results presented here on the inhibitory action of tolbutamide have since been confirmed by Misler's group (Gee et al., 1987, Misler et al., 1988, 1989), (who demonstrated a glucose-, ATP-, tolbutamide- and diazoxide-sensitive K^+ channel in the human ß-cell), and extended by Ashcroft et al., (1989b), who found that more than 100 µM tolbutamide was required for 50% inhibition of the ATP-sensitive channel in inside-out patches from human ß-cells, although the K_i for channel inhibition by tolbutamide in whole-cell experiments was only 18 µM. This latter value is in closer agreement with the results shown in figure 7.4: the different sensitivities can be reconciled if it is assumed that intracellular ADP increases the sensitivity of the human ß-cell to tolbutamide inhibition, as it has been shown to do in the rodent ß-cell (Zunkler et al., 1988). The relative insensitivty to tolbutamide of inside-out patches reported by Ashcroft et al. (1989b) was found in the absence of ADP, and although ADP was not included in the pipette solution used for their whole-cell recordings, it was probably formed by hydrolysis of the ATP. The K_i of 18 µM is well within the range of therapeutic plasma levels of free tolbutamide (Balant, 1981), lending support to the idea that inhibition of the ATP-sensitive channel may account for the hypogylcaemic action of the sulphonylureas in man.

Although there is good evidence that NIDDM is associated with disorders in the secretory function of the ß-cell which result in the failure of glucose to stimulate insulin release (Vague & Moulin, 1982), the ability of sulphonylureas to stimulate insulin release in non-insulin dependent diabetics suggests that the cellular mechanisms downstream of the ATP-sensitive K^+

channel remain intact. This being the case, the defect in these patients may be in i) glucose uptake by the ß-cell, ii) glucose metabolism, or iii) the ability of the channel to respond to glucose metabolism. It has been reported that changes in glucose metabolism are an early characteristic of NIDDM (Effendic et al., 1985) and it is interesting to note that the poor response to glucose of fetal ß-cells (Burr et al., 1971; Freinkel et al., 1984) is associated with a different pattern of glucose handling, such that the sugar fails to increase their ATP content, while the ATP- and tolbutamide-sensitivity of the ATP-sensitive K^+ channels in fetal rat ß-cells is similar to that of adult ß-cells (Rorsman et al., 1989). These results provide indirect support for the idea that the secretory defect in at least some forms of NIDDM may be a failure of glucose metabolism to generate ATP: studies on pancreatic ß-cells isolated from diabetic donors could quickly distinguish the three possibilities.

A number of patients with mitochondrial myopathies also develop diabetes mellitus (Petty et al., 1986). The cause of this is unclear, but one possibility is that defective ATP regulation in these myopathies (prehaps leading to low $[ATP]_i$ or a low ATP/ADP ratio) might result in an inability of glucose to close the ATP-sensitive channels of the ß-cell. If this were so, these patients should be sulphonylurea-sensitive.

Voltage-activated potassium currents

The activation range of the outward potassium current suggests that it might contribute to repolarisation of the action potential. The properties of this current are very similar to those of the delayed rectifier current reported by Rorsman and Trübe (1986) in mouse beta-cells. The greatest differences from the currents described in that paper are in the potential dependence of activation and inactivation and the rate of decay of the potassium tail currents (figures 7.6.A, 7.6B and 7.5.D). The midpoints of both activation and inactivation curves are apparently shifted to more positive potentials in the mouse. However, this discrepancy (10-15 mV), could be due largely to the different Ca_o in their experiments: the 10 mM Ca^{2+} in their extracellular solution might have caused a positive shift in the voltage-dependence of channel

gating, due to an increased screening of surface charges. In physiological Ca_o (~2 mM) all voltage parameters would be more negative than those given here. The time constant for potassium tail current deactivation in the experiments described here is three times faster than that found by Rorsman and Trübe (1986), (13 ms vs. 42 ms at -50 mV). This is again likely to be an effect of different extracellular calcium concentrations, 5 mM in these experiments against 2.56 mM in Rorsman and Trübe (1986). This is likely to have caused a shift in the voltage-dependence of the deactivation time constant to more positive potentials in our experiments. Since the time constant is highly voltage-dependent and increases with depolarisation, higher Ca_o will decrease the rate constant at -50 mV. There may also be some species difference in the channel properties.

The amplitude of the potassium currents seems to be much greater than that of the largest inward currents, but in the (mouse) beta-cell the spike potential rarely exceeds -10 mV (Henquin & Meissner, 1984) and the currents are comparable in amplitude up to this potential. The voltage-dependent inactivation illustrated in figure 6A will be of physiological significance during sustained depolarisations, such as during the plateau of the slow wave or in the continuous depolarisation achieved with high glucose concentrations. It is possible that a decrease in the amplitude of the delayed potassium current is required to balance the decreased amplitude of the calcium current towards the end of the plateau.

Several channel types were seen in excised membrane patches. It is likely that more than one channel type contributes to the outward current and to the repolarisation of the action potential; further characterisation would require a detailed analysis of single channel activity.

Calcium currents

Calcium currents are important in the ß-cell for both generation of electrical activity and provision of the calcium ions required for insulin secretion. Inactivation of calcium currents is likely to be important in shaping the pattern of ß-cell electrical activity and hence determining the rate of insulin secretion.

Inactivation of calcium currents has been shown in various cell types to be dependent on potential or on calcium entry, or both (see Eckert & Chad, 1984, for a review). Two characteristics of the inactivation of calcium currents in human beta-cells point to the inactivation being primarily calcium-dependent: first, the degree of inactivation roughly parallels the calcium influx. Secondly, inactivation is greatly reduced in barium solutions. Strong evidence supporting this view comes from the two-pulse experiments (figure 7.9): the voltage-dependence of inactivation of the current during the test pulse is very similar to the pre-pulse current-voltage relation, and the inhibition decreases at positive potentials, rather than increasing, as would be expected for voltage-mediated inactivation.

The conclusion that inactivation during short (200 ms) depolarisations is primarily calcium-dependent is in agreement with Plant (1988) who demonstrated calcium- dependent inactivation of calcium currents in mouse pancreatic beta-cells. Inactivation would presumably be more significant in the absence of EGTA (Eckert & Tillotson, 1981), and the degree of calcium-dependent inactivation in the intact cell will largely be determined by the rate and capacity of intracellular buffering.

It has been suggested (Plant, 1988) that if inactivation is purely calcium-dependent, the inactivation of the test current in a two-pulse protocol should depend only on the quantity of calcium entering during the first pulse and not on the potential at which it entered. Figure 7.10A illustrates the relationship between the degree of inactivation and the calcium influx during the prepulse. The relation shows that the prepulse potential does influence inactivation of the test current, apart from its effect in controling the quantity of calcium entry; figures 7.10A and 7.10B both show that Ca^{2+} entry is more effective at producing calcium current inactivation at more negative potentials. Neither potential- dependent inactivation nor an underestimation of charge entry at more positive potentials (due to a non-linear leak) can account for this effect; both would in fact act in the opposite direction.

If the elevation of cytosolic free Ca^{2+} is localised to small "domains" centered on active Ca channels (as in the model of Eckert & Chad, 1984), a small depolarisation will open few channels, producing discrete regions of high Ca_i. A large depolarisation producing the same macroscopic I_{Ca} (as in figure 10B) will activate more channels, but the single-channel currents

will be smaller because of the reduced driving force and the rectification predicted by the constant field theory. Thus the stronger depolarisation will produce a more diffuse distribution of calcium and correspondingly reduce the rate of single-channel closure. In the whole-cell recordings (figure 7.10) this is manifested in slower inactivation. The slower inactivation at more positive potential was previously noted in rodent beta-cells (Plant, 1988).

Evidence that the "domains" are not completely isolated from each other is provided in figure 7.12C. This figure shows calcium currents elicited by depolarisations to 0 mV from holding potentials of -100 mV, -70 mV and -40 mV. Not only does the peak amplitude decrease as the holding potential is made more positive, but the rate and extent of inactivation during the (200 ms) depolarisation decreases, even though the single channel current (and so the amount of calcium entering through each channel) must remain constant. Given that inactivation is predominantly calcium-dependent, the slower inactivation with more positive holding potentials implies that the local calcium concentration is lower, i.e. calcium "domains" must overlap at negative holding potentials. A second implication of the result discussed here is that calcium-dependent inactivation must be caused by calcium acting at a site accessible to cytosolic calcium, rather than at a site deep in the channel.

The lesser degree of inactivation seen with a holding potential of -40 mV might also be interpreted as an inactivating current which is abolished at positive holdng potentials: the currents in figure 7.12C resemble the currents demonstrated in Fox et al., (1987), where the lesser inactivation in currents at 0 mV elicited from a more positive holding potential was attributed to the presence of a third type of Ca^{2+} current (N-type). N-type channels contributed a declining component of inward current from a holding potential of -70 mV, but were inactivated at -40 mV. The inward currents reported in that paper, however, were Ba^{2+} currents, and the relaxation in currents elicited from a negative holding potential could not be ascribed to Ca^{2+}-dependent inactivation. The barium currents in human ß-cells show no sign of a rapidly inactivating component elicited from a holding potential of -70 mV: there is no evidence for more than two types of Ca^{2+} current in ß-cells. (The whole-cell evidence presented here for two types of barium current in the human ß-cell depends on the assumption that the cells were indeed ß-cells: although these particular cells were not shown to spike in response to glucose stimulation, cells from the same cover-slip possessed ATP-sensitive channels, which are not present in pancreatic alpha-cells).

Although inactivation of L-type calcium currents during 200 ms depolarisations seems to be almost entirely calcium-dependent (figures 9-11), longer depolarisations to -40 mV are sufficient to inactivate the calcium or barium currents almost entirely (fig. 7.12), this

inactivation developing over a time-course of several seconds (cf. Cavalie et al, 1986; Rosenberg et al., 1988).

The L-type barium currents in the human cells were unaffected by a change in holding potential from -100 mV to -70 mV, but were almost totally inactivated at -40 mV. The calcium currents were already partly inactivated at -70 mV. These results suggest that the calcium currents in human ß-cells are subject to both calcium- and voltage-dependent inactivation, as has been reported in other cells (e.g. Lee et al., 1985, but see Kalman et al., 1988, for lack of effect of potential and Rosenberg et al., 1986, for lack of effect of Ca_i). Plant (1988) found that changes in the holding potential between -100 mV and -50 mV had no effect on calcium current amplitude in the mouse. I have no explanation for this discrepancy, except that it may be due to the difference of species. A small degree of inactivation of calcium currents at -70 mV was also observed in the rodent beta-cell line HIT T15 (chapter 6).

The L-type calcium current seems sufficient to account for the upstroke of the action potential (Rorsman & Trübe, 1986, Findlay et al., 1989). If this is the case, it would seem that the decrease in the amplitude and frequency of spikes during the plateau phase of the slow wave (Meissner & Schmelz, 1974, Henquin & Meissner, 1984) can be ascribed to the combined effects of calcium-mediated and voltage-dependent inactivation.

CONCLUSION

The human ß-cell has electrophysiological properties very similar to those of the rodent. The human ß-cell posesses ATP-inhibited K^+ channels with conductance, kinetics, ATP- and tolbutamide-sensitivity similar to those of the channel in the rodent ß-cell. Large (200 pS, calcium- and voltage-activated) and small (20 pS) potassium channels are also present, as in the rat (Cook et al., 1984; Ashcroft et al., 1984; Dunne et al., 1985; Ashcroft et al., 1987, 1988) or mouse (Trübe et al., 1986). The voltage-activated currents elicited in the human ß-cell are also similar, in many respects, to those of the rodent ß-cell.

General discussion.

THE IONIC BASIS OF ELECTRICAL ACTIVITY.

Prior to the application of patch clamp methods to the ß-cell in the early 80's, microelectrode studies had characterised the electrical activity induced by glucose and had identified three main features, the initial depolarisation from the resting potential of -70 mV to a threshold potential of -50 mV, slow oscillations from -50 mV to -35 mV, and action potentials superimposed on these slow waves (figure 8.1). The intensity of the electrical activity is increased by those substances which promote insulin release, and is decreased by those which inhibit insulin secretion. Although not yet fully characterised, the ionic conductances responsible for these features have been largely clarified by three techniques, intracellular microelectrode studies, ion efflux studies and, recently, patch clamping.

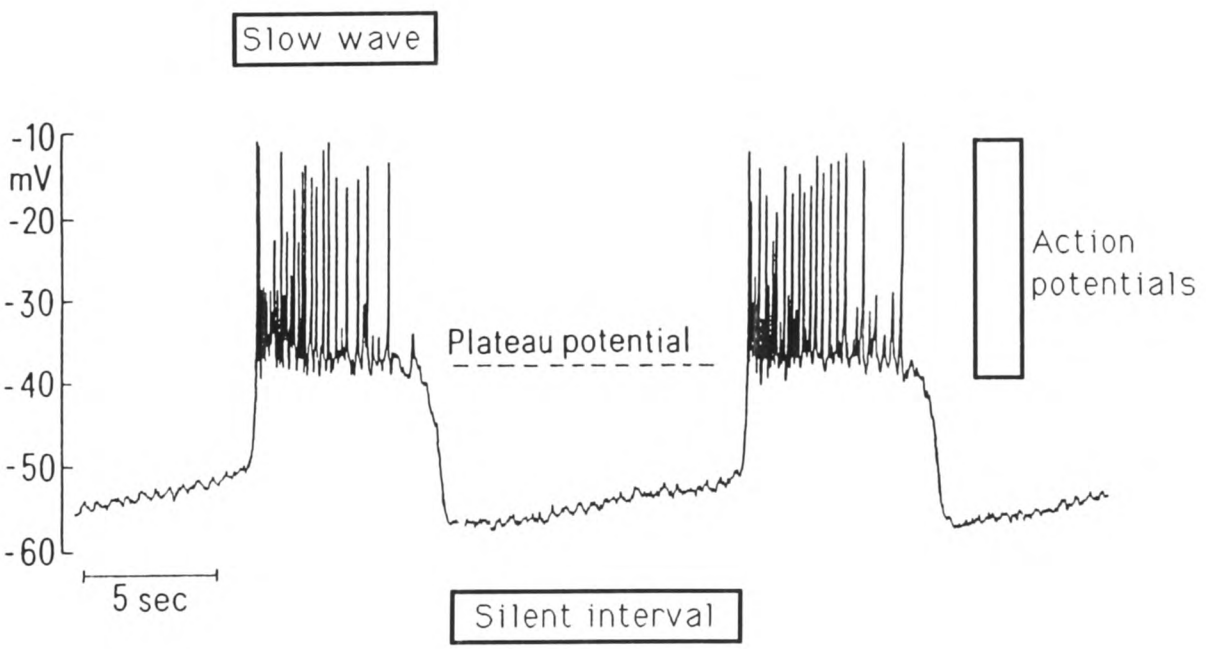


Figure 8.1. Electrical activity of the mouse ß-cell.

Two slow waves, showing the plateau, action potentials and the silent interval.

(Taken from Henquin & Meissner, 1984a).

The initial depolarisation.

The initial glucose-induced depolarisation to the threshold was established to be due to a decrease in P_K by Atwater's microelectrode studies demonstrating a decrease in input conductance, and by K^+ and Rb^+ efflux studies demonstrating reduced K^+ permeability (Sehlin & Taljedal, 1975; Henquin, 1978; Meissner et al., 1978; Boschero & Malaisse, 1979; Dawson et al., 1983), together with the observations that quinine, a known K^+ channel blocker, could depolarise the ß-cell to the plateau potential and stimulate continuous spike activity and insulin release in the absence of glucose (Atwater et al., 1979b; Henquin et al., 1975). Until the advent of patch clamping, however, this decrease in P_K was erroneously attributed to a decrease in the Ca^{2+}-activated potassium conductance.

The attribution of the initial depolarisation to a decrease in potassium permeability has been supported in recent years by patch clamp work, characterising a K^+-selective channel as the dominant conductance in the unstimulated ß-cell and showing it to be closed by stimulatory concentrations of glucose (Ashcroft et al., 1984, 1988a). This same channel has been shown to be sensitive to ATP (Rorsman & Trübe, 1985) and to be closed by a low concentration of quinine (Findlay et al., 1985c; Bokvist et al., 1990b) or sulphonylureas (Sturgess et al., 1985; Trübe et al., 1986).

As the Ca^{2+}-activated potassium conductance is relatively insensitive to quinine (Findlay et al., 1985c; Bokvist et al., 1990a; 1990b) and unaffected by sulphonylureas (Trübe et al., 1986), and as the ATP-sensitive potassium channel has been shown to have the appropriate rubidium permeability (chapter 3; Ashcroft et al., 1989c) the initial depolarisation can now be interpreted with confidence as being due to the closing of ATP-sensitive potassium channels.

Mechanism of bursting.

The initial depolarisation is followed by bursts of action potentials superimposed on a plateau potential around -40 mV (the 'slow wave'), and increases in the glucose concentration increase the plateau fraction by decreasing the interburst duration (the 'silent interval'). Evidence that the slow waves are supported by voltage-dependent Ca^{2+} current has been presented in chapter 1, and there is wide agreement that the rise of the plateau potential and the maintenance of the burst are due to a current of this type.

The process generating the termination of the burst and the mechanism by which glucose increases the slow wave duration are still disputed.

There have been four main theories to account for the burst termination:

1) Ca^{2+}-activated potassium channel activation by a progressive increase in Ca^{2+}_i during the slow wave.
2) ATP-sensitive potassium channel activation by a decrease in ATP due to membrane pump activation or Ca^{2+} inhibition of mitochondrial oxidation.
3) Ca^{2+} current inactivation.
4) activation of a potassium current by IP3-released Ca^{2+}_i.

Ca^{2+}-activated K^+ channel activation ?

The idea that slow Ca^{2+} accumulation during the plateau activated Ca^{2+}-activated K^+ channels to produce the hyperpolarisation terminating the slow wave and that Ca^{2+} efflux and sequestration during the silent interval reversed the activation of Ca^{2+}-activated K^+ channels, allowing the cell to depolarise slowly and trigger another slow wave was originally proposed by Atwater et al. (1979; Atwater et al., 1983), was supported by other groups (Ribalet & Biegelman, 1979; Cook et al., 1980; Cook et al., 1984), and was considered in early mathematical models of ß-cell electrical activity (Chay & Kreizer, 1983). In support of this idea, the input conductance of the ß-cell is greater at the beginning than at the end of the silent interval (Atwater et al., 1978; Ribalet & Biegelman, 1979; 1980), and Ca^{2+}-activated K^+ channels were indeed demonstrated to exist in the ß-cell by patch clamp methods shortly after

their introduction (Marty & Neher, 1982; Cook et al. 1984; Dunne et al., 1984; Findlay et al., 1985b).

Recent evidence has however ruled out this hypothesis. First, Soria's group have used the calcium-sensitive indicator Indo 1 to measure Ca^{2+}_i while simultaneously measuring membrane electrical activity in intact mouse islets. They reported that Ca^{2+}_i rapidly increases to a steady state level and does not progressively increase during the plateau (Valdeolmillos et al. 1989). Secondly, Kukuljan et al. (1991) have demonstrated that charybdotoxin, a specific blocker of the Ca^{2+}-activated K^+ channel, has no effect on the burst pattern in either cultured rat islets or microdissected mouse islets. Similarly, doses of TEA (1mM) which almost completely block Ca^{2+}-activated K^+ channels but have little effect on the ATP-sensitive K^+ channel or the delayed rectifier K^+ channel do not affect the duration of either the slow wave or the silent interval, although increasing spike amplitude (Atwater et al., 1979a; Henquin et al., 1989; Henquin, 1991).

ATP-sensitive K^+ channel activation ?

The decrease in input conductance during the silent interval (Atwater et al., 1978; Ribalet & Biegelman, 1979; 1980) is highly suggestive of a gK-decay model of bursting (Chay & Keizer, 1983; Keizer & Magus, 1989). If a role for the Ca^{2+}-activated K^+ channel has been ruled out, then perhaps the bursts could be due to cyclic activation of ATP-sensitive K^+ channels, as considered by Keizer and Magus (1989). The oscillation in ATP-sensitive potassium channel activity would reflect cyclic variation in the submembrane ATP/ADP ratio, due to the consumption of ATP and production of ADP by membrane ATPases, inhibition of mitochondrial oxidative phosphorylation by calcium entry during the burst, or indeed to intrinsic oscillations in the ATP-generating system.

Smith et al. (1990a) claimed to have excluded a role for ATP-sensitive K^+ channel activation in the slow wave repolarisation by showing that input conductance in a bursting single mouse ß-cell was identical during the plateau and the silent interval, although they acknowledged that they would be unable to detect a change in K-current of less than 0.5 pA.

Two other points are worth considering here: it is not clear how these results can be reconciled with the cyclic variations in input conductance in whole islets reported by Atwater et al. (1978), and it would also seem that an unchanged input conductance would rule out any model depending on an increase in gK to terminate the burst, such as the first and fourth models discussed here.

Finally, even if cyclic variations in ATP-sensitive potassium channel activity are not responsible for termination of the slow wave, it remains possible that regulation of ATP-sensitive potassium channel activity is the means by which glucose (or neurohormonal influences) regulate the periodicity of the slow wave (see below, page 102).

Ca^{2+} current inactivation ?

The role of Ca^{2+} current inactivation in terminating the burst is suggested by the possibility of a window current and the slow inactivation parameters of the Ca^{2+} current. The Ca^{2+} current appears to be inactivated by both Ca^{2+}_i and V_m, with the voltage-dependent inactivation having a time constant (in mouse islets) of ~ 2.75 s (Hopkins et al., 1991), and openings of the L-type calcium channel can be observed at potentials as negative as -70 mV. It seems likely that inactivation of L-type channels during the plateau results in fewer channels available for opening, leading to less frequent and smaller spikes, and possibly to an eventual regenerative deactivation of the calcium current, so terminating the plateau. In this scenario, recovery of the channels from inactivation would lead to the slow depolarisation and eventually to the regenerative activation of the calcium current on the upstroke of the plateau. (It should be remembered that not only has the plateau been shown to be underlain by a calcium current, (the evidence for which is reviewed in chapter 1), but also that the plateau potential can be reset in an all-or-none manner by a current pulse applied to an islet via a suction electrode (Cook et al. 1981b)). This model, then, suggests that the pacemaker current is due to progressive reactivation of L-type Ca^{2+} channels, rather than being due to gK decay (Cook et al. 1991). Mathematical simulations have shown that this type of model can reproduce islet electrical activity (Chay, 1990; Keizer & Smollen, 1991). Strengths of this model are that it does not

The action potential.

The action potential upstroke.

That the upstroke of the action potential in the rodent ß-cell is due to voltage-dependent activation of L-type Ca^{2+} channels is now undisputed, the evidence resting on the early microelectrode work on the effects of varying the external ion concentrations and applying Ca^{2+} channel blockers, on the early patch clamp studies of voltage-dependent currents in the ß-cell (Rorsman & Trübe, 1986) and on more recent patch clamp characterisations of the L-type current and channels (chapters 6 & 7; Rorsman et al., 1988; Plant, 1988; Velasco, 1988; Velasco et al., 1988; Smith et al., 1989b; Kelly et al., 1991).

In canine ß-cells, glucose-induced action potentials have been reported to be TTX-sensitive, and action potentials in one third to one half of human ß-cells could also by inhibited by omission of extracellular Na^+, suggesting that Na^+ current plays a role in action potential generation in non-rodent species (Pressel & Misler, 1990).

Action potential repolarisation.

The basis of repolarisation is more controversial. Attributed by Rorsman and Trübe (1986) to delayed rectifier potassium channels (K_{DR}), the part of the Ca^{2+}-activated K^+ channel has been proposed by other groups (Ribalet & Biegelman, 1980; Findlay & Dunne, 1985; Petersen & Velasco, 1987; Velasco & Petersen, 1987).

The interpretation of much of the data on the channel types underlying spike repolarisation depends on knowledge of the relative potencies of potassium channel blockers on the different channel types. These have recently been elucidated by Bokvist et al. (1989, a; b):

Blocking Kd:

	TEA	Quinine
KATP	22 mM	<10 µM
KCa	0.14 mM	0.1 mM
KDR	1.4 mM	4 µM

require a progressive increase in Ca^{2+}_i (ruled out by Valdeolmillos et al. 1989), and that it is consistent with the lack of effect of known potassium channel blockers. It would imply, however, an increasing input conductance during the silent interval, and so is difficult to reconcile with the results of Atwater et al. (1978).

IP3-activated K^+ current ?

Rorsman et al. have recently measured oscillations in IP3, Ca^{2+}_i and membrane noise in isolated mouse ß-cells. They report spontaneous oscillations in Ca^{2+}_i which they propose activate a Ca^{2+}-sensitive potassium channel which is not the 240 pS Ca^{2+}-activated K^+ channel reported by Cook et al. in 1984. This new K^+ channel they report to be very small (~ 0.6 pS) and to be insensitive to known potassium channel blockers (Rorsman et al. 1991, unpublished). They propose oscillations in IP3 leading to increases in Ca^{2+}_i and opening of this new K^+ channel in the glucose stimulated ß-cell, and attribute the slow depolarisation to gK decay. This model fits the pharmacology and input conductance data, but we are left to reconcile their periodic spikes in Ca^{2+}_i with the steady levels of Ca^{2+}_i shown by Soria's group. Rorsman et al. propose a model with compartmentalised Ca^{2+}_i, in which Ca^{2+}_i released by IP3 from internal stores is considered more effective than Ca^{2+} entering through plasma membrane Ca^{2+} channels in activating the proposed pacemaker channels.

In summary, it now seems unlikely that activation of either Ca^{2+}-activated or ATP-sensitive potassium channels contribute to slow wave repolarisation, but elements of both the Ca^{2+} current inactivation and IP3-mediated oscillations in potassium permeability seem attractive. Clearly, much remains to be clarified in this area, in particular the characterisation of the 'pacemaker' channel and the fluctuations in Ca^{2+}_i in the various intracellular compartments.

The separate question of the role of the ATP-sensitive K^+ channel in the regulation of the frequency of the slow waves and action potentials by glucose is considered below with the modulatory action of glucose on electrical activity (page 102).

In spite of this elucidation, a lot of the older data remains uninformative, for example, the report by Atwater et al. (1979a) that 10 mM TEA increases spike amplitude from 10 mV to 45 mV, with a concomitant increase in spike duration and a decrease in frequency, does not distinguish between involvement of the Ca^{2+}-activated K^+ channel or the delayed rectifier K^+ channel, as both would have been blocked at this concentration and even more recent work (Henquin, 1991) showing similar effects of 0.5 - 2 mM TEA cannot in this way dissect the role of the Ca^{2+}-activated K^+ channel from that of the delayed rectifier K^+ channel in action potential repolarisation.

The original evidence in favour of a role for the Ca^{2+}-activated K^+ channel in action potential repolarisation was provided by the microelectrode studies of Ribalet and Biegelman (1980), who demonstrated that an increase in the extracellular Ca^{2+} concentration increased the rate of action potential repolarisation, while a decrease in extracellular Ca^{2+} or the addition of Ca^{2+} channel blockers (Co^{2+}, 1.25 mM; Mn^{2+2+}, 2 mM; D600, 0.2 mM) decreased the rate of spike repolarisation. They further showed that high (40 mM) $Ca^{2+}{}_o$ partially reversed the effects of quinidine or TEA of the rate of repolarisation, but completely reversed those of Mn^{2+} on rates of depolarisation and repolarisation, a finding compatible with the idea that the decrease in rate of repolarisation by Mn^{2+} is due to a decrease in Ca^{2+} influx and consequent inhibition of Ca^{2+}-activated K^+ channels, while TEA has an additional action on some other potassium permeability contributing to repolarisation (presumably the delayed rectifier K^+ channel). The alternative view that the effect of Mn^{2+} is due to a decrease in P_K because of a shift in the activation curve to the right (Ashcroft & Rorsman, 1989b), seems unlikely, as it should not be overcome by an increase in $Ca^{2+}{}_o$.

Smith et al. (1990b) have shown that Ca^{2+}-activated K^+ channels account for 10-20% of the voltage-activated current in whole cell or nystatin-permeabilised cells, and concluded that Ca^{2+}-activated K^+ channels had little role in action-potential repolarisation as they saw only the 8 pS delayed rectifier K^+ channel openings following the action potential in cell-attached patches. On the other hand, Velasco and Petersen (1987) reported that the number of Ca^{2+}-activated K^+ channel openings seen in cell-attached patches depended on the local Ca^{2+}

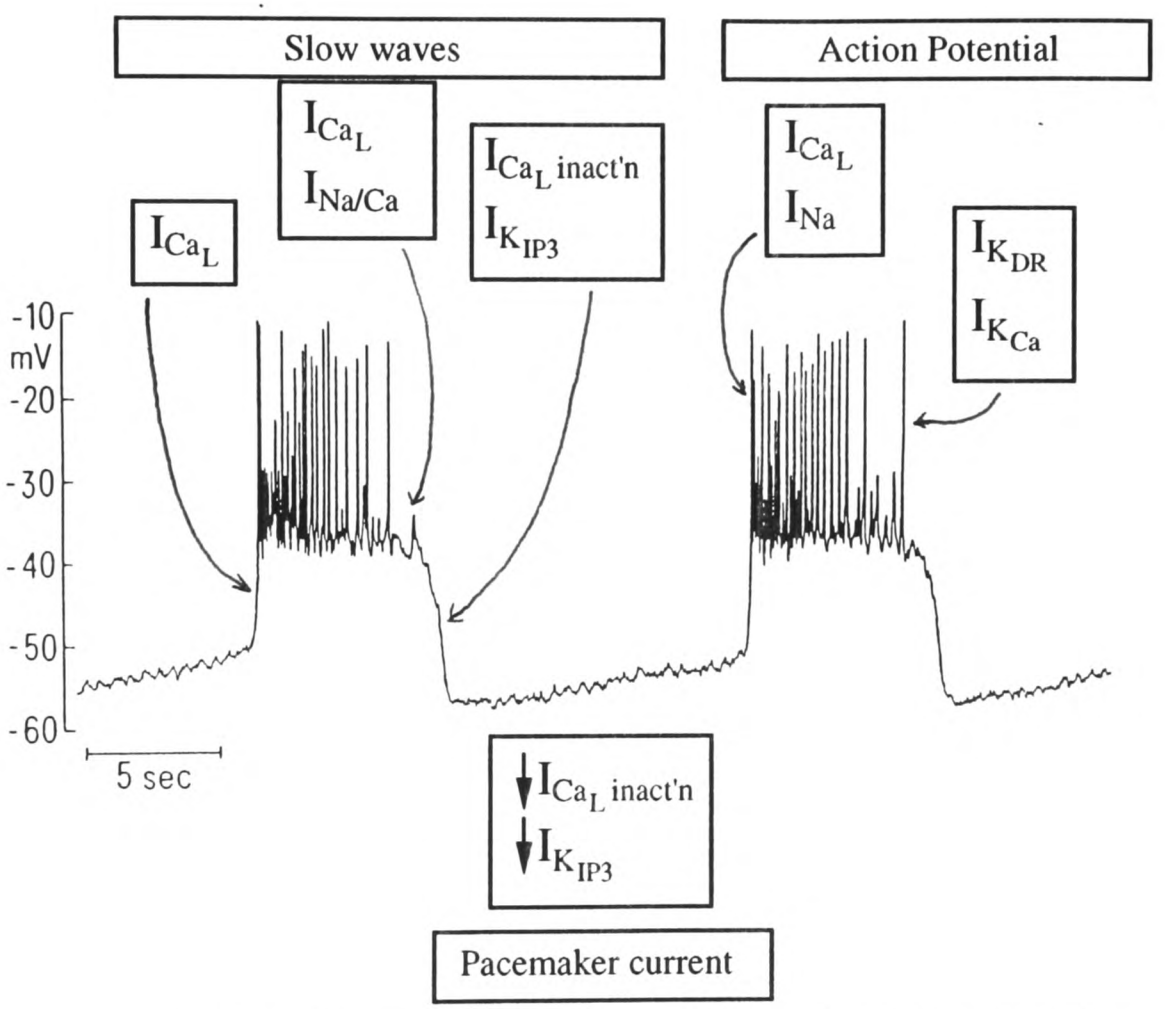


Figure 8.2. The ion channels underlying the various parts of ß-cell electrical activity.

concentration, with 2.5 mM Ca^{2+} in the pipette increasing the open probability of the Ca^{2+}-activated K^+ channel 10-fold compared with 0 mM Ca^{2+}_o, suggesting that Ca^{2+}-activated K^+ channels might open during the action potential repolarisation where they are in close proximity to open Ca^{2+} channels. Dean and Mathews (1970a) and Meissner and Schmeltz (1974) reported irregular repolarisation phases with large voltage fluctuations, and Bangham and Smith (1987) report that the permeability of the channel underlying the fluctuations is close to that of the Ca^{2+}-activated K^+ channel. The argument that these fluctuations are due to openings of the Ca^{2+}-activated K^+ channel is supported by the finding that the spikes are smoothed by 0.6 mM TEA, a concentration which should largely block Ca^{2+}-activated K^+ channels, while delayed rectifier K^+ channels should be relatively unaffected (Smith, 1988).

Successfully avoiding the problems of TEA's lack of specificity, Kukuljan et al. (1991) used CTX as a specific blocker of Ca^{2+}-activated K^+ channels, and found that the action potential frequency and rate of repolarisation were not affected at a dose which completely inhibited opening of Ca^{2+}-activated K^+ channels in cell-attached patches.

The A-currents recently demonstrated in mouse ß-cells seem unlikely to contribute to action potential repolarisation, as they are likely to be fully inactivated at the plateau potential (Smith et al., 1989a).

In conclusion, the dominant channel type underlying action potential repolarisation seems to be the delayed rectifer. A role for the Ca^{2+}-activated K^+ channel in spike repolarisation is unproven, at least at physiological Ca^{2+}_o, with evidence both for and against. There seems little doubt that the Ca^{2+}-activated K^+ channel can make a more important contribution to action potential repolarisation at elevated Ca^{2+}_o.

THE REGULATION OF THE ATP-SENSITIVE POTASSIUM CHANNEL.

The regulation of the ATP-sensitive potassium channel has become a massively complicated subject, with roles for adenosine, guanosine and pyridine nucleotides, pH_i, Mg^{2+} and Ca^{2+}, internal anions and GTP-binding proteins (see Ashcroft 1988; Ashcroft & Rorsman, 1989b). There remains a long-running dispute over the physiological regulation of the glucose-induced decrease in ATP-sensitive potassium channel activity. To summarise the present understanding of regulation of the channel in the ß-cell, modulation by pH_i seems unlikely as glucose has been reported to have no effect (Grapengiesser et al., 1989) or slightly to increase pH_i (Arkhammer et al., 1986) (which would tend to increase ATP-sensitive potassium channel activity), while protein kinase C now seems not to be involved in glucose-stimulated insulin secretion (see Wollheim & Regazzi, 1990 for a review) and the evidence is now overwhelming that the ATP/ADP ratio is the physiological regulator (reviewed in chapter 4). The lines of evidence in favour of this last point are that 1) ATP blocks the channel in excised patches and in whole-cell recordings (Cook & Hales, 1984; Rorsman & Trübe, 1985); 2) those substances which increase ATP_i decrease channel activity, while those which decrease ATP_i increase channel activity (Ashcroft et al., 1984; Misler et al., 1986; Ribalet & Ciani, 1987); 3) changes in ATP-sensitive potassium channel activity and the ATP/ADP ratio occur over the same glucose concentration range and similar time periods (Misler et al., 1986; Ashcroft et al., 1988a; Ashcroft et al., 1973; Kakei et al., 1986; Malaisse & Sener, 1987; Meglasson et al., 1989); 4) the effects of ATP on ATP-sensitive potassium channel kinetics in isolated patches resemble those of glucose on the channel in cell-attached patches. It seems likely that in the intact ß-cell, the great majority of ATP-sensitive potassium channels are inhibited even in the absence of glucose, that the effective ATP-sensitivity in the whole cell is much lower than that in excised patches and that this is in part due to a low submembrane ATP and in part to relief of ATP inhibition by ADP. Clearly, the ability to resolve ATP concentrations in different cellular compartments would be invaluable for understanding of ATP-sensitive potassium channel regulation.

RIN cells vs. ß-cells.

Part of the confusion with regard to regulation of the ATP-sensitive potassium channel stems from work on the RIN cell, which in this respect seems to be significantly different from the ß-cell, and worthy of a comment. In the RIN cell, glyceraldehyde (but not glucose) causes ATP-sensitive potassium channel inhibition, and the rise in ATP is not sufficiently fast to account for closure of the ATP-sensitive potassium channel (Wollheim et al., 1988). Glyceraldehyde, however, stimulates *de novo* synthesis of 1,2-DAG in RIN cells, and PMA and DC10 mimic the effects of glyceraldehyde in closing the ATP-sensitive potassium channel (Dunne & Petersen, 1987; Wollheim et al., 1988), and the increase in DAG concentration occurs sufficiently rapidly for Wollheim et al. (1988) to have proposed DAG to be the physiological regulator of ATP-sensitive potassium channel activity. Further confusion arose, however, from separate studies on the same cell line showing that the protein kinase C activators TPA (250 nM) or PMA (1µM) increased ATP-sensitive potassium channel activity (Ribalet et al., 1988; de Weille et al., 1989) and produced membrane hyperpolarisation (de Weille et al., 1989). It has also been reported that PMA has time-dependent effects on ATP-sensitive potassium channels, an early effect to decrease the activity of the ATP-sensitive potassium channel and a late effect to stimulate channel activity (Dunne et al., 1990b; Dunne, 1991). It may be that only the first effect is mediated by protein kinase C, and a direct effect of PMA revealed after protein kinase C is washed out of permeabilised cells, or the phenomenon could reflect the effects of two separate protein kinase C's (Nishizuka, 1988) with different rates of washout. This latter interpretation is supported by the observation that staurosporine (10 nM), a potent inhibitor of protein kinase C, produced activation of K_{ATP} channels, followed by inhibition (Dunne, 1991).

In the ß-cell, although glucose rapidly stimulates de novo synthesis of DAG (Peter-Riesch et al., 1988), protein kinase C activators do not decrease ATP-sensitive potassium channel activity (Plant, 1989; Henquin et al., 1989), protein kinase C is not redistributed to the plasma membrane (Easom et al., 1989; Persaud et al., 1989) and ATP_i rises sufficiently rapidly to

account for the closure of the ATP-sensitive potassium channel (Meglasson, 1989). Hence the protein kinase C pathway does not apear to be involved in glucose-stimulated ATP-sensitive potassium channel closure.

Finally, glyceraldehyde, unlike glucose, causes a decreae in cytoplasmic pH (Arkhammar et al., 1986), and this may contribute to its inhibitory effect on the ATP-sensitive K^+ channel (Misler et al., 1989), while the decrease in pH_i could contribute to the stimulaton of insulin release by causing mobilisation of Ca^{2+} from mitochondria (Prentki et al., 1983).

THE MODULATORY EFFECT OF GLUCOSE.

Glucose not only initiates electrical activity in the ß-cell, at suprathreshold concentrations glucose increases the plateau fraction and action potential frequency. Several groups, using various techniques, have now contributed to answering the question 'How does glucose modulate electrical activity after closing a sufficient number of ATP-sensitive potassium channels to trigger slow waves ?'

Slow waves.

There seem to be two main contenders for the current modulated by increasing glucose concentrations, ATP-sensitive potassium channel current and the voltage-sensitive L-type Ca^{2+} current. It is known that some ATP-sensitive potassium channels remain open at stimulatory glucose concentrations, in cell attached patches (Ashcroft et al., 1988a) and in whole-cell experiments (Ashcroft et al., 1990c), and that low doses of tolbutamide can produce bursts in the absence of glucose (Meissner & Henquin, 1983), while high concentrations can induce continuous spiking (Meissner et al., 1980) similar to that seen in high (>15 mM) glucose concentrations, and that diazoxide can convert continuous electrical activity to burst activity in the presence of 30 mM glucose (Henquin, 1988), suggesting that glucose could increase burst duration by decreasing the number of open ATP-sensitive potassium channels at superthreshold concentrations (Henquin, 1988; Ashcroft et al., 1990b). Only a very slight change in current would be required because of the high input resistance of the glucose-stimulated ß-cell (Smith et al., 1990a), as demonstrated by the potentiation of electrical activity by ouabain (Henquin & Meissner, 1982b) or argenine (Henquin & Meissner, 1981; Charles et al, 1982), which each produce a small net inward current by blocking the Na-K ATPase and by electrogenic membrane transport respectively.

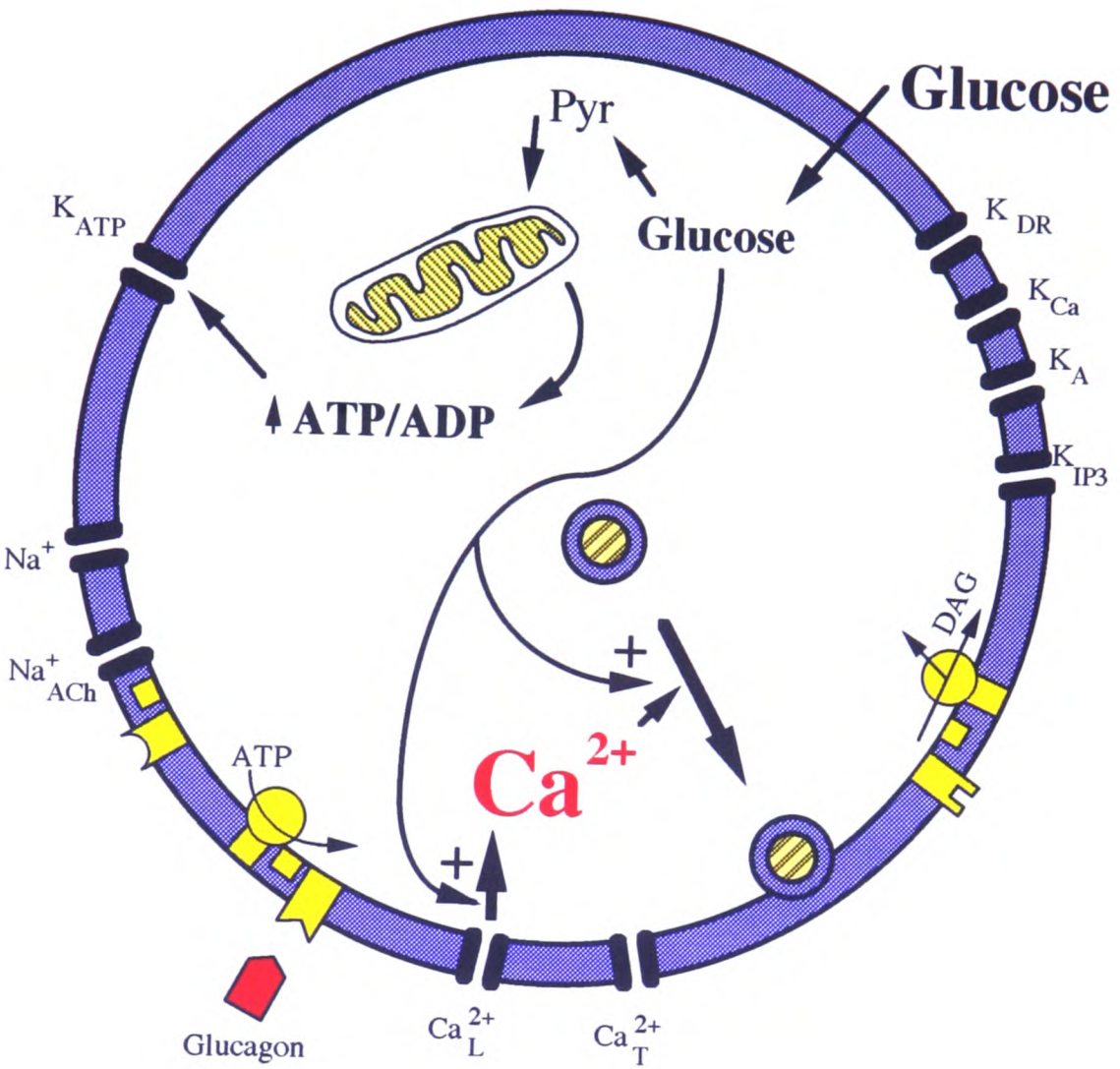


Figure 8.3. The actions of glucose in the ß-cell.
Glucose produces the initial depolarisation and subsequent increase in electrical activity by increasing the intracellular ATP/ADP ratio and closing ATP-sensitive K-channels. It also increases L-type Ca channel activity and sensitises the releasing mechanism to Ca. These actions all require glucose metabolism.

Action potential frrquency.

It seems that the role of glucose on electrical activity is not limited to causing the initial depolarisation and modulation of slow wave activity: Henquin has reported an effect of glucose in increasing action potential frequency, apart from that due to an increase in the plateau fraction at higher glucose concentrations (Bozem & Henquin, 1988). Bozem & Henquin (1988) investigated action potential frequency under conditions where the cell membrane was permanently depolarised to the plateau potential, and found that if this were achieved by a combination of 10 mM glucose and 1 mM Ca_o, raising the glucose concentration to 15 mM more than doubled spike frequency while addition of 5 µM tolbutamide increased it more than three-fold. Similarly, continuous depolarisation to the plateau potential could be achieved by a combination of 3 mM glucose and 100 µM tolbutamide at 2.5 mM Ca_o, under which conitions an increase in the glucose concentration to 10 mM resulted in a 50 % increase in action potential activity, similar to that produced by addition of 500 µM tolbutamide. Combining these observations with the known mechanisms of action of glucose and tolbutamide and the previous observation that the spike frequency can be increased by injection of a depolarising current during the slow wave, (Atwater et al., 1978), suggests that the increase in action potential frequency is due to inhibition by glucose or tolbutamide of ATP-sensitive K^+ channels remaining open during the continuous depolarisation.

Ca^{2+} current modulation.

A second mechanism by which glucose might influence electrical activity is the positive modulation of the voltage-sensitive Ca^{2+} current. Modulation of L-type Ca^{2+} current is well described in other systems (e.g. Reuter, 1987), and Petersen's group has reported that glyceraldehyde increases Ca^{2+} current and decreases the potential for Ca^{2+} current activation in the RIN cell (Velasco et al., 1988). It would seem that this mechanism is also active in the ß-cell. Smith et al. (1989b) have reported that glucose (20 mM compared with 0 mM) produces a two-fold increase in peak Ca^{2+} current in permeable-patch recordings from mouse ß-cells, and in the ensemble activity of L-type channels in cell-attached recordings in the voltage range

of the plateau and spikes (-40 mV to 0 mV) by decreasing the long closed time of this channel. This would tend to increase the calcium current and Ca^{2+} influx at high glucose concentrations, and could be a contributory factor in the progressive increase in electrical activity as the glucose concentration is increased. The effect was blocked by mannoheptulose (30 mM), and channel activity could be decreased below basal (i.e. that in 0 mM gluc) by oligomycin (2.4 μg/ml; Smith et al., 1989b).

The biochemical modulation of Ca^{2+} channels.

The nature of the link between glucose metabolism and calcium channel activation has not yet been established. L-type calcium channels are commonly modulated by cAMP-dependent phosphorylation (see Kameyama et al., 1885; Reuter, 1987; Armstrong & Eckert, 1989), but glucose has little effect on cAMP levels in the ß-cell (Prenki & Matschinsky, 1987). On the other hand, glucose and glyceraldehyde evoke rapid de novo synthesis of DAG in rat ß-cells (Peter-Riesch et al., 1988) and insulinoma cells (Wollheim et al., 1988). As Petersen & Wollheim (1990) have pointed out, since the cell permeable DAG analogue DC10 mimics the effect of glyceraldehyde on gating of L-type Ca^{2+} channels in the RIN cell (Velasco & Petersen, 1989), DAG could be the relevant intracellular messenger, acting via protein kinase C - mediated phosphorylation or an as yet unknown mechanism.

Against this argument, PMA (100 nM) had no effect on the same channel in the same cells (Velasco & Petersen, 1989), suggesting that either there are different varieties of C-kinase in RIN cells (Nishizuka, 1988), or the DC10 effect is not associated with activation of protein kinase C (see DiVirgilio et al., 1986, for an effect of PMA on RIN cell Ca^{2+} influx, see Hockberger et al., 1989, for inhibition of L-type Ca^{2+} channels by an external blocking action of OAG, DiC8, TPA, PDA and 4PDD, and see Plant, 1989 for attribution of the effects of DiC8 on voltage-activated currents in the ß-cell to a mechanism other than activation of protein kinase C).

MODULATION BY HORMONES AND NEUROTRANSMITTERS.

Glucagon.

Microelectrode studies.

Glucagon stimulates insulin secretion and potentiates electrical activity by increasing the duration of the slow wave and decreasing the duration of the silent interval (Ikeuchi & Cook, 1984). The effects of glucagon are thought to be mediated by cyclic AMP, as glucagon raises intracellular cyclic AMP (Schuit & Pipleers, 1985; Gorus et al., 1988) and dibutyryl cyclic AMP or those agents which increase intracellular cyclic AMP mimic the effects of glucagon on ß-cell electrical activity (Henquin & Meissner 1983; Henquin et al., 1983; Henquin & Meissner 1984b; Henquin & Meissner 1984c; Henquin et al., 1987). The proposal that glucagon increases electrical activity by increasing Ca^{2+} current (Henquin & Meissner, 1983) is supported by the report that those substances which increase intracellular cyclic AMP increase ß-cell Ca^{2+} influx, Ca^{2+} uptake and insulin release (Henquin et al., 1987) and is also supported by the report in the same paper that the delay to the first spike after addition of 25 µM tolbutamide to 3 mM glucose in the bath solution could be decreased by pretreatment with 1 µM forskolin (from 79s to 37s), even though this manoeuvre had no effect on the onset of depolarisation..

The action of glucagon in increasing insulin sectetion via an increase in Ca^{2+}_i is dependent on a decrease in the ß-cell membrane K^+ permeability by a fuel secretagogue (or a K_{ATP} channel blocker, such as tolbutamide), as it is without effect if the cell is not previously depolarised or is depolarised by alanine or arginine (Henquin & Meissner, 1986). Stimulation of cyclic AMP levels by forskolin has been reported not to increase Ca^{2+}_i as measured by quin 2 fluorescence in ob/ob mice ß-cells (Rorsman & Abrahamsson,1985) or in RIN cells (Wollheim et al., 1984), leading to suggestions that the mode of action of glucagon was not to increase Ca^{2+}_i, but to sensitise the ß-cell to Ca^{2+}_i. While it is certainly true that a major part of the action of glucagon is via a sensitisation of the secretory apparatus to Ca^{2+}_i, as for example the increase in insulin release by cyclic AMP is much greater than that expected from the

increase in electrical activity or Ca^{2+} influx (Henquin et al., 1987) and cyclic AMP can increase insulin release without change in membrane ion fluxes (Henquin & Meissner, 1986) (and see also the studies on permeabilised cells, e.g. Tamagawa et al., 1985; Jones et al., 1986), the increase in electrical activity induced by glucagon implies that part of its effect is via an increase in Ca^{2+} influx. It is possible that no increase in Ca^{2+}_i was observed in the studies mentioned above because quin 2 may not be sufficiently sensitive to pick up a relatively small change in Ca^{2+}_i, or one localised to the submembrane region.

Patch clamp studies.

The first patch clamp demonstration of cyclic AMP effects on the ß-cell Ca^{2+} current showed only a slowing in Ca^{2+} current inactivation, with no increase in peak Ca^{2+} current, when cAMP was included in the pipette (Rorsman & Ashcroft, 1989b), but Smith et al., (1990c) have now reported that 1 mM dibutyryl cyclic AMP or 10 µM forskolin added to the bath solution increase Ba^{2+} current up to three-fold (in a high-K^+ solution with 0.1 µM BAYK 8644). This is similar to the effects of cyclic AMP on Ca^{2+} current in other tissues, is consistent with the lack of effect of cyclic AMP on insulin secretion at low glucose concentrations, and is almost certainly the mechanism by which glucagon increases Ca^{2+} influx to the ß-cell.

Acetylcholine.

Microelectrode studies.

Acetylcholine is a secondary secretagogue, effective in vitro only at higher glucose concentrations, and its effect increasing with glucose concentration (see, for example, Gagerman et al., 1978). ACh or CCh have been shown to stimulate electrical activity already induced by glucose by increasing the slow wave frequency, decreasing the duration of both slow waves and silent intervals, with little change in plateau fraction. The effects are mimicked by muscarine, but not nicotine, and are abolished by atropine (Gagerman et al., 1978; Cook et al., 1981a; Hermans et al., 1987; Henquin et al, 1988). The mechanism of this muscarinic action on insulin secretion and electrical activity are still not clear. Changes in cyclic nucleotide concentrations are not involved (Gagerman et al., 1978; Wollheim et al., 1980; Mathias et al., 1985), but the roles of phosphoinositide breakdown and changes in ionic conductance are still being resolved. Muscarinic agonists generate IP3 from inositol-4,5-bisphosphate and so mobilise intracellular Ca^{2+} in islet cells and in insulinoma cells (Best & Malaisse, 1983; Biden et al., 1984; Joseph et al., 1984; Morgan et al., 1985; Wolf et al., 1985; Wollheim & Biden, 1986), but cholinergic stimulation of insulin release depends on the availability of Ca^{2+}_o (e.g. Wollheim et al., 1980; Mathias et al., 1985), suggesting that depolarisation of the ß-cell membrane and acceleration of Ca^{2+} influx is crucial for the action of ACh (e.g. Gagerman et al. 1978). In the presence of electrical activity, ACh decreases the slow wave repolarisation, i.e. the membrane potential during the silent interval is less negative than before (Gagerman et al., 1978; Cook et al., 1981a; Hermans et al., 1987; Henquin et al, 1988), and in a low glucose solution (Henquin et al., 1988) or in the presence of diazoxide (Hermans et al. 1987), ACh depolarises the membrane by about 5 mV without stimulating electrical activity. This depolarising effect was at first thought to be due to a decrease in K^+ permeability, but Henquin's group demonstrated that this was not so, as the depolarisation was not antagonised by agents which increase P_K, and was consistantly associated with an acceleration of $^{86}Rb^+$ efflux (Nenquin et al., 1984; Hermans et al., 1987)). The same group have demonstrated that ACh (20 μM) increases Na^+ influx and that omission of Na^+_o prevented muscarinic

depolarisation of the ß-cell, prevented the increase in Ca^{2+} influx and the increase in insulin release, while omission of Ca^{2+}_o did not prevent the stimulation of Na^+ influx. Unfortunately, technical reasons meant that the effect of 0 mM Ca^{2+}_o on depolarisation could not be determined (Henquin et al., 1988). The muscarinic breakdown of phosphoinositides (as measured by efflux of ^3H from ^3H-inositol labelled islets) was not affected by omission of Na^+_o. These results suggest that the increase in Ca^{2+} influx is secondary to an increase in P_{Na}, and are consistent with stimulation of Na^+ influx at 3 mM glucose or 10 mM glucose, but stimulation of Ca^{2+} influx only at 10 mM glucose. Since cholinergic agents mobilise intracellular stores, ACh has at least two mechanism for increasing Ca^{2+}_i. Sustained muscarinic stimulation of insulin release is, however, dependent on an increase in Ca^{2+} influx (Wollheim & Sharp, 1980; Best & Malaisse, 1983).

Patch clamp findings.

ACh-activated Na^+ channels have been reported in a recent review (Ashcroft & Rorsman, 1989b). The single-channel amplitude was 3.5 pA at -70 mV, the channel currents were dependent on the presence of external Na^+ and were abolished by atropine. That the maximum ACh-stimulated current in the ß-cell is ~ 10 pA implies that the number of opem channels (i.e. NP) must be very small.

Biochemical mediators.

Activation of these channels may be secondary to phosphoinositide breakdown, but it is not via protein kinase C activation, as depolarisation and the increase in Ca^{2+} influx are not duplicated by phorbol esters (Bozem et al., 1987). Another possibility is a coupling of the muscarinic receptor to the Na^+ channel via a G-protein (see Cohen-Armon et al., 1985; Cohen-Armon & Sokolovsky, 1986; Pfaffinger et al., 1985; Neer & Clapham, 1988).

Adrenaline

Adrenaline has long been known as an inhibitor of insulin secretion and electrical activity in the ß-cell (e.g. Milner & Hales, 1968; Dean & Mathews, 1970a). It has actions at several sites in the ß-cell, producing a decrease in electrical activity, an inhibition of adenylyl cyclase and exerting a distal inhibitory action on the secretory process. It seems that the mechanism of adrenaline action in decreasing ß-cell electrical activity has recently been elucidated by the report of Rorsman et al. (1991) that adrenaline (5 µM) acting via alpha-2 receptors activates K^+ channels distinct from the ATP-sensitive potassium channel. This 'new' channel has a linear slope conductance of ~ 0.6 pS (5.6 mM K^+_o), is insensitive to glibenclamide or TEA, is unaffected by application of forskolin or dibutyryl cyclic AMP and contributes ~ 11 pA of outward current at -70 mV (5 µM adrenaline). Activation of this channel by adrenaline could by inhibited by pretreatment with PTX, indicating involvment of an inhibitory G protein in channel activation.

Henquin's group has recently settled the disputed question as to whether the decrease in electrical activity is simply an epiphenomenon of the distal inhibitory action of adrenaline. They report that agents (high K^+_o, tolbutamide, arginine) which depolarise the cell membrane increased the K_i for adrenaline, while not diminishing the inhibitory effect of high concentrations, indicating that the decrease in electrical activity is the mediator of inhibition of insulin secretion by low concentrations of adrenaline (Debuyser et al., 1991). High concentrations of adrenaline exert additional, more distal, actions.

Galanin and somatostatin.

Rorsman et al. (1991), in their paper on the action of adrenaline, point out that the repolarising actions of galanin or somatostatin cannot be overcome by glibenclamide, and suggest that, contrary to what has previously been demonstrated in RIN cells (Dunne et al., 1989a; de Weille et al., 1988; 1989), ATP-sensitive potassium channel activation does not account for the inhibitory action of these peptides. As in the case of adrenaline, the inhibitory action of galanin is PTX-sensitive (Wahlander et al., 1991; Bokvist et al., 1991) and the effects of adrenaline and galanin are not additive, although those of galanin and diazoxide are (Drews et al., 1991). Rorsman's group have recently reported activation of the same class of K^+ channel by adrenaline, galanin and somatostatin (Bokvist et al., 1991), supporting the conclusion of Drews et al., (1990; 1991) that adrenaline and galanin act via the same mechanisms, including an increase in P_K that is not mediated by an increase in the activity of the ATP-sensitive potassium channel.

Ashcroft and Rorsman (1989b) report that not clonidine, galanin nor somatostatin activate ATP-sensitive potassium channels either whole-cell (Ashcroft & Rorsman, 1989b) or in perforated patch recordings (Ashcroft & Rorsman, 1989a), while in cell-attached patches the action of galanin in inhibiting glucose-induced spiking was usually not accompanied by ATP-sensitive potassium channel activation (Ahren et al., 1989). These various reports suggest that activation of the ATP-sensitive K^+ channel is not involved in the action of adrenaline, galanin or somatostatin on ß-cell electrical activity, although each of the reports was inconclusive, as occasionally an effect on ATP-sensitive K^+ channels was observed. The question of ATP-sensitive K^+ channel activation by inhibitors of secretion is therefore still not fully resolved.

In mouse ß-cells it has been impossible to demonstrate alpha-2 adrenergic inhibition of calcium currents (Ashcroft & Rorsman, 1989b) and indeed Wahlander et al. (1990) have reported that inhibition of insulin secretion by clonidine (5 µM) does not involve an inhibition of I_{Ca} in the mouse ß-cell, although adrenaline, clonidine, galanin and somatostatin have been demonstrated to inhibit Ca^{2+} current in HIT cells via a PTX-sensitive mechanism (Keahey et al., 1989b; Hsu et al., 1989) and in RIN cells (Homadian et al., 1991).

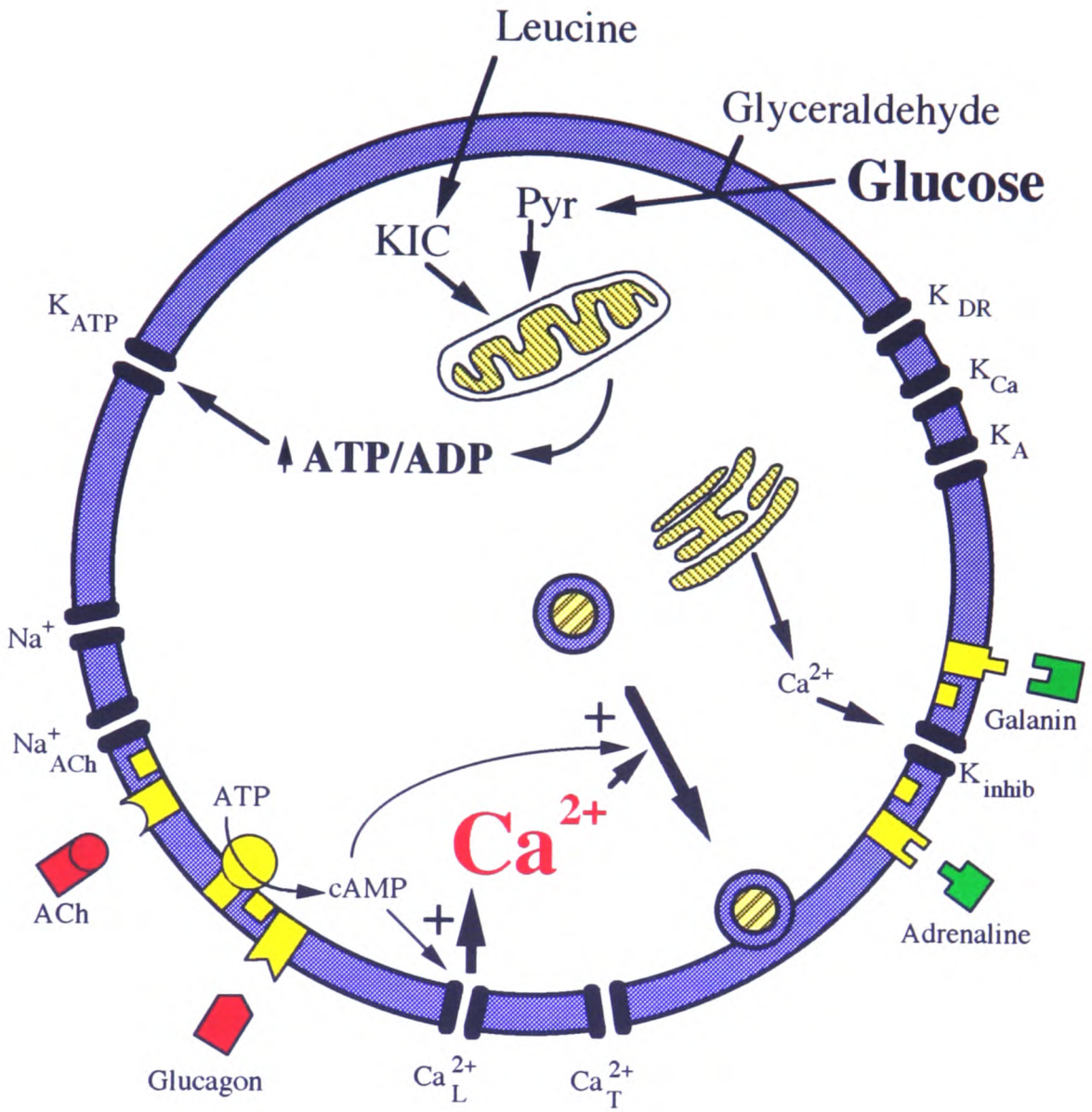


Figure 8.4. A schematic diagram of ß-cell membrane functions.
The diagram shows those ionic channels and second messenger systems discussed in the text. Several membrane functions contributing to ß-cell electrical activity are not represented, notably ion pumps and exchangers and cell-to-cell communications.

CONCLUSION.

Great progress has receently been made in identifying and understanding the mode of action of the initiators, potentiators and inhibitors of insulin secretion. A great deal remains to be done in elucidating the regulation and integration of these mechanisms, in particular at the interface of the biochemical and electrophysiological aspects of ß-cell function.

Much energy is presently being expended in the molecular characterisation of the regulatory pathways, and this should allow precise identification of the molecular intermediates. It would also be most helpful to be able to identify subcellular variations in ATP_i and Ca_i, in particular to measure their submembrane levels, as it is in this compartment that they control membrane ion channel activity and insulin release.

As the subtleties of ß-cell function are explored, the differences between species are becoming more apparent, and the deficiencies of the rodent as a model of the human ß-cell are becoming more obvious. More significantly, perhaps, insulinoma cells and virus-transformed cell lines have proved to be very different from the ß-cell in the regulation of both the ATP-sensitive K^+ channel and the L-type Ca^{2+} channel, the two channels central to the control of insulin secretion.

The key directions of future research are likely to be in clarifying the links between metabolism and electrical activity, identifying the nature and role of compartmentalisation within the cell and elucidating the regulatory and integrative aspects of the ß-cell microenvironment.

References.

Ahren, B., Berggren, P.-O., Bokvist, K. & Rorsman, P. 1989. Does galinin inhibit insulin secretion by opening of the ATP-regulated K^+ channel in the ß-cell ? *Peptides* **10,** 453-457.

Ammala, C., Bokvist, K., Larsson, O., & Rorsman, P. 1991. GTP-dependent periodic activation of a calcium-dependent potassium current in mouse ß-cells. *Diabetologia,* **34,** A87.

Arkhammer, P., Berggren, P.O. & Rorsman, P. 1986. Direct evidence for opposite effects of D-glucose and D-glyceraldehyde on cytoplasmic pH in mouse pancreatic ß-cells. *Bioscience Reports* **6**, 355-361.

Arkhammar, P., Nilsson, T., Rorsman, P. & Berggren, P.O. 1987. Inhibition of ATP-regulated K^+ channels precedes depolarisation-induced increase in cytoplasmic free Ca^{2+} concentration in pancreatic beta-cells. *Journal of Biological Chemistry* **262**, 5448-5454.

Arkhammer, P., Nilsson, T., Welsh, M., Welsh, N. & Berggren, P.-O. 1989. Effects of protein kinase C activation on the regulation of stimulus-secretion coupling in pancreatic ß-cells. *Biochemical Journal* **264**, 207-215.

Armando-Hardy, M., Ellory, J.C., Ferreira, M.G., Fleminger, S. & Lew, V.L. 1975. Inhibition of the calcium-induced increase in the potassium permeability of human red blood cells by quinine. *Journal of Physiology* **250**, 32-33P.

Armstrong, D. & Eckert, R. 1989. Voltage-activated calcium channels that must be phosphorylated to respond to membrane depolarisation. *Proceedings of the national Academy of Science of the USA* **84**, 2518-2522.

Ashcroft, S.J.H. 1980. Glucoreceptor mechanisms and the control of insulin release and biosynthesis. *Diabetologia* **18**, 5-15.

Ashcroft, F.M. 1988. Adenosine tri-phosphate sensitive K-channels. *Annual Reviews of Neuroscience* **11**, 97-118.

Ashcroft, S.J.H. & Ashcroft, F.M. 1989. Properties and functions of ATP-sensitive K-channels in stimulus-response coupling in the pancreatic ß-cell. *Cell Signalling* **2**, 197-214.

Ashcroft, F.M. & Kakei, M. 1987. Effects of internal Mg^{2+} on ATP-sensitive K-channels in isolated rat pancreatic ß-cells. *Journal of Physiology* **390**, 72P.

Ashcroft, F.M. & Kakei, M. 1989. ATP-sensitive K^+ channels in rat pancreatic ß-cells: modulation by ATP and Mg^{2+} ions. *Journal of Physiology* **416**, 349-67.

Ashcroft, F.M. & Rorsman, P. 1989a. ATP-sensitive channels: a link between ß-cell metabolism and insulin secretion. *Transactions of the Biochemical Society* **18**, 109-111.

Ashcroft, F.M. & Rorsman, P. 1989b. Electrophysiology of the pancreatic ß-cell. *Progress in Biophysics and Molecular Biology* **54**(2), 87-143.

Ashcroft, F.M & Stanfield, P.R. 1983. The influence of the permeant ions thallous and potassium on inward rectification in frog skeletal muscle. *Journal of Physiology* **343**, 407-428.

Ashcroft, S.J.H. & Stubbs, M. 1987. The glucose sensor in HIT cells is the glucose transporter. *FEBS Letters* **219**, 311-315.

Ashcroft, S.J.H., Weerasinghe, L.C.C. & Randle, P.J. 1973. Interrelationship of islet metabolism, adenosine triphosphate content and insulin release. *Biochemical Journal* **134**, 223-231.

Ashcroft, F.M., Harrison, D.E. & Ashcroft, S.J.H. 1984. Glucose induces closure of single potassium channels in isolated rat pancreatic beta-cells. *Nature* **312**, 446-448.

Ashcroft, F.M., Ashcroft, S.J.H. & Harrison, D.E. 1985. The glucose-sensitive potassium channel in rat pancreatic beta-cells is inhibited by intracellular ATP. *Journal of Physiology* **369**, 101P.

Ashcroft, S.J.H., Hammonds, P. & Harrison, D.E. 1986. Insulin secretory responses of a clonal cell line of simian virus 40-transformed B cells. *Diabetologia* **29**, 727-733.

Ashcroft, F.M., Ashcroft, S.J.H. & Harrison, D.E. 1987a. Effects of 2-keto-isocaproate on insulin release and single potassium channel activity in dispersed rat pancreatic ß-cells. *Journal of Physiology* **385**, 517-529.

Ashcroft, F.M., Kakei, M., Kelly, R.P. and Sutton, R. 1987b. ATP-sensitive K^+ channels in human isolated pancreatic B-cells. *FEBS Letters* **215**, 9-12.

Ashcroft, F.M., Ashcroft, S.J.H. and Harrison, D.E. 1988a. Properties of single potassium channels modulated by glucose in rat ß-cells. *Journal of Physiology* **400**, 501-527.

Ashcroft, S.J.H., Hughes, S.J. & Kerr, A.J. 1988b. Detection of the sulfonylurea-binding component of the ATP-sensitive K-channel in HIT T15 B-cells by electrophoresis on non-denaturing gels. *Diabetologia* **31**, 466A.

Ashcroft, F.M., Gray, D.E., Kelly, R.P. & Sutton, R. 1989a. Voltage-activated potassium and calcium currents in human isolated pancreatic ß-cells. *Journal of Physiology* **415**, 26P.

Ashcroft, F.M., Kakei, M., Gibson, J.S., Gray, D.W. & Sutton, R. 1989b. The ATP- and tolbutamide sensitivity of the ATP-sensitive K-channel from human pancreatic B cells. *Diabetologia* **32**, 591-8.

Ashcroft, F.M., Kakei, M. & Kelly, R.P. 1989c. Rubidium and sodium permeability of the ATP-sensitive K^+ channel in single rat pancreatic ß-cells. *Journal of Physiology* **408**, 413-430.

Ashcroft, F.M., Kelly, R.P. & Smith, P.A. 1990a. Two types of Ca channel in rat pancreatic ß-cells. *Pflügers Archiv* **415**, 504-506.

Ashcroft, F.M. Fewtrell, C., Oosawa, Y., Rorsman, P. & Smith, P.A. 1990b. ATP-regulated K channels modulate electrical activity in mouse isolated pancreatic ß-cells. *Journal of Physiology* **424**, 27P.

Ashcroft, F.M., Faehling, M., Fewtrell, C., Rorsman, P. & Smith, P.A. 1990c. Perforated patch recordings of ATP-regulated K-current and electrical activity in mutine pancreatic ß-cells. *Diabetologia* **33**, A78

Ashford, M.L.J., Sturgess, N.C., Gardner, N.J. & Hales, C.N. 1988. Adenosine 5'-triphosphate-sensitive ion channels in rat cultured central neurones. *Pflügers Archiv* **412**, 297-304.

Atwater, I. 1980. Effects of the calcium ionophore, A23187, on glucose-induced electrical activity in mouse pancreatic ß-cells. *Journal of Physiology* **303** 80P.

Atwater, I., Ribalet, B. & Rojas, E. 1978. Cyclic changes in potential and resistance of the B-cell membrane induced by glucose in islets of Langerhans from mouse. *Journal of Physiology* **278**, 117-139.

Atwater, I., Ribalet, B. & Rojas, E. 1979a. Mouse pancreatic ß-cells: Tetraethylammonium blockage of the potassium permeability increase induced by depolarisation. *Journal of Physiology* **288**, 561-574.

Atwater, I., Dawson, C.M., Ribalet, B. & Rojas, E. 1979b. Potassium permeability activated by intracellular calcium ion concentration in the pancreatic ß-cell. *Journal of Physiology* **288**, 575-588.

Atwater, I., Dawson, C.M., Scott, A., Eddlestone, G.T. & Rojas, E. 1980. The nature of the oscilatory behaviour in electrical activity from pancreatic ß-cell. *Hormone and Metabolism Research Supplement Series* **10**, 101-107.

Atwater, I., Frankel, B.J., Rojas, E. & Grodsky, G.M. 1983. ß-cell membrane potential and insulin release: role of calcium and calcium:magnesium ratio. *Quarterly Journal of Experimental Physiology* **68**, 233-245

Balant, L 1981 Clinical pharmokinetics of sulphonylurea hypoglycaemic drugs. *Clinical Pharmocokinetics* **6**, 215-241.

Bangham, J.A. & Smith, P.A. 1987. Nonconforming action potentials from isolated mouse islets of Langerhans. *Journal of Physiology* **392**, 15P.

Bean, B.P. 1989. Classes of calcium channel in vertebrate cells. *Annual Reviews of Physiology* **51**, 367-384.

Belles, B., Malecot, C.O., Heschler, J. & Trautwein, W. 1988. "Run-down" of the Ca current during long whole-cell recordings in guinea-pig heart cells: role of phosphorylation and intracellular calcium. *Pflügers Archiv* **411**, 353-360.

Bernadi, H., Fosset, M., Lazdunski, M. 1988. Chacterization, purification, and affinity labelling of the brain [^{3}H] glibenclamide-binding protein, a putative neuronal ATP-regulated K^+ channel. *Proceedings of the national Academy of Science of the USA* **85**, 9816-9820

Best, L. & Malaisse, W.J. 1983. Phosphatidylinositol and phosphatidic acid metabolism in rat pancreatic islets in response to neurotransmitter and hormonal stimuli. *Biochimica et Biophysica Acta* **750**, 157-163.

Biden, T.J., Prentki, M., Irvine, R.F., Berridge, M.J. & Wollheim, C.B. 1984. Inositol 1,4,5-trisphosphate mobilizes intracellular Ca^{2+} from permeabilized insulin-secreting cells. *Biochemical Journal* **223**, 467-473.

Blaustein, M.P. & Hodgkin, A.L. 1969. The effect of cyanide on the efflux of calcium from squid axons. *Journal of Physiology* **200**, 497-527.

Bokvist, K., Rorsman, P. & Smith, P.A. 1990a. Effects of external tetraethylammonium ions and quinine on delayed rectifying K^+-channels in mouse pancreatic ß-cells. *Journal of Physiology* **423**, 311-325.

Bokvist, K., Rorsman, P. & Smith, P.A. 1990b. Block of ATP-regulated and Ca^{2+}-activated K^+ channels in mouse pancreatic ß-cells by external tetraethylammonium and quinine. *Journal of Physiology* **423**, 327-342.

Bokvist, K., Ammama, C., Larsson, O., Wahlander, K. & Rorsman, P. 1991. A novel low - conductance K^+ channel, a common denominator in adrenergic and peptidergic inhibition of insulin release. *Diabetologia* **34**, A63.

Boschero, A.C. & Malaisse, W.J. 1979. Stimulus-secretion coupling of glucose-induced insulin release. XXIX. Regulation of ^{86}Rb efflux from perifused islets. *American Journal of Physiology* **236**, E139-E146.

Boschero, A.C., Kawazu, S., Duncan, G. & Malaisse, W.J. 1977. Effects of glucose on K^+ handling by pancreatic islets. *FEBS Letters* **83**, 151-154.

Boyd, A.E. 1988. Sulphonylurea receptors, ion channels and fruit flies. *Diabetes* **37**, 847-50.

Boyd, A.E., Hill, R.S., Oberwetter, A.M. & Berg, M. 1986. Calcium dependency and free calcium concentrations during insulin secretion in a hamster beta cell line. *Journal of Clinical Investigation* **77**, 774-781.

Bozem, M. & Henquin, J.C. 1988. Glucose modulation of spike activity independently from changes in slow waves of membrane potential in mouse ß-cells. *Pflügers Archiv* **413**, 147-152.

Bozem, M., Nenqiun, M. & Henquin, J.-C. 1987. The ionic, electrical and secretory effects of protein kinase C activation in mouse pancreatic ß-cells: studies with a phorbol ester. *Endocrinology* **121**, 1025-1033.

Brown, A.M., Camerer, H., Kunze, D.L. & Lux, H.D. 1982. Similarity of unitary Ca^{2+} currents in three different species. *Nature* **299**, 156-158.

Burr, I.M., Kanazawa, Y., Marliss, E.B. & Lambert, A.E. 1971. Biphasic insulin release from perifused cultured fetal rat Pancreas. *Diabetes* **20**, 592-597.

Carbone, E. & Lux, H.D. 1984. A low voltage-activated, fully inactivating calcium current in vertebrate sensory neurones. *Nature* **310**, 501-502.

Cavalie, A., Pelzer, D. & Trautwein, W. 1986. Fast and slow gating behaviour of single calcium channels in cardiac cells. Relation to activation and inactivation of calcium-channel current. *Pflügers Archiv* **406**, 241-258.

Charles, S., Tamagawa, T. & Henquin, J.-C. 1982. A single mechanism for the stimulation of insulin release and ^{86}Rb efflux from rat islets by cationic amino acids. *Biochemical Journal* **208**, 301-308.

Chay, T.R. 1990. Effects of compartmentalized Ca^{2+} ions on electrical bursting activity of pancreatic ß-cells. *American Journal of Physiology* **258**, C955-965.

Chay, T.R. & Kreizer. J. 1983. Minimal model for membrane oscillations in the pancreatic ß-cell. *Biophysical Journal* **42**, 181-190.

Ciani, S. & Ribalet, B. 1988. Ion permeation and rectification in ATP-sensitive channels from insulin-secreting cells RINm5F: effects of K^+, Na^+ and Mg^{2+}. *Journal of Membrane Biology* **103**, 171-180.

Cohen-Armon, M. & Sokolovsky, M. 1986. Interactions between the muscarinic receptors, sodium channels, and guanine nucleotide-binding protein(s) in rat atria. *Journal of Biological Chemistry* **261**, 12498-12505.

Cohen-Armon, M., Kloog, Y., Henis, Y.I. & Sokolovsky, M. 1985. Batrachotoxin changes the properties of the muscarinic receptor in rat brain and heart: possible interactions between muscarinic receptors and sodium channels. *Proceedings of the national Academy of Science of the USA* **82**, 3524-3527.

Cook, D.L. & Hales, C.N. 1984. Intracellular ATP directly blocks K-channels in pancreatic B-cells. *Nature* **311**, 271-273.

Cook, D.L. & Ikeuchi, M. 1988. ATP-inhibited K^+ channels (P_{KATP}) apppear to regulate glucose-induced electrical activity as well as subthreshold depolarization of ß-cells. *Diabetes* **37** (Suppl. 1), 7A.

Cook, D.L.& Perera, E. 1982. Islet electrical pacemaker response to alpha adrenergic stimulation. *Diabetes* **31**, 985-990.

Cook, D.L., Crill, W.E. & Porte, D. 1980. Plateau potentials in pancreatic islet cells are voltage-dependent action potentials. *Nature* **286**, 404-406.

Cook, D.L., Crill, W.E. & Porte, D. 1981a. Glucose and acetylcholine have different effects on the pacemaker potential of pancreatic islet cells. *Diabetes* **30**, 558-561.

Cook, D.L., Porte, D. & Crill, W.E. 1981b. Voltage-dependence of rhythmic plateau potentials of pancreatic islet cells. *American Journal of Physiology* **240**, E290-296.

Cook, D.L., Ikeuchi, M. & Fujimoto, W.Y. 1984. Lowering of pH_i inhibits Ca^{2+}-activated K^+-channels in pancreatic ß-cells. *Nature* **311**, 269-271.

Cook, D.L., Satin, L.S. & Hopkins, W.F. 1991. Pancreatic B cells are bursting, but how ? *Trends in Neuroscience* **14**, 411-414.

Corey, D.P. & Stevens, C.F. 1983. Science and technology in patch-recording electrodes. In *Single Channel Recording*. ed. Sakmann, B. & Neher, E. ch. 3. pp. 53-68. Plenum Press. NY.

Coronado, R.D. 1980. Ion conduction and selectivity in a potassium channel from sarcoplasmic reticulum. Ph.D. Thesis, Brandeis University.

Dawson, C.M., Croghan, P.C., Atwater, I. & Rojas, E. 1983. Estimation of potassium permeability in mouse islets of Langerhans. *BioMedical Research*, **4**, 389-392.

Dawson, C.M., Croghan, P.C., Scott, A.M. & Bangham, J.A. 1986. Potassium and rubidium permeability and potassium conductance of the B-cell membrane in mouse islets of Langerhans. *Quarterly Journal of Experimental Physiology* **71**, 205-222.

Dean, P.M. & Matthews, E.K. 1968. Electrical activity in pancreatic islet cells. *Nature* **219**, 389-390.

Dean, P.M. & Matthews, E.K. 1970a. Glucose-induced electrical activity in pancreatic islet cells. *Journal of Physiology* **210**, 255-264.

Dean, P.M. & Matthews, E.K. 1970b. Electrical activity in pancreatic islet cells: effects of ions. *Journal of Physiology* **210**, 265-275.

Dean, P.M. Mathews, E.K. & Sakamoto, Y. 1978. Pancreatic islet cells: effects of monosaccharides, glycolytic intermediates and metabolic inhibitors on membrane potential and electrical activity. *Journal of Physiology* **246**, 459-478.

Debuyser, A., Drews, G. & Henquin, J.C. 1991. Adrenaline inhibition of insulin release: role of B cell repolarisation. *Pflügers Archiv* **419**, 131-139.

DiVirgilio, F., Pozzan, T., Wollheim, C.B., Vicentini, L.M. & Meldolesi, J. 1986. Tumor promotor phorbol myristate acetate inhibits Ca^{2+} influx through voltage-gated Ca^{2+} channels in two secretory cell lines, PC12 and RINm5F. *Journal of Biological Chemistry* **261**, 32-35.

Drews, G., Debuyser, A., Nenquin, M. & Henquin, J.-C. 1990. Galinin and epinephrine act on distinct receptors to inhibit insulin release by the same mechanisms including an increase in K^+ permeability of the ß-cell membrane. *Endocrinology* **126**, 1646-1653.

Drews, G., de Timary, P., Debuyser, A. & Henquin, J.-C. 1991. Do adrenaline and galanin affect the same subset of K^+ channels in mouse B-cells ? *Diabetologia* **34**, A87.

Droogmans, G. & Callewaert, G. 1986. Ca^{2+}-channel current and its modification by the dihydropyridine agonist BAY k8644 in isolated smooth muscle cells. *Pflügers Archiv* **406**, 259-265.

Dunne, M. 1991. Evidence for dual modulation of ATP - regulated potassium channels by protein kinase C. *Diabetologia* **34**, A63.

Dunne, M.J. & Petersen, O.H. 1986a. Intracellular ADP activates K^+ channels that are inhibited by ADP in an insulin-secreting cell line. *FEBS Letters* **208**, 59-63.

Dunne, M.J. & Petersen, O.H. 1986b. GTP and GDP activation of K^+ channels that can be inhibited by ATP. *Pflügers Archiv* **407**, 564-565.

Dunne, M.J. & Petersen, O.H. 1987. Phorbol ester and cell-permeable diacylglycerol evoke closure of ATP-sensitive K+ channels in a cultured insulin-secreting cell line. *Journal of Physiology* **390**, 73P.

Dunne, M.J., Findlay, I. & Petersen, O.H. 1984. Patch-clamp study of voltage- and Ca^{2+}-activated K^+ channels in isolated rat pancreatic islet cells. *Journal of Physiology* **354**, 44P.

Dunne, M.J., Ilott, M.C. & Petersen, O.H. 1987. Interaction of diazoxide, tolbutamide and ATP^{4-} on nucleotide-dependent K^+ channels in an insulin-secreting cell line. *Journal of Membrane Biology* **99**, 215-224.

Dunne, M.J., Findlay, I. & Petersen, O.H. 1988a. The effects of pyridine nucleotides on the gating of ATP-sensitive K^+ channels in insulin-secreting cells. *Journal of Membrane Biology* **102**, 205-216.

Dunne, M.J., West-Jordan, J.A, Abraham, R.J., Edwards, R.H.T. & Petersen, O.H. 1988b. The gating of nucleotide-sensitive K^+ channels in insulin-secreting cells can be modulated by changes in the ratio of ATP^{4-}/ADP^{3-} and by non-hydrolysable derivatives of both ATP and ADP. *Journal of Membrane Biology* **104**, 165-177.

Dunne, M.J., Bullet, M.J., Wollheim, C.B. & Petersen, O.H. 1989a. Galanin activates nucleotide-dependent K^+ channels in insulin-secreting cells via a pertussis toxin-sensitive G-protein. *EMBO Journal* **8**, 413-420.

Dunne, M.J., Gallacher, D.V., Petersen, O.H. & Yule, D.I. 1989b. Na^+-dependent glucose-evoked depolarization and increase in $[Ca^{2+}]_i$ in the rat insulinoma cell line RINm5F. *Journal of Physiology* **415**, 93P.

Easom, R.A., Hughes, J.H., Landt, M., Wolf, B.A., Turk, J. & McDaniel, M.L. 1989. Comparison of the effects of phorbol esters and glucose on protein kinase C activation and insulin secretion in pancreatic islets. *Biochemical Journal* **264**, 27-33.

Eckert, R. & Chad, J.E. 1984. Inactivation of calcium channels. *Progress in Biophysics and Molecular Biology* **44**, 215-267.

Eckert, R. & Tillotson, D.L. 1981. Calcium-mediated inactivation of the calcium conductance in caesium-loaded giant neurones of *Aplysia californica*. *Journal of Physiology* **314**, 265-280.

Eddelstone, G.T., Oldham, S.B., Lipson, L.G., Premdas, F.H. & Biegelman, P.M. 1985. Electrical activity and insulin release in mouse islets of Langerhans. *American Journal of Physiology* **248**, C145-C153.

Eddelstone, G.T., Ribalet, B. & Ciani, S. 1989. Differences in K channel behaviour in glucose-reponsive and glucose-unresponsive insulin-secreting tumor cell lines. *Biophysical Journal* **55**, 541a.

Egan, T.M., Noble, D., Noble, S.J., Powell, T., Twist, V.W. & Yamaoka, K. 1988. On the mechanism of isoprenaline- and forskolin-induced depolarization of single guinea-pig myocytes. *Journal of Physiology* **400**, 299-320.

Fenwick, E., Marty, A. & Neher, E. 1982. Sodium and calcium channels in bovine chromaffin cells. *Journal of Physiology* **331**, 599-635.

Fernandez, J.M., Fox, A.P. & Krasne, S. 1984. Membrane patches and whole-cell membranes: a comparison of properties in rat clonal pituitary GH3 cells. *Journal of Physiology* **356**, 565-585.

Findlay, I. 1987. The effects of magnesium ions upon adenosine tri-phosphate sensitive potassium channels in a rat insulin- secreting cell line. *Journal of Physiology* **391**, 611-629.

Findlay I., & Dunne M.J., 1985. Voltage-activated Ca^{2+} currents in insulin-secreting cells. *FEBS Letters* **189**, 281-285.

Findlay I., & Dunne M.J., 1986a. ATP maintains ATP-inhibited K^+ channels in an operational state. *Pflügers Archiv* **407**, 238-240.

Findlay I., & Dunne M.J., 1986b. Ca^{2+} and K^+ currents in an insulin-secreting cell line (RINm5F). In Atwater, I., Rojas, E. & Soria, B. eds. *Biophysics of the pancreatic ß-cell.* Plenum Press. pp 177-187.

Findlay I., Dunne M.J. & Petersen, O.H. 1985a. ATP-sensitive inward rectifier and voltage- and calcium-activated K^+ channels in cultured pancreatic islet cells. *Journal of Membrane Biology* **88**, 165-172.

Findlay I., Dunne M.J. & Petersen, O.H. 1985b. High-conductance K^+ channel in pancreatic islet cells can be activated and inactivated by internal calcium. *Journal of Membrane Biology* **83**, 169-175.

Findlay I., Dunne M.J., Ullrich, S., Wollheim, C.B. & Petersen, O.H. 1985c. Quinine inhibits Ca^{2+}-independent K^+ channels whereas tetraethylammonium inhlbits Ca^{2+}-activated K^+ channels in insulin secreting cells. *FEBS Letters* **185**, 4-6.

Findlay, I., Ashcroft, F.M., Kelly, R.P., Rorsman, P. Petersen, O.H. & Trübe, G. 1989. Calcium currents in insulin-secreting beta-cells. *Annals of the New York Academy of Science* **560**, 403-409.

Fox, A.P., Nowycky, M.C. & Tsien, R.W. 1987a. Kinetic and pharmacological properties distinguishing three types of calcium currents in chick sensory neurones. *Journal of Physiology* **394**, 149-172.

Fox, A.P., Nowycky, M.C. & Tsien, R.W. 1987b. Single-channel recordings of three types of calcium channels in chick sensory neurones. *Journal of Physiology* **394**, 173-200.

Frankenhaeuser, B. 1957. The effect of calcium on the myelinated nerve fibre. *Journal of Physiology* **137**, 245-260.

Frankenhaeuser, B. & Hodgkin, A.L. 1957. The action of calcium on the electrical properties of squid axons. *Journal of Physiology* **137**, 218-244.

Gagerman, E., Idahl, L.A., Meissner, H.P. & Taljedal, I.B. 1978. Insulin release, cGMP, cAMP and membrane potential in acetylcholine-stimulated islets. *American Journal of Physiology* **234**, E493-500.

Gallacher D.V., Maruyama Y. & Petersen, O.H. 1984. Patch clamp study of rubidium and potassium conductance in single cation channels from mammalian exocrine accini. *Pflügers Archiv.* **401**, 361-367.

Gamkama, H.S., Groen, A.K., Wanders, R.J.A. & Tager, J.M. 1983. Measurement of binding of adenine nucleotides and phosphate to cytosolic proteins in permeabilised rat liver cells. *European Journal of Biochemistry* **131**, 447-451.

Gay, L.G. & Stanfield, P.R. 1978. The selectivity of the delayed potassium conductance of frog skeletal muscle fibres. *Pflügers Archiv* **378**, 177-179.

Gillespie, J.I. & Meves, H. 1980. The time course of sodium inactivation in squid giant axon. *Journal of Physiology* **299**, 289-347.

Gee, W., Gillis, K., Falke, L. & Misler, S. 1987. A metabollically regulated potassium channel in human pancreatic islet cells. *Journal of General Physiology* **90**, 19a.

Gorus, F.K., Schuit, F.C., In't Veld, P.A., Gepts, W. & Pipeleers, D.G. 1988. Interaction of sulphonylureas with pancreatic ß-cells. A study with glyburide. *Diabetes* **37**, 1090-1095.

Grapengiesser, E., Gylfe, E. & Hellman, B. 1989. Regulation of pH in individual pancreatic ß-cells as evaluated by fluorescence ratio microscopy. *Biochimica et Biophysica Acta* **1014**, 219-224.

Gray, D.W.R., McShane, P., Grant, A.M. & Morris, P.J. 1984. A method for isolation of islets of Langerhans from the human pancreas. *Diabetes* **33**, 1055-1061.

Hagiwara, N., Irisawa, H. & Kameyama, M. 1988. Contribution of two types of calcium currents to the pacemaker potentials of rabbit sino-atrial node cells. *Journal of Physiology* **395**, 233-253.

Hamill, O.P., Marty, A., Neher, E., Sakmann, B. and Sigworth, F.J. 1981. Improved patch-clamp techniques for high-resolution current recording from cells and cell-free membrane patches. *Pflügers Archiv* **391**, 85-100.

Harrison, D.E., Christie, M.R. & Gray, D.W.R. 1985. Properties of isolated human islets of Langerhans: insulin secretion, glucose oxidation and protein phosphorylation. *Diabetologia* **28**, 99-103.

Hebisch, S., Sobol, S., Schwenen, M. & Sies, H. 1984. Compartmentation of high energy phosphates in resting and working rat skeletal muscle. *Biochimica et Biophysica Acta* **746**, 117-124.

Hedeskov, C.J. 1980. Mechanism of glucose-induced insulin secretion. *Physiological Reviews* **60**, 442-509.

Hellman, B., Idahl, L.A. & Danielsson, A. 1969. Adenosine triphosphate levels of mammalian pancreatic B-cells after stimulation by glucose and hypoglycaemic sulphonylureas. *Diabetes* **18**, 509-516.

Henderson, P. 1908. *Zeitschrift fur Physikalische Chemie*. **63**, 325.

Henquin, J.C. 1978. D-glucose inhibits the potassium efflux from pancreatic islet cells. *Nature* **271**, 271-273.

Henquin, J.C. 1979. Opposite effects of intracellular Ca^{2+} and glucose on K^{+} permeability of pancreatic islet cells. *Nature* **280**, 66-68.

Henquin, J.C. 1980a. Metabolic control of the potassium permeability in pancreatic islet cells. *Biochemical Journal* **186**, 541-550.

Henquin, J.C. 1980b. The potassium permeability of pancreatic islet cells: mechanisms of control and influence on insulin release. *Hormone and Metabolic Research Supplement Series* **10**, 66-73.

Henquin, J.C. 1988. ATP-sensitive K^+ channels may control glucose-induced electrical activity in pancreatic B-cells. *Biochemical and Biophysical Research Communications* **156**, 769-775.

Henquin, J.C. 1991. Role of voltage- and Ca^{2+}-dependent K^+ channels in the glucose-induced electrical activity in pancreatic B-cells. *Pflügers Archiv* **416**, 568-572.

Henquin, J.C. & Meissner, H.P. 1981. Effects of amino acids on membrane potential and $^{86}Rb^+$ fluxes in pancreatic beta-cells. *American Journal of Physiology* **240**, E245-252.

Henquin, J.C. & Meissner, H.P. 1982a. Electrical and secretory events in pancreatic ß-cells of the mouse during mobilisation of intracellular calcium. *Diabetologia* **23**, 173.

Henquin, J.C. & Meissner, H.P. 1982b. The electrogenic sodium-potassium pump of mouse pancreatic ß-cells. *Journal of Physiology* **332**, 529-552.

Henquin, J.C. & Meissner, H.P. 1983. Dibutyryl cyclic AMP triggers Ca^{2+} influx and Ca^{2+}-dependent electrical activuty in pancreatic ß-cells. *Biochemical and Biophysical Research Communications* **112**, 614-620.

Henquin, J.C. & Meissner, H.P. 1984a. Significance of the ionic fluxes and changes in membrane potential for stimulus-secretion coupling in pancreatic beta-cells. *Experientia* **40**, 1043-1052.

Henquin, J.C. & Meissner, H.P. 1984b. The ionic, electrical and secretory effects of endogenous cyclic adenosine monophosphate in mouse pancreatic b-cells: studies with Forskolin. *Endocrinology* **115** 1125-1134.

Henquin, J.C. & Meissner, H.P. 1984c. Effects of theophylline and dibutyryl cyclic adenosine monophosphate on the membrane potential of mouse pancreatic ß-cells. *Journal of Physiology* **351**, 595-612.

Henquin, J.C. & Meissner, H.P. 1986. Cyclic adenosine monophosphate differently affects the response of mouse pancreatic ß-cells to various amino acids. *Journal of Physiology* **381**, 77-93.

Henquin, J.C., Hormans, B., Nenquin, M., Verniers, J. & Lambert, A.E. 1975. Quinine-induced modifications of insulin release and glucose metabolism by isolated pancreatic islets. *FEBS Letters* **57**, 280-284.

Henquin, J.C., Schmeer, W. & Meissner, H.P. 1983. Forskolin, an activator of adenylate cyclase, increases Ca^{2+}-dependent electrical activity induced by glucose in mouse pancreatic B-cells. *Endocrinology* **112**, 2218-2220.

Henquin, J.C., Schmeer, W., Nenquin, M. & Meissner, H.P. 1985. Effects of a calcium channel agonist on the ionic, electrical and secretory events in mouse pancreatic ß-cells. *Biochemical and Biophysical Research Communications* **16**, 980-986.

Henquin, J.C., Bozem, M., Schmeer, W.& Nenquin, M. 1987. Distinct mechanisms for two amplification systems of insulin release. *Biochemical Journal* **246**, 393-399.

Henquin, J.C., Garcia, M.C., Bozem, M., Hermans, M. & Nenquin, M. 1988. Muscarinic control of B-cell function involves sodium dependent depolarisation and calcium influx. *Endocrinology* **122**, 2134-2142.

Henquin, J.C., Nenquin, M. & Schmeer, W. 1989. The role of Ca-activated K (K-Ca) channels in glucose-induced electrical activity in B-cells. *Diabetes* **39**, 139A.

Hermans, M., Schmeer, W. & Henquin, J.C. 1987. Modulation of the effect of acetylcholine on insulin release by the membrane potential of B cells. *Endocinology* **120**, 1765-1773.

Hess, P., Lansman, J.B. & Tsien, R.W. 1984. Different modes of calcium channel gating behaviour favoured by dihydropyridine Ca agonists and antagonists. *Nature* **311**, 538-544.

Hill, R.S. & Boyd, A.E. III, 1985. Perifusion of a clonal cell line of simian virus-40 transformed beta cells. Insulin secretory dynamics in response to glucose, 3-isobutylmethylxanthine and potassium. *Diabetes* **34**, 115-120.

Hille, B. 1984. *Ionic channels of excitable membranes.* Sinauer Associates. Sunderland, MA, USA.

Hille, B. & Schwarz, W. 1978. Potassium channels as multi-ion single-file pores. *Journal of General Physiology* **72**, 409-442.

Hiriart, M. & Matteson,D.R. 1988. Na channels and two types of Ca channels in rat pancratic B cells identified with the reverse haemolytic plaque assay. *Journal of General Physiology* **91**, 617-639.

Hockberger, P., Toselli, M., Swandulla, D. & Lux, H.D. 1989. A diacylglycerol analugue reduces neuronal calcium currents independently of protein kinase C activation. *Nature* **388**, 340-242.

Hodgkin, A.L. & Huxley, A.F. 1952a. The components of membrane conductance in the giant axon of Loligo. *Journal of Physiology* **116**, 473-496.

Hodgkin, A.L. & Huxley, A.F. 1952b. A quantitative description of membrane current and its application to conduction and excitation in nerve. *Journal of Physiology* **117**, 500-544.

Hodgkin, A.L. & Katz, B. 1949. The effect of sodium ions on the electrical activity of the giant axon of the squid. *Journal of Physiology* **108**, 37-77.

Homaidian, F.R., Sharp, G.W.G. & Nowak, L.M. 1991. Galanin inhibits a dihydropyridine - sensitive Ca^{2+} current in the RINm5F cell line. *Diabetologia* **34**, A87.

Hopkins, W.F., Satin, L.S. & Cook, D.L. 1991. Inactivation kinetics and pharmacology distinguish two calcium currents in mouse pancreatic B-cells. *Journal of Membrane Biology* **119**, 229-239.

Horie, M., Irisawa, H. & Noma, A. 1987. Voltage-dependent magnesium block of adensoine triphosphate sensitive potassium channel in guinea-pig ventricular cells. *Journal of Physiology* **387**, 251-272.

Howell, S.L. & Montague, W. 1983. Adenylate cyclase activity in isolated rat islets of Langerhans. Effects of agents which alter rates of insulin secretion. *Biochimica et Biophysica Acta* **320**, 44-52.

Hsu, W.H., Xiang, H.D., Kunze, D.L., Rajan, A. & Boyd, A.E. 1989. Somatostatin decreases insulin secretion by inhibiting Ca^{2+}-influx through voltage-dependent Ca^{2+} channels in an insulin secreting cell line (HIT cells). *Journal of cellular Biology* **129**, 335A.

Hughes, S.J. & Ashcroft, S.J.H. 1988. Effect of secretagogues on cytosolic free Ca^{2+} and insulin release in the hamster clonal ß-cell line HIT-T15. *Journal of Molecular Endocrinology* **1**, 13-17.

Hutton, J.C., Sener, A., Herchulz, A., Atwater, I., Kawazu, S., Boschero, A.C., Somers, G., Devis, G. & Malaisse, W.J. 1980. Similarities in the stimulus-secretion coupling mechanisms of glucose- and 2-keto acid-induced insulin release. *Endocrinology* **106**, 203-219.

Ikeuchi, M. & Cook, D.L. 1984. Glucagon and forskolin have dual effects upon islet cell electrical activity. *Life Science* **35**, 685-691.

Ikeuchi, M., Fujimoto, W.Y. & Cook, D.L. 1984. Rat islet cells have glucose-dependent periodic electrical activity. *Hormone and Metabolism Research* **16**, 125-127.

Isenberg, C., Schröter, K. & Trübe, G. 1988. Kinetics of single ATP-dependent K-channels in the membrane of murine pancreatic ß-cells. *Pflügers Archiv* **411** Suppl 1, R111.

Jahnsen, H. & Llinas,R. 1984. Ionic basis for the electroresponsiveness and oscillatory properties of guinea-pig thalamic neurones *in vitro*. *Journal of Physiology* **349**, 227-247.

Jones, D.P. 1986. Intracellular diffusion gradients of O_2 and ATP. *American Journal of Physiology* **250**, C663-675.

Jones, P.M., Fyles, J.M., Howell, S.L. 1986. Regulation of insulin secretion by cAMP in rat islets of Langerhans permeabilised by high voltage discharge. *FEBS Letters* **205**, 205-209.

Joseph, S.K., Williams, R.J., Corkey, B.E., Matschinsky, F.M. & Williamson, J.R. 1984. The effect of inositol triphosphate on Ca^{2+} fluxes in insulin-secreting cell lines. *Journal of Biological Chemistry* **259**, 12952-12955.

Kalman,D., O'Lague, P.H., Erxleben, C. & Armstrong, D.L. 1988. Calcium-dependent inactivation of the dihydropyridine-sensitive calcium channel in GH3 cells. *Journal of General Physiology* **92**, 531-548.

Kakei, M. & Ashcroft, F.M. 1987. A microflow superfusion system for use with excised membrane patches. *Pflügers Archiv* **409**, 337-341.

Kakei, M. & Noma, A. 1984. Adenosine-5-triphosphate sensitive single potassium channel in the atrio-ventricular node cell of the rabbit heart. *Journal of Physiology* **352**, 265-284.

Kakei, M., Noma, A. & Shibasaki, T. 1985. Properties of adenosine triphosphate-regulated potassium channels in guinea-pig ventricular cells. *Journal of Physiology* **363**, 441-462.

Kakei, M., Kelly, R.P. & Ashcroft, S.J.H. & Ashcroft, F.M. 1986. The ATP- sensitivity of K^+ channels in rat pancreatic B-cells is modulated by ADP. *FEBS Letters* **208**, 63- 66.

Kalman, D. O'Lague, P. Exrleben, C. & Armstrong, D. 1988. Calcium-dependent inactivation of the dihydropyridine-sensitive calcium channels in GH3 cells. *Journal of General Physiology* **92**, 531-548.

Kameyama, M., Hoffman, F. & Trautwein, W. 1985. On the mechanism of ß-adrenergic regulation of the Ca channel in the guinea-pig heart. *Pflügers Archiv* **405**, 285-293.

Keahey, H.H., Rajan, A.S., Boyd, A.E. & Kunze, D.L. 1989a. Characterization of voltage-dependent calcium channels in a ß-cell line. *Diabetes* **38**, 188-193.

Keahey, H.H., Boyd, A.E. & Kunze, D.L. 1989b. Catecholamine modulation of calcium currents in clonal pancreatic ß-cells. *American Journal of Physiology* **257**, C1171-C1176.

Keizer, J. 1988. Electrical activity and insulin release in pancreatic beta cells. *Mathematical Biosciences* **90**, 127-138.

Keizer, J. & Magnus, G. 1989. ATP-sensitive potassium channels and bursting in the pancreatic beta cell. A theoretical study. *Biophysical Journal* **56**, 229-242.

Keizer, J. & Smollen, P. 1991. Bursting electrical activity in pancreatic ß-cells caused by Ca^{2+}- and voltage-inactivated Ca^{2+} channels. *Proceedings of the national Academy of Science of the USA* **88**, 3897-3901.

Kelly, R.P. & Ashcroft, F.M. 1988. ATP-sensitive K-channels in HIT-T15 insulin-secreting cells. *Diabetologia* **31**, 507A.

Kelly, R.P., Sutton, R. & Ashcroft, F.M. 1991. Voltage-activated calcium and potassium currents in human pancreatic ß-cells. *Journal of Physiology* **443**, 175-192.

Kniffki, K.D. Siemen, D. & Vogel, W. 1978. Delayed development of sodium permeability inactivation in the nodal membrane. *Journal of Physiology* **284**, 92P.

Kramer, W., Oekonomopoulos, R., Punter, J. & Summ, H.D. 1988. Direct photoaffinity labelling of the putative sulphonylurea receptor in rat ß-cell tumor membranes by [^{3}H] glibenclamide. *FEBS Letters* **229**, 355-359.

Kukuljan, M., Goncalves, A.A. & Atwater, I. 1991. Charybdotoxin-sensitive $K_{(Ca)}$ channel is not involved in glucose-induced electrical activity in pancreatic ß-cells. *Journal of Membrane Biology* **119**, 187-195.

Lansman, J.B., Hess, P. & Tsien, R.W. 1986. Blockade of current through single calcium channels by Cd^{2+}, Mg^{2+} and Ca^{2+}. *Journal of General Physiology* **88**, 321-347.

Lauger, P. 1973. Ion transport through pores: a rate theory analysis. *Biochimica et Biophysica Acta* **311**, 423-441.

Lee, K.S., Marban, E. & Tsien, R.W. 1985. Inactivation of calcium channels in mamallian heart cells: joint dependence on membrane potential and intracellular calcium. *Journal of Physiology* **364**, 395-411.

Malaisse,W.J & Herchuelz, A. 1982. Nutritional regulation of K^+ conductance: An unsettled aspect of pancreatic ß-cell physiology. In *Biochemical actions of hormones*. ed. Litwack, G. Academic Press. NY.

Malaisse, W.J. & Sener, A. 1987. Glucose-induced changes in cytosolic ATP content in pancreatic islets. *Biochimica et Biophysica Acta* **927**, 190-195.

Malaisse, W.J., Malaisse-Lagae, F., Wright, P.H. & Ashmore, J. 1967. Effects of adrenergic and cholinergic agents on insulin secretion *in vitro*. *Endocrinology* **80**, 975-978.

Malaisse,W.J., Boshero, A.C., Kawazu, S. & Hutton, J.C. 1978. The stimulus-secretion coupling of glucose-induced insulin release. XXVII. Effects of glucose on K^+ fluxes in isolated islets. *Pflügers Archiv* **373**, 237-242.

Malaisse,W.J., Hutton, J.C., Kawazu, S., Herschulz, A, Valverde, I. & Sener, A. 1979. The stimulus-secretion coupling of glucose-induced insuin release. The links between metabolic and cationic events. *Diabetologia* **16**, 321-341.

Malecot, C.O., Feindt, P. and Trautwein, W. 1988. Intracellular N-methyl-D-glucamine modifies the kinetics and the voltage-dependence of the calcium current in guinea pig ventricular heart cells. *Pflügers Archiv* **411**, 235-242.

Marty, A. & Neher, E. 1982. Ionic channels in cultured rat pancreatic islet cells. *Journal of Physiology* **326**, 36P.

Mathias, P.C.F., Best, L. & Malaisse, W.J. 1985. Stimulation by glucose and carbamylcholine of phospholipase C in pancreatic islets. *Cell Biochemistry and Function* **3**, 173-177.

Matthews, E.K. & Sakamoto, Y. 1975. Electrical characteristics of pancreatic islet cells. *Journal of Physiology* **246**, 421-437.

Meglasson, M.D., Nelson, J., Nelson, D. & Erecinska, M. 1988. Glucose stimulation of the pancreatic islet energy state. *Diabetes* **37** (Suppl. 1), 5A.

Meglasson, M.D., Nelson, J., Nelson, D. & Erecinska, M. 1989. Bioenergetic response of pancreatic islets to stimulation by fuel molecules. *Metabolism* **38**, 1188-1195.

Meissner, H.P. 1976. Electrical characteristics of the beta-cells in pancreatic islets. *Journal de Physiologie (Paris)* **72**, 757-767.

Meissner, H.P. & Boschero, A.C. 1977. Calcium antagonists and islet function. XI. Effect of nifedipine. *Hormone Research* **8**, 203-209.

Meissner, H.P. & Henquin, J.C. 1983. Comparison of the effects of glucose, amino acids and sulphonamides on the membrane potential of pancreatic ß cells. In *Diabetes 1982*, pp. 353-360. (ed. Mngola, E.N.) International Congress Series 600, Excerpta Medica, Amsterdam.

Meissner, H.P. & Preissler, M. 1979. Glucose-induced changes in the membrane potential of pancreatic B cells: their significance for the regulation of insulin release. In *Treatment of early diabetes*, ed. Camerini-Davalos, R.A. & Hanover, B.pp. 97-107. Plenum Press. NY.

Meissner, H.P. & Preissler, M. 1980. Ionic mechanisms of the glucose-induced membrane potential changes in B-cells. *Hormone and Metabolism Research Supplement* **10**, 91-99.

Meissner, H.P. & Schmeer, W. 1981. The significance of calcium ions for the glucose-induced electrical activity of pancreatic ß-cells. In *The mechanism of gated calcium transport across biological membranes*. ed. Ohnisi, S.T. & Endo, M. pp. 157-165. Acad. Press. NY.

Meissner, H.P. & Schmelz, H. 1974. Membrane potential of B-cells in pancreatic islets. *Pflügers Archiv* **351**, 195-206.

Meissner, H.P., Henquin, J.C. & Preissler, M. 1978. Potassium dependence of the membrane potential of pancreatic B-cells. *FEBS Letters* **94**, 87-89.

Meissner, H.P., Preissler, M. & Henquin, J.C. 1980. Possible ionic mechanisms of the electrical activity induced by glucose and tolbutamide in pancreatic ß cells. In *Diabetes 1979*, pp. 166-172. (ed. Waldhausl, W.K.) International Congress Series 500, Excerpta Medica, Amsterdam.

Milner, R.D.G. & Hales, C.N. 1969. The interaction of various inhibitors and stimuli of insulin release studied with rabbit pancreas in vitro. *Biochemical Journal* **113**, 473-479.

Misler, S., Falke, L.C., Gillis, K. & McDaniel, M.L. 1986. A metabolite regulated potassium channel in rat pancreatic ß-cells. *Proceedings of the National Academy of Sciences of the U.S.A.* **83**, 7119-7123.

Misler, S., Gee, W.M., Manchester, J., Scharp, D.W. & Falke, L.C. 1988. A metabolically regulated potassium channel in human islet cells. *Diabetes* **37**, 6A.

Misler, S., Gee, W.M., Gillis, K., Scharp, D.W. & Falke, L.C. 1989. A metabolite regulated ATP-sensitive K^+ channel in human pancreatic islet cells. *Diabetes* **38**, 422-427.

Morgan, N.G., Rumford, G.M. & Montague, W. 1985. Studies on the role of inositol triphosphate in the regulation of insulin secretion from isolated rat islets of Langerhans. *Biochemical Journal* **228**, 713-718.

Moure, C., Ben Ari, Y., Bernardi, H., Fosset, H. & Lazdunski, M. 1989. Antidiabetic sulphonylureas: localization of binding sites in the brain and effects of the hyperpolarisation induced by anoxia in hypocampal slices. *Brain Research* **486**, 159-164.

Neer, E.J.& Clapham, D.E. 1988. Roles of G protein subunits in transmembrane signalling. *Nature* **333**, 129-134.

Neher, E. & Steinbach, J.H. 1978. Local anaesthetics transiently block currents through single acetylcholine-receptor channels. *Journal of Physiology* **277**, 153-176.

Nelson, T.Y., Gaines, K.L., Rajan, A.S., Berg, M., Boyd, III A.E. 1987. Increased cytosolic calcium. A signal for sulfonylurea-stimulated insulin release from ß-cells. *Journal of Biological Chemistry* **262**, 2608-2612.

Nenquin, M., Atwouters, P., Mathot, F. & Henquin, J.C. 1984. Distinct effects of acetylcholine and glucose on 45-calcium and 86-rubidium efflux from mouse islets. *FEBS Letters***176**, 457-461.

Niki, I., Kelly, R.P., Ashcroft, S.J.H. & Ashcroft, F.M. 1989. ATP-sensitive K-channels in HIT T15 ß-cells studied by patch-clamp methods, ^{86}Rb efflux and glibenclamide binding. *Pflügers Archiv* **408**, 133-138.

Nishizuka, Y. 1988. The molecular heterogeneity of protein kinase C and its importance for cell regulation. *Nature* **334**, 661-665.

Noma, A. 1983. ATP-regulated K-channels in cardiac muscle. *Nature* **305**, 147-148.

Noma, A. & Shibasaki, T. 1985. Membrane current through adenosine-triphosphate-regulated potassium channels in guinea-pig ventricular cells. *Journal of Physiology* **363**, 463-481.

Nowycky, M.C., Fox, A.P. & Tsien, R.W. 1984. Multiple types of calcium channel in dorsal root ganglion cells distinguished by sensitivity to cadmium and single channel properties. *Society for Neuroscience* **101**, 526.

Nowycky, M.C., Fox, A.P. & Tsien, R.W. 1985. Three types of neuronal calcium channel with different calcium agonist sensitivity. *Nature* **316**, 440-443.

Ohno-Shosaku, T., Zunkler, B.J. & Trübe, G. 1987. Dual effects of ATP on K^+ currents in mouse pancreatic B-cells. *Pflügers Archiv* **408**, 133-813.

Pace, C.S. & Goldsmith, K.T. 1985. Action of a phorbol ester on ß-cells: potentiation of stimulant-induced electrical activity. *American Journal of Physiology* **248**, C527-534.

Panten, U. & Lenzen, S. 1988. Alterations in energy metabolism of secretory cells. In *The energetics of secretion responses*, ed. Akkerman, J.W.N. Boca Raton, Fla. CRC in press.

Persaud, S.J., Jones, P.M., Sugden, D. & Howell, S.C. 1989. Translocation of protein kinase C in rat islets of Langerhans. Effects of a phorbol ester, carbachol and glucose. *FEBS Letters* **245**, 80-84.

Peter-Riesch, B., Fathi, M., Schlegel, W. & Wollheim, C.B. 1988. Glucose and carbachol generate 1,2-diacylglycerols by different mechanisms in pancreatic islets. *Journal of Clinical Investigation* **81**, 1154-1161.

Petersen, O.H., Findlay, I. 1987. Electrophysiology of the pancreas. *Physiological Reviews* **67**, 1054-1116.

Petersen, O.H. & Velasco, J.M. 1987. Voltage-activation of high-conductance K^+ channel is dependent on local extracellular Ca^{2+} concentration in the RINm5S cell lime. *Journal of Physiology* **382**, 127P.

Petersen, O.H. & Wollheim, C.B. 1990. Diacylglycerol as messenger. *Nature* **344**, 300.

Pfaffinger, P.J., Martin, J.M., Hunter, D.D., Nathanson, N.M. & Hille, B. 1985. GTP - binding proteins couple cardiac muscarinic receptors to a K channel. *Nature* **317**, 536 - 538.

Pipleers, D.G., Schuit, F.C., int Veld, P.A., Maes, E., Hooghe-Peters, E.L., van de Winkel, M. & Gepts, W. 1985. Interplay of nutrients and hormones in the regulation of insulin release. *Endocrinology* **117**, 824-833.

Plant, T.D. 1988. Properties and calcium-dependent inactivation of calcium currents in cultured mouse pancreatic B-cells. *Journal of Physiology* **404**, 731-747.

Plant, T.D. 1989. Effects of 1,2-dioctanoyl-*sn*-glycerol (DiC_8) on ionic currents in cultured mouse pancreatic B-cells. *Journal of Physiology* **418**, 21P.

Prentki, M. & Matschinsky, F.M. 1987. Ca^{2+}, cAMP, and phospholipid-derived messengers in coupling mechanisms of insulin secretion. *Physiological Reviews* **67**, 1185-1249.

Prentki, M., Janjic, D. & Wollheim, C.B. 1983. The regulation of extramitochondrial steady state free Ca^{2+} concentration by rat insulinoma mitochondia. *Journal of Biological Chemistry* **258**, 7597 - 7602.

Pressel, D.M. & Misler, S. 1990. Sodium channels contribute to action potential generation in canine and human pancreatic islet cells. *Journal of Membrane Biology* **116**, 273 - 280.

Rane, S.G., Holz, G.G. & Dunlap, K. 1987. Dihydropyridine inhibition of neuronal calcium current and substance P release. *Pflügers Archiv* **409**, 361-366.

Reuter, H. 1987. Modulation of ion channels by phosphorylation and second messengers. *News in Physiological Science* **2**, 168-171.

Ribalet, B. & Beigelman, P.M. 1979. Cyclic variation of K^+ conductance in pancreatic ß-cells: Ca^{2+} and voltage dependence. *American Journal of Physiology* **237**, C137-C146.

Ribalet, B. & Beigelman, P.M. 1980. Calcium action potentials and potassium permeability activation in pancreatic ß-cells. *American Journal of Physiology* **239**, C124-C133.

Ribalet, B. & Beigelman, P.M. 1981. Effects of divalent cations on ß-cell electrical activity. *American Journal of Physiology* **241**, C59-C67.

Ribalet, B. & Ciani, S. 1987. Regulation by cell metabolism and adenine nucleotides of a K channel in insulin-secreting ß-cells (RINm5F). *Proceedings of the national Academy of Science of the USA* **84**, 1721-1725.

Ribalet, B., Eddlestone, G.T. & Ciani, S. 1988. Metabolic regulation of the K(ATP) and a maxi-K(V) channel in insulin-secreting RINm5F cell. *Journal of General Physiology* **92**, 219-237.

Ribalet, B., Ciani, S. & Eddlestone, G.T. 1989. ATP mediates both activation and inhibition of K(ATP) channel activity via cAMP dependent protein kinase in insulin secreting cell lines. *Journal of General Physiology* **94**, 693-717.

Rojas, E. & Hidalgo, C. 1968. Effect of temperature and metabolic inhibitors on ^{45}Ca outflow from squid giant axons. *Biochimica et Biophysica Acta* **163**, 550-556.

Rorsman, P. 1986. Patch clamp studies on pancreatic glucagon- and insulin-secreting cells. PhD thesis. Acta Universitatis Upsaliensis.

Rorsman, P. 1988. Two types of Ca^{2+} currents with different sensitivities to organic Ca^{2+} channel antagonists in guinea pig pancreatic a2 cells. *Journal of General Physiology* **91**, 243-254.

Rorsman, P. & Abrahamsson, H. 1985. Cyclic AMP potentiates glucose-induced insulin secretion without increasing cytosolic free Ca^{2+}. *Acta Physiologica Scandinavia* **125**, 639-647.

Rorsman, P. & Hellman, B. 1988. Voltage-activated currents in guinea-pig pancreatic a_2 cells. *Journal of General Physiology* **91**, 223-242.

Rorsman, P. & Trübe, G. 1985. Glucose-dependent potassium channels in pancreatic B-cells are regulated by intracellular ATP. *Pflügers Archiv* **405**, 305-309.

Rorsman, P. & Trübe, G. 1986. Calcium and delayed potassium currents in mouse pancreatic beta-cells under voltage-clamp conditions. *Journal of Physiology* **374**, 531-550.

Rorsman, P. & Trübe, G. 1989. Biophysics and physiology of ATP-regulated K^+-channels (KATP). In *Potassium Channels: Structure, Classification and Therapeutic Potential*, pp. 96-116 (ed. N.S. Cook) Ellis Horwood, Chichester, UK..

Rorsman, P., Ashcroft, F.M. & Trübe, G. 1988. Single Ca channel currents in mouse pancreatic B-cells. *Pflügers Archiv* **412**, 597-603.

Rorsman, P., Arkammar, P., Bokvist, K. Hellerstrom, C, Nilsson, T, Welsh, M., Welsh, N. & Berggren, P.O. 1989. Failure of glucose to elicit a normal response in fetal pancreatic beta-cells results from glucose-insensitivity of the ATP-regulated K^+ channels. *Proceedings of the national Academy of Sciences of the USA* **86**, 4505-4509.

Rorsman, P., Bokvist, K., Ammala, C., Arhammer, P., Berggren, P.-O., Larsson, O. & Wahlander, K. 1991. Activation by adrenaline of a low-conductance G protein-dependent K^+ channel in mouse pancreatic ß-cells. *Nature* **349**, 77-79.

Rosario, L.M. & Rojas, E. 1986. Potassium channel selectivity in mouse pancreatic B cells. *American Journal of Physiology* **250**, C90-94.

Rosenberg, R.L., Hess, P. & Tsien, R.W. 1988. Cardiac calcium channels in planar lipid bilayers. *Journal of General Physiology* **92**, 27-54.

Sanguinetti, M.C. & Kass, R.S. 1984. Regulation of cardiac calcium channel current and contractile activity by the dihydropyridine Bay K8644 is voltage-dependent. *Journal of Molecular and Cellular Cardiology* **16**, 667-670.

Santana de Sa, S., Ferer, R., Rojas, E. & Atwater, I. 1983. Effects of adrenaline and noradrenaline on glucose-induced electrical activity of the mouse pancreatic ß-cell. *Quarterly Journal of Experimental Physiology* **68**, 247-258.

Santerre, R.F., Cook, R.A., Crisel, R.M.D., Sharp, J.D., Schmidt, R.J., Williams, D.C. & Wilson, C.P. 1981. Insulin synthesis in a clonal cell line of SV40 transformed hamster B-cells. *Proceedings of the National Academy of Sciences of the U.S.A.* **78**, 4339-4343.

Satin, L.S. & Cook, D.L. 1985. Voltage-gated inward currents in pancreatic islet B-cells. *Pflügers Archiv* **404**, 385-387.

Satin, L.S. & Cook, D.L. 1986. Voltage-gated Ca current in pancreatic islet ß-cells. In Atwater, I., Rojas, E. & Soria, B. eds. *Biophysics of the pancreatic ß-cell.* Plenum Press. pp 189-193.

Satin, L.S. and Cook, D.L. 1988. Evidence for two calcium currents in insulin-secreting cell lines. *Pflügers Archiv* **411**, 401-409.

Schuit, F.C. & Pipeleers, D.G. 1985. Regulation of adenosine 3', 5'- monophosphate levels in the pancreatic ß-cell. *Endocrinology* **117**, 834-840.

Schultz, S.G. 1980. Basic properties of membrane transport. Cambridge University Press.

Sehlin, J. & Taljedal, I.-B. 1975. Glucose-induced decrease in Rb^+ permeability in pancreatic B-cells. *Nature* **253**, 635-636.

Smith, P., Boquist, K. & Rorsman, P. 1989a. Demonstration of A-currents in pancreatic islet cells. *Pflügers Archiv* **413**, 441-443.

Smith, P., Rorsman, P. & Ashcroft, F.M. 1989b. Modulation of dihydropyridine-sensitive Ca^{2+} channels by glucose metabolism in mouse pancreatic ß-cells. *Nature* **342**, 550-553.

Smith, P., Ashcroft, F.M. & Rorsman, P. 1990a. Simultaneous recordings of glucose dependent electrical activity and ATP-regulated K^+-currents in isolated mouse pancreatic ß-cells. *FEBS Letters* **261**, 187-190.

Smith, P., Boquist, K. Arkammar, P., Berggren, P.O. & Rorsman, P. 1990b. Delayed rectifying and calcium-activated K channels and their significance for action potential repolarization in mouse pancreatic beta-cells. *Journal of General Physiology* **95**, 1041-59.

Smith, P.A., Fewtrell, C. & Ashcroft, F.M. 1990c. Cyclic AMP potentiates L-type Ca-channel activity in murine pancreatic ß-cells. *Diabetologia* **33**, A104.

Spruce, A., Standen, N.B., Stanfield, P.R. & Wilson, S.W. 1984. Rubidium ions prolong potassium channel opening in frog skeletal sarcolemma. *Journal of Physiology* **357**, 45P.

Spruce, A., Standen, N.B. & Stanfield, P.R. 1987. Studies on the unitary properties of adenosine tri-phosphate regulated potassium channels of skeletal muscle. *Journal of Physiology* **382**, 213-237.

Standen, N.B. & Stanfield, P.R. 1980. Rubidium block and rubidium permeability of the inward rectifier of frog skeletal muscle fibres. *Journal of Physiology* **304**, 415-435.

Sturgess, N.C., Ashford, M.L.J., Cook, D.L. & Hales, C.N. 1985. The sulphonylurea receptor may be an ATP-sensitive potassium channel. *Lancet* **8453**, 474-475.

Sturgess, N.C., Hales, C.N. & Ashford, M.L.J. 1987. Calcium and ATP regulate the activity of a non-selective ion channel in a rat insulinoma cell line. *Pflügers Archiv* **409**, 607-615.

Sturgess, N.C., Kozlowski, R.Z., Carrington, C.A., Hales, C.N. & Ashford, M.L.J 1988. Effects of sulphonylureas and diazoxide on insulin secretion and nucleotide-sensitive channels in an insulin-secreting cell line. *British Journal of Pharmacology* **95**, 83-94.

Swope,. S.L. & Schonbrunn, A. 1984. Bombesin stimulates insulin secretion by a pancreatic islet cell line. *Proceedings of the National Academy of Science of the USA* **81**, 1822-1866.

Tamagawa, T. & Henquin, J.C. 1983. Epinefrine modifications of insulin release and of $^{86}Rb^{+}$ or $^{45}Ca^{2+}$ fluxes in rat islets. *American Journal of Physiology* **244**, E245-E252.

Tamagawa, T., Niki, M. & Niki, A. 1985. Insulin release independent of a rise in cytosolic free Ca^{2+} by forskolin and phorbol ester. *FEBS Letters* **183**, 430-432.

Tarvin, J.T. & Pace, C.S. 1981 Glucose-induced electrical activity in the pancreatic ß-cell: effect of veratridine. *American Journal of Physiology* **242**, C127-134.

Trübe, G. & Hescheler, J. 1983. Inward-rectifying channels in isolated patches of the heart cell membrane: ATP-dependence and comparison with cell-attached patches. *Pflügers Archiv* **501**, 178-184.

Trübe. G. & Rorsman, P. 1986. Calcium and potassium currents recorded from pancreatic ß-cells under voltage-clamp control. In Atwater, I., Rojas, E. & Soria, B. eds. *Biophysics of the pancreatic ß-cell.* Plenum Press. pp 167-175.

Trübe. G., Rorsman, P. & Ohno-Shosaku, T. 1986. Opposite effects of tolbutamide and diazoxide on the ATP-dependent K^{+} channel in mouse pancreatic ß-cells. *Pflügers Archiv* **407**, 493-499.

Trübe, G., Hescheler, J. & Schroter, K. 1989. Regulation and function of ATP-dependent K^+ channels in pancreatic B-cells. In *Secretion and its control.* Society of General Physiologists Series Vol. 44. (eds. Armstrong, C.M. & Oxford, G.S.) Rockerfeller University Press, N.Y. in press.

Tsien, R.W., Lipscombe, D., Madison, D.V., Bley, K.R. & Fox, A.P. 1988. Multiple types of neuronal calcium channels and their selective modulation. *Trends in Neuroscience* **11**, 431-438.

Valdeolmillos, M., Santos, R.M., Contreras, D., Soria, B. & Rosario, L.M. 1989. Glucose-induced oscillations of intracellular Ca^{2+} concentration matching bursting electrical activity in single mouse islets of Langerhans. *FEBS Letters* **259**, 19-23.

Vasseur, M., Debuyser, A. & Joffre, M. 1986. Effects of verapamil and nifedipine on glucose-induced electrical activity in pancreatic ß-cells. In Atwater, I., Rojas, E. & Soria, B. eds. *Biophysics of the pancreatic ß-cell.* Plenum Press. pp 195-200.

Velasco, J.M. 1988. Calcium channels in insulin-secreting RINm5F cell line. *Journal of Physiology* **398**, 15P.

Velasco, J.M. & Petersen, O.H. 1987. Voltage-activation of high-conductance K^+ channels in the insulin-secreting cell line RINm5F is dependent on local extracellular Ca^{2+} concentration. *Biochimica et Biophysica Acta* **896**, 305-321.

Velasco, J.M. & Petersen, O.H. 1989. The effect of a cell-permeable diacylglycerol analogue on single Ca^{2+} (Ba^{2+}) channel currents in the insulin-secreting cell line RINm5F. *Quarterly Journal of Experimental Physiology* **74**, 367-370.

Velasco, J.M., Petersen, J.U.H. & Petersen, O.H. 1988. Single-channel Ba^{2+} currents in insulin-secreting cells are activated by glyceraldehyde stimulation. *FEBS Letters* **231**, 366-370.

Wahlander, K., Ammala, C., Bokvist, K., Arkhammar, P., Berggren, P.O. & Rorsman, P. 1990. Adrenergic inhibition of insulin secretion from mouse ß-cells does not involve reduced calcium current. *Diabetologia* **33**, A27.

Wahlander, K., Ammala, C., Berggren, P.O., Bokvist, K., Juntti-Berggren, L. & Rorsman, P. 1991. Galanin inhibits ß-cell electrical activity by a G-protein regulated sulphonylurea-insensitive mechanism. In Hokfelt, T. ed. Wenner-Gren International Symposium Series, in press.

Walsh, K.B., Begenisich, T.B. & Kass, R.S. 1989. ß-adrenergic modulation of cardiac ion channels. Differential sensitivity of potassium and calcium currents. *Journal of General Physiology* **93**, 841-854.

Weidmann, S. 1955. The effects of calcium ions and local anaesthetics on electrical properties of Purkinje fibres. *Journal of Physiology* **129**, 568-582.

de Weille, J.R., Schmid-Antomarchi, H., Fosset, M. & Lazdunski, M. 1988. ATP-sensitive K^+ channels that are blocked by hypoglycaemia-inducing sulphonylureas are activated by galanin, a hyperglycaemia-inducing hormone. *Proceedings of the National Academy of Science of the USA* **85**, 1312-1316.

de Weille, J.R., Schmid-Antomarchi, H., Fosset, M. & Lazdunski, M. 1989. Regulation of ATP-sensitive K^+ channels in in insulinoma cells: Activation by somatostatin and protein kinase C and the role of cAMP. *Proceedings of the National Academy of Science of the USA* **86**, 2971-2975.

Wolf, B.A., Comens, P.G., Ackermann, K.E., Sherman, W.R. & McDaniel, M.C. 1985. The digitonin-permeabilised islet model. Effect of myoinositol 1,4,5-trisphospate on Ca^{2+} mobilization. *Biochemical Journal* **227**, 965-969.

Wollheim, C.B. & Biden, T.J. 1986. Second messenger function of inositol 1,4,5-trisphosphate. Early changes in inositol phosphates, cytosolic Ca^{2+} and insulin release in carbamylcholine-stimulated RINm5F cells. *Journal of Biological Chemistry* **261**, 8314-8319.

Wollheim, C.B. & Regazzi, R. 1990. Protein kinase C in insulin secreting cells. Putative role in stimulus secretion coupling. *FEBS Letters* **268**, 376-380.

Wollheim, C.B., Siegel, E.G. & Sharp, G.W.G. 1980. Dependency of acetylcholine-induced insulin release on Ca^{++} uptake by rat pancreatic islets. *Endocrinology* **107**, 924-929.

Wollheim, C.B., Ullrich, S. & Pozzan, T. 1984. Glyceraldehyde, but not cyclic AMP-stimulated insulin release is preceeded by a rise in cytosolic free Ca^{2+}. *FEBS Letters* **117**, 17-22.

Wollheim, C.B., Dunne, M., Peter-Riesch, B. Bruzzone, R., Pozzan, T. & Petersen, O.H. 1988. Activators of protein kinase C depolarize insulin-secreting cells by closing K^+ channels. *EMBO Journal* **7**, 2443-2449.

Woodhull, A.M. 1973. Ionic blockage of sodium channels in nerve. *Journal of General Physiology* **61**, 687-708.

Zunckler, B.J., Lenzen, S., Manner, K., Panten, U., Trübe, G. 1988a. Concentration-dependent effects of tolbutamide, meglitinide, glipizide, glibenclamide and diazoxide on ATP-regulated K currents in pancreatic B-cells. *Archivs of Pharmacology* **337**, 225-230.

Zünckler, B.J., Lins, S., Ohno-Shosaku, T., Trübe, G. & Panten, U. 1988b. Cytosolic ADP enhances the sensitivity to tolbutamide of ATP-dependent K^+ channels from pancreatic B-cells. *FEBS Letters* **239**, 241-244.